Smart Nord

Final Report

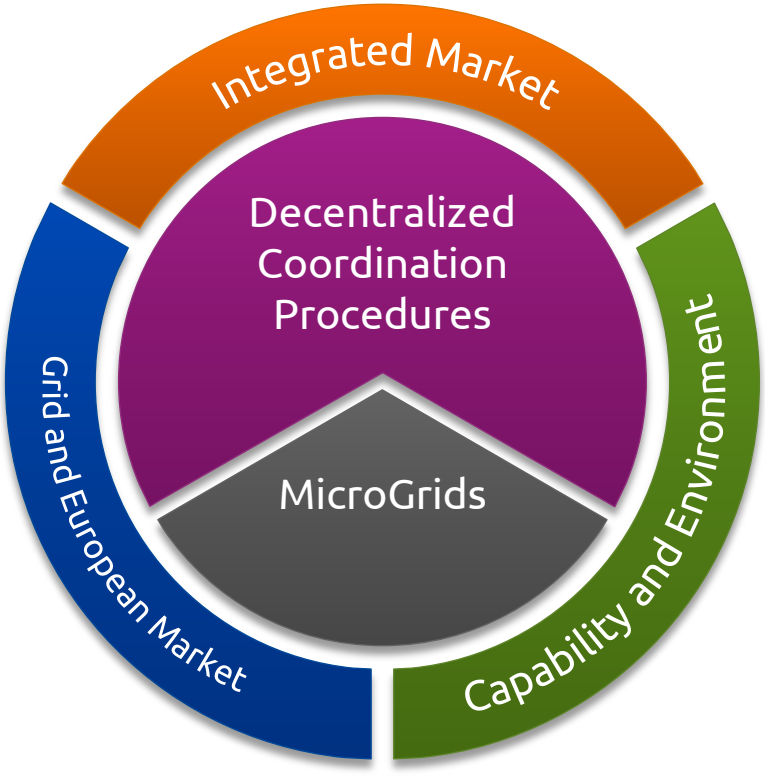

April 2015

Smart Nord

Final Report

Editors:

Prof. Dr.-Ing. habil. Lutz Hofmann

and

Prof. Dr. rer. nat. habil. Michael Sonnenschein

The Lower Saxony research network “Smart Nord” acknowledges the support of the Lower Saxony Ministry of Science and Culture through the “Niedersächsisches Vorab” grant programme (grant ZN2764/ZN 2896).

Hanover, April 2015

Please cite the contributions to this report in the following manner:

Author(s), “Full Title of the Work Package or Full Title of the Sub-Project,” in L. Hofmann and M. Sonnenschein, “Smart Nord - Final Report”, pp. #-#, Hanover, April 2015.

ISBN: 978-3-00-048757-6

Printed by: Druckerei Hartmann GmbH, Hannover

Preface

The Lower Saxony research network "Smart Nord" has achieved its goals. In this research network supported by Lower Saxony's Ministry of Science and Culture through the "Niedersächsisches Vorab" grant programme with an amount of 4.1 Million €, about 40 scientists of the universities of Oldenburg, Brunswick, Hanover and Clausthal as well as the OFFIS Institute for Information Technology, the Energy Research Centre of Lower Saxony and NEXT ENERGY, the EWE-Research Center of Energy Technology e. V. worked together for three years in six sub-projects.

In the past three years (from 3/2012 to 2/2015) the interdisciplinary research network Smart Nord aimed to create contributions to coordinated, decentralized provision of active power, control power and reactive power in distribution grids which allow a stable system operation. Therefore, the development of a new ICT infrastructure which includes all the new components of the distribution grids is required.

The sub-projects were motivated by the transformation of the European and especially German power system which includes the shutdown of nuclear power plants, the replacement of fossil power plants with converter based decentralized generation units, the ever intensifying European power market and installation of Smart Grids and their ICT infrastructure. In addition to these changes, a high amount of new power lines and transformers to fulfil the changing transmission and distribution tasks will be included in all grid voltage levels as well as new control strategies.

Based on this transformation of the power system, sub-project (SP) 1 was focused on methods for decentralized coordinated active power management to allow decentralized and especially renewable generation units to contribute to the power market. Another market which can be opened to these units is the market for ancillary services, especially provision of control power and reactive power, to support the power grid and the realization of the technical requirements (SP 2). The design and requirements of these above mentioned future markets had to be set within the project (SP 3). This included the design of new products and marketing opportunities. Based on the unit dispatch which resulted from SP 1-3, the resulting states of the transmission and distribution grids were evaluated in stationary and dynamic simulations to analyse the frequency stability in order to identify measures to ensure frequency stability in future grids (SP 4). The control strategies for distribution grids with a high amount of volatile converter connected generation units were also evaluated (SP 5). This included strategies for distribution grids connected to the transmission grid and islanding distribution grids without connection to other grids. SP 6 aimed at the analysis of the potential for the construction of new renewable generation units based on environmental conditions.

The following report introduces Smart Nord to you and shows the various results of the sub-projects and their work packages. For further information please visit www.smartnord.de.

Prof. Dr.-Ing. habil. Lutz Hofmann
Institute of Electric Power Systems
Leibniz Universität Hannover

Prof. Dr. rer. nat. habil. Michael Sonnenschein
Department of Computing Science
Carl von Ossietzky Universität Oldenburg

Table of Contents

Introduction

Smart Nord

"Smart Nord – Intelligente Netze Norddeutschland" which stands for "smart grids in northern Germany" is an interdisciplinary research network supported for three years (from 3/2012 to 2/2015) by the Lower Saxony Ministry of Science and Culture through the "Niedersächsisches Vorab" grant programme with 4.1 Million €. Smart Nord was organized in six sup-projects with research partners from up to four universities and research institutes which were:

Sub-Project One - Decentralized Provision of Active Power
coordinated by Michael Sonnenschein

Research partners:
University of Oldenburg
OFFIS – Institute for Information Technology
Technische Universität Braunschweig

Sub-Project Two - Grid Stabilizing Ancillary Services
coordinated by Sebastian Lehnhoff

Research partners:
OFFIS – Institute for Information Technology
University of Oldenburg
Leibniz Universität Hannover
Technische Universität Braunschweig

Sub-Project Three - Integrated Market
coordinated by Michael Kurrat

Research partners:
Technische Universität Braunschweig
OFFIS – Institute for Information Technology
Leibniz Universität Hannover

Sub-Project Four - Distribution and Transmission System
coordinated by Lutz Hofmann

Research partners:
Leibniz Universität Hannover
Technische Universität Braunschweig
EWE-Forschungszentrum für Energietechnologie e.V.

Sub-Project Five - System Theory for Active Distribution Grids
coordinated by Hans-Peter Beck

Research partners:
Clausthal University of Technology
University of Oldenburg

Sub-Project Six – SmartSpatial
coordinated by Christina von Haaren

Research partners:
Leibniz Universität Hannover

On the following pages an overview over the research aims of the six sub-projects is given. They are introduced with a brief explanation and visualisation of the contents as well as their interaction and collaboration, especially in the sub-projects 1-4 within the work group scenario design.

Overview on Smart Nord

The following pictures and annotations shall give a general overview and understanding of the connections and collaborations between the system layers market, function, information, hardware, grid and environment, which are handled in the sub-projects 1-6 and the collaborations between the sub-projects.

Figure 1 shows the setup and connections of the sub-projects 1-4. The main research areas of these sub-projects are the operation of an interconnected energy system spreading over four voltage levels with a high amount of decentralized renewable generation. In the SP new decentralised market structures are examined in addition to a market based interface. A necessary part of the market is the market for ancillary services which is based on so far existing units. In the lower voltage levels of the distribution grid, the units are organised within virtual dynamic coalitions. These coalitions are subjected to a decentralized regulation and control strategy which is realized by an agent-based information and communication technology (ICT) infrastructure.

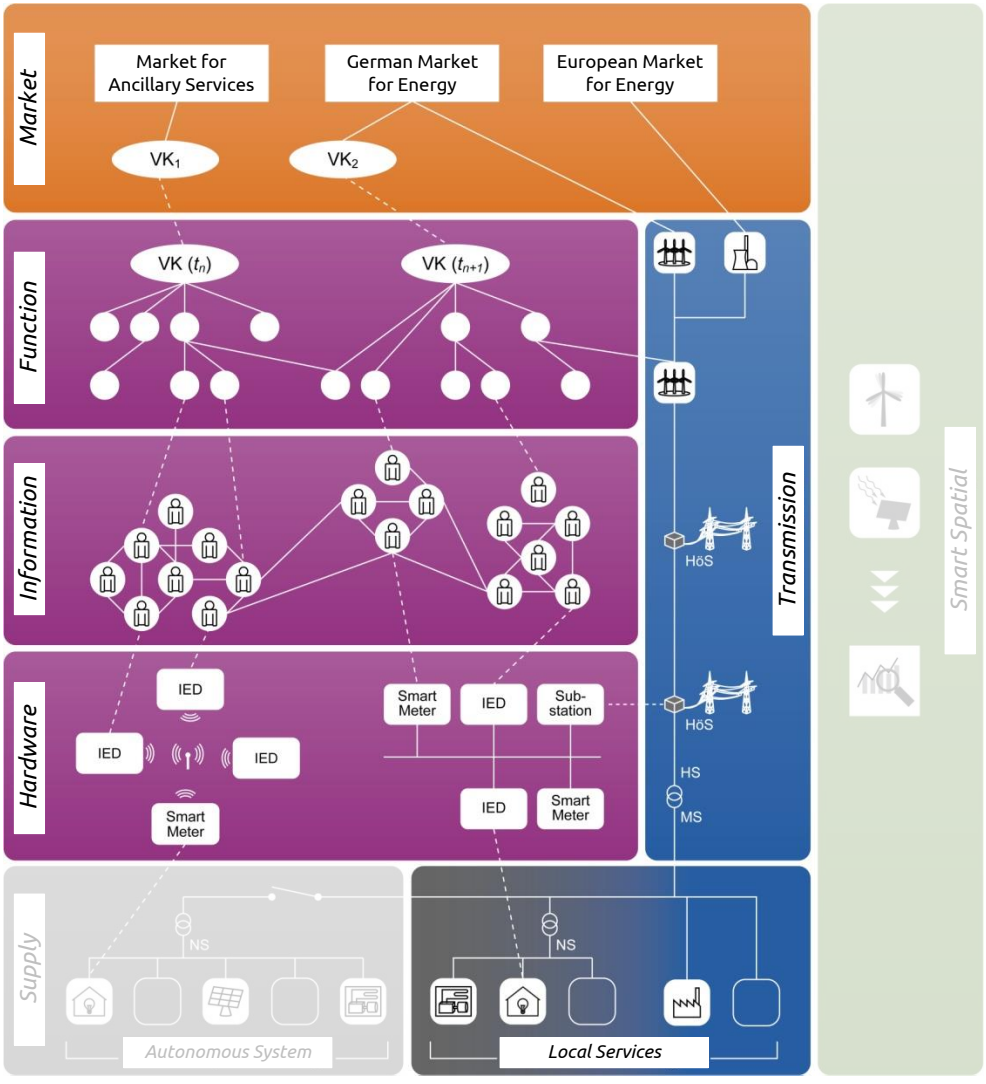

Figure 1: Setup and connections of sub-projects 1-4

Based on the design of new tradable products and the results of the markets, further analysis is possible. The stationary operational behaviour of the system under the constraints of decentralised provision of active and reactive power as well is calculated for several stationary cases and evaluated with regard to operational and technical boundary conditions. In addition to stationary analysis, the decentralised provision of ancillary services to ensure the frequency stability and measures to ensure the frequency stability in future systems are analysed.

In order to work together on comprehensive topics, specialised work groups were established. The work group Scenario Design has developed joint scenarios and herewith corresponding grid models as joint evaluation environment for the studies in sub-projects 1-4 to allow a common simulation at several research institutes and an exchange of research results.

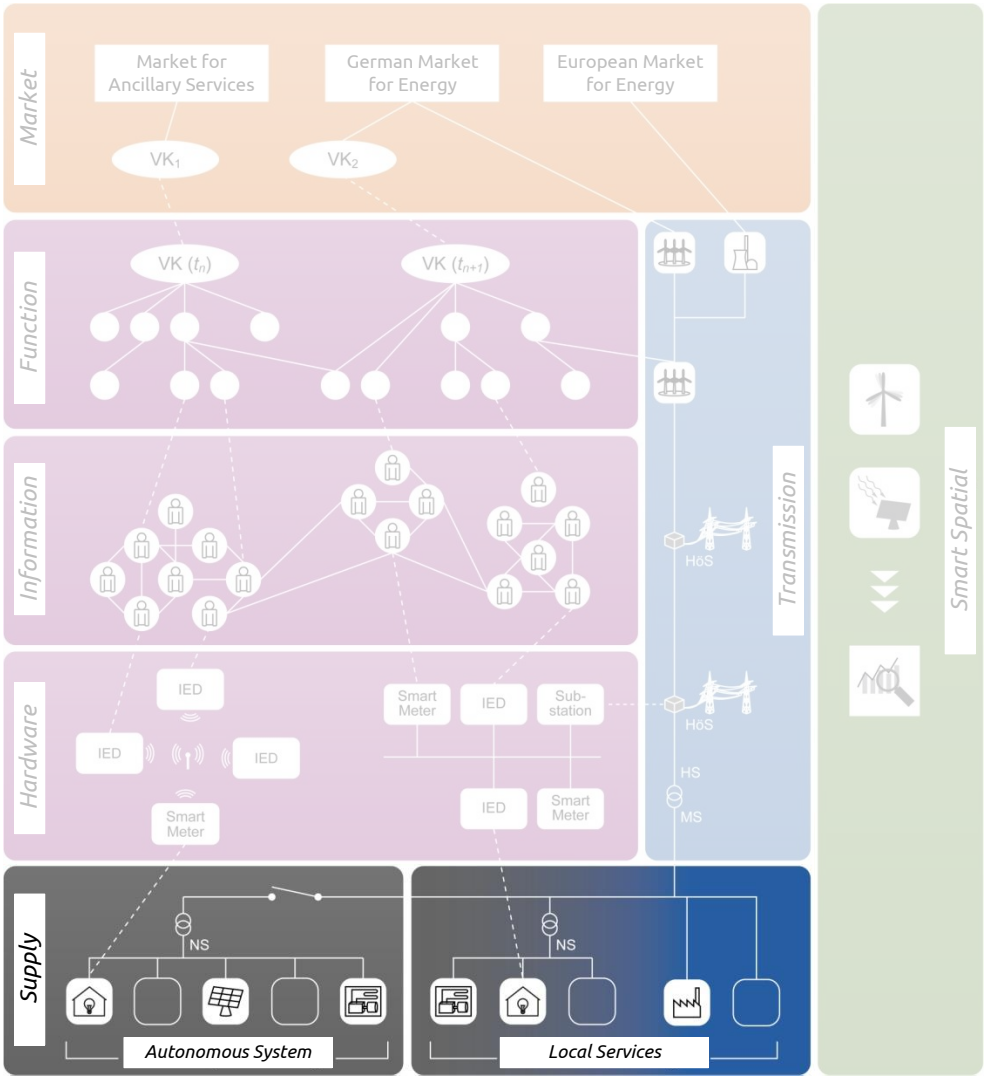

Figure 2: Setup of SP 5

Figure 2 shows the setup of SP 5 and possible connections to the other SP. Within this SP, MicroGrids with a high amount of renewable generation units are evaluated. These MicroGrids are simulated as islanded grids without any connections to neighbour grids and as part of the interconnected energy system. In addition, the possibilities of a virtual synchronous generator for providing ancillary services with the use of converters are evaluated. The second part of this SP is a system-theoretical approach influenced by the stochastic disturbance of regenerative systems. The last part of this SP is the construction of a demonstrator to evaluate the simulations in real power systems.

Figure 3 shows the setup of SP 6. This SP evaluated the local potential of possible construction sites for renewable generation units. It identifies the potential of several renewable energy sources in predesigned regions and identifies an efficient energy mix for a specific region under consideration of environmental requirements.

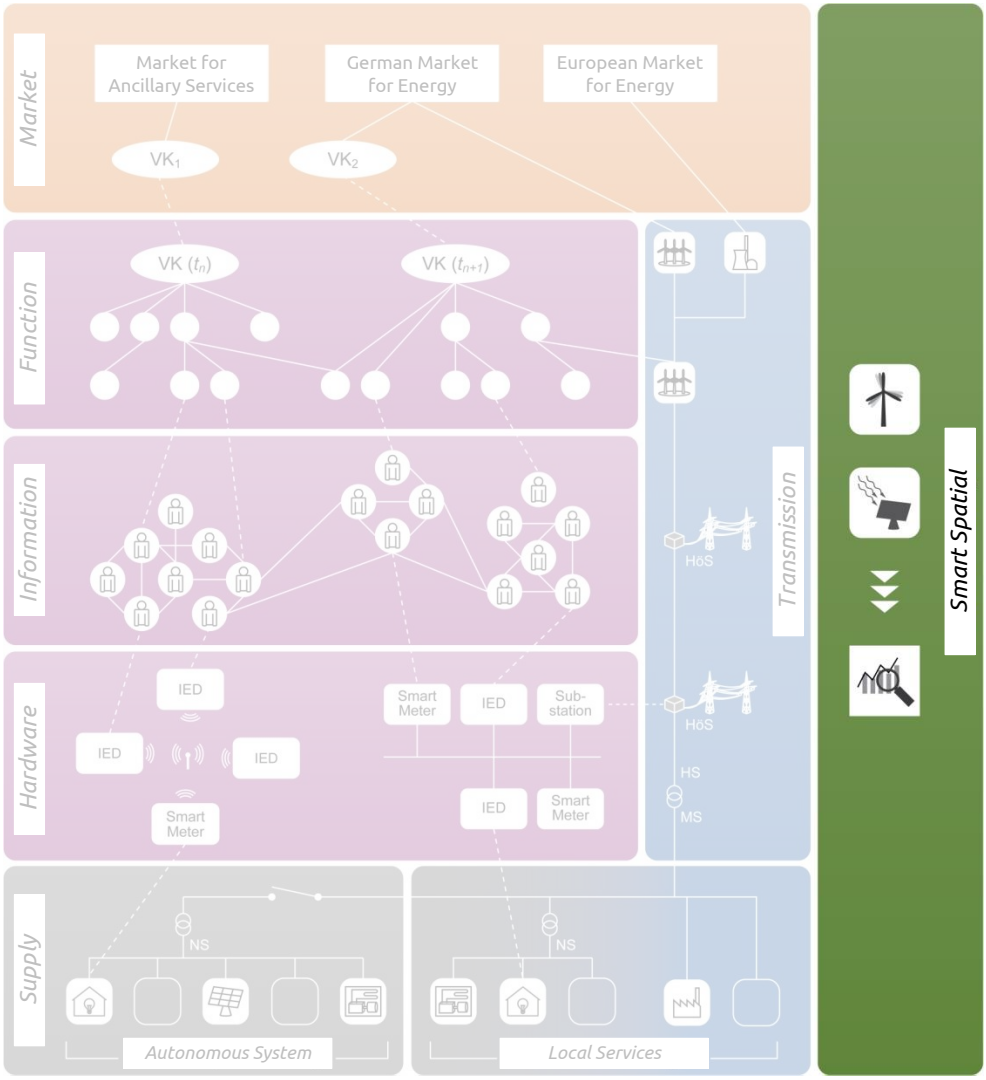

Figure 3: Setup of SP 6

On the following pages detailed reports of each SP are given. These detailed reports are headed by an introduction of the joint evaluation scenarios which were created by the work group scenario design for the sub-projects 1-4.

Work Group:
Scenario Design for Sub-Projects 1-4

Work Group: Scenario Design

Marita Blank[1], Timo Breithaupt[2], Jörg Bremer[1], Arne Dammasch[3], Steffen Garske[2], Thole Klingenberg[4], Stefanie Koch[3], Ontje Lünsdorf[4], Astrid Nieße[4], Stefan Scherfke[4], Lutz Hofmann[2] and Michael Sonnenschein[1]

1 Goals

Within the multi-disciplinary research project Smart Nord, different research questions have been addressed which concern different fields and system levels. However, several work packages require cross-disciplinary information and models and are dependent on results from other project partners. A simulation of the whole system taking into account all research questions within all work packages was not available and could not be realised at once. Nevertheless, the evaluation of the SP 1-4 had to be built on the same basic assumptions in order to guarantee compatible and comparable project results. For this reason, the work group Scenario Design – consisting of researchers from all partner institutes and work packages – has developed joint scenarios and herewith corresponding grid models as evaluation environment for all partners in the SP 1-4.

The scenarios had to be valid for all voltage levels from ultra-high voltage to low voltage and have been transferred to the corresponding grid models. Furthermore, the present regional structure of loads and generating units had to be represented as well as estimations for their future development according to actual studies (see Section 3). With the developed scenarios characteristic points in time (high load, low load) and time horizons (e.g. winter, summer) can be investigated in order to evaluate the different algorithms und approaches within the project under different case studies.

2 Related Work

The terms scenario and scenario design are used in different ways depending on the domain under investigation [1] (e.g. in companies, energy system, algorithm design) and the purpose the scenarios are used for. In companies, scenarios for future development can be used to identify new business strategies [2]. For energy systems, the design of future scenarios is an essential step for research studies. There, scenarios are used, e.g., to define goals for future energy systems (e.g. the energy concept of Germany [3]) or to make assumptions or predictions on future developments of the overall energy system. The predictions can be utilised to evaluate the development of different system parameters such as the need for network expansion depending on, e.g., different energy mixes or different assumption on energy consumption ([4], [5], [6] and [7]). Moreover, structural and economic effects can be investigated for different scenarios and conclusions can be drawn for different approaches such as the need of flexibility (e.g. [8]). In [9] migration paths are described for information and communication technologies of different Smart Grid scenarios. Furthermore, scenario design is an important step during algorithm engineering especially for applications in Smart Grid approaches [10].

[1] University of Oldenburg, 26129 Oldenburg, Germany,
{forename.surname}@uni-oldenburg.de, Department of Computing Science
[2] Leibniz Universität Hannover, 30167 Hanover, Germany,
{surname}@iee.uni-hannover.de, Institute of Electric Power Systems (IEH)
[3] Technische Universität Braunschweig, 28106 Braunschweig, Germany,
{first letter.surname}@tu-braunschweig.de, elenia
[4] OFFIS – Institute for Information Technology, 26121 Oldenburg, Germany,
{forename.surname}@offis.de, R&D Division Energy

However, a uniform or standardised process for scenario design does not exist [1]. The vast amount of scenarios and their different usage shows that the design of scenarios strongly depends on the purpose and investigations to be conducted.

3 Methodology

For the development of the scenarios within this research project as a first step, the work group Scenario Design collected requirements from the different work packages to ensure that the scenarios are suitable for the investigations of all work packages. Two main scenarios - a reference scenario 2011 and a future outlook of the year 2030 - have been aligned. Based on these requirements a process has been developed to define and realise the scenarios in the available evaluation environments in all SP. This process is visualised in Figure 1.

First, the Basic Assumptions (4.1) were made on which the scenarios were built. These include all basic information as grid, load and generation data for as well the reference year 2011 as the future outlook of the year 2030. The assumptions are mainly based on the governmental plans for the transformation of the energy supply system and furthermore the corresponding studies regarding grid expansion in transmission and distribution grids (Section 4.1). Furthermore, requirements from the simulation environments available and used at each SP have been identified which were necessary to adapt to the scenario requirements and to obtain an overall coherent simulation environment. Thus as the second step, the transmission grid model used in the work package 4.1 has been determined in order to define coupling points to underlying grid levels (see Section 4.2 Top-Down). As a third step, requirements from the distribution grid have led to defining coupling points to the higher voltage levels (see Section 4.3 Bottom-Up). In a fourth step, the unit distribution within the distribution grid has been computed in order to represent the actual and regional structure of load and generation. Hence the according units have been distributed and connected to the grid model nodes followed by a validation and verification of the grid compatibility of these generated grid models (cf. work package 4.2).

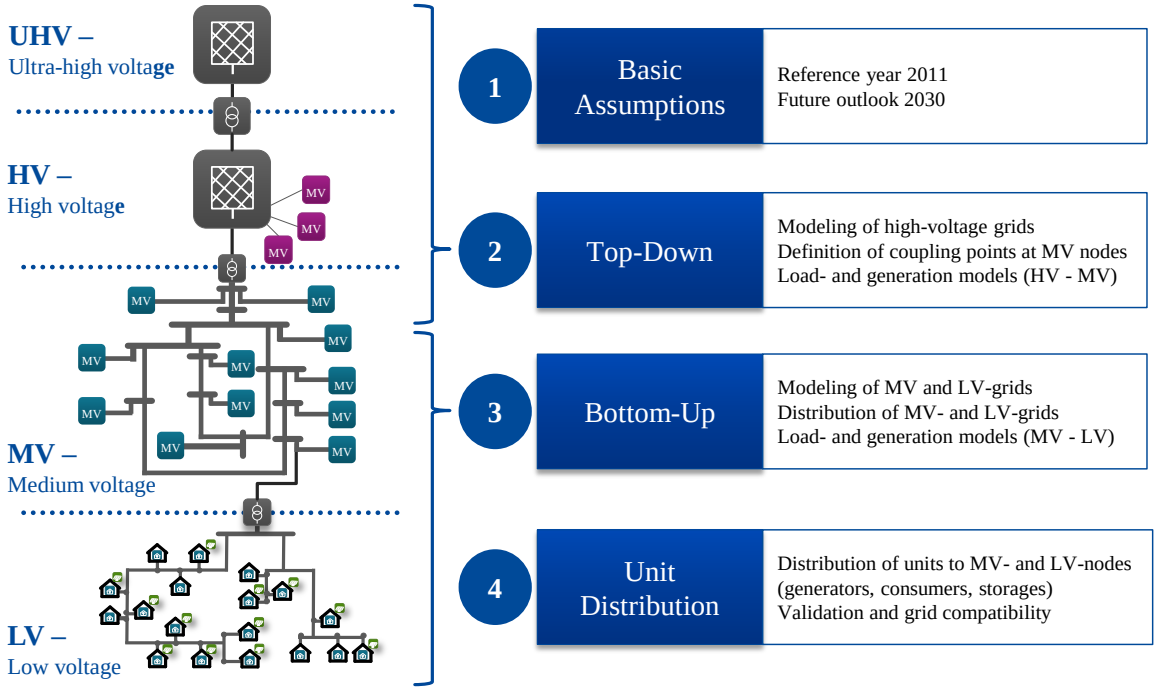

Figure 1: Process for scenario definition

In both analyses – the top-down and bottom-up step – requirements and data interfaces for load and generating units were identified that comply with the assumptions and coupling points. The results of this process are coherent grid models for both distribution and transmission grid within this research project with corresponding load and generation distribution for both scenarios (2011 and 2030).

4 Main Results

As the process itself is a main result of the work group, the individual steps of the process introduced in the previous section of this chapter are being presented in more detail. Furthermore excerpts of the results and realisation of the scenarios are shown as well. For more detailed descriptions refer to the corresponding work packages and further [11] and [12].

4.1 Basic Assumptions

The Basic Assumptions form the foundation for the scenarios, since they establish the scope for investigations of the SP 1-4. The steps 2-3 (Figure 1) are the realisation of the scenarios in order to obtain a setting and environment to conduct experimental evaluations.

For investigations of a segment of the distribution grid, the structure of loads and distributed generating (DG) units for rural grids were chosen to represent the structure of rural regions in Lower Saxony. To this end, statistical data of population of rural regions was utilised [13]. In order to reflect the installed capacity in Lower Saxony according to the different voltage levels, the asset master data of all installed renewable energy sources (RES) in the German transmission grid operators [14] has been filtered. The joint reference year has been chosen to be 2011, whereas the future horizon was specified to be the year 2030 because for this horizon a good basis of data and studies were at hand. Predictions of growth of renewable and distributed energy resources as well as assumptions on grid expansion had to be consistent throughout all voltage levels. The following studies have been chosen to build the assumptions on 2030: BMU[5] Long-term scenarios 2011 [8], Netzentwicklungsplan 2012 [15], ENTSO-E[6] Ten Years Network Development Plan (TYNDP) [6], ENTSO-E Scenario Outlook & Adequacy Forecasts (SOAF) [7], Dena[7] Verteilnetzstudie [4], and BMWi[8] Verteilernetzstudie [5].

4.2 Top-Down

The approach of the top-down step is based on an integrated grid and market simulation developed in MATLAB[9] by the IEH (refer to [11], [16] and [17]) which is used for simulations of the European transmission system in this research project (cf. work package 4.1). The integrated simulation is based upon several databases like e.g. measured load data of the ENTSO-E, a grid model of the ENTSO-E interconnected continental transmission grid, generation data of all power plants with an installed capacity greater than 50 MW and further generation as well as RES and DG generation (all units smaller than 50 MW) as regional aggregated data [11], [10], [17]. The first result of the simulation is an energy market simulation based on a merit order of marginal costs (see work package 4.1). The according power plant dispatch is the input value for the load flow calculations of the transmission system.

[5] Bundesministerium für Umwelt, Naturschutz, Bau und Reaktorsicherheit (Federal Ministry for the Environment, Nature Conservation, Building and Nuclear Safety), http://www.bmub.bund.de/en/
[6] European Network of Transmission System Operators for Electricity, https://www.entsoe.eu
[7] Deutsche Energie-Agentur (German Energy Agency), www.dena.de/en/
[8] Bundesministerium für Wirtschaft und Energie (Federal Ministry for Economic Affairs and Energy), www.bmwi.de/EN/
[9] http://www.mathworks.com

In this simulation environment the assumptions of the future outlook scenario 2030 have been implemented into the generation data with the 2011 scenario as the existing reference scenario (see Figure 3 as an example for the German transmission system model).

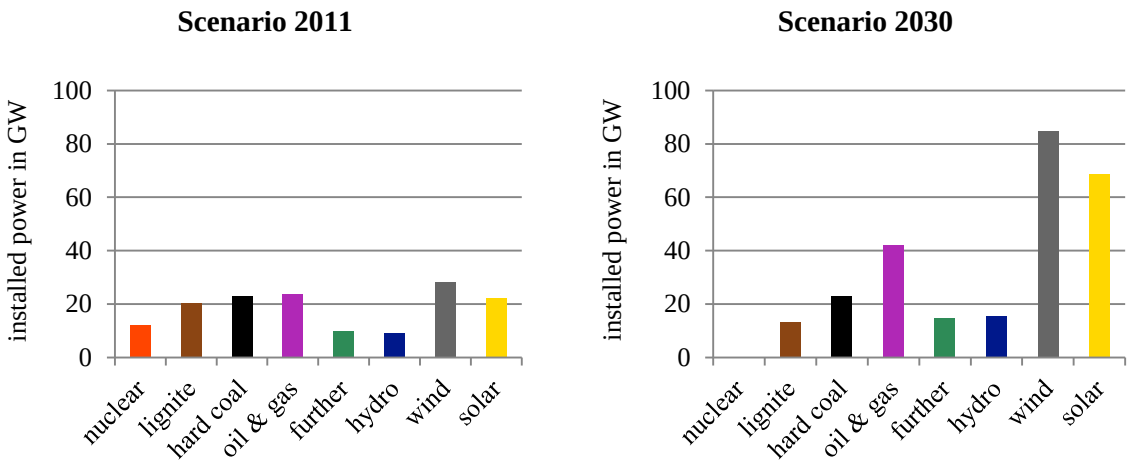

Figure 2: The scenarios 2011 and 2030 in the generation data for the transmission system model

The forward projection of the power generation is based on the power plant database of the grid and market model (see work package 4.1) and the Vision 3 of the SOAF [7]. The forecast in the SOAF gives only information about the installed capacities of the different energy sources. Hence different concepts for the distribution of the various types have been developed within this research project to calculate the shares and the geographical allocation of each generation type within the simulation model (see Figure 3).

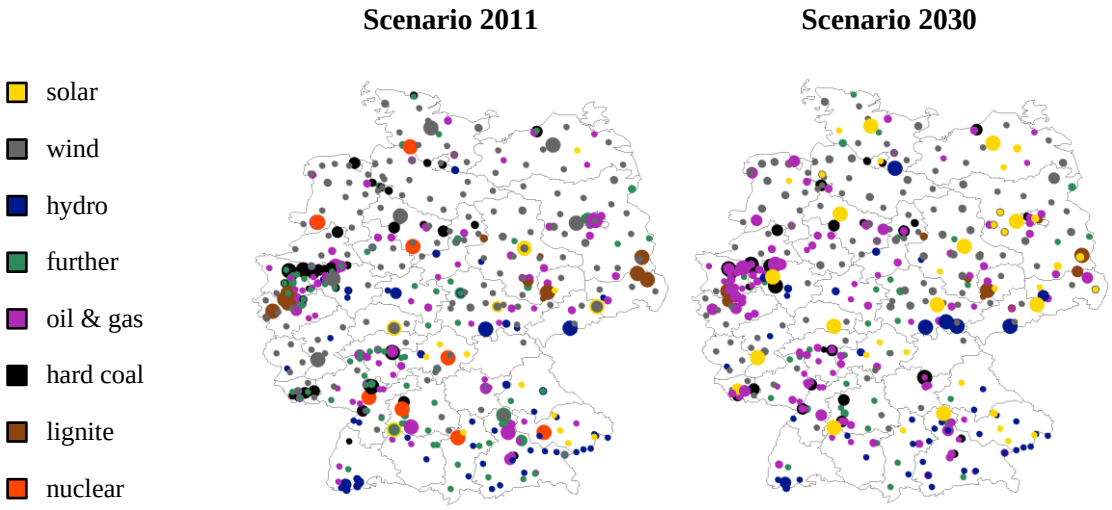

Figure 3: The scenarios 2011 and 2030 in the generation allocation data for the transmission system model

For biomass, garbage and not clearly identifiable energy sources all characteristics of the single power plants listed remain the same except the nominal power. To estimate the nominal power for every power station a scaling factor is calculated in relation of the target value (SOAF) and the sum

of the nominal power listed in the database. Wind and solar power plants are scaled with the target values and the geographical allocation of the power plants remains unchanged. Thermal power plants and hydropower plants are first analysed regarding their expected lifetime within the database [18], [19], [20]. Power plants whose lifetime ends before 2030 are removed. If the remaining cumulative capacity is greater than the target value, the power plants starting with the oldest are removed until the target value is reached. If the cumulative capacity is smaller than the target value, new power plants are built in the second step using a trend line with consideration of the average relative deviation for nominal power and efficiency at the same location. The trend lines and the average relative deviations are estimated from existing and planned power plants [21]. As the nominal power of run-of-the-river power plants and storage power plants is strongly influenced by the local conditions, the nominal power remains the same when these power plants are rebuilt. Due to the small amount of heavy oil-fuelled power plants the identification of a trend line is not possible. If the cumulative capacity is still smaller than the target value the missing capacity needs to be added manually.

Within each scenario load flow calculations can be analysed for various characteristic points in time. As the simulation model is based on the reference scenario 2011, the new generation allocation (see Figure 3), which is based on the stated studies and the described allocation algorithm, is not compatible with the present grid data. The extensive transformation of the European energy supply system leads to a high need of grid expansion (compare [6], [15]). Thus this required grid expansion according to the stated studies, including the high-voltage direct current (HVDC) lines within the German transmission system (see Figure 4), had to be implemented in the simulation model. Furthermore, because of divergences of the simulation model and the stated studies, further grid expansions within the transmission grid model have been implemented.

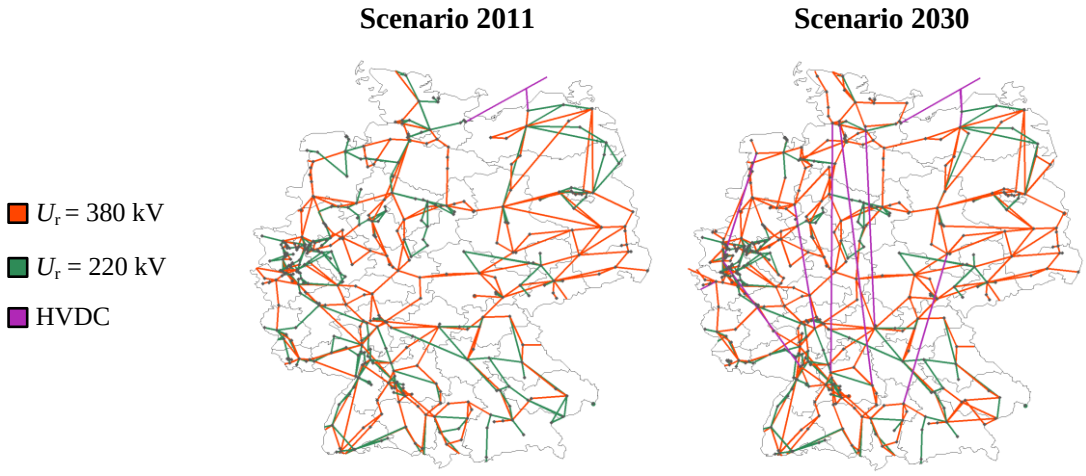

Figure 4: The scenarios 2011 and 2030 in the transmission system model including the NEP 2012

One main research question of the project Smart Nord is the provision of active, reactive and control reserve by dynamic virtual power plants (DVPP) in the underlying voltage levels to the transmission system. Hence the distribution grid had to be implemented into the existing transmission system model. This was realised with the stated top-down and bottom-up approach in addition with distributed load and generation data models. On selected UHV nodes the existing load and RES data was substituted with distributed HV and MV load and DG models in one

distribution grid section model (see Figure 1). Therefrom, the top-down requirements for the bottom-up coupling points are defined. The distribution section from HV to MV is based on synthetic grids for the HV-level and a modification of a common MV-Benchmark grid [22] (see 4.3). With the distribution grid sections coupled to the transmission system with individual load and RES data for each node, both scenarios can be evaluated in an integrated transmission and distribution system model [12].

4.3 Bottom-Up

Within the project, data of rural LV grids have been available from which realistic grid parameters were identified such as data of transformers, number of house connection nodes, line lengths and line types. This data was the basis for modelling eight LV-grids with typical rural grid structures. For completion, household profiles were generated (cf. [23]). To this end, different domestic consumers were modelled depending on size of households and technical equipment, e.g. how domestic warm water is prepared. The resulting profiles of domestic consumption for one year were validated by checking the correlations with the standardised load profile H0 from BDEW[10]. For simplification, commerce and industry were neglected within the MV and LV level.

As a model for an MV-grid a sub-network of the Cigre-Benchmark Grid [22] was chosen and adapted according to the requirements of the research project. According to Figure 5 the sub-network I has been used for evaluations in Smart Nord. The LV model-grids have been randomly connected to the MV-nodes according to the maximum load at the MV/LV-transformers and furthermore the specification of maximum power at the coupling point (HV/MV) from the top-down step. For modelling the scenario grids of the distribution level, the software DIgSILENT PowerFactory[11] was used. Due to the many opportunities and the high adaptability of the software, the lower voltage levels (LV, MV) were completely simulated using PowerFactory within the work package 4.2 and further as one part of the top-down step in the transmission system model (work package 4.1) in the MATLAB simulation.

[10] Bundesverband der Energie- und Wasserwirtschaft e.V. (Federal Association of the Energy and Water Industry), https://www.bdew.de/

[11] PowerFactory is a professional network calculation tool, which can be adjusted via freely programmable scripts (DPL Programming Language). The program is also capable of calculating very large power grids. Far from the modeling PowerFactory includes all common analysis tools such as load flow, short-circuit, harmonic calculations, contingency calculation and reliability analysis.

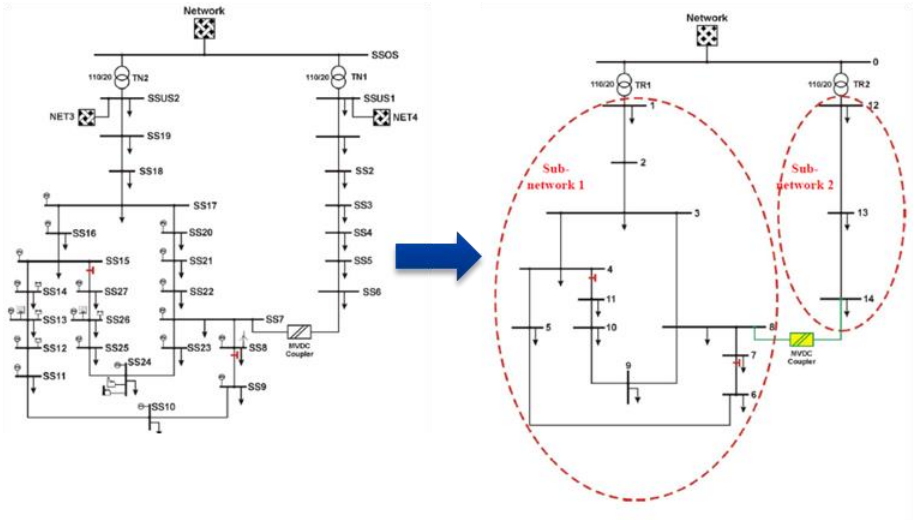

Figure 5: Graph of a German medium-voltage grid [22] (left) and aggregation of lines used for Smart Nord (right); sub-network I was has been used as evaluation basis

The MV-grid with connected LV-grids represents the evaluation environment for the SP 1-2. However, in order to evaluate the various concepts and algorithms of the single work packages detailed models of the units are necessary. As already introduced, domestic load models have been generated. Moreover, nine different models of photovoltaic units were generated in form of normalised time series of power feed-in (i.e. the time series have been scaled with respect to peak power) for different angles (15°, 30°, and 45°) and tilts (east, south, and west) of the photovoltaic-module. In order to generate a profile for the power feed-in of a wind turbine, a synthetic reference wind turbine was utilised. Furthermore, physical models were available for storage devices from work package 1.1 as well as combined heat and power plants and heat pumps. The grid models together with the unit models form the basis to connect grid nodes with unit simulators, i.e. the unit distribution presented in the subsequent section.

4.4 Unit Distribution

With the grid models as a part of a distribution grid with suitable household loads, the next step is to assign other consumer units, generating units as well as storage devices to the various nodes of the grid model in order to reflect the energy mix of the region of interest – in this case Lower Saxony. However, the following procedure can be applied to other regions, too.

First, typical unit sizes per technology are chosen. This can be done according to the frequency of appearance of installed capacity. To this end, for renewable energy units the asset master data [14] has been filtered. Typical unit sizes are determined for each technology and voltage level. Second, the installed power per technology and voltage level of Lower Saxony has been mapped to the grid model via per-head installed power. The population in Lower Saxony has been inferred from statistical data [13]. With the information of the installed power per technology and voltage level from the asset master data [14], the per-head installed power in a region has been computed. The population in the grid model has been determined from the household loads. From this, the annual energy demand has been known at each node and conclusions have been drawn on the number of households and inhabitants. With the per-head installed power of the region the installed power in the grid model has been calculated. Together with the typical unit size, the number of units to be distributed in the grid model was known.

Given the number of units, in a third step the units have been randomly and automatically assigned to nodes in the grid model. To this end, the co-simulation framework mosaik[12] has been used: the grid models have been processed and simulators of distributed units were connected to the grid nodes. After that, the distribution is being checked for plausibility (e.g., units are connected to the right voltage level; no unrealistic combinations of units appear at one node).

Besides the plausibility check, it must also be evaluated whether the random unit distribution to realistic grid structures leads to any grid related problems. To this end, operational equipment is investigated with respect to contingencies and overloads according to actual guidelines. In case these limits are exceeded the grid is expanded accordingly. Details on the distribution grid calculations and grid expansions methodologies can be found in the report of work package 4.2.

4.5 Results

In Figure 6, the results of the units distributed in the model distribution grid are shown as aggregated data representing the rural structure of Lower Saxony for the reference scenario 2011 as well as the future scenario 2030. The models of the distribution grid and the corresponding unit distribution are the basis for simulations.

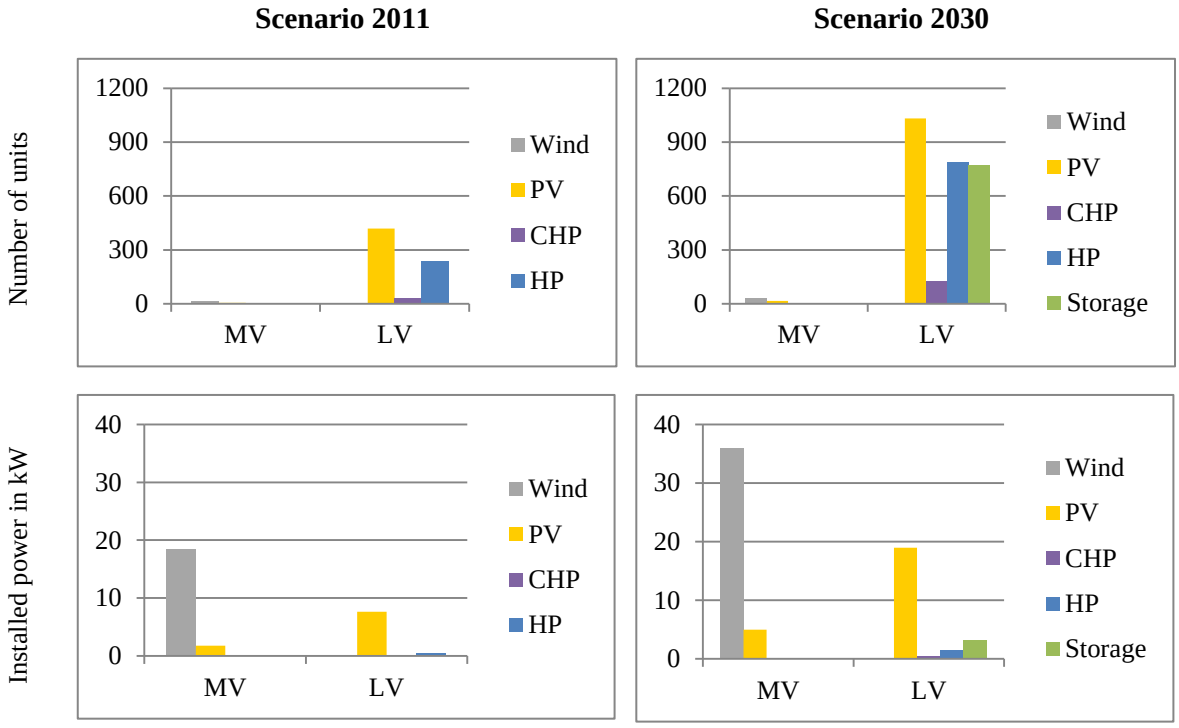

Figure 6: Results of unit distribution in model distribution grid
(PV: photovoltaic, CHP: combined heat and power plant, HP: heat pump)

Using the suitable unit models developed within this research project, investigations can be conducted concerning different load and generation ratios. Figure 7 shows exemplary results for a week in the winter of the scenarios 2011 and 2030, respectively. For simulations of the units' power feed-in and consumption, the tool mosaik has been used. The different unit distribution allocated within the distribution grid models lead to different load and generation characteristic for

[12] https://mosaik.offis.de/

the different scenarios and different periods under observation (summer or winter, high load or low load).

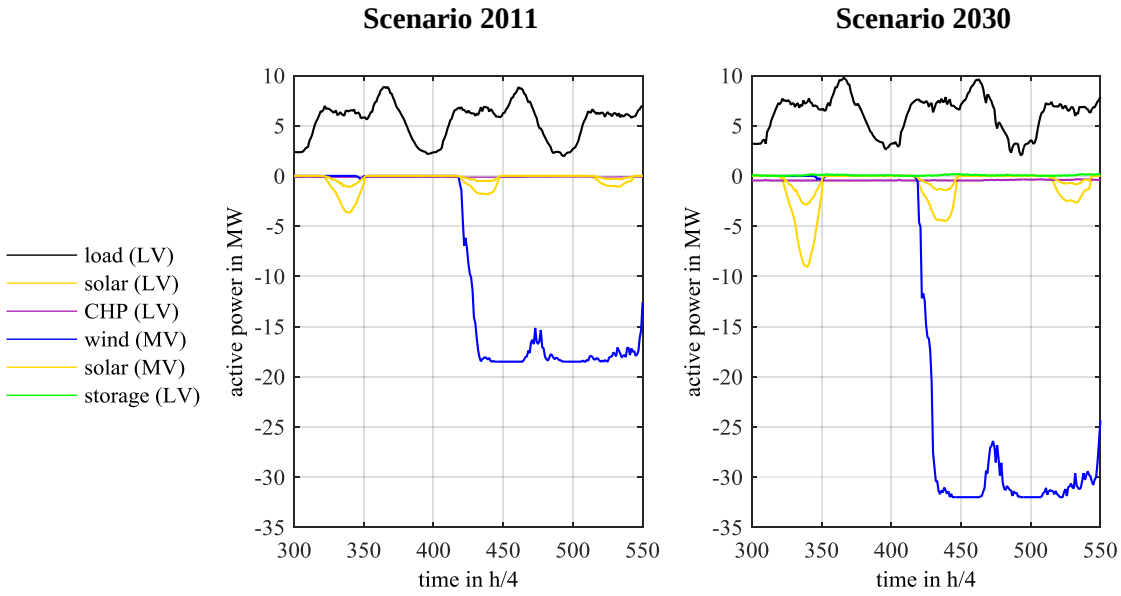

Figure 7: Aggregated consumption and distributed generation within the scenarios 2011 (left) and 2030 (right)

The scenarios developed within the simulation environments of this research project provide a wide range of characteristic points in time and realistic evaluation. Hence, both simulations of the distribution grid (see Figure 7) are based on the same time series of load and generation data the time course of the aggregated active power is basically the same, but the share of the single components differs as well as the unit distribution within the grid models. With the implementation of the different distribution grid models (2011 and 2030) in the transmission system simulation as components for the distribution grid section for as well the reference scenario 2011 and the future outlook 2030 the scenarios can be evaluated consistently in all voltage levels and in large-scale evaluations.

5 Conclusion and Outlook

The work group Scenario Design has been an interdisciplinary work group within the research project Smart Nord of the sub-projects 1-4. Consistent and compatible scenarios have been defined and existing simulation infrastructure has been adapted to comply with the scenario definition. Since a single simulation environment for the whole system from low- to ultra-high-voltage levels was not available and realisable, coupling points between the different levels and simulation environments were defined such that requirements from top-down to bottom-up have been taken into account and mapped to the according point of coupling. Corresponding grid models were adapted and generation, consuming and storage units were distributed in the distribution grid models in order to reflect the energy mix of Lower Saxony. The scenarios and accordingly adapted simulation environments have been used as a basis for investigations and evaluations of the various research questions in the different work packages of Smart Nord sub-projects 1-4.

References

[1] H. Kosow, R. Gaßner, "Methoden der Zukunfts- und Szenarioanalyse: Überblick, Bewertung und Auswahlkriterien," WerkstattBericht Nr. 103, Institut für Zukunftsstudien und Technologiebewertung (IZT), Berlin, September 2008.

[2] J. Gausemeier, C. Wenzelmann, C. Plass, "Zukunftsorientierte Unternehmensgestaltung: Strategien, Geschäftsprozesse und IT-Systeme für die Produktion von morgen," Hanser Verlag, 2009.

[3] "Energieszenarien für ein Energiekonzept der Bundesregierung," Prognos AG, EWI, GWS, Projekt Nr. 12/10 des Bundesministeriums für Wirtschaft und Technologie, 2010.

[4] A.-C. Agricola et al., "Dena Verteilnetzstudie. Ausbau- und Innovationsbedarf der Stromverteilnetze in Deutschland bis 2030," final report, dena, 2012.

[5] J. Büchner et al., "Moderne Verteilernetze für Deutschland (Verteilernetzstudie)," BMWi, 2014.

[6] "Ten Years Network Development Plan," ENTSO-E, 2014.

[7] "Scenario Outlook & Adequacy Forecasts 2014-2030," ENTSO-E, 2014.

[8] J. Nitsch et al., "Langfristszenarien und Strategien für den Ausbau der erneuerbaren Energien in Deutschland bei Berücksichtigung der Entwicklung in Europa und global," final report, DLR, Fraunhofer IWES, IFNE, 2012.

[9] H.-J. Appelrath, H. Kagermann, C. Mayer (Ed.), "Future Energy Grid: Migration to the Internet of Energy," acatech STUDY, Munich 2012.

[10] A. Nieße, M. Tröschel, M. Sonnenschein, "Designing Dependable and Sustainable Smart Grids – How to Apply Algorithm Engineering to Distributed Control in Power Systems," Environmental Modelling and Software, December 2, 2013.

[11] T. Rendel, C. Rathke, T. Breithaupt, L. Hofmann, "Integrated Grid and Power Market Simulation," IEEE PES General Meeting, San Diego, CA, USA, 22.-26. July 2012.

[12] T. Breithaupt, S. Garske, T. Rendel, L. Hofmann, "Methodological Approach for Integrated Grid and Market Simulation of Coherent Distribution and Transmission Systems," EnviroInfo 2013, Hamburg, Germany, 02.-04. September 2013.

[13] Landesamt für Statistik, "Statistische Erhebungen: Bevölkerungsfortschreibung, Tabelle K1020111," 2012.

[14] 50Hertz Transmission, Amprion GmbH, TenneT TSO GmbH, TransnetBW GmbH, "Informationsplattform der Deutschen Übertragungsnetzbetreiber EEG-Anlagenstammdaten,", 2011.

[15] "Netzentwicklungsplan Strom," 50Hertz Transmission GmbH, Amprion GmbH, TenneT TSO GmbH, TransnetBW GmbH, 2012.

[16] T. Breithaupt, T. Rendel, C. Rathke, L. Hofmann, "Modeling the Reliability of Large Thermal Power Plants in an Integrated Grid and Market Model," 2012 IEEE International Conference on Power System Technology (Powercon), Auckland, New Zealand.

[17] T. Rendel, C. Rathke, L. Hofmann, "Integrated Grid and Power Market Simulator," in ew - das Magazin für die Energiewirtschaft, no. 20, pp. 20-23.

[18] Deutsche Energie-Agentur GmbH, "Kurzanalyse der Kraftwerksplanung in Deutschland 2020 (Aktualisierung)," Berlin, 2010.

[19] O. Mayer-Spohn, S. Wissel, A. Voß, U. Fah, M. Blesl, "Lebenszyklusanalyse ausgewählter Stromerzeugungstechniken - 2005," Institut für Energiewirtschaft und Rationelle Energieanwendung, Stuttgart, 2007.

[20] Deutsche Energie-Agentur GmbH, "Untersuchung der elektrizitätswirtschaftlichen und energiepolitischen Auswirkungen der Erhebung von Netznutzungsentgelten für den Speicherstrombezug von Pumpspeicherwerken," Berlin, 2010.

[21] S. Wissel, U. Fahl, M. Blesl, A. Voß, "Erzeugungskosten zur Bereitstellung elektrischer Energie von Kraftwerksoptionen 2015," Institut für Energiewirtschaft und Rationelle Energieanwendung, Stuttgart, 2010.

[22] K. Rudion et al., "Design of Benchmark of Medium Voltage Distribution Network for Investigation of DG Integration," IEEE Power Engineering Society General Meeting, 2006.

[23] M. Bunk, H. Loges, B. Engel, "Innovative Last- und Erzeugungsannahmen präzisieren die künftige Netzplanung," in ew - das Magazin für die Energiewirtschaft, no. 8, pp. 68-71, 2014.

Sub-Project One:
Decentralized Provision of Active Power

Overview on Sub-Project[13] One: Decentralized Provision of Active Power

Michael Sonnenschein[14], H.-Jürgen Appelrath[15], Wolf-Rüdiger Canders[16], Markus Henke[16], Mathias Uslar[15], Sebastian Beer[15], Jörg Bremer[14], Ontje Lünsdorf[15], Astrid Nieße[15], Jan-Hendrik Psola[16], Christine Rosinger[15]

1 Goals

Distributed energy resources like photovoltaic (PV) plants, wind turbines or small scale combined heat and power (CHP) plants entered the energy market in many European countries, especially Germany, with the financial security of guaranteed electrical feed-in tariffs. With their share in the market still rising, a concept is needed to integrate them into the very same regarding both real power and ancillary services to reduce subsidy dependence and follow the goals as defined by the European Commission.

Virtual power plants are a well-known concept for the aggregation of distributed energy resources (DER) to deliver both energy products and ancillary services [2]. Besides the control of generation by distributed energy resources like combined heat and power plants (CHPs), photovoltaic (PV) plants and wind turbines, shiftable loads like heat pumps, water boilers or air conditioners can be controlled to adapt the load profile regarding different optimization targets. Electrical storage may additionally be a new player in this scene, delivering even more flexibility for the optimized use of distributed generation (DG). To address these three aspects, generation, load and storage, we will refer to distributed energy units (DEU) for the rest of this chapter.

Currently virtual power plants are *statically* structured coalitions of small power suppliers (and possibly controllable loads and storage systems) controlled by a *centralized control unit*. To tap the full flexibility potential of all energy units in the distribution grid we set up the following domain-driven paradigms for our model of *dynamic* virtual power plants (DVPPs) (cf. [3]) controlled by *distributed, agent-based methods*:

- Distributed energy units have to trade their services on markets, not only for active power products, but for ancillary services as well (as far as possible; see e.g. [4] for the position of the German Federal Network Agency regarding this topic). DVPPs for ancillary services are addressed in sub-project two.
- To dynamically adapt to current power system operational states and handle the vast amount of energy units in the distribution grid, an approach based on self-organization principles is used. By this means, characteristics like robustness, scalability and adaptivity of the overall system should be gained.
- DVPPs should be set up on a per-product base, thus allowing for optimal aggregation of energy units regarding the products needed. The paradigm of a dynamic VPP with respect to the product obligation is completely different from current virtual power plant concepts. We want to evaluate, if we can extract more flexibility from the distribution grid with such a highly dynamic approach.

[13] Parts of this section have previously been published in [1], [3], [14], [15]
[14] University of Oldenburg
[15] OFFIS – Institute for Information Technology
[16] Technische Universität Braunschweig

- The potential of DVPPs for power system control lies in their units' flexibility. Therefore a generic representation of these flexibilities is needed, building the foundation for all DVPP mechanisms concerned with DEU scheduling.
- For active power delivery on energy markets, the operation of distributed energy units is controlled using operation schedules for all different types of units. The resolution of the DEUs' operation schedules should reflect current schedule resolutions by indicating mean active power values for each 15 min. time interval. This is different to the current handling of renewable energy sources – current systems work with prognoses and use schedules only for controllable generating electricity units.
- To deliver ancillary services with locality constraints (like voltage control – see sub-project two), DVPPs have to be able to reflect the grid topology. Therefore grid topology should be an optional parameter in the aggregation process and within the operation of DVPPs.

Within this context, the objective of this sub-project is to introduce a seamless process chain for day-ahead based active power provision by means of DVPPs. We develop a multi-agent system (MAS) realizing the aggregation algorithm, the scheduling heuristic as well as the flexibility modelling used for DVPP management and control.

Two important prerequisites for the reliable and secure operation of DVPPs are also addressed in this sub-project:

- The application of multi-agent systems for operational control of a virtual power plant leads to a higher threat potential as a result of new and more intelligent actors, additional interfaces and data exchange. So, in addition to common security considerations and data privacy concepts a trust model has to support the trustworthy formation of DVPPs.
- In order to obtain a reliable energy supply with a high amount of (fluctuating) renewable energy, energy storages will become inevitable. So, technology selection, location and scaling of energy storage components in the power grid are important to enable DVPPs to fulfil their tasks reliably.

2 Related Work

The operational management of energy systems involves a number of complex tasks ranging from technical aspects like supervisory control and data acquisition (SCADA) to organizational measures performed by business management systems (BMS). These are coupled within an energy management system (EMS) based on information and communication technology (ICT). Traditionally, the EMS was implemented as a centralized control system. However, given the increasing share of distributed energy resources as well as flexible loads in the distribution grid today, the evolution of the classical, rather static (from an architectural point of view) power system to a dynamic, continuously reconfiguring system of individual decision makers endangers the feasibility of such centralized control schemes. In the seminal work of Wu et al. [5], the need for decentralized control has been identified as follows: "Control centers today are in the transitional stage from the centralized architecture of yesterday to the distributed architecture of tomorrow. [. . .] To summarize, in a competitive environment, economic decisions are made by market participants individually and system-wide reliability is achieved through coordination among parties belonging to different companies, thus the paradigm has shifted from centralized to decentralized decision making." In line with this vision, the International Energy Agency (IEA) describes a possible transition to decentralized control in three steps [6]:

1) **Accommodation**. Distributed generation is accommodated into the current market with the right price signals. Centralized control of the networks remains in place.
2) **Decentralization**. The share of DG increases. Virtual utilities optimize the services of decentralized providers through the use of common communications systems. Monitoring and control by local utilities is still required.
3) **Dispersal**. Distributed power takes over the electricity market. Microgrids and power parks effectively meet their own supply with limited recourse to gridbased electricity. Distribution operates more like a coordinating agent between separate systems rather than controller of the system.

The concept of a virtual utility mentioned therein was introduced in the late nineties and describes a "[. . .] flexible collaboration of independent, market-driven entities that provide efficient energy service demanded by consumers [. . .]." [7] Subsequently, virtual power plants (VPP) have been studied extensively as a derivation from this concept. For example, a number of successful VPP realizations can be found in [8]. Additionally, different operational targets have been defined and implemented for VPPs, like aggregating energy (commercial VPPs) or delivering system services (technical VPPs) [1]. These VPP concepts form a basis for the decentralization stage in the transition path above. However, such VPPs usually focus on the long-term aggregation of generators (and sometimes storages) only and are each still operated in a centralized manner. For an implementation of the dispersal stage in the transition path, a more flexible concept is required. In the last years, a significant body of research emerged on this topic. For instance, [9] surveys the use of agent-based control methods for power engineering applications. Exemplary applications can be found in [10], [11], [12]. Finally, a research agenda in this context was proposed recently in [13].

In contrast to the work referenced above, the concept of DVPPs explicitly takes the current market situation into account for the process of forming aggregations of DEUs: DVPPs form with respect to concrete products at an energy market, and will dissolve after delivering a product. Additionally, fully distributed control algorithms are being used, as will be shown in the following sections of this chapter, building the foundation for the dispersal stage in the mentioned transition path. A preliminary description of the concept including a detailed differentiation from related approaches was given in [3].

3 Methodology

In developing the integrated process of DVPP operation, we followed the Smart Grid Algorithm Engineering (SGAE) approach described in [14]. The SGAE process model is motivated by the main objective of contributing application-oriented research results on a sound methodological background, thus striving for an engineering aspiration within the domain of Smart Grids. The process model is set up with an initial conceptualization phase followed by an iterable cycle of five phases with both analytical and experimental parts, giving detailed information on inputs and results for each phase and identifying the needed actors for each phase. It is displayed in Figure 1.

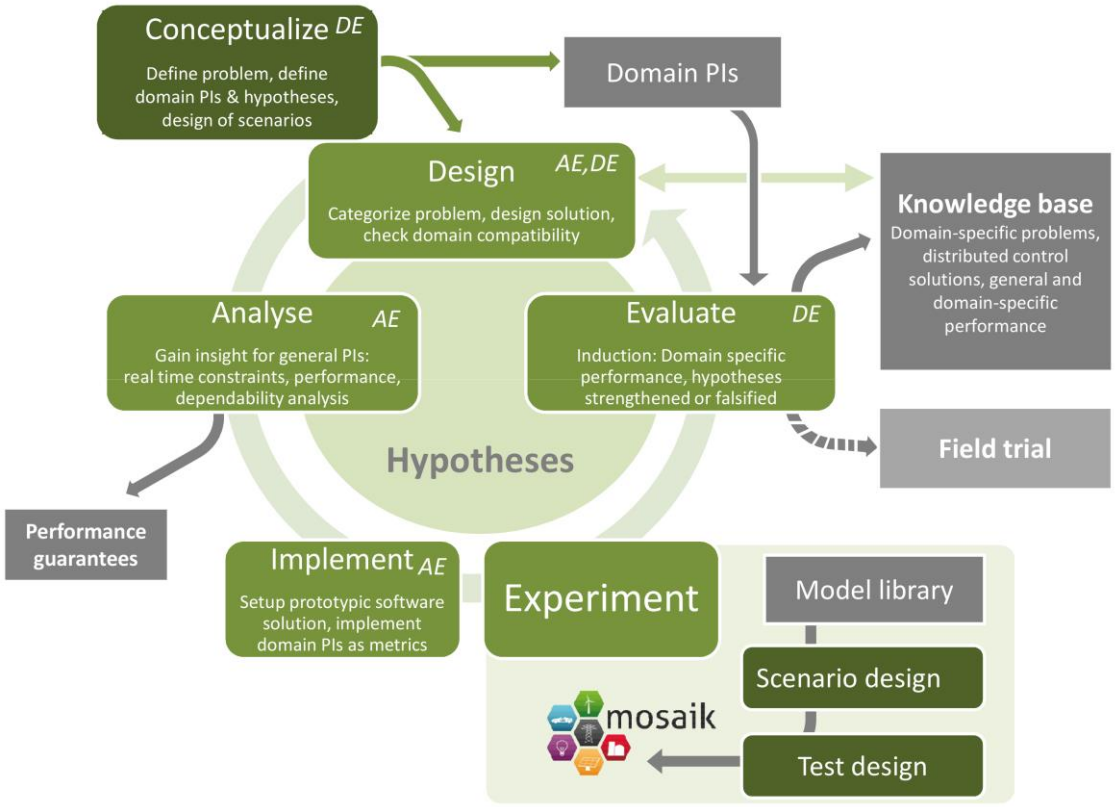

Figure 1: Overall Process of Smart Grid Algorithm Engineering [14]

4 Main Results

To introduce the concept of dynamic virtual power plants and show which tasks have to be performed by the software agents, we refer to the use case of active power products traded on the day-ahead power market, where product trading is based on an auction mechanism as described in [3] (see Figure 1).

From the market perspective, three different phases have to be distinguished. In the first phase, bids can be placed in the so-called order book for predefined product types. Once the order book is closed (e.g. at 12 a.m. for active power products traded day-ahead in Germany at EPEX SPOT) a matching mechanism clears supply and demand bids to set up the market price. In the last phase, these products have to be delivered, but no distinct market actions are entangled with this phase: the surveillance of product delivery and associated actions for balancing are subject to balancing group management.

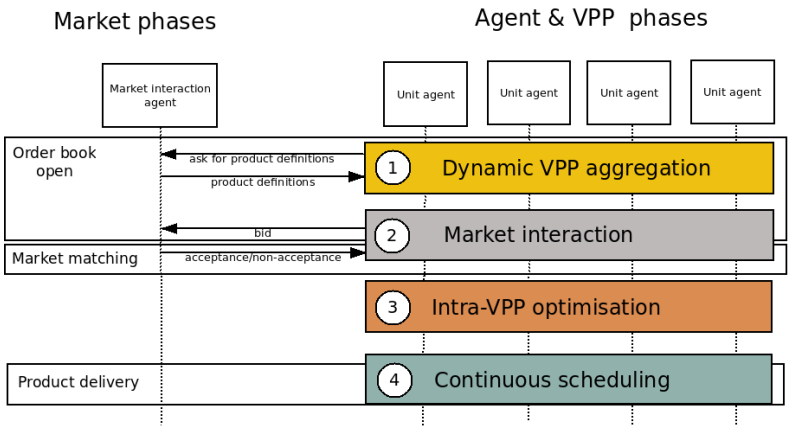

Figure 2: VPP delivering energy products on a day-ahead market [1]

To implement this with regard to DVPPs, unit agents are set up to represent distinct DEUs within a multi-agent system. Four sequential phases within these unit agents are needed for active power delivery on day-ahead markets, as can be seen on the right hand side of Figure 2:

1) Dynamic VPP aggregation: First, energy units have to be appropriately aggregated to DVPPs with the goal to deliver common active power products. Trust values for agents have to be integrated into the matching algorithm for security reasons. Grid topology has to be an optional parameter in this phase.

2) Market interaction: In the second phase, DVPPs place their active power products on the market by means of a representative agent for each respective DVPP and are informed about acceptance after market-matching. Thus, after market matching the units' obligations regarding their power contributions are known.

3) Intra-DVPP optimization: Within a third phase, an intra-DVPP optimization is performed, taking into account these obligations and updated prognoses regarding the units' operational states.

4) Continuous scheduling: The last phase is concerned with continuous energy scheduling to ensure product fulfilment. In case of an incident endangering product delivery a rescheduling of the units has to be performed.

The methodologies and algorithms to implement these phases are described below in the subsections for the work packages of sub-project one.

An exemplary result of DVPP aggregation for the common evaluation scenario 2030 is shown in Figure 3 – Figure 5. DVPPs are formed from 789 heat pumps, 1048 photovoltaic systems, 122 CHPs, and 789 redox-flow batteries for a day at the end of January. For reasons of clarity, 24 1h-products are selected by the initiating agents aggregating DVPPs.

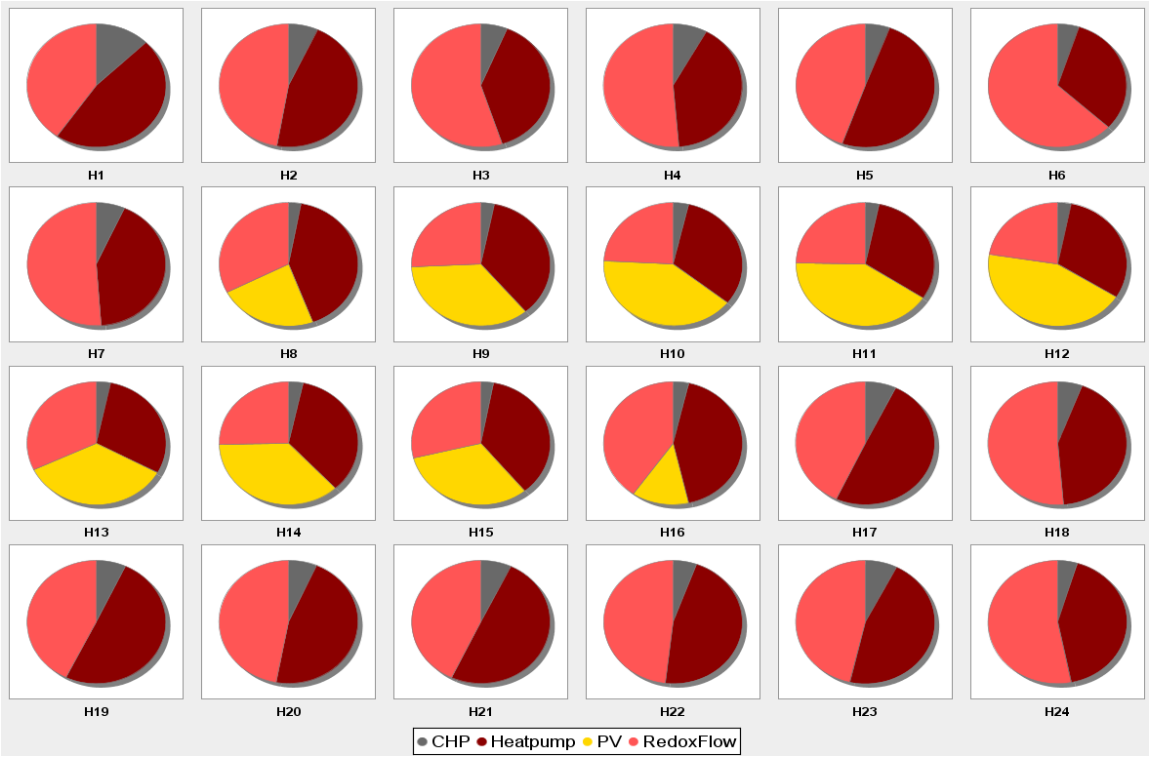

Figure 3: Relative part of units of different technologies within the DVPPs for all 24 1h-products

Figure 3 shows the relative part of units of different technologies within the DVPPs for all 24 1h-products. Figure 4 shows the absolute number of DVPPs for every hour, and Figure 5 shows the relative part of power delivery for different technologies within the DVPPs for the 24 hours.

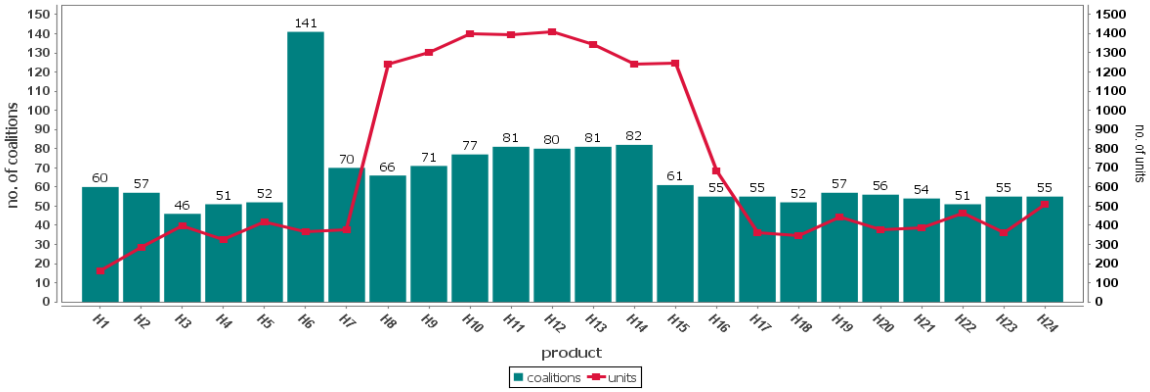

Figure 4: Absolute number of DVPPs for every hour

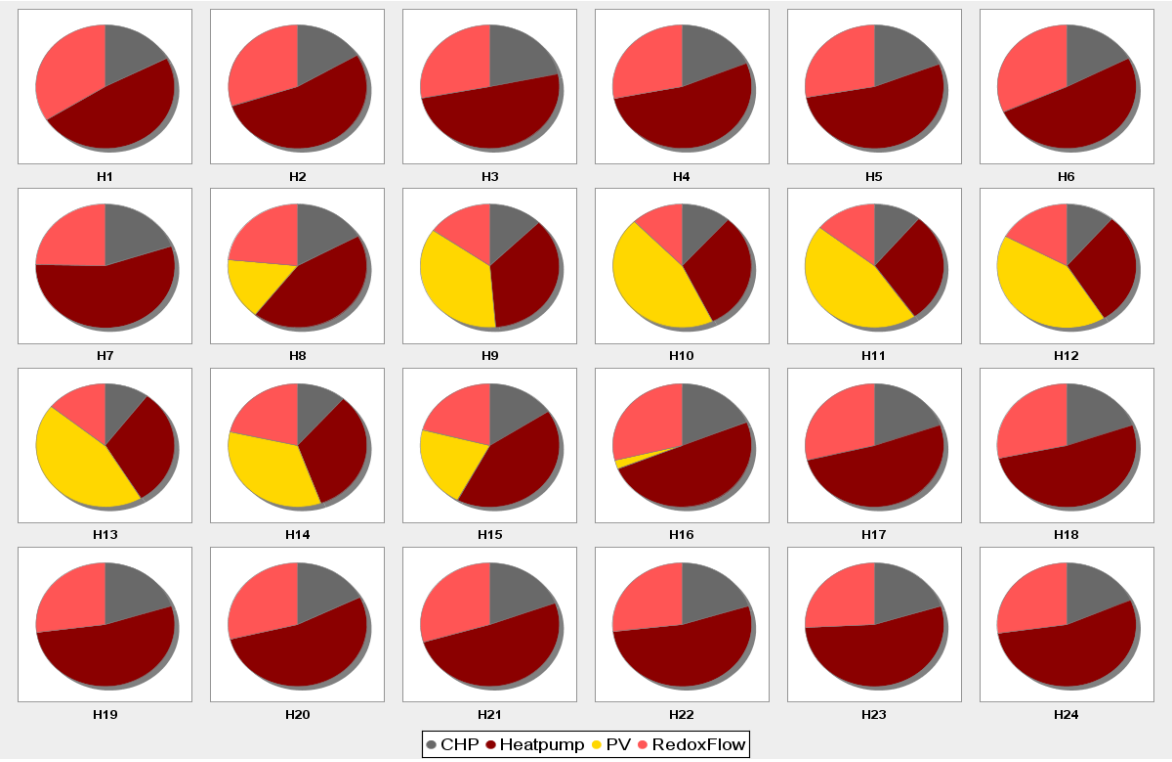

Figure 5: Relative part of power delivery for different technologies within the DVPPs for the 24 hours

If we have a look at an exemplary coalition of micro-CHPs forming a DVPP delivering 50 kW for an hour (separated into 4 intervals of 15 min. each), then due to prognosis errors the delivery based on the original day-ahead schedule could be as shown in the left part of Figure 6. Delivery of single micro-CHPs is illustrated by different colours. In this example, several CHPs are not able to deliver power after half an hour due to operational constraints. Optimizing product schedules again just before the delivery period starts, i.e. taking into account actual constraints for rescheduling, the CHPs can be rescheduled to deliver power as shown in the right part of Figure 6. Thus, by rescheduling the DVPP is able to fulfil its obligation to deliver 50 kW for an hour.

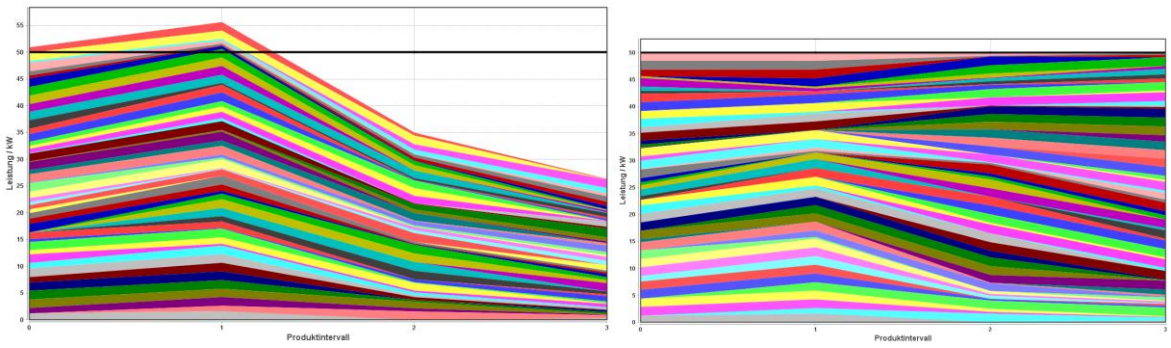

Figure 6: Delivery of CHPs in a DVPP before (left) and after (right) rescheduling just before product delivery

5 Conclusion and Outlook

With the concept of DVPPs a fully distributed, self-organizing operational scheme for VPPs has been developed. In [15] the algorithmic concept of DVPP has been mapped to two different realization options. In the first realization option, the DVPPs are an internal construct within a central VPP system. Thus, they are a substitute for commercial optimizers to fulfil the tasks of unit

commitment and economic re-dispatch for all energy units aggregated in a virtual power plant. Self-organization in this concept can be drilled down to distributed optimization applied within a VPP system with full control of all DEU integrated in the system. In the second realization option, DVPP are realized in the field with software agents running on the intelligent electronic devices (IEDs) controlling the DEU. The VPP system is reduced to a VPP service provider (VPP TP), delivering information retrieved from other actors like distribution system operators (DSO) (for grid locational information) and access to the market.

Following a new methodology that combines IEC/PAS 62559 and technological migration paths as defined in [16], some main findings of the work in [15] sum up as follows:

- As the requirements of both DVPP concepts clearly exhibit dependencies, migration paths for a transfer of self-organization concepts to the field could be defined. Although self-organization seems to be easier to realize as an algorithmic solution on enterprise level as compared to field level, the main technological requirements follow the same critical paths.
- The main benefits of self-organization on the field level can be found in the distribution of information: Detailed information on single households, plants and flexible loads are not transferred to a central information system as an important aspect regarding privacy.
- DVPP are compliant with current energy system and market roles as defined by ENTSO-E. Further work should be done on the extension regarding new concepts like the data access point manager [17].

Additional findings have been made regarding the allocation of self-organization on the SGAM levels and lead to new hypotheses: The closer to the field level self-organization algorithms are realized, the more relevant become safety issues. The more levels in the SGAM are crossed, the higher becomes the vulnerability of the resulting system (as already has been defined by NIST in IR 7628 [18]), thus security issues are more important.

From simulation results it can be derived that battery storage systems play an important role in the operation of future energy grids. However, an algorithmic attempt to the optimal dimensioning of battery storage systems in the grid is still challenging. Additionally the need for long term storage systems in the grid has to be investigated with respect to the short-term operation of (D)VPPs. Another direction for future research on control algorithms could be a combination of self-organization methods for DVPP operation with the observer/controller concept of organic computing [19]. This attempt promises an additional way to control convergent evolution in self-organizing systems.

Work Package 1.1: Use of Electrical Energy Storages to Support a Schedule-Based Energy Management

Jan-Hendrik Psola[17], Wolf-Rüdiger Canders[17] and Markus Henke[18]

1 Goals and Integration in the Sub-Project

The energy conversion chain is going to change from conventional fossil fuel-based plants to renewable energies as wind and photovoltaic plants. These technologies will be widely spread throughout the grid but their energy conversion is volatile due to seasonal weather conditions. In order to keep the energy supply based on a high amount of renewable energies reliable, energy storages will become inevitable. Hereby, it is important to choose a suitable storage solution based on the individual grid situation. The geographical location and scaling of energy storage systems are important in order to obtain grid stability and fulfil the desired operations. In addition to technical aspects, the storage operation has to be economically optimized. Therefore, an understanding of fluctuations of renewable energy and the cost structure of different storage technologies is needed.

For the storage operation several aspects have to be investigated with relation to several market options, e.g. system services or optimization of private household consumption. However, the primary aspect is to ensure a reliable and stable energy supply. According to some aspects, certain storage technologies or combinations thereof have to be preferred over others.

The impact of energy storages is examined in several use cases. The resulting effects on the grid as well as economic parameters as energy losses due to conversion and losses due to self-discharges as well as the storage installation costs are studied.

2 Related Work

Several models on energy storage technologies are implemented for the simulation process in MATLAB/Simulink. The storage models are based on datasheets as well as measurement series. For example, a redox flow battery model based on measurements from a real system at the EFZN (Energie-Forschungszentrum Niedersachsen) in Goslar is implemented. The modelling approach, more details and further information can be found in [20]. In Figure 7, a voltage curve for a six hour discharge with three variations in power demand is depicted. The figure shows the measurement data as well as the model behaviour. The measurement data confirms general parameter of a redox flow battery found in literature.

[17] Technische Universität Braunschweig, 38106 Braunschweig, Germany,
{first initial.surname}@.tu-braunschweig.de, Institute for Electrical Machines, Traction and Drives
[18] Technische Universität Braunschweig, 38106 Braunschweig, Germany,
markus.henke@.tu-braunschweig.de, Institute for Electrical Machines, Traction and Drives

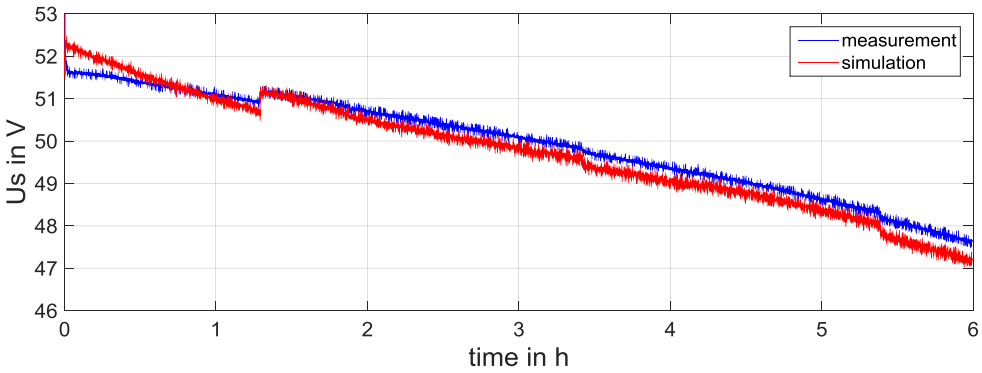

Figure 7: Voltage plot during discharge

Furthermore, the correlation of energy generation by wind and photovoltaic is investigated. Renewable energies can be combined with storage systems. An optimal ratio between portfolio solutions has to be calculated in order to adopt positive effects depending on their different generation behaviour. Therefore, data gathered from Braunschweig 2011, Germany is studied. Generally, there is a negative correlation between these renewable energies over the seasons. However, if the observed time period is reduced to 15 minutes this effect vanishes [21], [22]. Thus, for short-term storages no reliable positive effect by combining these two renewable energies can be identified (Figure 8).

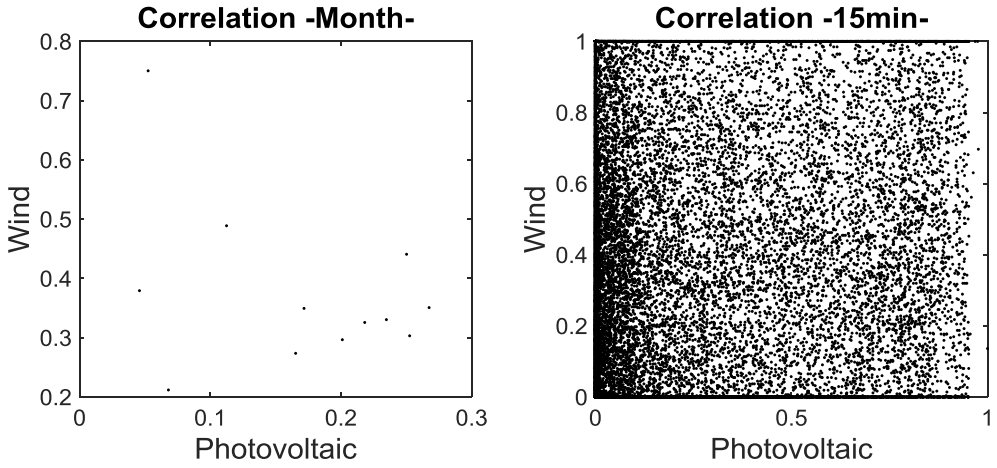

Figure 8: Correlation between wind and photovoltaic

3 Methodology

In a first step, the technical and economical behaviour and attributes of the available energy storage technologies is collected. Based on the technical data, simulation models are developed, which are either based on data sheets or system measurements. According to the simulation environment, these models are adapted and tailored to the necessary parameters for real power applications. Depending on the technology specifications and constraints, the relevant technologies are selected for further research.

For simulation, a part of the Smart Nord grid that is modelled using DIgSILENT PowerFactory has been chosen. The aim of the simulations is to evaluate the impact of different storage ratings and technologies on the so called sub-scenarios. Hereby, the installed power of renewable energies and the loads are varied. In order to maximize the fluctuation, only photovoltaic plants are used as

renewable energy sources. In order to maximize the simultaneous feed-in of these decentralized systems, both the same orientation and inclination are used. The photovoltaic models from TP4 are used. Throughout the various sub-scenarios, the energy capacity and the power of the energy storages are varied. The methodology is shown in Figure 9.

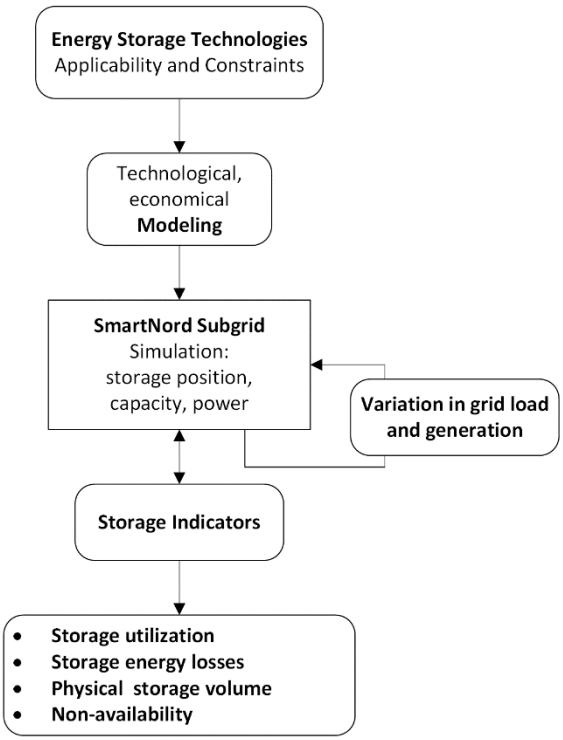

Figure 9: Methodology of storage scaling and selection

A utility function is used in order to measure the storage applicability. Under certain conditions, specific characteristics are more important than others, therefore, a factor-based rating method is deemed appropriate.

4 Main Results

In order to determine how to select and parametrize an energy storage relevant technology, data has to be gathered. Therefore, the important technical specifications for several energy storage technologies are presented in Table 1.

	Cycle efficiency in %	Rated power in MW	Capacity in MWh	Self-discharge	Lifetime in years	Lifetime in cycles
PHS*	70 – 85	10 – 1,000	< 8,000	neglectable	70	> 30,000
CAES*	30 – 54 (diabatic) 60 – 70 (adiabatic)	10 – 600	500 – 5,000	-	30	> 30,000
Flywheel	90 – 95	< 10	< 2	< 20 %/hour	20	>> 100,000
SuperCaps	90 – 95	< 0.2	< 0.05	0.5 %/hour	./.	./.
SMES*	90 – 95	0.01 – 100	< 0.03	>>15 %/day	30	./.
Lead-Acid	70 – 85	< 50	< 10	5 %/month	10 – 15	200-2,000
Sodium-Sulfur	75 – 90	< 35	< 10	-	15 – 20	1,000-5,000
Lithium-Ion	85 – 95	< 50	< 10	5-10 %/month	10 – 15	1,000-5,000
Redox-Flow	70 – 80	< 10	< 100	neglectable	10	> 10,000
Hydrogen	20 – 40	kW - GW	GWh	neglectable	20	./.
Methane	30 – 40	kW - GW	GWh	-	20	./.

* PHS: Pumped-hydro Storage, CAES: Compressed-Air-Energy-Storage, SMES: Superconducting Magnetic Energy Storage

Table 1: Technical storage parameter [23], [25]

Another technology classification is done according to operational concepts for the energy storage technologies. One can mainly distinguish between real power market arbitrages and system services. Both operational concepts have different storage parameters as primary conditions (see Table 2).

Real Power Market Arbitrage	System Service
High cycle efficiency	High rated power
Low self-discharge	High capacity
High capacity	Fast response time
High rated power	Low self-discharge

Table 2: Storage requirements according to [23]

The overall abilities for the technologies to operate within the market are shown in Table 3. Within system services, primary, secondary and replacement services can be distinguished between.

	Real Power Market Arbitrage	System Services		
		Primary	Secondary	Replacement
PHS*	X		X	X
CAES*	X			X
Flywheel	X	X		
SuperCaps		X		
SMES*		X		
Lead-Acid	X	X		
Sodium-Sulfur	X	X		
Lithium-Ion	X	X		
Redox-Flow	X	X		
Hydrogen	X		X	X
Methane	X		X	X

* PHS: Pumped-hydro Storage, CAES: Compressed-Air-Energy-Storage, SMES: Superconducting Magnetic Energy Storage

Table 3: Operation for energy storage technologies from [23]

In addition to the technology and operation concepts, there are restrictions imposed by certain technologies. Pumped hydro and compressed air energy storages depend on geographical conditions. Therefore, these technologies may not be placed and scaled without context in a grid scenario. Another restriction applies to the sodium-sulfur battery being a high temperature technology and alas, sodium fire is difficult to be extinguished, so this technology may not be placed in every urban environment.

Furthermore, an understanding of the cost structure of energy storage technologies is indispensable. Therefore, specific cost data is collected and an economic ragone chart has been developed for Figure 10.

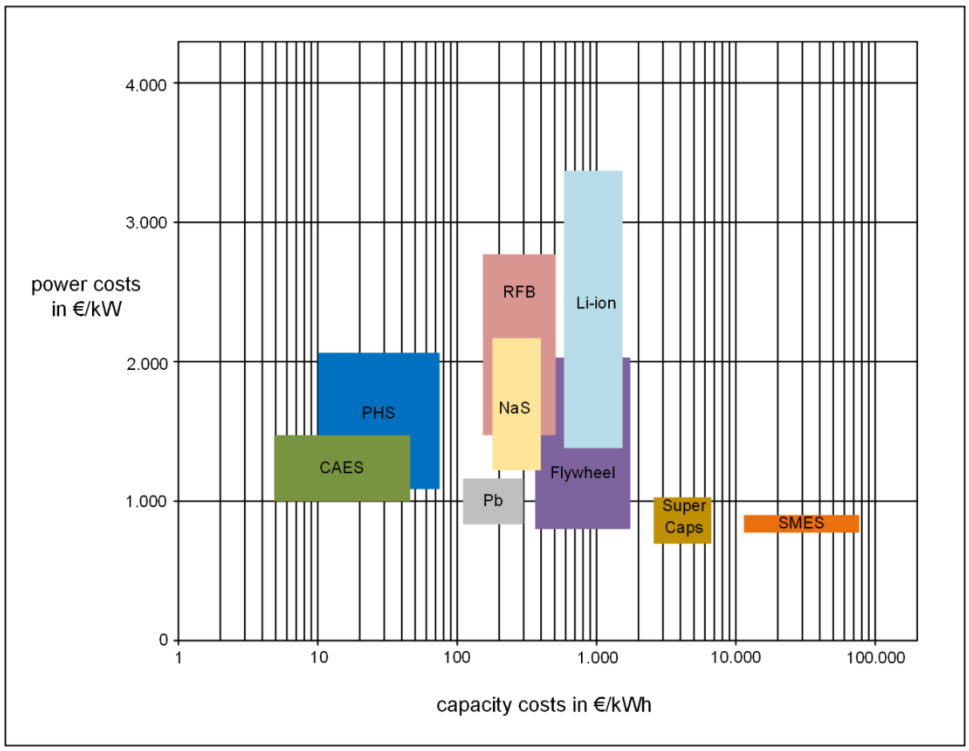

Figure 10: Economical ragone chart on energy storage technologies [24] - [27]

Due to technical and economic parameters and restrictions, battery storage technologies are most suitable for decentralized energy operations. These systems include an inverter, which enables them to deliver system services.

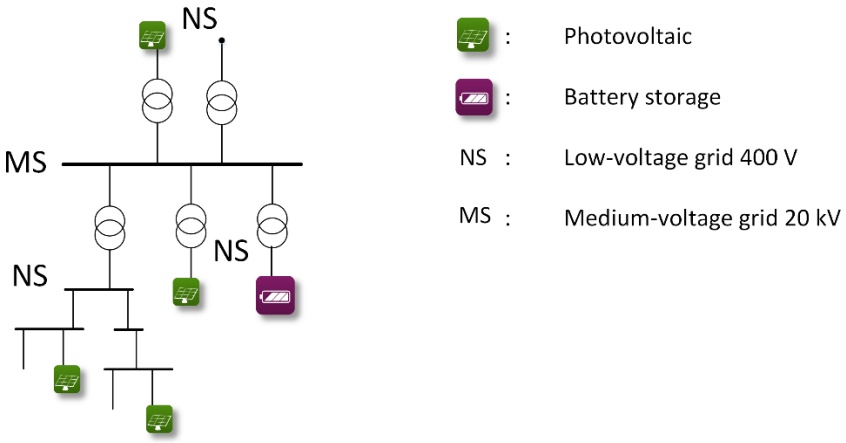

Figure 11: Example on simulations grid and technology distribution

In the following paragraphs, two simulation scenarios are described and discussed. The rating of the storages for different applications is shown. For case (1), the intent of the storage is to avoid a higher grid load caused by photovoltaic panels. To achieve this, the power at the coupling point has to be kept within the same limits, as it would be without additional generation. For case (2), the approach is to balance the grid load to its annual average. However, for case (2) the storage energy is limited to ten hours full power output. The simulation runs are based on a data of the Smart Nord grid that is used in various WP. However in WP 1.1 a smaller section is used for the simulation and the geographical distribution of renewable energies and storages is adjusted (Figure 11).

For the cases (1) and (2) the load varies between 48 – 413 kW. The installed photovoltaic capacity has an energy rating of 840 kWp with an identical generation behaviour and can deliver 80 % of the annual electricity demand of the sub-grid.

The results for rated power, rated energy and equivalent full-cycles for the two cases are shown in Table 4.

	Case (1)	**Case (2)**
Storage power rating in kW	120	563
Storage energy capacity in kWh	150	5630
Full-cycle per year	40	61

Table 4: Simulation results energy storage rating

It can be seen that for case (1) the power and energy rating of the storage is moderate, whereas for case (2) a much higher rating results. The number of full-cycles differs by around 33 %, hereby it must be taken into account that in case (2) the storages have nearly 38 times the capacity compared to case (1). This results in much higher energy losses in the storage operation. The full-cycles in general are moderate so that it can be concluded that the storage could be operated according to its lifetime or to its cycle time.

The delivered power and the energy stored in the storages are shown in Figure 12 for case (1) and in Figure 13 for case (2). For case (1), it can be concluded that the storage has less operation time compared to case (2). For case (2), the storage reaches its fully charged state several times during summer period.

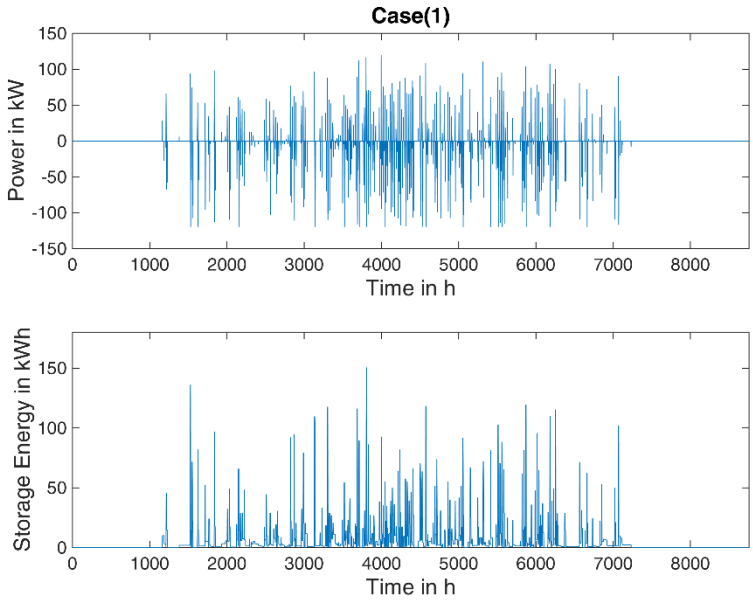

Figure 12: Storage energy and power for case (1)

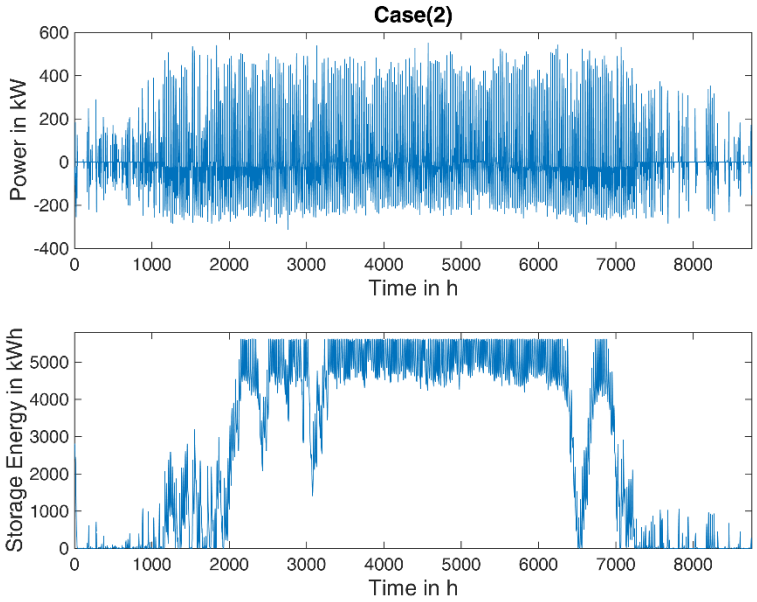

Figure 13: Storage energy and power for case (2)

5 Conclusion and Outlook

Battery storages are most suitable way to install energy storages all over the grid. These storage systems can be installed without any restrictions in the grid. They only refer to the grid power restrictions whereas other technologies are limited in scaling or depend on specific geographical conditions. Therefore, battery storages could be placed in a decentralized way like renewable energies (e.g. photovoltaic panels). In addition to their ability to store energy for consumption, battery storages are capable of delivering system services. This capability can offer additional operation and business strategies for energy storage systems and operation of grids.

Due to the limited number of life cycles of battery systems, a combination with flywheels to a hybrid system seems to be a suitable approach. Flywheels are most effective for fast response and primary reserve.

Battery storages can be placed easily within a building structure. As they are also DC-sources like photovoltaics and fuel cells, they offer a solution within a Smart Building where a DC-energy-supply may be used.

Other storage approaches might include electrical vehicles in a decentralized storage concept or extend the scenarios to the heat sector.

In order to have long-term storage capacities, the research on hydrogen and methane as energy storages systems will be indispensable.

Work Package 1.2: Decentralized Active Power Provision

Sebastian Beer[19] and H.-Jürgen Appelrath[20]

1 Goals and Integration in the Sub-Project

General goal of WP 1.2 was the development of an agent-based mechanism for the self-organized aggregation of decentralized energy units (producers, consumers, and storage) in order to provide active power products in electricity markets. Forming respective coalitions generally allows small-scale actors to directly participate in current wholesale markets and compensate stochastic effects which cause production or consumption values to deviate from contractually specified amounts at time of supply. In contrast to centralized pooling paradigms like virtual power plants, the aspired approach was intended to be temporally flexible and fully decentralized in the sense that agents autonomously act as representatives for their units in the market and form product-related coalitions in a self-organized fashion according to current economic and technological conditions.

Given this main goal, the research in WP 1.2 particularly aimed at the development of the following concepts:

- *A method for product portfolio generation* that allows agents to identify a set of aspired target products for which coalitions to form. The choice of products should be based on economic aspects like expected market prices as well as the operational capabilities of their supervised units.
- *A mechanism for neighbourhood formation* which allows agents to form (potentially expendable) neighbourhoods in order to initially restrict the number of cooperation partners and thus reduce communication and computational cost. The concept was generally intended to take grid-related aspects into account in order to provide for a future provision of topology-aware products.
- *A method for coalition formation* which allows agents to form coalitions within the built neighbourhoods in order to provide their initially identified target products. In particular, the approach should be applicable to a high number of participants and allow for a decentralized and temporally flexible formation by restricting the organizational binding of coalition members to the provision of the provided product only.
- *A mechanism for value distribution* which allows coalitions to distribute the payoff gained from a traded product among their members. The distribution method was particularly intended to be fair in in terms of game theoretical concepts.

With regard to its integration in the sub-project, WP 1.2 makes use of the search space model of WP 1.3 to represent the operation schedule space of an agent's unit. Moreover, the coalitions being formed as output of WP 1.2 represent the input of WP 1.5 which provides an approach for reactive scheduling in case unplanned events make units deviate from their contributions to specific target products. Finally, the mechanism of WP 1.2 conceptually integrates agent-related trust values which are part of the work of WP 1.6.

[19] OFFIS – Institute for Information Technology, 26121 Oldenburg, Germany
sebastian.beer@offis.de, R&D Division Energy
[20] OFFIS – Institute for Information Technology, 26121 Oldenburg, Germany
appelrath@offis.de, R&D Division Energy

2 Related Work

Theoretical and practical concepts for the formation of coalitions and the distribution of value have been studied in the domains of game theory and distributed artificial intelligence for years.

In game theory (more specifically in one of its branches termed cooperative game theory), the problem of coalition formation is formalized as a characteristic function game (or coalitional game) $G = \langle A, v \rangle$, where A is a set of agents and $v: 2^A \rightarrow R$ is referred to as the characteristic function of the game assigning a real-valued payoff $v(C)$ to a coalition C. Now, cooperative game theory provides different solution concepts for coalitional games addressing the two essential questions of which coalitions to form and how to divide the gained payoff among members. Well-known examples for solution concepts include the core, representing the set of all distributions guaranteeing stable coalitions (in the sense that no subset of agents has the incentive to leave because of a higher payoff), or the Shapley value, which allows a fair distribution by specifying the payoff based on the average marginal contribution an agent makes to a coalition [28].

Although appealing because of their mathematical justification, most game theoretical results are associated with several disadvantages when it comes to their practical application, particularly when considering IT-related, distributed systems. First, many concepts are associated with combinatorial calculations which become intractable when coping with a larger set of agents. Second, most solutions are not suitable to be calculated in a decentralized, parallel fashion, which contradicts the general paradigm of distributed systems.

Thus, in the course of the last years several approaches have been proposed in the field of distributed artificial intelligence which account for the requirement of practical applicability, often adjusting game theoretical concepts to reduce complexity. In this domain, the problem of coalition formation is often considered as a three phase process comprising the steps of (1) coalition structure generation, (2) solving the optimization problem under consideration, and (3) distributing the resulting payoff [29]. In particular the first problem, coalition structure generation (CSG), has gained much attention in the course of the last years. Based on the notion of characteristic function games, general goal of CSG is the partitioning of a set of agents into mutually disjoint coalitions such that global value is maximized. Being a NP-hard optimization problem, several methods have been proposed to reduce computational complexity which can be generally classified into dynamic programming (DP), anytime and heuristical algorithms [30]. General idea of DP approaches is to recursively divide the optimization problem into subtasks to avoid redundant computations. Prominent candidates offering respective capabilities were proposed by Rothkopf et al. [31] and Rahwan and Jennings [30]. While DP approaches generally offer the lowest worst case complexity with regard to an optimal solution, they do not provide anytime capabilities which is particularly disadvantageous when coping with larger sets of agents. According anytime algorithms generally start with a first solution which is guaranteed to be in a bound from optimum and steadily improve on it until the latter is found or another termination condition is met. Corresponding approaches were proposed by Sandholm et al. [29], Dang and Jennings [32], or Rahwan et al. [33]. In particular, Michalak et al. proposed an anytime algorithm for solving the CSG problem in a decentralized manner [34]. Finally, a number of heuristic methods have been proposed to reduce computational costs. For instance, Shehory and Kraus [35] put constraints on the size of coalitions to reduce computational complexity, while Sen and Dutta [36] apply an order-based genetic algorithm to search for (near-) optimal partitions. Heuristic approaches do not make any guarantees regarding the quality of their solutions but generally scale up well with the number of agents

3 Methodology

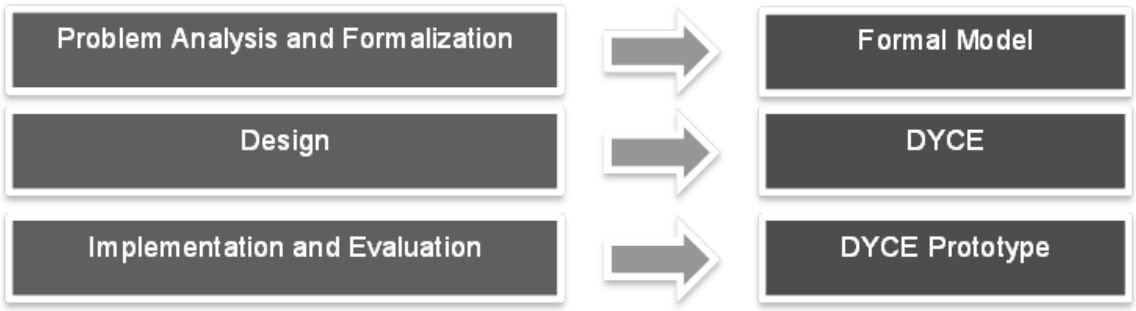

Figure 14: Methodology of WP 1.2

The methodology which was applied in WP 1.2 in order to achieve the aspired research goals is shown in Figure 14. As depicted, the work was split into three major steps which resulted in corresponding outputs as shown on the right. The different phases comprised the following tasks:

- *Problem Analysis and Formalization*: In a first step, a detailed problem analysis was conducted with regard to the considered problem of coalition formation for active power trading. This task particularly addressed the actual process of coalition formation itself as well as aspects of related fields like power grids or electricity markets. The analysis resulted in a detailed formal model comprising a concise specification of all concepts relevant for the considered context.
- *Design*: Based on the problem specification as defined by the formal model, the second step comprised the development of the actual agent-based approach for coalition formation, referred to as DYCE (DYnamic Coalition formation in Electricity markets). This particularly included the design of the four concepts as described in section 1 of this chapter which were conceived taking into account the output of other work packages. The developed processes formed the basis for the agent-based IT architecture of the final system.
- *Implementation and Evaluation*: In a last step, the architectural design of the second step was implemented in coordination with other work packages in order to create an integrated multiagent system. The resulting prototype was evaluated in a comprehensive simulation study harnessing concepts from the field of design of experiments (to be published in [40]). Moreover, the approach was applied to large-scale scenarios which were by participating institutions in an interdisciplinary effort in order to create a common basis for evaluation.

4 Main Results

The following section describes the main results which were developed in the context of WP 1.2. It starts by discussing the formal model which resulted from the problem analysis of the first work step. As already mentioned, this comprises formal definitions of all concepts relevant for the examined problem. Since coalition formation is a well-known topic in game theory and artificial intelligence, according definitions were adapted where appropriate. As shown on the right hand side of Figure 15, the specified concepts are generally categorized into four different domains covering respective aspects of the considered problem. All in all, the model consists of 40 definitions which result in the specification of an *electricity market* in the context of which coalition formation takes place. The market area is given by a *power grid* comprising a set of electrotechnical units which are supervised by autonomous intelligent agents. General goal of each agent is an economically optimized provision of active power, where participants are able to cooperate with each other and form *coalitions* for *value maximization* (domain 1). General purpose of each coalition is the provision of a power *product* which is supplied or demanded within a

temporal *product horizon* reflecting the time of fulfilment (domain 2). Through its participation, an agent makes a *contribution* to a coalition's *cumulative contribution* by providing an amount of electrical energy with an estimated error at a specified cost (domain 4). Each contribution is reflected by the *operation schedule* of its supervised unit, where the general time frame for planning (and thus coalition formation) is determined by a temporal *planning horizon* (domain 3).

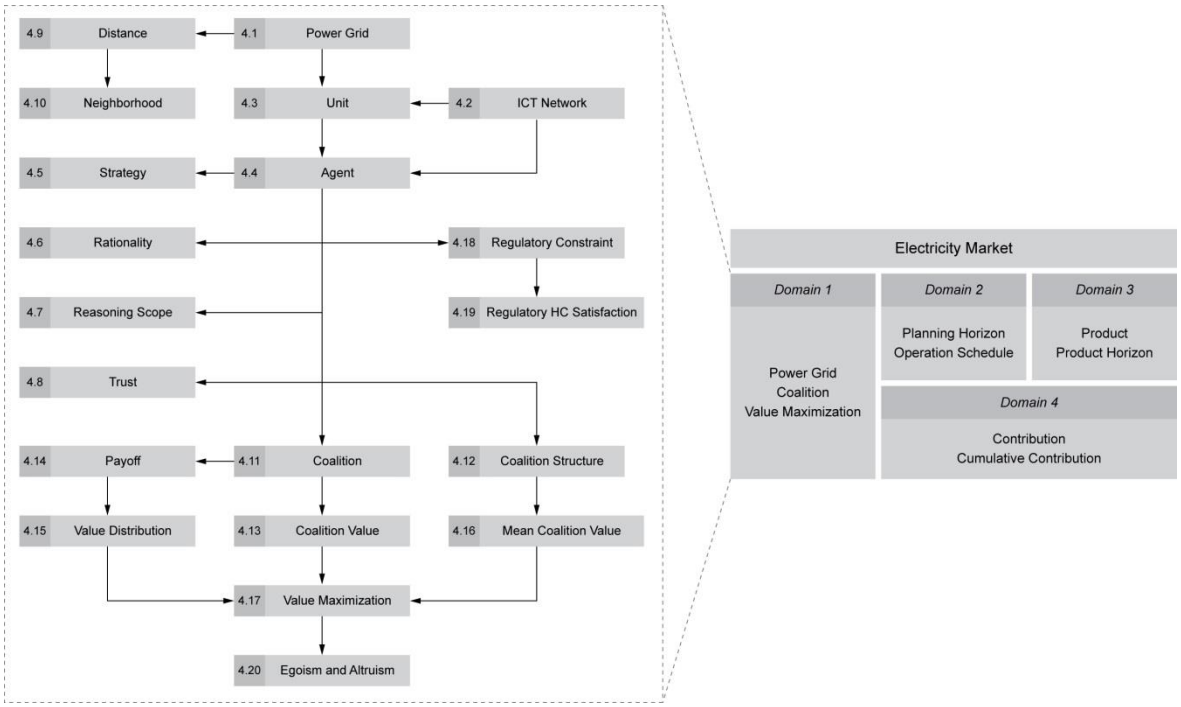

Figure 15: DYCE formal model

As shown on the left hand side of Figure 15, each domain comprises a set of concepts pertaining to the addressed topics. Each concept is specified by means of a concise formal definition (not shown) which put the different notions into context. A detailed description of all domains as well as the according formal specifications can be found in [41].

Based on the specified model, the actual mechanism for coalition formation in electricity markets was developed. As shown in Figure 16, the approach comprises four main activities which are carried out by each agent in the course of each planning cycle in order to finally supply or demand a product on the market. In the following, we provide an overview of each of these subprocesses. To facilitate discussion, we consider a use case in which producers form coalitions day-ahead in order to provide active power products at the spot market of the European Energy Exchange.

Product Portfolio Generation: In the course of the first activity, each agent creates an individual product portfolio PP comprising a set of target products which it is willing to trade on the market depending on a chosen operation schedule OS_U from the operation schedule space of its supervised unit U. The product portfolio is generally defined based on a catalogue of product templates which is provided by the market. For instance, the EPEX SPOT specifies a catalogue of 41 different single hour and block product templates (like baseload or peakload) which can be chosen by an agent for the specification of its target products. However, as the templates partly overlap with regard to their time of fulfilment and an agent can only participate in one coalition at each point in time, it has to choose a combination which is first temporally consistent and second provides most expected benefit given the operational capabilities of its unit. Depending on the size of the template

catalogue, this combinatorial problem may become highly complex and computationally intractable to solve. For instance, the set of 41 product templates of the EPEX SPOT results in a general search space of 2^{41} product combinations (including those candidates not satisfying the required constraint of temporal consistency). Thus, DYCE provides a respective heuristic for identifying both a product portfolio and an operation schedule which in conjunction maximize expected benefit. Given the determined portfolio, an agent executes the following three activities for each of the comprised target products.

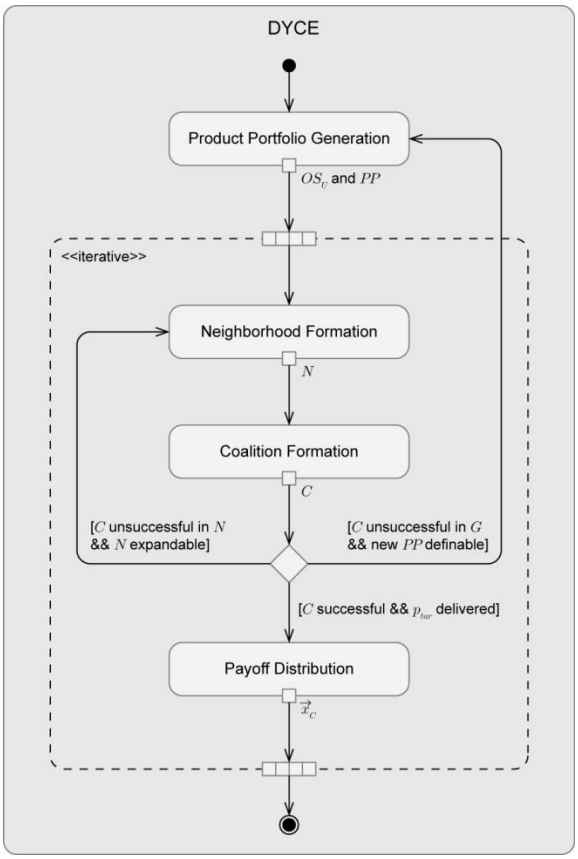

Figure 16: DYCE activity diagram

Neighbourhood Formation: As the total number of participants is typically very high, in the course of the second activity agents initially restrict the number of potential cooperation partners by forming neighbourhoods N of nearest neighbors based on a distance function which quantifies physical distance between units in the grid. Thus, neighbourhoods allow to reduce communication and calculation costs while taking grid-related aspects into account. Moreover, a respective approach generally allows for the provision of topology-aware power products within a specified grid area and procures system services like redispatch capacities for congestion management. However, neighbourhoods are not necessarily fixed because agents can iteratively expand their scope if coalition formation within the current one was unsuccessful.

Coalition Formation: As third activity, agents form coalitions C within their previously defined neighbourhoods in order to join forces and collectively fulfil common target products. The decentralized coordination process for coalition formation is based on the standardized Contract Net Protocol [37] as shown in Figure 17. Accordingly, agents can either take on the role of an initiator or a responder. While the former starts a formation process by sending requests to agents of its neighbourhood, the latter reacts to respective queries by sending appropriate replies. More

precisely, an initiator starts an iteration by initially determining the trust values of its potential cooperation partners. If these satisfy a defined threshold, it sends a call for proposal to the respective agents including its current coalition as payload. Each addressed responder then determines if the members of the initiator's coalition satisfy its own trust threshold and, if this is the case, checks for a utility maximizing regrouping of the initiator and responder coalition. If an according rearrangement is possible, it sends a respective proposal to the initiator. For each received reply, the latter first verifies the trust values of the new members and then checks for a utility maximizing regrouping taking all responder coalitions into account. Based on the result, it informs the responders about the acceptance or refusal of their proposals including the calculated coalitions as payload. If its proposal was accepted, a responder then starts the actual regrouping and notifies the initiator about the result. In case the restructuring was successful, the initiator conducts the required regrouping actions as well. Finally, if the formation process made the initiator fulfil its target product and the latter was successfully delivered, both agents update their trust values according the actual behaviours of the agents (for a more detailed description of trust-related issues see [37]. Contrary, if the initiator has not fulfilled its target product yet, it has different options depending on its former actions. First, it can execute the protocol again and start another try to extend its coalition within the current neighbourhood. Second, if the number of attempts has reached a maximum threshold but the neighbourhood is still expandable, it can widen the scope of the very same in order to increase the number of potential cooperation partners. Third, if the neighbourhood already covers the whole grid, the initiator can go back to the first activity and identify a new product portfolio along with an according operation schedule. However, if all of these options are not feasible, the agent terminates coalition formation for the given target product. For all other target products which were successfully traded and delivered, it executes the last step of value distribution.

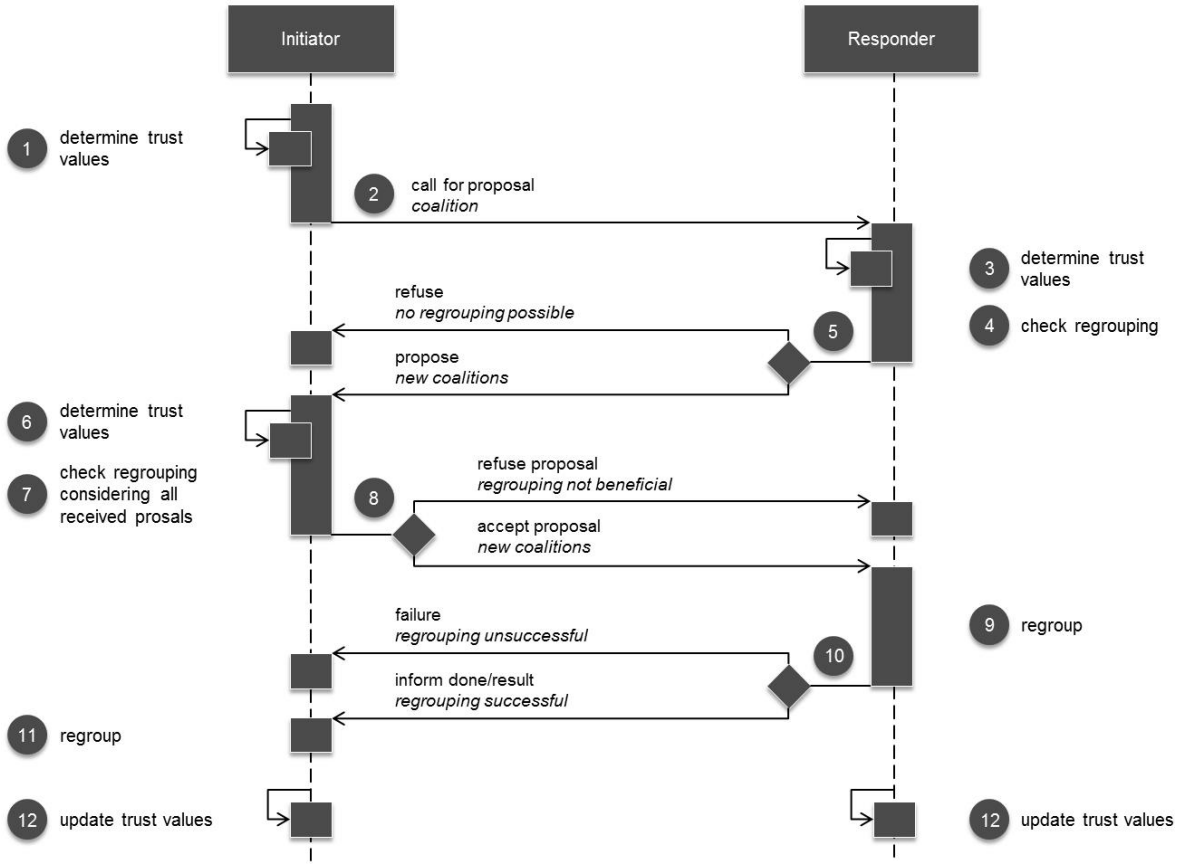

Figure 17: Communication protocol for coalition formation

Value distribution: After the transaction of a delivered product is completed, agents distribute the value gained from cooperation among each other. The approach developed for this purpose is based on a game theoretical model which allows an (at least approximately) fair distribution of the payoff using the Shapley value as solution concept. The latter generally determines the individual shares according the average marginal contributions the agents make to a delivered product. More precisely, the developed approach considers the contributions which an agent makes to the different attributes of the target product. The latter are given by the target electricity amount to be delivered, the target cost at which the energy is provided, as well as the target error by which the delivered energy approximately deviates from the contractually specified amount. Given these, the approach uses concepts from cooperative game theory and defines a k-majority game which puts the contributions of the members to the different attributes into context. Based on the specified game, the Shapley value of each agent can be calculated reflecting its average marginal distribution to the target product and thus a fair distribution according the defined fairness axioms (see [28] for a more detailed description of the Shapley value). Although respective calculations are computationally intractable for high numbers of players, the specific model allows for the application of an approximation method being efficient even for large coalition sizes [39].

5 Conclusion and Outlook

The research in WP 1.2 yielded a comprehensive approach for the self-organized formation of coalitions in electricity markets. In particular, the developed mechanism provides concepts for the identification of utility maximizing product portfolios, the formation of topology-aware neighbourhoods, the decentralized formation of coalitions, and a fair distribution of the final payoff. The approach was evaluated in a comprehensive DOE study investigating its algorithmic characteristics and applied to scenarios which were developed in an interdisciplinary effort by

participating institutions of Smart Nord. With regard future work, the following topics may be further examined:

- *Overlapping coalitions:* DYCE currently restricts agents to join only one coalition at each point in time. Future work may examine the case of overlapping coalitions in which members can make contributions to several coalitions concurrently.
- *Alternative mechanisms for value distribution*: As described in the previous section, DYCE uses the Shapley value in order to allow a fair distribution of a coalition's gain. Future work may investigate alternative game theoretical solution concepts like the core which provides for a stable division of the obtained payoff.
- *Unreliable communication:* The DYCE mechanism does currently not provide concepts for the management of unreliable communication. For instance, in the course of coalition formation messages may arrive out of order or even get lost. Respective communication errors have to be appropriately handled in order to guarantee reliable system performance.
- *Integration of business processes:* The provision of power products is generally associated with according business processes like the metering of the produced electricity or the execution of the respective financial transactions. Corresponding activities are currently not part of DYCE and may be integrated in order to allow for an automation of the according tasks.

Work Package 1.3: Optimization of Cluster Schedules

Jörg Bremer[21], Astrid Nieße[22] and Michael Sonnenschein[21]

1 Goals and Integration in the Sub-Project

A crucial question regarding all smart grid related optimization algorithms is how to achieve feasible solutions if different individually configured and operated energy resources are involved. As we regard scenarios where distributed devices are independently operated by different operators, all devices are individually configured with a not publicly known setup. Dynamically, such devices are clustered into different groups of co-operating units.

This dynamics will inevitably lead to a necessary co-operation of unacquainted energy units. Without central control (with a central, static model) individual search spaces of different units – representing the individual capabilities within a group – have to be integrated to a model for the optimization problem at runtime and thus be automatically derived. Each individually operated unit has its own set of different schedules to offer for a scheduling algorithm. This flexibility depends on the current, individual configuration of the unit, several (technical) constraints for operation, current operational state, and, if applicable, on state and requirements of coupled units – e.g. on the thermal demand of a house in case of a co-generation plant.

Modelling the optimization problem that determines an optimal (with regard to target load profile resemblance, cost-efficient and eco-friendly operation, preservation of reserve flexibility for control tasks, asf.) operation schedule for each member of the group such that the group as a whole achieves the given targets cannot be attained a priori as a static model. Due to the dynamic nature of the problem and permanent re-organization, the model of the current optimization problem (one for each group) has to be derived automatically right after forming a new group of electrical units. Individual flexibilities and constraints of these units have to be integrated on the fly.

The aim of this work package is to find an appropriate method to provide scheduling algorithms with a means for exploring the search space of arbitrary devices without any domain specific knowledge (in the sense of device operation, constraints or cost models). The method should work independently of any specific schedule setting for timely resolution, duration and integrate current operational setting of the device.

The main target of this work package is support for scheduling algorithms. Nevertheless, the integration into sub-project one is defined by several interactions between work packages. Work package 1.2 needs a means for generating a product portfolio that consist of feasible schedules which must be generated without knowing the specific unit modelling. Schedules in the portfolio need cost indictors for evaluating suitability of the schedules for use during coalition formation. Work package 1.4 is responsible for continuous re-scheduling which directly involves the flexibility model from this work package for ensuring feasibility during scheduling and therefor took over the integration of distributed optimization into the concept of DVPP (see Overview of the Sub-Project section 3). Work package 1.1 delivers unit models for batteries that are used here.

[21] University of Oldenburg, 26111 Oldenburg, Germany,
{forename.surname}@informatik.uni-oldenburg.de, Department of Computing Science,
[22] OFFIS – Institute for Information Technology, 26121 Oldenburg, Germany
astrid.niesse@offis.de, R&D Division Energy

2 Related Work

Effectively solving real world optimization problems often suffers from the presence of constraints that have to be obeyed when looking for feasible solutions. This holds especially true for problems from the smart grid domain where each electricity unit has its own individually configured and constrained search space of alternatively operable schedules [42], [43], [44]. Several techniques for handling constraints during optimization have already been developed; mostly for general purpose. Nevertheless, almost all are concerned with special cases of NLP or require a priori knowledge on the problem structure in order to be properly adapted [45]. Some prominent representatives of such techniques are: the introduction of a penalty into the objective function that devalues a solution that violates some constraint, the introduction of a repair mechanism for infeasible solution [46], or treating constraints as separate objectives. A good overview on constraints-handling techniques can for instance be found in [47] or, more recently, in [48].

In order to give an algorithm hints on how to construct a solution, so called decoders may impose a relationship between feasibility and a special representation: the decoder solution. For example, [48] proposed a homomorphous mapping between an n-dimensional hyper cube and the feasible region in order to transform the problem into a topological equivalent one that is easier to handle. Earlier approaches used Riemann mapping [50] or Schwarz-Christoffel mapping [51]. Such space mapping techniques are usually used in engineering with the objective to substitute computationally expensive models with a coarser grained surrogate model [52], [53].

Another use case that exploits a space mapping approach by deriving a decoder for constrained search spaces from a support vector based surrogate model has been presented in [54], [55]. With this approach the authors propose a two-step process: First, they have a support vector model of the feasible region learned, i.e. a classifier that distinguishes between operable and not operable schedules. In this work, this model is further extended. A decoder function is derived, that is able to map an arbitrary solution candidate to an as far as possible similar but feasible solution. In this way, they get a means that guides a search algorithm where to look for feasible solutions and the constrained problem is transferred into an unconstrained one that is much easier to solve.

3 Methodology

Each unit has an individual flexibility, i.e. a set of alternative possibilities for operation. As we consider day-ahead planning within this work package, we are interested in the set of alternative schedules that are all operable for a unit for the following day.

In order to design a device independent standardized model for representing this flexibility and all restricting constraints in a way that arbitrary planning algorithms may integrate the models on the fly to a problem specific optimization model, different sub-problems had to be solved. This includes at a first stage the abstraction from device specific models by representing the individual flexibilities with the help of sets of feasible schedules. Such a set of schedules must be generated with the help of a device specific simulation model. This is the only stage where expert knowledge is necessary for adapting a simulation model to a specific instantiation of a device and to the specific embedding into the devices' operational environment. Though, this task might become at least a semi-automatic task by follow-up work.

From these sets of feasible schedules that already represent as a stencil for the feasible region the individual flexibilities and indirectly incorporate individual constraints, a formal representation has to be derived, that can be used by different planning algorithms in a standardized manner. First we derive a machine learning model from a training set consisting of feasible schedules that automatically learns a model for the hidden functional relationship that determines feasibility

within a training set. Such a model is already capable of telling feasible and infeasible schedules apart without having to know anything about the original device, restricting operational constraints or any device specific modelling of operation. But, for efficient optimization, a means for systematically generating feasible solutions is needed. In many criteria scenarios, such a means should also be capable of generating good solutions with respect to different objectives. Again, this should be possible without giving the planning algorithm any direct and specific model for individual cost calculation for these different objectives.

To achieve this, we refined the concept of a so called decoder [49] that is capable of systematically generating feasible solutions from an unconstrained solution representation. Such a decoder can easily be integrated into most common optimization approaches.

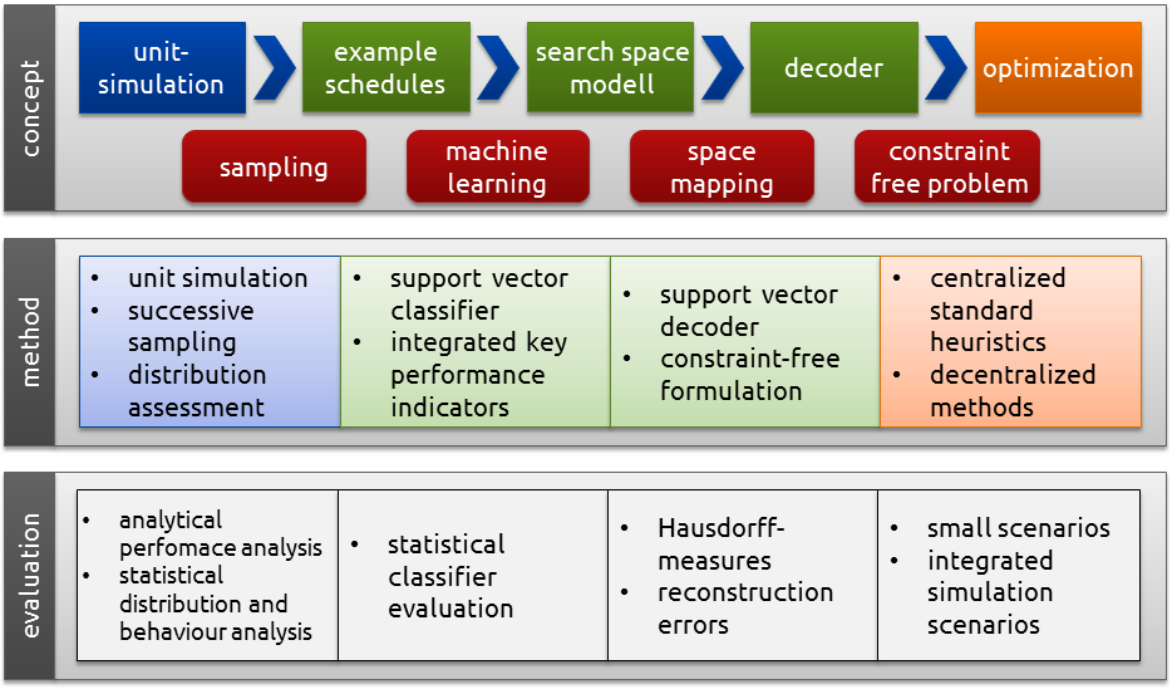

Figure 18: Procedure model and evaluation concept of WP 1.3

Due to a lack of available real power units, all concepts and implementations of this work package have been evaluated and tested by simulation studies. A design science approach had been chosen as a research concept for designing and developing the artifacts that constitute the optimization approach of this work package. In this way, well-defined sub problems may be scrutinized and solved separately [56] in order to minimize the risk of a complete failure. Artifacts represent structured entities, such as software prototypes, mathematical models or logical constructs. These artifacts were subject to rigorous evaluation both by analytical methods and by function tests. Results can for example be found in [57], [58], [59].

Additionally, the process model for Smart Grid algorithm engineering [60] proposes a strong integration of domain knowledge during conception stage, which was brought in from the Smart Nord project community.

4 Main Results

The main result of this work package consists of the conceptual and formal description of a process chain for flexibility modelling (c.f. Figure 18, constrained handling, and optimization as well as the prototypical implementation artifacts of all modules.

The main outcome of this work package is the decoder that finally enables the integration of arbitrary energy devices' flexibilities into optimization algorithms without a need for implementation of or adaption to device specific modelling, constraint description or objective specific evaluation. To gain this result, several prerequisites had to be solved. Thus, this section lists the results of the sub-tasks that finally led to the decoder construction.

4.1 Flexibility Model

Each energy resource foremost has to serve the purpose it has been built for. But, often such a task may be achieved in different alternative ways. For example, it is the main purpose of a co-generation plant to deliver enough heat for a varying heat demand in a house at every moment in time. Nevertheless, heat usage is usually decoupled from heat production by using a thermal buffer store. Thus, different production profiles may be used for generating the heat. In turn, this leads to different respective electric load profiles that may be offered as alternatives to a scheduling controller.

Each individual energy unit offers a set of operable schedules for a given (future) time horizon. We regard a schedule not as a time series but as a vector $x \in \mathbb{R}^d$, with the number of periods d (typically 96 for day-ahead planning) and the i-th element denoting the respective amount of electric energy produced or consumed in this period or – equivalently – the mean active power output or input during this period. With operable, we denote a schedule that might be operated without violating any technical constraint. Constraints restrict the vector space that contains the set of feasible (operable by a specific device) schedules. These constraints can be interpreted geometrically. Without any constraint, the whole hypercube $[0,1]^d$ (active power between 0 and 100 %) would be a model for the region of feasible schedules. With every constraint, different parts (regions) of the hypercube fall off the feasible region, because the respective schedules are not operable due to the constraint. Only the finally remaining region (hypercube minus superposition of all regions prohibited by constraints) is the feasible region of the DER. Only from this region, schedules might be taken during optimization. Please refer to [44] for an in-depth discussion with evaluation results.

It has been shown in [51] that the feasible region of operable schedules is not necessarily a convex polytope or a single and connected region. For this reason, concavity and clusters have to be taken into account, too. These considerations led to black-box models based on machine learning approaches that capture the topological traits of the feasible region as a compact description. Support vector data description [61] has shown good performance for this use case. Given a set of schedules, the inherent structure of the region where they reside in is derived as follows: After mapping the data to a high dimensional feature space, the smallest sphere is determined that encloses all images of the schedules. When mapping back the sphere to schedule space, its pre-image forms a contour (not necessarily connected) enclosing the sample. A detailed explanation of the mathematical background and the model can for example be found in [62], [63]. In the following, the approach is briefly summarized.

The feasible region that forms a sub-space inside the vector space of all schedules and that only contains the operable schedules is described by a decision function. This decision function distinguishes the feasibility of a given schedule by comparison with a schedule from the boundary

of the feasible region. As usual in support vector methods [64] the learning algorithm selects a subset from the training set that represents the rest of data best. This support vector subset can be used in conjunction with a derived decision function for classification of arbitrary other schedules. The feasible region is represented as some high dimensional ball. All support vectors lie on the boundary of the feasible region, thus there images in the high dimensional space of the ball lie on the surface of the ball. Thus the distance of the image of a given schedule to the centre of the ball can be compared with the distance of a support vector. A larger distance indicates that the image of the questionable schedule lies outside the ball and thus the schedule lies outside the feasible region and thus it is not operable by the device.

In this way, the feasible region of the search space of an arbitrary energy unit, i.e. the flexibility or the set of alternative operable schedules, is represented as the pre-image of a high-dimensional ball.

Only the comparably small set of support vectors together with a vector of non-zero values for weighing the support vectors is needed for modelling the flexibility of a device. The model might be used as a black-box that abstracts from any explicitly given form of constraints and allows for an easy and efficient decision on whether a given solution is feasible or not. Moreover, as the distance (decision) function maps to $\mathbb{R}$ and hence allows for comparing two solutions with regard to their feasibility.

4.2 Sampling

A prerequisite for learning the model is the availability of a training set consisting of feasible schedules. This training set serves as a stencil for the feasible region of a specific energy unit operated starting from a given specific initial situation. For building up such a training set, a new sampling method has been developed.

In general, the domain of an indicator function that map schedules to {true, false} depending on the operability of a schedule with respect to a given device and a given start configuration has to be sampled so as to get a set consisting merely of feasible schedules. To achieve this, sets of schedules have to be tested against a simulation model that may decide on whether the given schedule would be operable by the device or not. Unfortunately, standard sampling methods hardly work for schedules with higher dimensionality due to the very fast shrinking likelihood to randomly guess a schedule that is actually operable. In order to avoid intractability, a successive sampling method has been developed that builds a training-set and at the same time forces the simulation model only to implement a minimal interface. The method constructs feasible schedules step by step instead of trying to guess complete schedules at a time. A detailed description of the new methods and its time saving features can for example be found in [59].

4.3 Decoder

As the core concept for integrating the flexibility model with arbitrary optimization methods, a decoder has been developed. Basically, a decoder is a constraint handling technique that gives an algorithm hints on where to look for feasible solutions. It imposes a relationship between a decoder solution and a feasible solution and gives instructions on how to construct a feasible solution [47]. For example, [49] proposed a homomorphous mapping between an n-dimensional hyper cube and the feasible region in order to transform the problem into one that is easier to handle.

The solution here derives a mapping function from the support vector flexibility model that is capable of mapping an arbitrary given (not necessarily feasible) schedule to a respective one that lies inside the feasible region and is therefore operable by the respective device.

The black-box support vector model represents the flexibility of a unit as pre-image of a high-dimensional ball. This representation has some advantageous properties. Although the pre-image

might be some arbitrary shaped non-continuous blob in $\mathbb{R}^d$ (left side of Figure 19), the high-dimensional representation is still a ball and thus geometrically easier to handle (right side of Figure 19). The relation is as follows: If a schedule is feasible, i.e. can be operated by the unit without violating any technical constraint, it lies inside the feasible region (grey area on the left side in Figure 19). Thus, the schedule is inside the pre-image (that represents the feasible region) of the ball and thus its image in the high-dimensional representation lies inside the ball. An infeasible schedule lies outside the feasible region and thus its image lies outside the ball. But we know some relations: the centre of the ball, the distance of the image from the centre and the radius of the ball. Hence, we can move the image of an infeasible schedule along the difference vector towards the centre until it touches the ball. Finally, we calculate the pre-image of the moved image and get a schedule at the boundary of the feasible region: a repaired schedule that is now feasible. We do not need a mathematical description of the feasible region or of the constraints to do this.

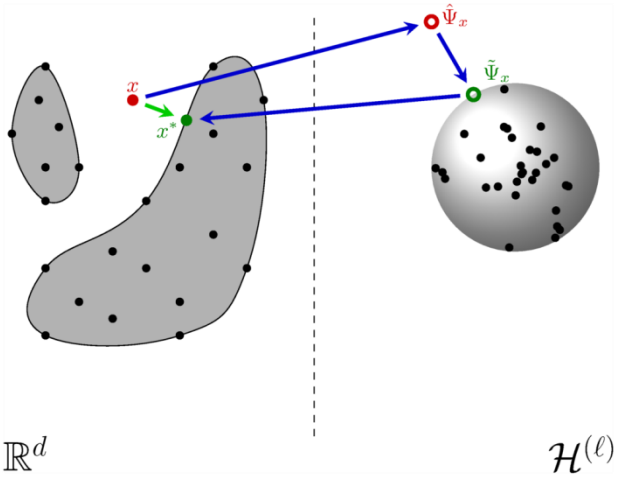

Figure 19: General scheme for the proposed decoder scheme

4.4 Optimization

Integration into optimization has been evaluated with different optimization approaches. Among them are centralized approaches as well as distributed approaches.

The integration works in two successive stages: a decoder training phase and the actual planning phase. During the training phase a decoder is calculated for each unit. These calculations can be done fully parallel. During the succeeding planning phase, these decoders are used by an optimization algorithm. The aim of the optimization is to find a schedule for each unit in a cluster such that the sum of all schedules in the cluster resembles a wanted target schedule. For optimization, the search is defined on the whole set of all schedule. In this way, no precaution has to be taken to deal with any (apart from the box constraint of always being between 0 and 100 % of maximum power) technical constraints of the units. The optimization algorithm does not need to know which schedules are operable and which are not while navigating through search space.

In each iteration, new candidate solutions are generated. Formally in our active power planning use case, this candidate is a feature vector from search space comprising *d* values of mean active power (one for each time slot) and some predefined describing indicator values. Such indicators characterize the load schedule with respect to different optimization objectives. As a candidate solution is taken from the unconstrained vector space of all possible solutions regardless of the set of constraints that prohibits the operation of certain schedules, infeasible solutions are naturally also taken. In order to repair such infeasible solutions, the decoder is harnessed for repairing

infeasible solutions prior to evaluation. The decoder then constructs a new vector with the following properties:

1) The first *d* elements are values of active power that constitute a power schedule ($p'_1,\ldots,p'_d$) that is operable by the respective unit for the given time frame.
2) The schedule has been constructed such that the distance $\delta(p\text{-}p')$ is small.
3) The next *l* elements are indicator values that correctly describe the constructed (not the original) schedule's performance in achieving additional objectives. The relationship had been learned with the SVDD, too.

Now, the feasible candidate solution *p'* can be evaluated for comparison with other solutions to pick the best. In a many objective problem, evaluation is done with respect to the global objective of minimizing the distance to the target schedule and with the help of each indicator that describes the schedule with respect to further objectives.

Many types of optimization algorithms are suitable. For scalability reasons, heuristics (evolutionary algorithms like simulated annealing, population based approaches or genetic algorithms) or distributed approaches are most promising.

As a first attempt, model and decoder have been tested with centralized optimization methods. For this approach there are mainly two reasons: easier (and leaner) implementations and better control during tests and the chance to use approved, standard optimization methods from widely accepted libraries. The tested centralized approaches can be categorized into population based heuristics and other evolutionary approaches. An example is given by the use of Parallel Tempering in [65].

The integration into distributed optimization was done in a two-step approach. First, a new greedy approach has been developed especially suitable for the decoder [54]. Implementation for the DVPP approach was done by adapting the distributed, approved optimization approach COHDA [66] (constrained optimization heuristics for distributed agents), which had beforehand already been successfully integrated with the decoder approach for constraint handling [66]. The integration with COHDA in Smart Nord was done by work package 1.4 and is in greater detail described there. Many-objective optimization was integrated in the COHDA approach, but had also been tested with centralized approaches [65].

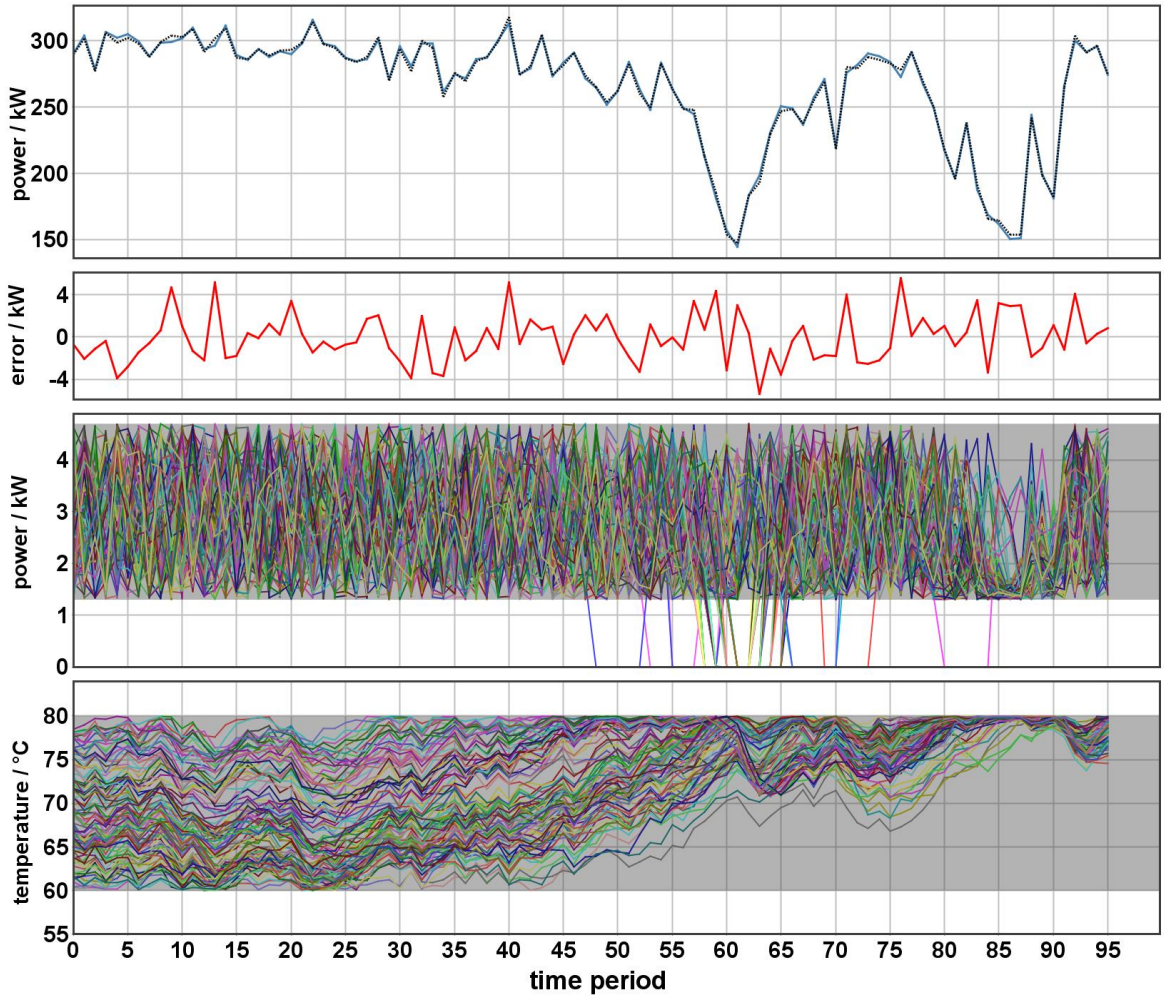

Figure 20: Example result for a cluster with 100 co-generation plants

Figure 20 shows an example result for a cluster with 100 co-generation plants that jointly want to achieve a given target schedule for a whole day. The graph on the top shows the target schedule together with the optimization result: the cluster schedule that resembles the product. The residual error is displayed beneath. The two lower graphs show the more important aspect: the compliance of the result with different constraints. The grey bands show the allowed ranges for active power of the modulating plants and of the temperatures of attached thermal buffer stores respectively. The individual schedules stay within the allowed range during optimization. An additional constraint for a minimum down-time of one hour after shut-down is also obeyed. Thus, the set of decoders for this individual optimization problem instance generated a valid result without knowing anything about specific modelling or constraints.

5 Conclusion and Outlook

In this work package, we presented a new approach for constraint handling especially for applications in smart grid load planning scenarios where devices with private or otherwise not publicly known modelling have to be integrated on the fly into common optimization models even without explicitly know models of the units, their technical or economical setting, constraints, or any specific relation to different optimization objectives.

The process chain that produces the decoder that is capable of systematically producing feasible solutions in the device’s place during optimization or planning has been presented with focus on the different stages: starting with abstracting from the device simulation model by generating a

surrogate from example schedules (as a general an device independent representation of the feasibility) and ending with an automated process of deriving the decoder that generates operable schedules together with assigned performance indicators (describing the result with respect to a configurable set of objectives for many objective planning).

Integration into many optimization algorithms has been successfully tested. With the help of the decoder approach any algorithm gained the capability of producing valid solutions without any explicit model of the energy units that are to be orchestrated. The presented approach is already applicable for generating decoders for the representation of individual devices. An extension to the representation of a group of devices by a single decoder (e.g. in cases where the set of devices of a larger organization such as a manufactory is represented by a single agent) still demands some further development. Especially the distribution of feasible schedules will need some additional attention in order to adapt the sampling properly to the folding of individual schedule distributions when representing combined flexibilities.

For future integrated optimization of active and reactive power some further improvements regarding the representation of the schedules are possible. This could for example be achieved by using complex valued support vector machines instead of real valued.

Work Package 1.4: Continuous Scheduling

Astrid Nieße[23], Jörg Bremer[24] and Michael Sonnenschein[24]

1 Goals and Integration in the Sub-Project

It is the core idea of the dynamic virtual power plant (DVPP) to identify an optimal (with respect to several given objectives) schedule for each device within a group of energy units such that the accumulated schedules of all units resemble a market given active power schedule (a product) as close as possible. If each unit can actually operate the assigned schedule during the whole product delivery phase, the cluster delivers the product as committed on market. But, in reality usually unforeseen events often inhibit a direct implementation of the initial plan. A co-generation plant might shut down earlier due to unexpected low thermal demand, a device might go offline due to a malfunction, or some forecasts for weather conditions might have changed. In any case, a deviation of the actual operation from the initial plan has to be detected and actions have to be taken to steer the rest of the group in a way that it stays on track during product fulfilment. All unit agents have to follow the same task in the last phase, from unit schedule configuration until the product delivery is finished: They have to ensure the delivery of the DVPP active power product. Therefore, the unit agents continuously (e.g. on a minute base) check the unit's operational state and check it for schedule compliance. If a unit is not following the desired schedule and if the overall DVPP active power contribution will not fulfil the defined product, as a consequence a rescheduling is performed within the DVPP agents.

This leads to a need for continuous monitoring of the energy production (or equivalently consumption) by the energy units themselves. A rescheduling is needed in those cases, where the summed deviations of the DVPP's energy units hinder product fulfilment. If product fulfilment cannot be guaranteed anymore, rescheduling is triggered. In such cases, a new optimization run for the deviating cluster has to be conducted for the remaining time frame and with changed situation as the new initial state. The optimization function for continuous rescheduling therefore has to be formulated as time-dependent optimization function, where these factors are convexly combined and given hard constraints like product fulfilment and other criteria (e.g. power grid related criteria or cost functions) are taken as side conditions.

As the general methodology used for optimization in this work package is strongly related to the optimization approaches from WP 1.3, both work packages are linked in terms of abstraction from the real energy unit by using the same meta model for representation of the feasible region of an energy unit's operable schedules for dynamically building up the model for optimization within a newly formed cluster. The optimization problem scrutinized in this work package is an extended version of the one from WP 1.3. Thus, the solution for optimization developed in this work package is also used for the initial internal optimization of a DVPP. The set of coalitions from WP 1.2 gives the set of DVPPs that continuously have to control their own product delivery and that are hence the subject of optimization in this work package. Additionally, dependencies of units that are members in more than just one coalition (in consecutive products) have to be solved within this work package.

[23] OFFIS – Institute for Information Technology, 26121 Oldenburg, Germany
astrid.niesse@offis.de, R&D Division Energy
[24]University of Oldenburg, 26111 Oldenburg, Germany,
{forename.surname}@informatik.uni-oldenburg.de, Department of Computing Science

2 Related Work

An overview on related work regarding dynamic aggregation of energy units in the distribution grid is given by [67]. Several approaches for distributed scheduling algorithms with applications to large scale problems in the energy domain have been scrutinized in this work package. Among them are algorithms for autonomous virtual power plants [68], stigmergy based multi agent planning systems [69], adjusting algorithms [70], and holon-organized clusters of energy units [71]. Important for the DVPP approach is a support for decentralized evaluation as all concepts of the approach have to be decentralized due to a lack of a common memory or a designated leader within the DVPP. Moreover, support for the integration of private constraints is mandatory. Integration of continuous re-scheduling can be integrated into most approaches. Stigspace [69] supports private constraints and decentralized evaluation but fails to handle complete schedules as it is just appropriate for one single planning period. Thus, the approach COHDA [72] looks most promising for adaption to the use case of continuous rescheduling in a DVPP.

Moreover, to cope with possible voltage range deviations the grid topology should be an optional parameter in the aggregation process and within the operation of DVPPs. In contrast to the transmission grid, where a continuous measurement allows for detecting violations of operational constraints, no such infrastructure is available in the distribution grid. Due to the large amount of units in the distribution grid, the identification of the most efficient unit to avoid a critical grid state cannot be deduced manually. Additionally, the underlying optimization problem of identifying the most efficient mitigation actions is challenging due to the non-linearity and non-differentiability of the underlying power flow equations as shown by [73]. Therefore, state-of-the-art control systems on the transmission level cannot be transferred directly to the lower voltage levels due to a lack of real-time information and the large complexity of the re-dispatch problem. Recently, a lot of work has been done to overcome these problems like e.g. the work done in [74]. In this work package, a simplified graph based approach has been developed for this purpose.

3 Methodology

The strength of the used distributed optimization approach COHDA [72] is its ability to advance the improvement in achieving the overall objectives during optimization solely based on local decisions. An agent takes these decisions based on believes about other the agents' actions derived from received messages. In this way, any agent decides on its own actions such that the global goal of resembling the target schedule defined by the energy product is put forward best while at the same time each agent is acting to its own interest. More precisely, the behaviour of an agent comprises three stages:

1) **Perceive** – Incoming data from other agents are imported into the local working memory.
2) **Decide** – If new data has been received in the "perceive" stage, the agent now decides upon adapting its current schedule selection regarding better alternatives with respect to the updated knowledge. Here, both global constraints (e.g. the costs of a schedule selection in the global context) as well as local constraints (e.g. preferences of the unit regarding individual schedules) are taken into account.
3) **Act** – Again, if new data has been received in the "perceive" stage, the agent now forwards the new data to its neighbouring agents (including the possibly adapted schedule selection from the "decide" stage).

The process terminates autonomously, when no agent is able to adapt its schedule in the "decide" stage any more, thus producing no new data. More details on COHDA can be found in [72]. In its

existing form, however, the COHDA approach lacks some essential features for the continuous scheduling in DVPPs. Thus the following extensions had to be developed:

Product dependency – In the DVPP concept, an agent can participate in multiple consecutive products within the planning horizon. Each product corresponds to an individual DVPP composition. Hence, the data model of COHDA was extended to reflect the affiliation of data to specific DVPPs. Moreover, schedule adaptations of an agent during a rescheduling process within a DVPP may in principle endanger product fulfilment of subsequent DVPPs the agent is a member of, because the subsequent state trajectory of the energy unit (and thus the remaining flexibility) is modified by a schedule change. To compensate for this effect, all commitments of an agent have to be taken into account while selecting schedules during a rescheduling, such that subsequent DVPPs are not affected.

Secondary objectives – Integration of secondary objectives into the schedule selection and evaluation process during optimization has to be tackled on two different levels. First, on the global level, the evaluation of selected schedules has to be done for different optimization objectives. This is achieved by building the evaluation function as a convex combination of all criteria. In this work, exemplarily two objectives have been chosen: product quality and cost. With this criteria, it has been shown that product fulfilment can be achieved at lower cost if integrated into the evaluation function. Second, local objectives are modelled along the approach from work package 1.3. This includes local hard constraints (i.e. feasibility of schedules, see section 1) as well as local soft constraints such as profit limits or costs. Those are integrated directly into the search space model, cf. Figure 21:

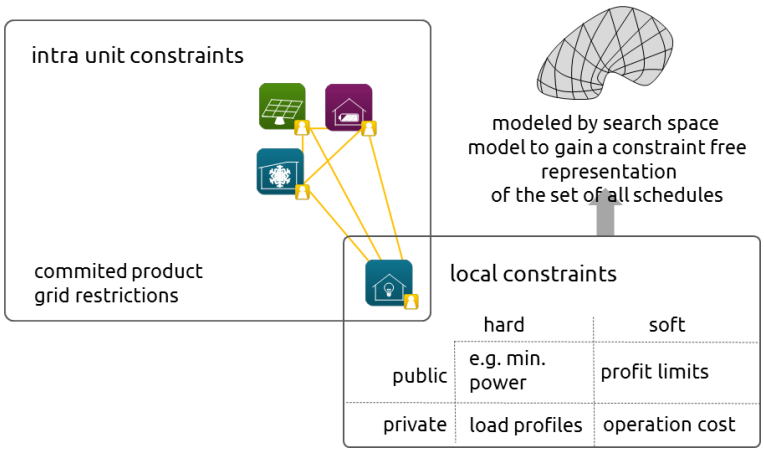

Figure 21: Concept for modelling unit constraints in re-scheduling

Without private preferences for schedule selection, the decoder would generate merely valid schedules for improving the optimization result regarding quality of product delivery and global soft constraints. Integrating private preferences into the process of building the search space model enables for automatically generating valid schedules with annotated indicators for local preferences and for automated exclusion of undesired schedules. A detailed explanation of this procedure can for example be found in [75].

Continuous scheduling – The COHDA approach is designed for solving distributed combinatorial optimization problems. Regarding the continuous scheduling in the DVPP context, the capabilities of the agents had to be extended significantly. In particular, agents have to monitor their associated energy units in order to detect incidents during product delivery, and take measures to compensate unwanted effects. Moreover, with the possibility of agents being part of more than just one

coalition, the treatment of incidents becomes a complex task that has possibly to be carried out by several DVPPs. Therefore it has to be ensured that the distributed scheduling approach still converges to valid and sufficient solutions under these circumstances.

4 Main Results

The main artifact developed in this work package is *DynaSCOPE – Dynamic Scheduling Constraint Optimization for Energy Units*. The approach is capable of detecting events that cause a demand for reactive scheduling in DVPPs (self-diagnosis) as well as performing the rescheduling of units within DVPPs (self-healing). As the approach thus realizes both an agent-based planning and control system, a hybrid agent architecture derived from the InterRRaP architecture [76] is employed. The resulting architecture organizes the behaviour and the knowledge of an agent in successive layers, which directly resemble the tasks an agent performs in the approach (cf. Figure 22).

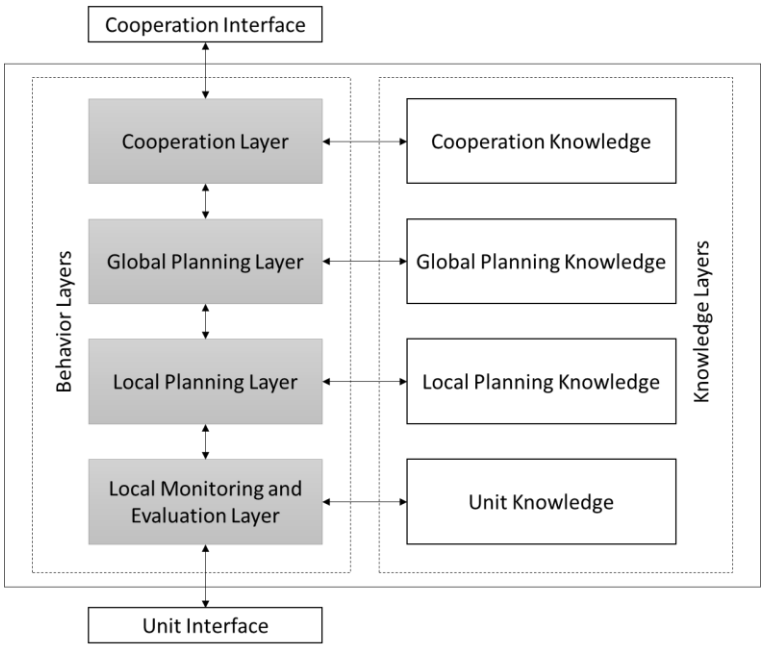

Figure 22: Hybrid agent model of DynaSCOPE

Focusing on the treatment of incidents, the architecture is described from bottom to top as follows:

Local monitoring and evaluation – This layer realizes the interaction with the energy unit under control. In particular, this comprises the configuration of the unit (e.g. setting a schedule) and the detection of incidents, possibly causing a rescheduling.

Local planning – This layer covers the schedule selection task with respect to the energy unit under control only. More precisely, the search space of feasible schedules is searched whenever needed. For instance, such a situation occurs when an incident has been detected at the monitoring layer that invalidates the currently configured schedule. The agent now tries to find an alternative schedule that compensates the incident on the one hand, thus maintaining product fulfilment, and satisfies unit-specific soft constraints on the other hand. If such a schedule cannot be found, a local compensation of the incident is not possible. The detected incident is then escalated to the global planning layer for further treatment in the agent system.

Global planning – This layer contains the algorithmic components for the conjoint scheduling within a DVPP. Primarily, this comprises logic concerning the selection, processing and integration of data exchanged with other agents.

Cooperation – This layer finally handles aspects regarding interaction with the agent system, such as maintaining communication channels to other agents, dispatching outgoing messages or the preprocessing of incoming messages.

With this bottom-up approach regarding the treatment of incidents, an agent primarily is responsible for keeping its energy unit in a state that does not impair the delivery of power products the unit participates in (i.e. the product fulfilment of the DVPPs the unit is a member of). Figure 23 visualizes this process in detail.

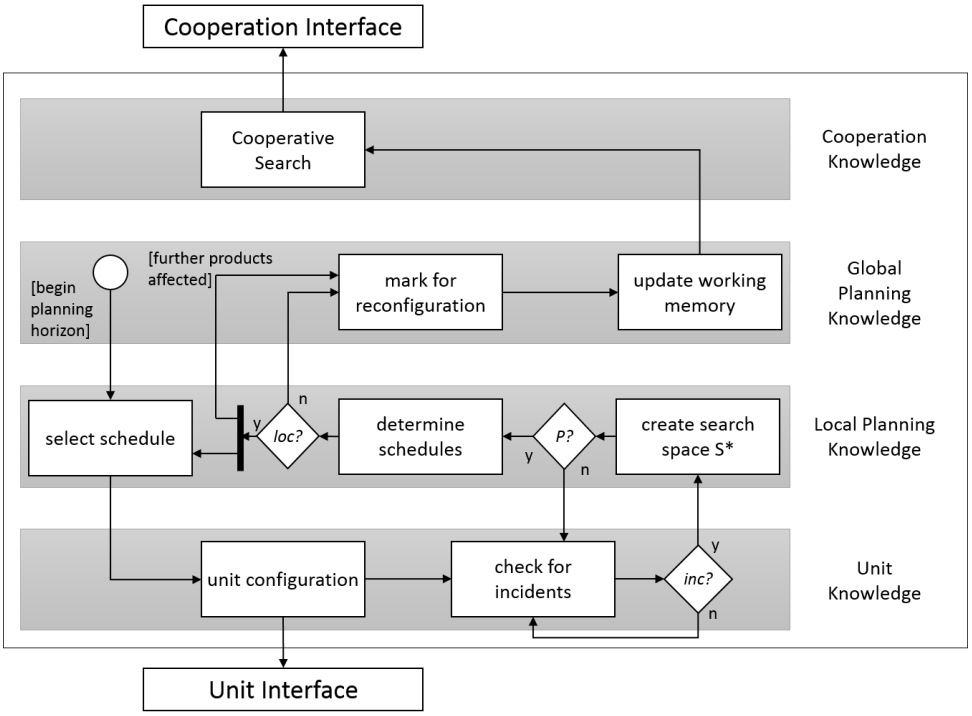

Figure 23: Workflow of a DynaSCOPE agent during product delivery

During the delivery of a power product, each agent continuously monitors its respective energy unit for deviations from the configured schedule (bottom right in the figure). If a detected deviation exceeds a preconfigured sensitivity threshold (*inc?*), an incident is reported to the local planning layer. Here, the search space model has to be recreated first, as the incident invalidates the previously calculated search space model. Then it is checked whether the incident impairs the delivery of a product the agent participates in (*P?*), i.e. if a sensitivity threshold is exceeded. If this is not the case, the incident can be discarded, as no immediate action is required, and the agent continues monitoring the energy unit. Otherwise, the agent tries to compensate the incident locally, by calculating alternative schedules with respect to the recreated search space model. If a suitable schedule (respecting both global and local constraints) can be found (*loc?*), it is selected as active schedule, and the energy unit is configured accordingly. If a local compensation is not possible, or if subsequent products are affected by this incident, the global planning layer is activated. As reconfigurations of energy units regarding this incident have to be finished at the end of the current delivery interval, less than 15 minutes are available for the cooperative reactive scheduling. Hence, the agent marks the point in time, in which the energy unit has to be reconfigured with a potential

alternative schedule at the latest. Then the incident is inserted into the global planning knowledge, which subsequently is sent to neighbouring agents, in order to begin the cooperative scheduling process based on the COHDA heuristic.

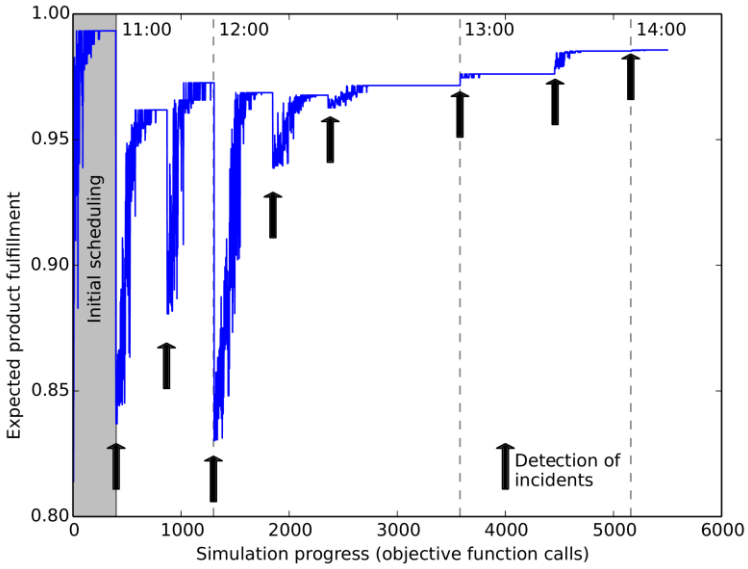

Figure 24: Cooperative problem solving after the occurrence of incidents

In this experiment, a total number of 10 incidents (CHP outages for 30 minutes each) was simulated. The arrows in the figure depict the detection of incidents. The incidents occurred randomly during product delivery, thus some of them were detected simultaneously by the agents. In Figure 25, the results from a series of experiments with different amounts of incidents in the same DVPP as above is shown. Each experiment was repeated 100 times with different random placements of the incidents.

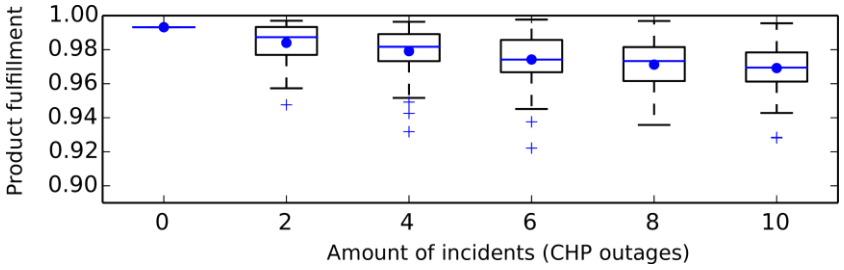

Figure 25: Actual product fulfilment after the occurrence of incidents

Obviously, the final product quality deteriorates steadily with an increasing amount of incidents. However, the analysis of the raw simulation data reveals that, in all shown cases, the triggered rescheduling processes yield far superior product qualities in total than in the case without a rescheduling.

Regarding the integration of costs, the following global objective function is set up:

$$f(\gamma_\psi) = (1-\alpha)\cdot q_{e_p} + \alpha \cdot \frac{1}{c_\psi}, \qquad c_\psi > 0$$

Here, γ_ψ describes a solution candidate with respect to the DVPP denoted by ψ. The product fulfilment criterion is identified by q_{e_p}, while c_ψ depicts the associated costs. Then α constitutes a weighting factor, such that both optimization criteria are combined using a convex combination. In Figure 26, the results from a series of experiments with different values for α are visualized.

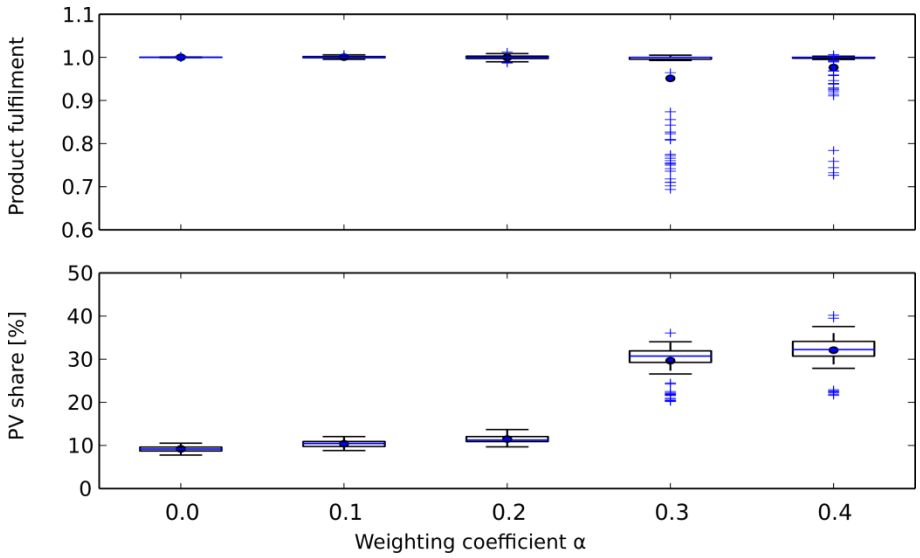

Figure 26: Product fulfilment compared to PV share with respect to the weighting coefficient α

Each experiment in this series comprises 100 energy units, divided into 69 PV systems and 31 CHP units. For the former, a cost factor of 0.0 ct/kWh was assumed, while for the latter 0.20 ct/kWh was assumed. For each value of α, a total of 100 simulation runs have been performed. The results show a substantial increase in the share of PV power in the final product delivery with increasing significance of the costs. Meanwhile, the product fulfilment criterion deteriorates predominantly in terms of outliers when preferring costs over product compliance.

Finally, in addition to the self-organized treatment of incidents with DynaSCOPE, a heuristic method for estimating the effects of a scheduling action on the grid was developed. This allows approaches like DynaSCOPE to account for required ancillary services due to rescheduling directly in the objective function of the optimization algorithm. The method comprises a grid related cluster schedule resemblance as a metric to analyse the grid usage changes using a graph based approach, as depicted in Figure 27.

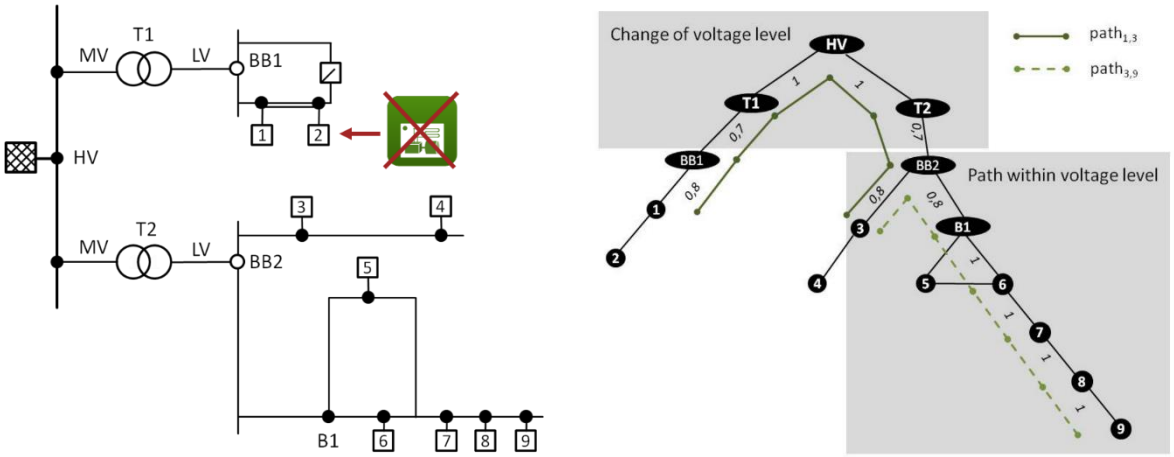

Figure 27: Grid related cluster schedule resemblance. Left: Exemplary medium-voltage grid, showing an incident at node 2. Right: A weighted graph representation of the grid upon the incident.

This metric can be used to compare different rescheduling options regarding grid usage for both dynamic clusters of distributed energy resources and for rescheduling of static clusters like virtual power plants. For more details, please refer to [77].

5 Conclusion and Outlook

The results of this work package clearly show the feasibility of implementing the continuous scheduling for tracking and updating the operations of a DVPP to ensure product fulfilment at any time during delivery in a fully distributed way. For the first time, a fully distributed method has been developed which ensures feasible cluster schedules dynamically after incidents during product delivery. All results from validation scenarios, which will be published soon as [78], show suitable behaviour regarding performance and scalability.

However, improvements are still to be made considering the dependencies between different consecutive DVPP if units are member in more than one cluster. In this case, controller conflicts emerge during optimization due to interference for other clusters' re-scheduling. Further studies are needed to find an optimal balance between the frequency of dynamic reconfigurations of DVPPs and efficient scheduling of units.

As a closing remark for this work package it should be noted, that this approach of distributed re-scheduling of units could also be applied to schedule supply and demand in a micro grid minimizing its residual load.

Work Package 1.5: Information Security in Agent-Based Energy Management Systems

Christine Rosinger[25] and Mathias Uslar[25]

1 Goals and Integration in the Sub-Project

Overall goal of this work package 1.5 (WP 1.5) is the improvement of security for agent-based energy management systems. Therefore, this WP elaborated results in the following three main topics of information security in the energy domain: *security* consideration in general, a data *privacy* concept and a conceptualization of a *trust model* to support the coalition formation process of the energy agents, which is the main part of this WP.

The reorganization from a monopolistic electricity market to a distributed smart grid and also the liberalization of this market with its unbundling induces the need of more information and communication technologies (ICT) [79]. The increasing ICT leads to a higher *threat potential*, as a result of new and more intelligent actors and additional interfaces and data exchange that are introduced in the energy domain [80]. Thus, the energy domain requires more revised and in some cases even new *security measures* because of the special requirements of the energy domain [81].

Because of former non-existence of ICT for power supply, data *privacy* legislation was also not an issue in this domain. With the upcoming Smart Grid, more individual-related data is exchanged in this field. For example, in a continuous metering scenario with assumed quarter-hourly measurement data transfers, there are 35,040 transmissions per household/meter per year [82]. Especially the prevention of profiling of households needs new privacy protection concepts.

The main motivation using a *trust model* is the occurrence of malicious agents. Different attack motivations [83] like e.g. achieving economic advantages can mislead malicious agents to misuse the system for their own advantage. In a so called worst case scenario, malicious agents can create a system blackout if they cooperate as a so called botnet. To thwart such attacks, the application of a reputation or a trust system [84] shall prevent this. Additionally, such a trust model should restrict the actions of the malicious agents and acts as one security measure, respectively, increases information security.

The three described topics of this WP act as cross-departmental function in this project because security always addresses every layer in an ICT infrastructure. The developed trust model is used in the coalition formation processes in work package 1.2 of sub-project one as one criterion for the decision making of going into a coalition with one special agent or not. Overall, the developed results in this WP 1.5 lead to a more robust and resilient system.

2 Related Work

Related work in the context of this work package focusses upon *security*, *privacy* and *trust* related issues. In general, the following initiatives and projects could be identified and classified into the categories of Smart Grid Security in general, data privacy, trust models and information security.

In the field of *Smart Grid Security* in general, the following references were mainly considered: The “Protection Profile for the Gateway of a Smart Metering System” [85] by the Federal Office for Information Security, Germany; the IEC 62351 with the title “Power systems management and

[25] OFFIS – Institute for Information Technology, 26121 Oldenburg, Germany
{forename.surname}@offis.de, R&D Division Energy

associated information exchange - Data and communications security" [86]; the ISO/IEC 27019 [87] as the domain specific component of the ISO 27k series with the title "Information security management guidelines based on ISO/IEC 27002 for process control systems specific to the energy utility industry"; and the NISTIR 7628 [88] with the title "Guidelines for Smart Grid Cyber Security" which gives recommendations for security issues in the energy domain. Additionally besides only security topics and standards, standardization of smart grids has to be considered [89].

Besides the previous mentioned literature, for the *trustworthiness facet information security* there was some common security literature: For the assessment of security realizations, security metrics were used [90]. To realize an improvement over existing systems or even in the development of architectures, risk analyses [91], [92] and principles like security by design [79] were applied.

For *data protection* and *privacy* concerns for the smart grid domain also the NISTIR 7628 [88], and several further publications [82], [85], [93], [94] were considered. Additionally, some sources for metrics were necessary [90], [95].

Trust related literature can be divided into references for common trust considerations [96], [97], [98], [99], trust in multi-agent systems [100], [101] and also the results and publication of the DFG-funded project OC-TRUST [102], [103], [104] were in main focus in this work package.

3 Methodology

For this work package, the methodology and processes applied can be defined as follows. Even in the methodology the three main topics security, privacy and trust can be identified, as can be seen in the illustration of the methodology in Figure 28. The common *security* considerations were derived from risk analysis standards and a classification was created. Of particular importance was the application of a risk analysis for the yellow pages agent as a critical part of the Smart Nord architecture. Additionally, an emphasis was on the *privacy* concept, creating a categorization with eight levels to be applied in Smart Nord. This classification provides an analysis of the interfaces exchanging critical data. Afterwards, the *trust* model is developed for the trustworthy coalition formation of time-table-based active power provision taking into account the identified trustworthiness facets. The next section will describe the most important aspects and results from the three main pillars.

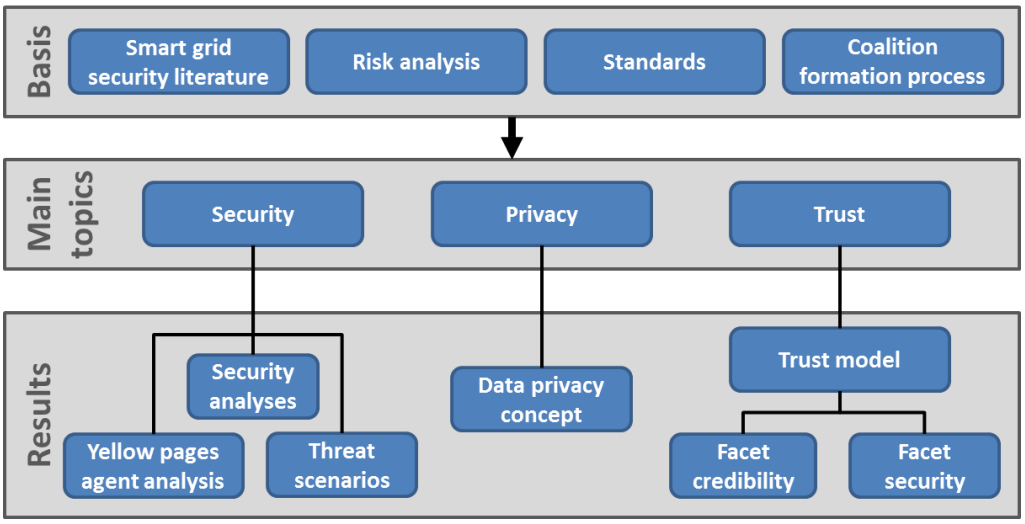

Figure 28: Methodology of WP 1.5

4 Main Results

As described before, the results of this work package 1.5 are divided into three parts: a common security consideration, a privacy concept and a trust model for the coalizing energy agents. The results of these topics are described in this section.

4.1 Common Security Considerations

Attackers have motivations and use security vulnerabilities to penetrate a system and to reach their goal(s). They are endangering the compliance to different security goals. In the operational scenario of the project are three different agent types – unit, market, and grid agents – which have different goals as malicious agents. Another important factor for security is the attacker's origin, i.e. if he is an intrinsic or extrinsic attacker. In this work package several threat scenarios were identified which cover different categories in various combinations, as can be seen in [83]. This threat identification is derived by common risk analyses of security standards by BSI or NIST [89].

Beyond the threat identification, a common security analysis for the yellow pages agent – who operates as directory service[26] for the coalizing agents – mostly for the security goal authentication was executed for different use cases of the yellow pages agent. This analysis identifies and treats security issues of the yellow pages agent. A conclusion of this analysis is shown in Table 5.

Nr.	Title	Threat	Security Measures
1	Registration at yellow pages agent	Entering malicious agent data reduces benefit of yellow pages, can in worst case lead to system breakdown.	First authentication via Postident procedure or eID of ID card or passport; creation of organizational or monetary obstacle
2	Status-Response	Notification of wrong/not-its-own-data results bad quality of service.	Min. identification via login and password
3	Updating of data	Update of not own data can lead to wrong search results.	Min. identification via login and password
4	Sign-Out	Sign-Out of another unit than the own unit leads to gaps in the database of the directory service.	Min. identification via login and password
5	Search request	Using search requests not for coalition formation but for data collection.	Restriction of frequency and only local search results; cannot be avoided completely

Table 5: Security consideration of the yellow pages agent

4.2 Data Privacy Concept for Energy Agents

The data privacy concept can be applied for the development of ICT architectures as privacy-by-design principle. With this concept, exchanged data of energy agents in coalition formation processes are analysed and categorized to identify the privacy risk of one particular date. With that categorization further privacy measures can be recommended.

After a first draft of the ICT architecture, this concept can be applied for the analysis of the exchanged data to categorize the degree of personalization. For this, a metric is used which is based on security metrics of security compliance monitoring. The eight categories of the analysis – where from category 1 to 8 the need of privacy measures increases – are:

[26] Further realization of the yellow pages agent and the corresponding directory service can be seen in WP2.3.

Cat. 1: Date is not individual-related.

Cat. 2: Date is individual-related with several additional external sources.

Cat. 3: Date is individual-related with one additional external source.

Cat. 4: Date is individual-related with several additional intern sources.

Cat. 5: Date is individual-related with one additional intern source.

Cat. 6: Date is individual-related with several additional sources of the coalition formation process.

Cat. 7: Date is individual-related with one additional source of the coalition formation process.

Cat. 8: Date is individual-related without any additional sources.

The privacy metric analyses the quantity of privacy relevant data for one communication relationship. The following Table 6 shows an example for the categorization of the exchanged data of an agent for a photovoltaic plant in a coalition formation process. With that categorization the privacy risk can be identified and used for privacy measures recommendations – like for example reducing the exchanged data or encrypt the data – to get a privacy compliant communication.

	Categories							
Date	**1**	**2**	**3**	**4**	**5**	**6**	**7**	**8**
IP address					X			
Location			X					
Max. power	X							
Power forecast	X							
Total	2	0	1	0	1	0	0	0

Table 6: Data privacy categorization for energy agent

4.3 Trust Model for Coalizing Energy Agents

The trust model which was developed in this WP 1.5 supports the trustworthy coalition formation of time-table-based active power provision and is the main part of this work package. The process of the coalition formation, where this trust model is applied, is illustrated in work package 1.2 of this sub-project one. The trust model consists of two parts: the *structure* and the *application* of the trust model which will be described in the next paragraphs.

5 Structure of the Trust Model

The common structure of the trust model is shown in Figure 29.

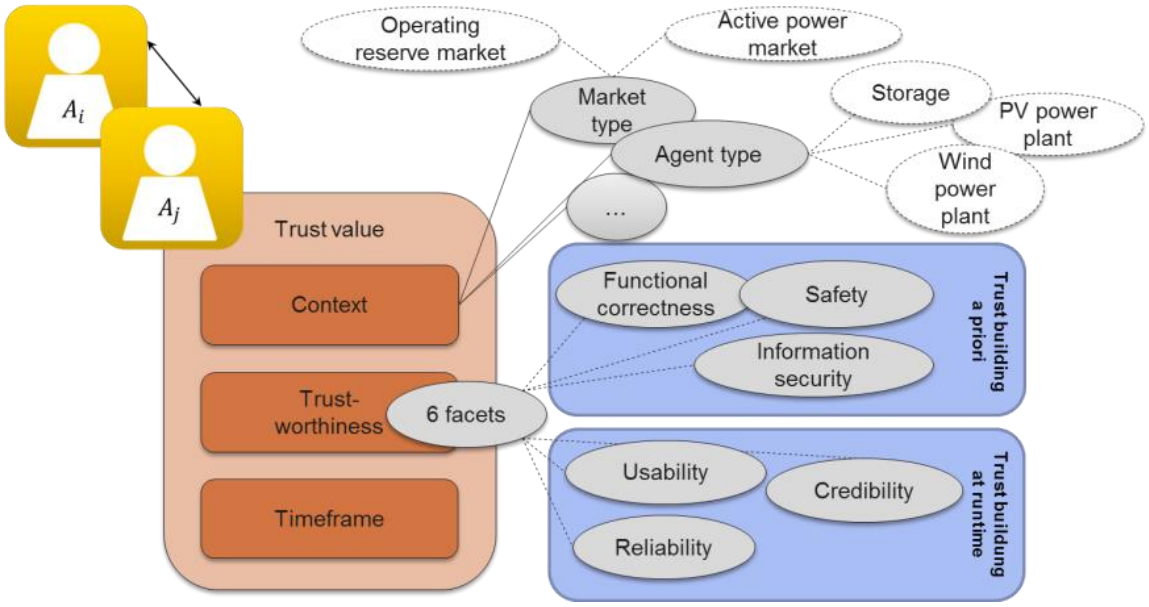

Figure 29: Illustration of trust model

One main component of this structure is the integration of different facets of trustworthiness [104] and combining these facets to one trust value [83], [84]. Trustworthiness facets considered in the project *"Smart Nord"* are:

Credibility represents the former behaviour of an agent.

Reliability forms a prediction value of technical data from the plant for the product delivery performance. This facet was examined in WP 2.2.

Information security assesses realized security measures of the agent/plant system.

Figure 29 shows an illustration of the trust model. Besides the described facets, there are different ones that will not be considered in the project *"Smart Nord"* but can still affect trustworthiness. Generally, the facets are distinguished into trust building a priori and at runtime. Additionally, the trust value of an agent A_j from the viewpoint of A_i always refers to a context and is also time-dependent.

The different facets of trustworthiness are used in combination or as single value as trust building factor for the decision making in the coalition formation process. The considered facets in this work package – credibility and information security – are described in the following paragraphs.

5.1 Credibility

Credibility [105] is one trustworthiness facet and was considered in detail in this work package. By [104] it is defined as: "The belief in the ability and willingness of a cooperation partner to participate in an interaction in a desirable manner. Also, the ability of a system to communicate with a user consistently and transparently."

In this project this facet credibility represents the former behaviour of a particular agent in previous coalition formation processes the agent took part in. The credibility value is structured into four parts. First there is the *singular credibility* which describes the credibility of an agent after a coalition formation process. Then there is the *direct overall credibility* which describes the direct

experiences (of singular credibility) in a relationship between one agent and another developed over a time period. The third part is the *indirect overall credibility* which describes recommendations of other agent to another agent over a time period. Finally, the *overall credibility* comprises the direct and indirect relationships and calculated an overall credibility value for an agent. In the following enumeration the different parts of the credibility value are described:

Singular Credibility: Singular credibility depends on the percentage contribution in a coalition formation process – a higher percentage contribution means higher credibility – and the estimated reliability – a higher estimated reliability means a lower credibility. For the singular credibility between two agents the following formula is assumed: $z = f(x, y) = MIN(1, x \cdot ((x + (1 - y))))$. As result, the value 0 means a minimal credibility and the value 1 means a maximum credibility.

Direct credibility: Direct credibility of one agent A_i to another agent A_j over a number of coalition formations is built on own experiences. The formula for direct credibility is applied as follows: $C_{all}^{dir}(A_i, A_j) = \frac{\sum C(A_i, A_j)}{\#(C(A_i, A_j))}$ which means a mean value over all direct experiences agent A_i has about A_j. Figure 30 shows the development of the value over a time period in four different use cases.

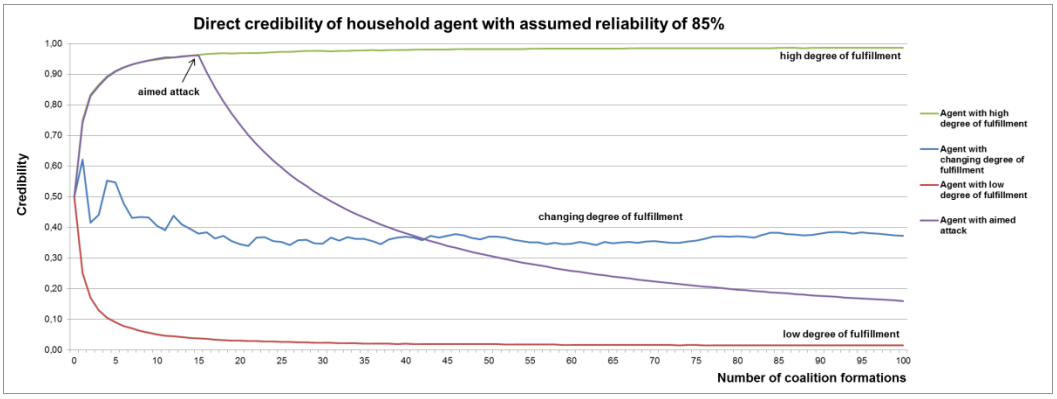

Figure 30: Example of direct overall credibility

Indirect credibility: The indirect credibility is built on recommendations from other agents. This value can be used if an agent has no direct experiences with another agent with whom the agent wants to form a coalition with or if the agents wants to improve the own value. The formula for the indirect overall credibility – where the agents A_j's recommendation of A_k is weighted by the direct trust relationship between A_i and A_j – is applied as follows:

$$C_{all}^{ind}(A_i, A_k) = \frac{1}{N} \cdot \sum_{n=1}^{N} \left(C_{all}^{dir}(A_i, A_n) \cdot C_{all}^{dir}(A_n, A_k) \right)$$

Figure 31 shows how the agents are interrelated for the direct and indirect trust relationships.

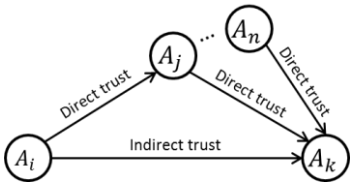

Figure 31: Direct and indirect relationship

Overall credibility: The overall credibility combines the direct and indirect overall credibility. The combined formula (1) is applied as follows:

$$C_{all}(A_i, A_j) = \begin{cases} C_{all}^{dir}(A_i, A_j), \text{ if } \#\left(C(A_i, A_j)\right) > x \\ C_{all}^{ind}(A_i, A_j), \text{ if } \#\left(C(A_i, A_j)\right) = 0 \\ \frac{1}{2} \cdot \left(C_{all}^{dir}(A_i, A_j) + C_{all}^{ind}(A_i, A_j)\right), \text{ if } 0 < \left(C(A_i, A_j)\right) \leq x \end{cases} \quad (1)$$

This formula shows if an agent has a certain number x of direct experiences with agent A_j the agent can use only the direct credibility, if the agent has no direct experiences he can use only the indirect credibility and if he has some direct experiences but wants to improve this value by recommendations the agent can use a combination of both – direct and indirect – credibility. Figure 32 shows an example of the overall credibility of an agent with the use case aimed attack from the view of another agent compared to the agent's direct credibility. This shows that the usage of recommendations by others can help getting a more precise value.

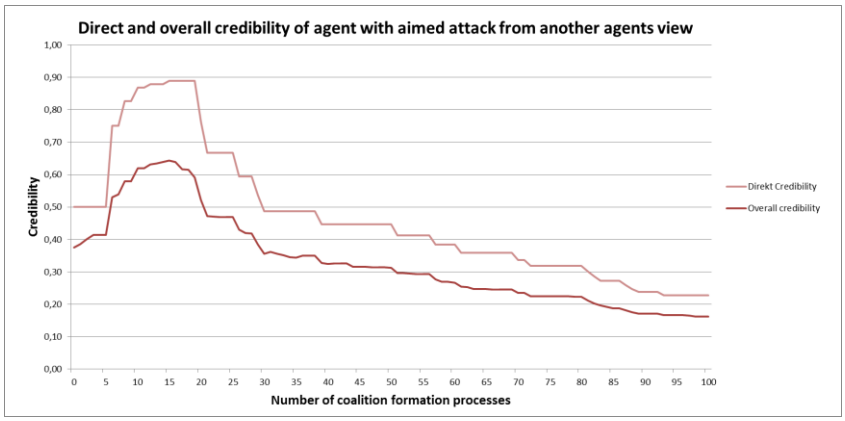

Figure 32: Example of overall credibility

5.2 Information Security

Information security [106] is one of the previous described trustworthiness facets which were examined in particular in this WP. This facet takes into account that the more security measures a system of an agent applies, the higher is the assumed trustworthiness of the agent. Additionally, for this information security facet it is expected that if an agent realizes its security measures in a standard-based way, the agent is considered more trustworthy. Information security as trustworthiness facet can be used as trust building a priori or as a factor for the initial trust. In the following two sections the concept of the security assessment is described.

Basic security assessment model

In Figure 33 an overview of the basic security assessment model as ontology is depicted.

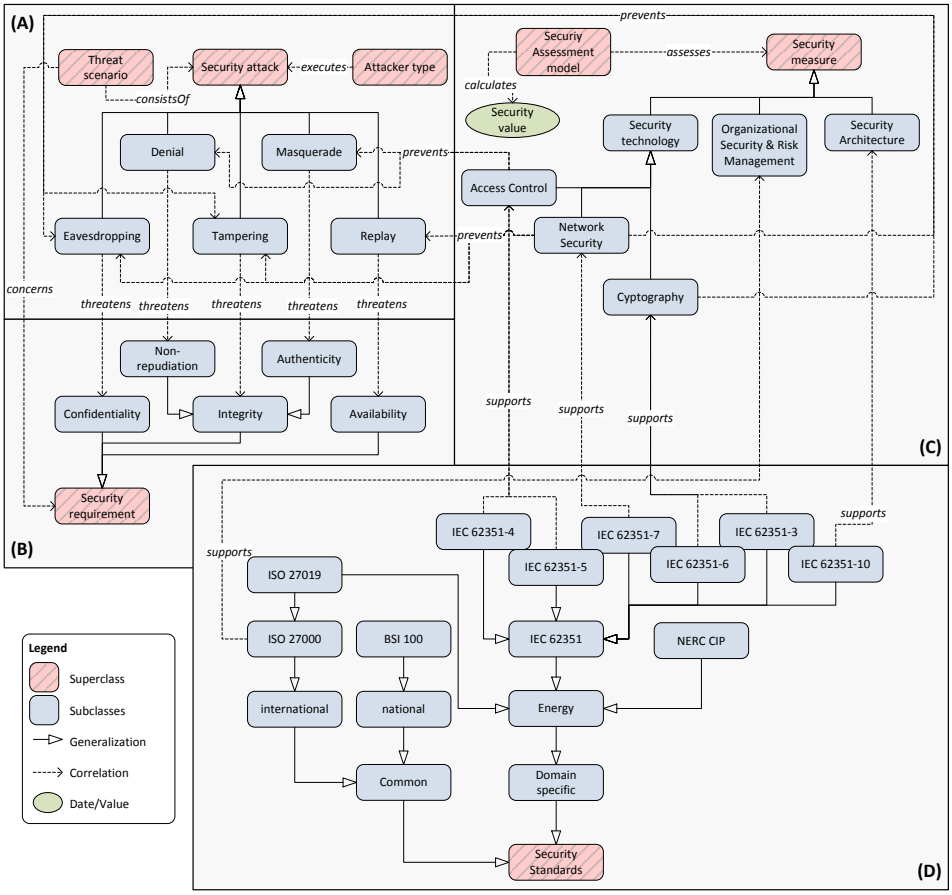

Figure 33: Assessment of implemented information security measures

The solid lines represent hierarchical relationships between the concepts shown in blue and red-striped boxes and the dashed lines are object-property relationships, which can be reasoned. The green oval shows the security value which is calculated by the security assessment model and which represents the result of the assessment phase.

The basic security assessment model in Figure 33 is segmented into four parts. Part (A) shows different *security attacks* while part (B) shows several *security requirements*. Part (C) shows *security measures* which are related with the appropriate *security standard*s depicted in part (D). Even in part (C) – the most relevant concept for this assessment – the *security assessment model* concept is associated with the *security measure* concept over the object property *assesses*. Finally, this *security assessment model* concept with its assessment functions realizes the overall *security value*. A more detailed description of this model can be found in [106].

Security value assessment method

Security assessment consists of assumptions because there are always different requirements and every user has to decide by oneself which security requirements are the most important for his particular use case. The security assessment method is based on a regular risk analysis [91], [92] with the assumption that the more security requirements are covered the more trustworthiness can be expected. Thus, the security assessment per agent consists of three parts: The assessment per security requirement A, the consideration of security standards St and a weighting factor $Prio$. For the final security assessment per agent $Sec(Agent)$ a weighted average with the single assessment per security requirement $A(i)$, the assessment of standard-based realization per security requirement $St(i)$, and the priority per security requirement $Prio(i)$ can be built which can be seen in formula (2). $\#secreq$ implies in this case the number of security requirements.

$$Sec(Agent) = \frac{\sum_{i=1}^{\#secreq} A(i) * St(i) * Prio(i)}{\sum_{j=1}^{\#secreq} Prio(j)} \quad (2)$$

6 Application of the Trust Model

The second main part of the trust model is the consideration of different phases a trust value has to go through during its lifecycle, which is shown in Figure 34.

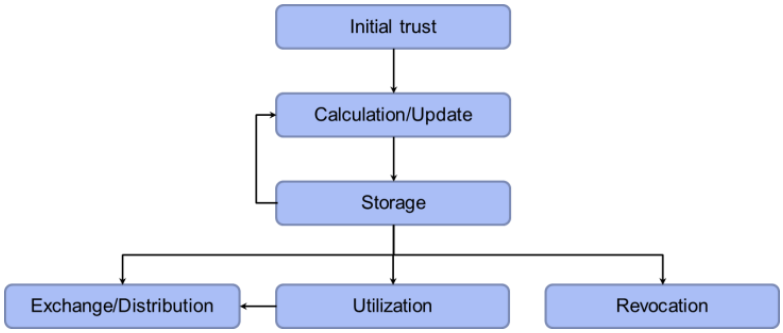

Figure 34: Life cycle of the trust model

The first appearance of a trust value is in the *initial trust* phase. This occurs when an agent is generated or joins the community. In this phase it has to be decided and determined which value the trustworthiness will be. Facets that have a trust building a priori can be applied in this *initial trust* phase. After this, the *calculation* or *update* phase takes place where e.g. the former behaviour of an agent is regarded. This behaviour is then included into the value or the value is updated. The *storage* phase considers where and how the different facets are stored and how tampering can be prevented. After a value was stored, there is a relationship back to the *calculation* and *update* phase because this is the main life circle of the value. After *storage* there are different other possibilities what happens next with the value. The *exchange/distribution* phase is concerned with the method how the values are exchanged and distributed between the agents and also a secure transfer of the values is considered. In the *utilization* phase, the different facets of the trust value are combined, goal functions are applied and guidance recommendations are given. If a value is compromised by malicious agents, revocation of the value has to be initiated.

7 Conclusion and Outlook

This work package examined different issues from the security domain for energy related topics especially for coalition formation processes of energy agents in a multi-agent system. Several results were elaborated like a trust model and common security and privacy analyses for coalition formation processes of energy agents. We showed some approaches for security considerations, like the appropriate threat scenarios and the security consideration of the yellow pages agent. The privacy concept supports the privacy-by-design-principle and shows a categorization of individual-related data in this use case. Finally, the trust model represents the main part of this work package which is divided into the structure and the application of the trust model. In this trust model the trustworthiness facets credibility and information security were examined primarily. The concepts of these facets were also described in the "main results" section of this chapter.

For further work, the security and privacy concepts has to be examined empirically. Additionally for the trust model, a combination of different trustworthiness facets has to be considered, for example how different facets should be weighted or in which phase of the life cycle of the trust model diverse facets can be utilized. Additionally, an integration of this model into the existing

NIST measures, described in e.g. [107] has to be evaluated. Secure storage and avoiding of manipulated exchange of the several trust values has also be considered in the future.

References

[1] A. Nieße, S. Beer, J. Bremer, C. Hinrichs, O. Lünsdorf, M. Sonnenschein, "Conjoint Dynamic Aggregation and Scheduling Methods for Dynamic Virtual Power Plants," In Proceedings of the 2014 Federated Conference on Computer Science and Information Systems, pp. 1505-1514.

[2] O. Abarrategui, J. Marti, A. Gonzalez, "Constructing the Active European Power Grid," in Proceedings of WCPEE09, Cairo, 2009, pp. 1–4.

[3] A. Nieße, S. Lehnhoff, M. Tröschel, M. Uslar, C. Wissing, H.-J. Appelrath, M. Sonnenschein, "Market-based self-organized provision of active power and ancillary services: An agent-based approach for smart distribution grids," in Complexity in Engineering (COMPENG), 2012.

[4] Bundesnetzagentur, "'Smart Grid' and 'Smart Market'," 2012.

[5] F. Wu, K. Moslehi, A. Bose, "Power system control centers: Past, present, and future," Proceedings of the IEEE, vol. 93, no. 11, pp. 1890–1908, 2005.

[6] International Energy Agency, "Distributed Generation in Liberalised Electricity Markets," OECD Publishing, 2002.

[7] S. Awerbuch, A. M. Preston, Eds., "The Virtual Utility: Accounting, Technology & Competitive Aspects of the Emerging Industry," ser. Topics in Regulatory Economics and Policy. Kluwer Academic Publishers, 1997, vol. 26.

[8] D. Coll-Mayor, R. Picos, E. Garciá-Moreno, "State of the art of the virtual utility: the smart distributed generation network," International Journal of Energy Research, vol. 28, no. 1, pp. 65–80, 2004.

[9] S. McArthur, E. Davidson, V. Catterson, A. Dimeas, N. Hatziargyriou, F. Ponci, T. Funabashi, "Multi-agent systems for power engineering applications – Part I: Concepts, approaches, and technical challenges," IEEE Transactions on Power Systems, vol. 22, no. 4, pp. 1743–1752, 2007.

[10] R. R. Negenborn, Z. Lukszo, H. Hellendoorn, Eds., "Intelligent Infrastructures," ser. Intelligent Systems, Control and Automation: Science and Engineering. Springer, 2010, vol. 42.

[11] S. D. Ramchurn, P. Vytelingum, A. Rogers, N. R. Jennings, "Agentbased homeostatic control for green energy in the smart grid," ACM Trans. Intell. Syst. Technol., vol. 2, no. 4, pp. 35:1–35:28, Jul. 2011.

[12] G. Anders, F. Siefert, J.-P. Steghöfer, H. Seebach, F. Nafz, W. Reif, "Structuring and Controlling Distributed Power Sources by Autonomous Virtual Power Plants," in IEEE Power and Energy Student Summit (PESS 2010). IEEE Power & Energy Society, 2010.

[13] "Putting the 'smarts' into the smart grid: A grand challenge for artificial intelligence," Commun. ACM, vol. 55, no. 4, pp. 86–97, Apr. 2012.

[14] A. Nieße, M. Tröschel, M. Sonnenschein, "Designing Dependable and Sustainable Smart Grids - How to Apply Algorithm Engineering to Distributed Control in Power Systems," Environmental Modelling and Software, vol. 56, pp. 37-51, 2014.

[15] A. Nieße, S. Lehnhoff, M. Sonnenschein, M. Tröschel, "Dynamic Virtual Power Plants in Future Energy Grids: Defining the Gap to the Field," in Proceedings VDE Kongress 2014, VDE Verlag.

[16] H.-J. Appelrath, H. Kagermann, C. Mayer Eds., "Future Energy Grid (acatech study)," acatech, Munich, 2012.

[17] F. Korb, S. Lehnhoff, C. Mayer, M. Uslar, "Data Access-Point Manager – definierte Informationsflüsse für Betriebsführung und Markt," Energiewirtschaftliche Tagesfragen, 64(3), 2014.

[18] The Smart Grid Interoperability Panel Cyber Security Working Group. Introduction to NISTIR 7628 Guidelines for Smart Grid Cyber Security, 2010.

[19] U. Richter, M. Mnif, J. Branke, C. Müller-Schloer, H. Schmeck, "Towards a Generic Observer/Controller Architecture for Organic Computing," in Informatik 2006. LNI P-93, pp. 112-119, 2006.

[20] J. Psola et al., "Modeling of a Redox Flow Battery Storage for Grid Applications," in PCIMasia 2013, Shanghai, China, 2013.

[21] J. Psola et al., "Optimization of energy output by combining energy storages with renewable energies," in PCIMasia 2014, Shanghai, China, 2014.

[22] J. Widén, “Correlation Between Large-Scale Solar and Wind Power in a Future Scenario for Sweden,” in. IEEE Transactions on Sustainable Energy, Vol. 2, No. 2, p. 177-184, 2011.

[23] J. Psola et al., “Technologies and Operational Concepts for Energy Storages,” in EnviroInfo 2013, Hamburg, Germany, 2013.

[24] J. Psola, W. Canders, “Klassifizierung von Energiespeichern,” in FEN - Bericht des IMAB zum TP2, Braunschweig, Germany, 2009.

[25] H. L. Ferreira et al., “Characterisation of electrical energy storage technologies,” in Energy 53 (2013), p. 288-298, 2013.

[26] F. Díaz-González et al., “A review of energy storage technologies for wind power applications,” in: Renewable and Sustainable Energy Reviews 16 (2012), p. 2154-2171, 2012.

[27] H. Chen et al., “Progress in electrical energy storage systems: A critical review,” in Progress in Natural Science 19 (2009), p. 291-312, 2009.

[28] Y. Shoham, K. Leyton-Brown, “Multiagent Systems: Algorithmic, Game-Theoretic, and Logical Foundations,” Cambridge University Press, 2000.

[29] T. Sandholm, K. Larson, M. Andersson, O. Shehory, F. Thomé, “Coalition structure generation with worst case guarantees,” in Artificial Intelligence, 111, 209-238.

[30] T. Rahwan, N. R. Jennings, “An Improved Dynamic Programming Algorithm for Coalition Structure Generation,” in Proc. of 7th Int. Conf. on Autonomous Agents and Multiagent Systems, 2008.

[31] M. H. Rothkopf, A. Pekei, R. M. Harstad, “Computationally Manageable Combinatorial Auctions,” Center for Discrete Mathematics & Theoretical Computer Science, 1995.

[32] V. D. Dang, N. R. Jennings, “Generating coalition structures with finite bound from the optimal guarantees,” in 3rd International Conference on Autonomous Agents and Multi-Agent Systems, 2004.

[33] T. Rahwan, S. Ramchurn, N. Jennings, A. Giovannucci, “An Anytime Algorithm for Optimal Coalition Structure Generation,” in Journal of Artificial Intelligence Research (JAIR), 34, 521–567, 2009.

[34] T. Michalak, J. Sroka, T. Rahwan, J. Wooldridge, P. McBurney, N. R. Jennings, “A Distributed Algorithm for Anytime Coalition Structure Generation,” in Proc. of 9th Int. Conf. on Autonomous Agents and Multiagent Systems (AAMAS 2010), 2010.

[35] O. Shehory, S. Kraus, “Methods for task allocation via agent coalition formation,” in Artificial Intelligence, 101, 165-200, 1998.

[36] S. Sen, P. S. Dutta, “Searching for optimal coalition structures,” in Proceedings of the Fourth International Conference on MultiAgent Systems, 2000.

[37] C. Rosinger, S. Beer, “Glaubwürdigkeit in dynamischen Wirkleistungsverbünden,” in Informatik-Spektrum, 2014, pp. 1-8.

[38] R. G. Smith, “The Contract Net Protocol: High-Level Communication and Control in a Distributed Problem Solver,” in IEEE Transactions on Computers, C-29(12), 1104–1113.

[39] S. S. Fatima, M. Wooldridge, N. R. Jennings, “A Linear Approximation Method for the Shapley Value,” in Artificial Intelligence, 172, 1673-1699.

[40] S. Beer, “Dynamic Coalition Formation in Electricity Markets,” PHD thesis, Dept. of Computing Science, University of Oldenburg, Oldenburg, Niedersachsen, planned to be submitted 2015-04.

[41] S. Beer, “A Formal Model for Agent-based Coalition Formation in Electricity Markets,” in 4th IEEE/PES Innovative Smart Grid Technologies Europe (ISGT EUROPE), Kopenhagen, pp. 1-5, 2013.

[42] A. Nieße, S. Lehnhoff, M. Tröschel, M. Uslar, C. Wissing, H.-J. Appelrath, M. Sonnenschein, “Market–Based Self–Organized Provision of Active Power and Ancillary Services,” IEEE, 06 2012.

[43] M. Blank, S. Gerwinn, O. Krause, S. Lehnhoff, “Support Vector Machines for an efficient Representation of Voltage Band Constraints,” in Innovative Smart Grid Technologies. IEEE PES, 2011.

[44] J. Bremer, B. Rapp, M. Sonnenschein, “Support Vector based Encoding of Distributed Energy Resources’ Feasible Load Spaces,” in IEEE PES Conference on Innovative Smart Grid Technologies Europe, Chalmers Lindholmen, Gothenburg,Sweden, 2010.

[45] Z. Michalewicz, M. Schoenauer, “Evolutionary algorithms for constrained parameter optimization problems,” Evol. Comput., 4:1–32, March 1996.

[46] G. E. Liepins, M. D. Vose, “Representational issues in genetic optimization,” in Journal of Experimental and Theoretical Artificial Intelligence, 2, 1990.

[47] C. A. Coello Coello, “Theoretical and numerical constraint-handling techniques used with evolutionary algorithms: a survey of the state of the art,” Computer Methods in Applied Mechanics and Engineering, 191(11-12):1245–1287, January 2002.

[48] O. Kramer, “A review of constraint-handling techniques for evolution strategies,” Appl. Comp. Intell. Soft Comput., 2010:1–19, January 2010.

[49] S. Koziel, Z. Michalewicz, “Evolutionary algorithms, homomorphous mappings, and constrained parameter optimization,” Evol. Comput., 7:19–44,March 1999.

[50] D. G. Kim, “Riemann mapping based constraint handling for evolutionary search,” in SAC, pages 379–385, 1998.

[51] W. Squire, “Computer implementation of the schwarz-christoffel transformation,” Journal of the Franklin Institute, 299(5):315{322}, 1975.

[52] J. W. Bandler, R. M. Biernacki, S. H. Chen, P. A. Grobelny, R. H. Hemmers, “Space mapping technique for electromagnetic optimization,” Microwave Theory and Techniques, IEEE Transactions on, 42(12):2536–2544, 1994.

[53] J. W. Bandler, R. M. Biernacki, S. H. Chen, R. H. Hemmers, K. Madsen, “Electromagnetic optimization exploiting aggressive space mapping,” Microwave Theory and Techniques, IEEE Transactions on, 43(12):2874–2882, 1995.

[54] J. Bremer, M. Sonnenschein, “A Distributed Greedy Algorithm for Constraint-based Scheduling of Energy Resources,” in Maria Ganzha, Leszek A. Maciaszek,and Marcin Paprzycki, editors, Federated Conference on Computer Science and Information Systems - FedCSIS 2012, Wroclaw, Poland, 9-12 September 2012,Proceedings, pages 1285–1292, 2012.

[55] J. Bremer, M. Sonnenschein, “Constraint-handling for Optimization with Support Vector Surrogate Models – A Novel Decoder Approach,” in J. Filipe and A.L.N. Fred, editors, ICAART 2013 – Proceedings of the 5th International Conference on Agents and Artificial Intelligence, volume 2, pages 91–105, Barcelona, Spain, 2013.SciTePress.

[56] A. Hevner, S. March, J. Park, S. Ram, “Design Science in Information Systems Research,” MIS Quarterly (28:1) 2004, pp. 75-105.

[57] J. Bremer, M. Sonnenschein, “Automatic Reconstruction of Performance Indicators from Support Vector based Search Space Models in Distributed Real Power Planning Scenarios,” in M. Horbach (Hrsg.): Lecture Notes in Informatics 220, Proceedings of the Informatik 2013 - Informatik angepasst an Mensch, Organisation und Umwelt. 16.-20. September, Koblenz, Germany. LNI 220, ISBN 978-3-88579-614-5, pp. 1441-1454, 2013.

[58] J. Bremer, M. Sonnenschein, “Model-based Integration of Constrained Search Spaces into Distributed Planning of Active Power Provision,” Computer Science and Information Systems, Vol. 10, No. 4, 1823-1854, 2013.

[59] J. Bremer, M. Sonnenschein, “Sampling the Search Space of Energy Resources for Self-organized, Agent-based Planning of Active Power Provision,” in B. Page, A.G. Fleischer, J. Göbel, V. Wohlgemuth (Eds.): Environmental Informatics and Renewable Energies - 27th International Conference on Informatics for Environmental Protection. Shaker Verlag, ISBN: 978-3-8440-1676-5, pp. 214-222, 2013.

[60] A. Nieße, M. Tröschel, M. Sonnenschein, “Designing dependable and sustainable Smart Grids – How to apply Algorithm Engineering to distributed control in power systems,” in Environmental Modelling & Software, 2013

[61] D. M. J. Tax, R. P. W. Duin, “Data Domain Description using Support Vectors,” in European Symposium on Artificial Neural Networks – ESANN, S. 251–256, 1999.

[62] A. Ben-Hur, H. T. Siegelmann, D. Horn, V. Vapnik, “Support Vector Clustering,” in Journal of Machine Learning Research 2, S. 125–137, 2001.

[63] J. Bremer, B. Rapp, M. Sonnenschein, “Encoding distributed Search Spaces for Virtual Power Plants,” in IEEE Symposium Series on Computational Intelligence 2011 (SSCI 2011). Paris, France, April 2011.

[64] I. Steinwart, A. Christmann, “Support Vector Machines,” 1st. Springer Publishing Company, Incorporated. ISBN: 0387772413, 2008.

[65] J. Bremer, M. Sonnenschein, “Parallel tempering for constrained many criteria optimization in dynamic virtual power plants,” IEEE Symposium on Computational Intelligence Applications in Smart Grid (CIASG). Doi: 10.1109/CIASG.2014.7011551, 2014

[66] C. Hinrichs, J. Bremer, M. Sonnenschein, “Distributed Hybrid Constraint Handling in Large Scale Virtual Power Plants,” in IEEE PES Conference on Innovative Smart Grid Technologies Europe (ISGT Europe 2013). IEEE Power & Energy Society, 2013.

[67] A. Nieße, S. Lehnhoff, M. Tröschel, M. Uslar, C. Wissing, H.-J. Appelrath, M. Sonnenschein, “Market-based self-organized provision of active power and ancillary services: An agent-based approach for Smart Distribution Grids,” in Complexity in Engineering (COMPENG), Aachen, 2012.

[68] G. Anders, F. Siefert, J.-P. Steghöfer, H. Seebach, F. Nafz, W. Reif, “Structuring and Controlling Distributed Power Sources by Structuring and Controlling Distributed Power Sources by Autonomous Virtual Power Plants,” in Proceedings of the IEEE Power and Energy Student Summit 2010.

[69] R. Li, J. Li, G. Poulton, “Agent-Based Optimisation Systems for Electrical Load Management,” in The 20th Australian Joint Conference on Artificial Intelligence. Queensland, Australia.

[70] E. Pournaras, “Multi-level Reconfigurable Self-organization in Overlay Services,” Thesis,TU Delft. 2013.

[71] M. Tröschel, “Aktive Einsatzplanung in holonischen Virtuellen Kraftwerken,” Dissertation. Universität Oldenburg. 2010.

[72] C. Hinrichs, S. Lehnhoff, M. Sonnenschein, “COHDA: A Combinatorial Optimization Heuristic for Distributed Agents,” in Agents and Artificial Intelligence, Communications in Computer and Information Science, vol. 449, J. Filipe and A. Fred, Eds. Berlin, Heidelberg: Springer Berlin Heidelberg, 2014, pp. 23–29.

[73] E. Handschin, C. Rehtanz, H. F. Wedde, O. Krause, S. Lehnhoff, “On-line stable state determination in decentralized power grid management,” in Proceedings of the 16th Power Systems Computation Conference (PSCC’08), pages 07–14, Glasgow, Scotland, UK, 2008.

[74] O. Krause, S. Lehnhoff, “Generalized Static-State Estimation,” in 22nd Australasian Universities Power Engineering Conference (AUPEC), 2012.

[75] J. Bremer, M. Sonnenschein, “Automatic Reconstruction of Performance Indicators from Support Vector based Search Space Models in Distributed Real Power Planning Scenarios,” in Lecture Notes in Informatics 220, Proceedings of the Informatik 2013 - Informatik angepasst an Mensch, Organisation und Umwelt. Koblenz, Germany. pp. 1441-1454. 2013.

[76] M. Wooldridge, “Intelligent Agents,” in Multi-Agent Systems, 2nd ed., G. Weiss, Ed. MIT Press, 2013.

[77] A. Nieße, M. Sonnenschein, “Using Grid Related Cluster Schedule Resemblance for Energy Rescheduling – Goals and Concepts for Rescheduling of Clusters in Decentralized Energy Systems,” in SMARTGREENS, 2013.

[78] A. Nieße, “Verteilte kontinuierliche Einsatzplanung in Dynamischen Virtuellen Kraftwerken,” Ph.D. thesis, Dept. of Computing Science, Univ. of Oldenburg, Germany (to appear 2015).

[79] M. Sonnenschein, H.-J. Appelrath, L. Hofmann, M. Kurrat, S. Lehnhoff, C. Mayer, A. Mertens, M. Uslar, A. Nieße, M. Tröschel, “Dezentrale und selbstorganisierte Koordination in Smart Grids,” VDE Kongress 2012.

[80] M. Postina, S. Rohjans, U. Steffens, M. Uslar, “Views on service oriented architectures in the context of Smart Grids,” First IEEE international conference on Smart grid communications (SmartGridComm), 2010.

[81] A. Suhr, C. Rosinger, H. Honecker, “System Design and Architecture – Essential Functional Requirements vs. ICT Security in the energy domain,” Int. ETG-Kongress 2013 (ETG-FB 139), p. 9, 2013.

[82] A. Roßnagel, S. Jandt, “Datenschutzkonformes Energieinformationsnetz - Risiken und Gestaltungsvorschläge,” DuD - Datenschutz und Datensicherheit, S. 373-378, 2010.

[83] C. Rosinger, M. Uslar, J. Sauer, “Threat Scenarios to evaluate Trustworthiness of Multi-agents in the Energy Data Management,” EnviroInfo2013 – Environmental Informatics Renewable Energies, 2013.

[84] C. Rosinger, M. Uslar, F. Hockmann, “Reputationssysteme für selbstorganisierte Multi-Agenten-Systeme in Energiemanagementsystemen,” VDE-Kongress 2012, 2012.

[85] Federal Office for Information Security, Germany, “BSI–CC–PP–0073: Protection Profile for the Gateway of a Smart Metering System (Smart Meter Gateway PP)”, 2014.

[86] International Electrotechnical Commission (IEC), “IEC 62351 part 1 - 11, Power systems management and associated information exchange - Data and communications security”, 2007 – 2013.

[87] International Organization for Standardization (ISO), International Electrotechnical Commission (IEC), “ISO/IEC TR 27019: Information technology - Security techniques - Information security management guidelines based on ISO/IEC 27002 for process control systems specific to the energy utility industry”, 2013.

[88] The Smart Grid Interoperability Panel Cyber Security Working Group, “NISTIR 7628 - Guidelines for Smart Grid Cyber Security vol. 1-3,” August 2010.

[89] M. Uslar, M. Specht, C. Dänekas, J. Trefke, S. Rohjans, J. M. Gonzalez, C. Rosinger, R. Bleiker, “Standardization in Smart Grids,” Springer Publishing, 2013.

[90] A. Jaquith, “Security Metrics: Replacing Fear, Uncertainty, and Doubt,” Addison-Wesley, 2007.

[91] International Organization for Standardization (ISO), “ISO 27005: Information technology — Security techniques — Information security risk management”.

[92] CEN-CENELEC-ETSI Smart Grid Coordination Group, final document in mandate M/490 group SGIS “Smart Grid Information Security”, 2012.

[93] D. Laupichler, S. Vollmer, H. Bast, M. Intemann, “Das BSI-Schutzprofil: Anforderungen an den Datenschutz und die Datensicherheit für Smart Metering Systeme,” in DuD – Datenschutz und Datensicherheit, 8:542 – 546, 2011.

[94] O. Raabe, M. Lorenz, F. Pallas, E. Weis, A. Malina, “14 Thesen zum Datenschutz im Smart Grid,” in DuD – Datenschutz und Datensicherheit, 8:519 – 523, 2011.

[95] A. Sowa, “Metriken - der Schlüssel zum erfolgreichen Security und Compliance Monitoring,” Wiesbaden: Vieweg + Teubner Verlag, 2011, ISBN 978–3–8348–1480–7.

[96] L. Capra, “Engineering human trust in mobile system collaborations,” in Proceedings of the 12th ACM SIGSOFT twelfth international symposium on Foundations of software engineering, ACM SIGSOFT Softw. Eng. Notes, p. 10, 2004.

[97] C. Castelfranchi, R. Falcone, “Trust theory: A socio-cognitive and computational model,” Wiley, 2010.

[98] A. Jøsang, “The right type of trust for distributed systems,” Proceeding NSPW ’96 Proc. 1996 Work. New Secur. Paradigm., pp. 119–131, 1996.

[99] S. P Marsh, “Formalising trust as a computational concept,” PhD-Thesis University of Stirling, 1994.

[100] A. Das, M. M. Islam, “SecuredTrust: A Dynamic Trust Computation Model for Secured Communication in Multiagent Systems,” IEEE Trans. Dependable Secur. Comput., vol. 9, no. 2, pp. 261–274, Mar. 2012.

[101] H. Yu, Z. Shen, C. Leung, C. Miao, V. R. Lesser, “A Survey of Multi-Agent Trust Management Systems,” IEEE Access, vol. 1, pp. 35–50, 2013.

[102] R. Kiefhaber, S. Hammer, B. Savs, J. Schmitt, M. Roth, F. Kluge, E. Andre, T. Ungerer, “The Neighbor-Trust Metric to Measure Reputation in Organic Computing Systems,” 2011 Fifth IEEE Conf. Self-Adaptive Self-Organizing Syst. Work., pp. 41–46, Oct. 2011.

[103] R. Kiefhaber, G. Anders, F. Siefert, T. Ungerer, W. Reif, “Confidence as a Means to Assess the Accuracy of Trust Values,” 2012 IEEE 11th Int. Conf. Trust. Secur. Priv. Comput. Commun., pp. 690–697, Jun. 2012.

[104] J.-P. Steghöfer, R. Kiefhaber, “Trustworthy organic computing systems: Challenges and perspectives,” in Autonomic and Trusted Computing and Trusted Computing, Springer Berlin Heidelberg, 2010.

[105] C. Rosinger, S. Beer, “Glaubwürdigkeit in dynamischen Wirkleistungsverbünden,” in Informatik-Spektrum, pp. 1–8, Dezember 2014.

[106] C. Rosinger, M. Uslar, J. Sauer, “Using Information Security as a Facet of Trustworthiness for Self-Organizing Agents in Energy Coalition Formation Processes,” EnviroInfo2014 – Environmental Informatics Renewable Energies, 2014.

[107] M. Uslar, C. Rosinger, S. Schlegel, “Security by Design for the Smart Grid: Combining the SGAM and NISTIR 7628,” IEEE 38th International Computer Software and Applications Conference Workshops (COMPSACW), IEEE Publishing 2014.

Sub-Project Two:
Grid Stabilizing Ancillary Services

Overview on Sub-Project Two: Grid Stabilizing Ancillary Services

Sebastian Lehnhoff[27], Marita Blank[28], Robert Bleiker[27], Thole Klingenberg[27], Klaus Piech[27], Mathias Uslar[27], Walter Schumacher[29], Mauro Calabria[29], Axel Mertens[30], René Dietz[30] and Felix Fuchs[30]

1 Goals

The increase in renewable power generation causes an overall decrease in conventional power generation from large-scale and highly predictable fossil power plants. Aside from market-based provision of active power schedules, these power plants are crucial for the provision of short-term reactive ancillary services such as frequency and voltage control. Substituting these plants for renewable generation units requires the latter to be capable of providing these ancillary services in order to guarantee a reliable and stable power supply. In this sub-project key challenges of providing reliable ancillary services from unreliable distributed renewable energy sources are addressed:

- Setting up coordinated coalitions for real-time provision of ancillary services (work package 2.1)
- Reliable contribution planning and risk management of coordinated coalitions for the provision of ancillary services (work package 2.2)
- Interoperability and performance issues of coalition formation for ancillary services (work package 2.3)
- Stability of automated controllers in ancillary service coalitions in low-voltage grids (work package 2.4)
- Grid-supporting services through inverters and stable lower-level control (work package 2.5)

2 Related Work

Transforming the electric power system to incorporate an increasing share of renewable, distributed generation implicates new challenges for the control of the system: control methods have to cope with many individually configured, distributed, small generation units (photovoltaic (PV) systems, combined heat and power plants (CHP), wind energy converters, etc.) as well as with the fluctuation in their feed-in depending on foremost meteorological conditions. A paradigm shift from the current centralized control method assuming a static set of large controllable power plants to a decentralized, self-organized system of agents representing small active units (generators, loads, storages) in the power supply system has been proposed by the Smart Grid community for several years, and several self-organization approaches for coordinating these units have been proposed [1], [2], [3], [4].

[27] OFFIS – Institute for Information Technology
[28] University of Oldenburg
[29] Technische Universität Braunschweig
[30] Leibniz Universität Hannover

Compared with these approaches, within the Smart Nord project a method for agent-based aggregation of distributed generation as well as consumer appliances into so called coordinated coalitions has been developed that is not only capable of matching appropriate products at traditional markets for active power schedules (e.g. day-ahead or intra-day) but additionally capable of providing ancillary services to stabilize the grid. Additional related work relevant to each work package is presented in the context of the appropriate following work packages.

3 Main Results

In order to enable coordinated coalitions to deliver ancillary services in real-time a hybrid approach has been developed. At first each unit's power contribution is estimated based on long-term as well as (more reliable) short-term forecasts and coordinated coalitions are formed following economical aspects. This communication-based (multi-agent system) economical optimization yields a coordinated coalition – strictly adhering to a certain minimum reliability level – that is capable of activating power reserves for stabilizing grid frequency (primary control reserve). In order to guarantee short-term activation in real-time each unit parameterizes a local controller (droop) through appropriate configuration of the connected inverter, which exhibits the desired behaviour of a frequency-proportional power response. The main results of this sub-project are the coordination formation algorithms, taking into account the reliability constraints of ancillary services as well as inverter-based distributed controller design optimizing small-signal stability of such coalitions [5], [6], [7], [8].

4 Conclusion and Outlook

While the sub-project has demonstrated that reliable and stable provision of primary control reserve through appropriate inverter configuration is possible and can be operated following economical targets of ancillary service markets, damping issues and small-signal stability has proven to be a much more important challenge than initially expected. A PDT-controller has been designed to optimize the dynamic behaviour of coordinated coalitions in low-voltage grids. However, it has been proven that dynamic interactions between nodes of a power grid can turn the system unstable and thus it is foreseeable that additional distributed controller optimization and damping mechanisms are required when extending the frequency response regime with other controllers, e.g. voltage/var control or schemes for optimal generation curtailment. These will not only introduce more complex dynamics but very likely will influence each other, which has to be investigated further.

Work Package 2.1: Coordinated Coalitions for Real-time Provision of Ancillary Services

Thole Klingenberg[31] and Sebastian Lehnhoff[31]

1 Goals and Integration in the Sub-Project

Within this sub-project a method for agent-based aggregation of distributed generation as well as consumer appliances into so called coordinated coalitions has been developed that is not only capable of matching appropriate products at traditional markets for active power schedules (e.g. day-ahead or intra-day) but additionally capable of providing ancillary services to stabilize the grid.

Active power has been traded on energy markets for several years now yielding a desirable impact on the energy provision: especially in connection with liberalization and unbundling policies, the price for active power has been subject to functional markets instead of monopolistic structures. At the same time, the share of fluctuating renewable energy sources (RES) has increased drastically, particularly in the distribution grid, and many countries set up subsidization programs for RES to promote this change resulting in large energy capacities from RES at today's power markets.

Despite their sheer amount, RES are not yet capable of completely substituting conventional power plants, whose role goes beyond market-based active power generation and scheduling. In order to substitute fossil power plants and ensure a safe and reliable power supply, a new approach is required for the provision of the ancillary services through RES needed to operate the grid.

For instance, frequency response reserve must be provided as an automatic reaction to a loss in supply or demand (immediately following that event) in order to stabilize the frequency. This is typically provided by large power plants through a governor or controller yielding a small boost or drop in generation to balance demand and supply, respectively, thus stabilizing the frequency. As these droop-controlled power reserves are necessary for a stable power supply, the provision of an ancillary service such as this must be guaranteed and thus has to fulfil specific reliability constraints.

Hence, coordinated coalitions providing such frequency response power must adhere to the same functional as well as non-functional constraints. The functional constraint is the power-frequency-droop with which the coalition has to respond to frequency deviations matching the behaviour of a large-scale governor-controlled power plant. The non-functional requirements on the other hand are the reliability, with which the provision of this stabilizing ancillary service has to be guaranteed, as well as the dynamic stability of a distributed frequency response system.

2 Related Work

Research on relevance as well as technical and economical feasibility of aggregations of small generation units has been conducted for over a decade now. Initially, static virtual power plants (VPP) have been designed to overcome market barriers on active power markets [8], [10]. Nowadays, several operators of such VPPs are active participants on energy markets. The underlying concept, though, has three major flaws regarding its portability to larger scale. First, the VPPs are static regarding the pool of aggregated units – dynamic changes within the pool will create substantial engineering overhead driving the VPP's operational costs or might not even be

[31] OFFIS – Institute for Information Technology, 26121 Oldenburg, Germany
{forename.surname}@offis.de, R&D Division Energy

possible at all. Second, the control architecture is centralized, i.e. a single VPP control centre typically supervises and controls each single unit based on centrally optimized schedules – with the obvious shortcomings regarding scalability and complexity in the reflection of local constraints. Third, these VPPs were not designed to take system stability into account. VPPs of this kind only optimize economic integration of distributed energy resources (being a very important issue nonetheless).

In the project FENIX, a new aggregation type was defined to overcome some of these shortcomings – using a technical VPP concept. Operational feasibility aspects are integrated into the market mechanism for commercial VPPs [11], [12]. A similar concept has been presented in [13] where grid aspects are taken into account. However, both types of aggregation are still prone to flexibility and scalability issues. Also, dynamic system stability has not been subject to market processes.

With the PowerMatcher approach, a more dynamic and agent-based concept was proposed, which was initially dedicated to matching supply and demand locally [14]. Small generating units and loads in the distribution grid trade their schedules locally and thus try to reduce the necessity of electricity transport from or to other voltage levels. A similar concept is proposed in [15] and [16], focusing on real-time requirements and explicitly taking the grid topology as the basic hierarchy for the multi-agent system into account. In contrast to the concept presented in this paper, both systems work fully reactive – the main concept being predictive planning on the basis of (e.g. short-term) forecasts within the current electricity system – and the energy market is not part of these works. Thus, the integration into the current electricity system and energy markets remains unclear.

Ramchurn et al. [3] introduce a predictive planning phase in their agent-based energy management concept. However, the work is still in progress and cannot be evaluated in terms of adhering to current electricity system rules and adopting its actors.

A clear focus on the compatibility with the current European energy market rules can be seen within the ADDRESS project [17]. The aggregation approach within this project is based on the idea of aggregating demand-side flexibility using energy management gateways for each household. These gateways communicate with an aggregator function, e.g. located at the DSO, to economically optimize the utilization of the locally available demand-side flexibility. Local decisions are based on dynamic price signals calculated by the aggregation function. This idea is heavily based on a hierarchical control concept with central decision-making. Ancillary services are not subject to this approach.

The need for ancillary service provision from distributed units has been stated in several publications within the last two years e.g. [18]. Schnettler [19] and Frey [20] define requirements on how this should be realized, but hint to the missing incentives for a market-based control of ancillary-service provision by distributed small generation units. We therefore focus on both market design and agent-based provision of active power and ancillary services in the distribution grid within the Smart Nord project.

3 Methodology

In this sub-project we focus on the distributed provision of frequency response reserve (or primary control reserve) i.e. the power that is provided by power plants and used to automatically compensate an imbalance between generation and consumption within a few seconds through corresponding frequency/power (f/P)-droop-controllers thus leading to the stabilization of the frequency in the interconnected electricity grid. This frequency response reserve is activated automatically through the utilization of generator governors (more generally, the unit controllers)

in power plants. Activation is triggered when the frequency deviates from the nominal value of 50 Hz (in the EU), whereby the activated primary control power increases or decreases proportionally to the magnitude of the deviation. Maximum activation (subject to a-priori worst-case scenarios) takes place in the event of a frequency deviation of 200 mHz. A unit must guarantee that this maximum activation is realized, at latest, 30 seconds after the corresponding frequency deviation occurs and that it remains available for at least 30 minutes.

In the Smart Nord setup this primary control reserve has to be provided through distributed (renewable) units connected to the medium-voltage and low-voltage distribution grid. Each unit is equipped with a power inverter and controlled by a software agent within the Smart Nord multi-agent system. An inverter is a piece of power-electronics hardware accountable for the conversion of the unit's input power and its injection into the grid. An agent is a software component capable of computing and carrying out control actions for a given unit that follow certain (predefined) objectives or strategies. The unit's agent configures adequate droop-control settings at the unit's inverter, in order to meet the real-time constraints for the provision of frequency response reserve and guarantee its availability. Each inverter then reacts to the system's frequency with the programmed droop and injects energy accordingly, yielding the appropriate effect on the interconnected systems' frequency.

Within a planning scheme for the frequency response reserve of an individual agent, it determines the amount of power its corresponding unit is able to provide for an ancillary service product within a given product horizon. As one RES agent typically cannot meet the requirements (power quantity, reliability) alone, coalitions are formed in order to meet appropriate prequalification (foremost reliability) and overcome market entry barriers. Hence, a coalition is an aggregation of agents with the same objective, e.g. the provision of ancillary services.

4 Main Results

In Smart Nord, frequency response reserve is provided by *base coalitions* and corresponding *core coalitions* (see Figure 1). The purpose of a base-coalition is to aggregate and to represent a group of agents at an energy market. This way, agents that are not capable of providing the required amount of power for the entire delivery period of a given ancillary service product on their own gain access to the market and thus may take part in placing bids on the product. A base coalition whose bid is accepted by the market is responsible for providing the specified amount of frequency response reserve and has to guarantee that this amount can be called throughout the whole product horizon.

Core coalitions are subsets of base coalitions. Their purpose is to provide the full reserve of the coalition over a period of time shorter than the original delivery period of the frequency response product. As the quality and thus the reliability of forecasts typically increases with shorter forecasting horizons, the contribution of individual units of a given core coalition might be larger over this shorter period of time than initially anticipated within the base coalition's delivery period. Thus, a more efficient utilization of units within a base coalition can be obtained through more precise short-term forecasts. In case of an activation of an ancillary service all units in the core coalition must automatically deliver the demanded amount whereas all other units in the base coalition do not react. In other words, units being in the core coalition are actively responsible for ancillary service provision and the remaining units play a passive role until a coalition restructuring is necessary that yields a new core coalition.

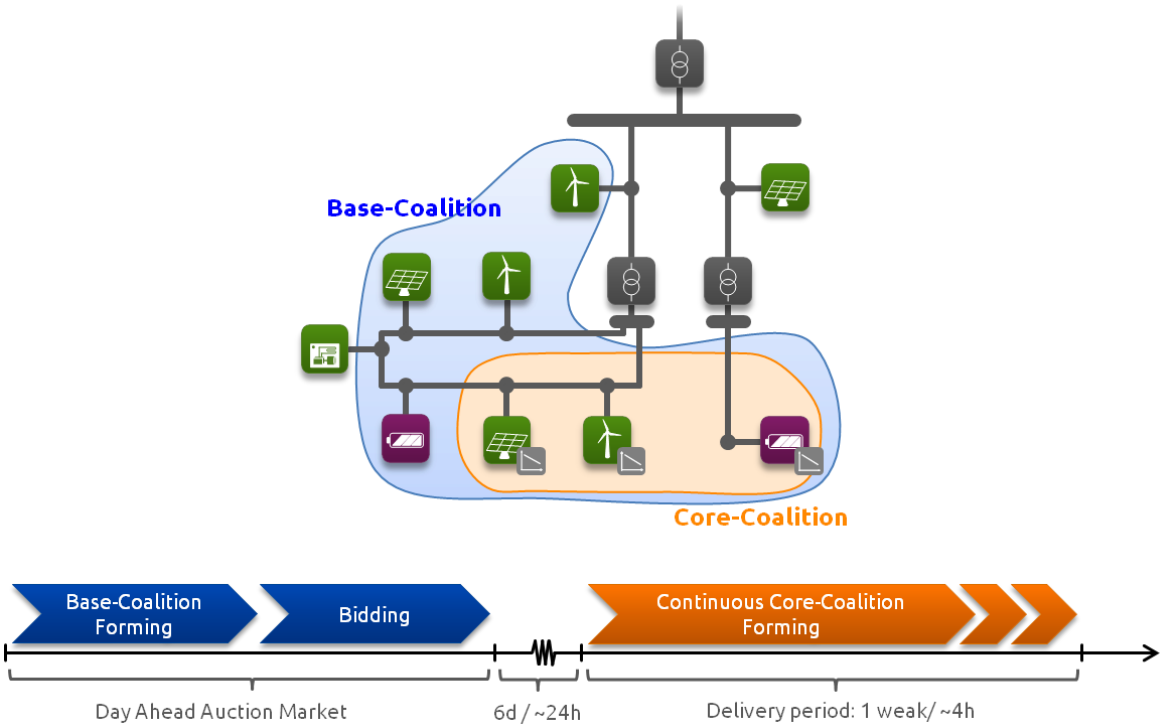

Figure 1: Market regime of base coalition and core coalition

During the product horizon internal restructuring, by identifying a new core coalition, will be necessary on a regular basis in order to guarantee the activation of the necessary amount of reserve power with at least the minimum acceptable reliability across several core coalitions and ultimately for the whole product delivery period. Figure 2 visualizes the decrease of a coalition's reliability through the increase of its forecasting errors over time and the respective reconfiguration of the coalition, i.e. the contribution of its members for different time intervals. Here, C_{Core} denotes a core coalition within a base coalition C consisting of 13 units U_i with $i \in \{1,2,\dots,13\}$.

In the following we focus on the formation of core coalitions within a given base coalition (i.e. a set of available units capable of providing the necessary amount of power) for frequency response reserve. Therefore, properties of agents participating in an ancillary service coalition and their attributes are introduced.

Each agent consists of a cost value specific to its corresponding unit expressed in ct/kW. In the long run, these costs should suffice to cover the prime costs of the unit. However, since only short-term planning is conducted at this stage in the Smart Nord project, prime costs are not yet considered but the unit should at least get financial compensation for power it cannot trade on active power markets (opportunity costs). For the sake of conceptual clarity appropriate cost factors are assumed.

The agent is assumed to know the forecast of its unit's power feed-in and consumption. Since this forecast is subject to inherent uncertainties (e.g. weather-based generation) the agent must take those uncertainties into account when planning for its unit. To this end, the agent has a model of the magnitude of uncertainties, i.e. the prediction error. Based on this, the agent calculates a reliability value. This is a measure of how certain it can provide an amount of power within a given time interval. This amount is a possible contribution to an ancillary service product. The determined contribution and respective reliability value is then communicated for the purpose of coalition formation. The reliability model is presented in work package 2.2.

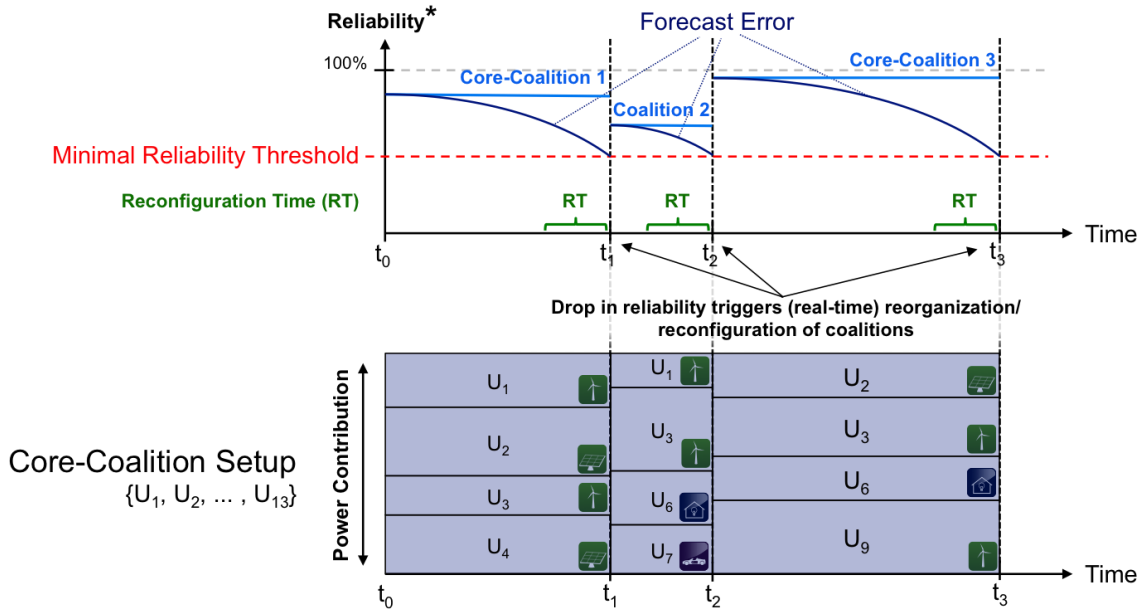

Figure 2: On-line reconfiguration of core coalitions to meet the dynamic decrease in reliability

In order to activate the amount of power being necessary after a frequency deviation triggering primary frequency control, each agent within the core coalition of a primary frequency response coalition sets the droop control parameter of its unit. This parameter determines an agent's power response proportionally to the frequency deviation as kW per Hz. As already indicated, the agents' droop control parameter is a result of the core coalition formation such that all agents within the core coalition in combination fulfil the frequency-power-droop specified in the contracted ancillary service product. Agents that do not participate in the current core coalition have a droop control parameter of 0 kW/Hz since they do not actively contribute to the ancillary service product. Small-signal stability of such distributed controller formations is investigated in work package 2.4.

As mentioned before, primary frequency control must be available up to its full amount at any moment within its appropriate delivery period. To this end, units participating in the provision of ancillary services must guarantee their ability to do so. Especially wind turbines and solar panels are subject to fluctuating weather conditions but also e.g. combined heat and power plants bear uncertainties because of the unpredictability in the thermal demand it must fulfil. The resulting uncertainties must be included into the planning process for providing frequency control reserves since those units cannot guarantee the provision of ancillary services with a reliability of 100 %. In order to take this into account a new model for reliability was introduced in [35] that reflects not only the availability of a unit to provide ancillary services but also the guaranteed amount of power. The reliability of a coalition with respect to the provision of an ancillary service product is defined as the probability with which this product is available within a product horizon under normal conditions (i.e. for instance without the existence of vicious agents or extreme weather conditions such as tornados). The model for calculating the contribution-specific and delivery-horizon-dependent reliability of a coalition is presented in the subsequent work package 2.2.

In order to demonstrate how agent coalitions can be found that provide ancillary services meeting a specific reliability target a core coalition of agents with a commitment for the provision of an ancillary service product must be identified. To this end, an optimization problem is solved, that chooses a core coalition with maximum lifespan and minimal costs based on the agents' attributes, assuring a specified reliability. For the sake of simplicity the formalization of an exemplary setup of a 4-agent-coalition is presented.

Identifying "good" core coalitions within a base coalition is a challenging task because, on the one hand, an ideal core coalition has a long lifespan such that the total amount of coalition reconstructions and therefore direct interferences with the controllers/governors of the units participating in the base coalition is kept to a minimum. On the other hand an ideal core coalition has low costs such that the overall financial gain of the base coalition is maximized. Both of these objectives conflict with one another, as becomes clear when the effect of longer coalition lifespans on reliable unit contributions and thus total coalition costs is taken into account: the maximum amount of reserve a unit can provide with a given reliability decreases the longer the considered period of time of the provision, i.e. coalitions with short lifespans can more likely be composed of a few units with low costs, whereas coalitions with longer lifespans have to include more units with potentially higher costs. This concept is schematically depicted in Figure 3.

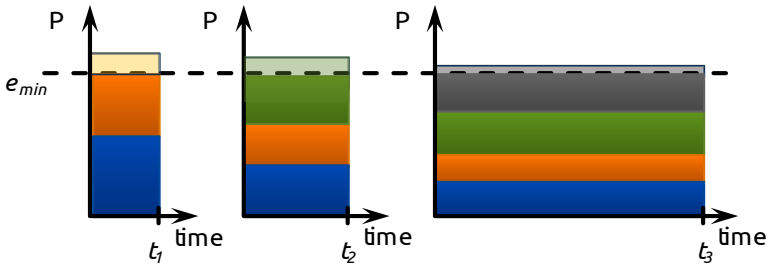

Figure 3: Core coalitions of various lengths and individual unit commitment (each colour represents an individual unit)

Three different core coalitions comprising two to four units can be chosen in order to provide the reserve e_{min}. The depicted unit contributions (colours) are assumed to be ordered by cost increasing from bottom to top. If the shortest coalition lifespan t_1 is chosen, the reserve can be provided by the two units with lowest costs. If coalition lifespan t_2 or t_3 is chosen, the contributions of these two units shrink due to decreased reliability and thus other more expensive units have to be accepted into the coalition in order to provide the reserve e_{min} fulfilling the required minimum coalition reliability. However, choosing lifespan t_1 requires the reconstruction of a new core coalition shortly thereafter thus increasing the overall management overhead.

Let $T_{pl} = [t_0, t_m]$ be the planning horizon of a core coalition formation and let $pred_a(T_{pl})$ be the short-term forecast of agent a. With t_C denoting the core coalition's lifespan, the core coalition exists during the interval $T_C = [t_0, t_0 + t_C]$. Thus, the core coalition lifespan t_C must be chosen from $[0, t_m - t_0]$ and unit contributions must be chosen from $[0, \max(pred_a(T_{pl}))]$ such that all functional and non-functional constraints are fulfilled in order to find feasible coalitions.

Let $cost_a$ denote the cost of reserve power provided by agent a. The total cost of the reserve provided by a core coalition during its lifespan can then be expressed as

$$cost_C(T_C) = t_C \sum_{i=1}^{n} e_{cont,a_i}(T_C) \cdot cost_{a_i} \quad (1)$$

A straightforward approach for the identification of "good" core coalitions is to solve the optimization problem described above using a solver like IBM ILOG CPLEX. This approach comprises the following two optimization steps:

First, in order to identify core coalitions with maximum lifespan that are able to provide the amount e_{min} of reserve power at least with the reliability ρ_{min}, a cost value $acceptableCost$, has to be

preconfigured, which serves as an upper bound for the total core coalition cost. Then, the following optimization problem has to be solved yielding the maximum coalition lifespan t_{max}.

$$\begin{aligned} &maximize\ t_C \\ &subject\ to:\ cost_C(T_C) \leq acceptableCost \\ &\rho_C(T_C) \geq \rho_{min} \\ &e_{cont,C}(T_C) \geq e_{min} \end{aligned} \tag{2}$$

In a next step, the coalition costs are minimized by solving the following optimization problem yielding pareto-optimal contributions for each agent.

$$\begin{aligned} &minimize\ cost_C(T_C) \\ &subject\ to:\ t_C = t_{max} \\ &\rho_C(T_C) \geq \rho_{min} \\ &e_{cont,C}(T_C) \geq e_{min} \end{aligned} \tag{3}$$

The latter two constraints in equations (2) and (3) take into account the reliability requirements introduced in work package 2.2.

In the following example the method proposed so far will be applied to the low-voltage grid shown in Figure 4.

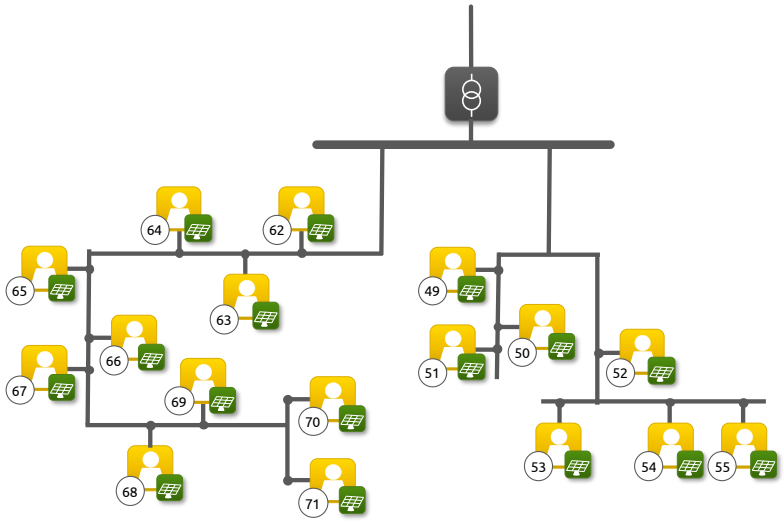

Figure 4: Low-voltage grid exemplary setup

It consists of 17 nodes: each connected to a PV unit, which is monitored and controlled by an agent. For the sake of conceptual clarity, the forecasts and prediction error models of all units are identical and linear: $pred_a(t) = 3 + 0.01t$ and $\sigma_a^2(t) = 0.01 + 0.01t$. Setting the planning horizon to $T_{pl} = [0, 5]$ it is obvious that all possible coalitions of at least four units should be able to provide a reserve of $e_{min} = 10$ kW, at least for a couple of short-term planning time steps. Agents 62, 63, 64 and 65 have a cost value of $c_1 = 25$ and all other agents have a cost value of $c_2 = 30$. The required reliability target for the ancillary service product to be provided by the agent coalition is $\rho_{min} = 0.9$. Choosing an acceptable cost value of $maxCost = 900$ for the first optimization step yields the coalition $C_1 = \{49, 62, 63, 65\}$ with lifespan $t_{C_1} = 3$ and costs $cost_{C_1}(T_{C_1}) = 765.0$. As expected the second optimization step then chooses the coalition with

lowest costs yielding the coalition $C_2 = \{62, 63, 64, 65\}$ with lifespan $t_{C_2} = 3$ and costs $cost_{C_2}(T_{C_2}) = 750.0$. The contributions of the agents are 2.58, 2.42, 2.42 and 2.58 kW. Both resulting coalitions have a reliability of $\rho = 0.99$.

5 Conclusion and Outlook

In this work package we have developed a reconfiguration scheme made up of base and core coalitions continuously replacing one another in order to hold available the necessary frequency response reserve initially contracted by the base coalition. This continuous reconfiguration facilitates the utilization of high-precision short-term power forecasts, which were unavailable at the time of base-coalition formation. In the basic example, the continuous optimization problem is solved with a central IBM ILOG CPLEX solver. This central optimization scheme can be easily distributed onto a multi-agent-based system using the contract-net protocol introduced in sub-project one. Due to page limitations this has not been shown here. However, as with all heuristic relaxations optimality and goodness become a challenge that have only been addressed preliminarily and will be subject to on-going work.

Work Package 2.2: Reliable Contribution Planning and Risk Management of Coordinated Coalitions for the Provision of Ancillary Services

Marita Blank[32] and Sebastian Lehnhoff[33]

1 Goals and Integration in the Sub-Project

System stabilization in form of short-term activation of provided power reserves, e.g. for frequency stability are necessary for secure and reliable operation of the electrical power system. Power plants that take over those tasks must fulfil certain pre-qualification tests such that it can be proved that certain minimum technical requirements are given, as specified e.g. in the ENTSO-E handbook [21].

In order to provide such system-critical services by coordinated coalitions of distributed energy resources (DER) reliable and stable system operations have to be guaranteed. Thus it is necessary to be able to make statements about the reliability taking into account the volatile and stochastic behaviour of DER. Therefore, the aim of work package 2.2 is to develop a procedure to determine the reliability with which ancillary services can be provided by coordinated coalitions such that it can be incorporated during planning the individual contributions units can make for an ancillary-service product. Accordingly, this can be included in the coalition formation process of work package 2.1. The possible contributions depend on actual forecasts for the units' power feed-in or consumption. Different factors influence the reliability of contributions. Those factors must be identified and a method for reliability assessment must be developed that incorporates these factors. This method is the basis for evaluating a coalition regarding its ability to fulfil given reliability requirements.

Furthermore, a model must be developed to assess the remaining risk when coordinated coalitions are utilized to provide ancillary services. With this not only the risk can be estimated but also requirements for coalition formation for work package 2.1 can be given.

2 Related Work

As pointed out in the previous section, two main topics are in the focus of work package 2.2: first, the planning of contributions for a reliable provision of ancillary services by coordinated coalitions of DER, and second, risk assessment of ancillary-service provision by those coordinated coalitions.

The usage of probabilistic methods for reliability assessment of the electrical power system and according models have been developed (see e.g. [22], [23]) and improved during the last decades to enable simulative evaluation (e.g. [24], [25]). However, these methods mainly refer to operational equipment and different load situations in order to estimate reliability indices. They do incorporate probabilistic models of loads and generators but they do not investigate how single units can provide ancillary services. In [26] it was investigated how wind park pools can prepare bids for tendering proposals together with the development of verification procedures for prequalification for the provision of frequency control reserves based on probabilistic forecast methods. Additional work for assessing the capability of wind turbines for the provision of frequency reserves has

[32] University of Oldenburg, 26129 Oldenburg, Germany,
marita.blank@uni-oldenburg.de, Department of Computing Science
[33] OFFIS – Institute for Information Technology, 26121 Oldenburg, Germany,
sebastian.lehnhoff@offis.de, R&D Division Energy

appeared (e.g. [27]). Uncertainties of forecasts and corresponding statistical models can be incorporated in the dimensioning of frequency control reserves [28]. This may also lead to dynamic dimensioning of control reserves [29]. This shows that statistical and dynamic models gain more acceptance in the operation of the power system. However, methods for assessing the reliability of ancillary-service products by distributed coalitions are still lacking.

For risk assessment of real systems simplified models are used in order to identify and represent relevant interrelations. In [30], a common methodology is presented for different domains and different technical systems to assess risk as a function of frequency and consequence. In [31] a corresponding model is given for ICT-systems. Furthermore, the method of Value-at-Risk (VaR) modelling already is used for dimensioning frequency control reserves but it also finds attention for scheduling of virtual power plants [32] and on energy markets [33], [34].

3 Methodology

In this section, an outline of the methodical approach is given that was conducted in work package 2.2. A process model is visualized in Figure 5.

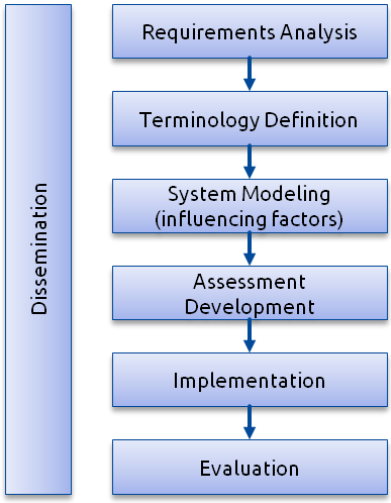

Figure 5: Process model for reliability and risk assessment modelling

As stated in the previous section, one of the main tasks of work package 2.2 was to develop a method for assessing the reliability and remaining risk with which a coordinated coalition can provide an ancillary-service product. To this end, in a first step the requirements given by an ancillary-service product that must be fulfilled by a coalition were analysed as well as the resulting requirements for reliability and risk assessment. The main requirements are (more detail can be found in [35]):

- a coalition is able to provide a constant amount of power during a given product horizon,
- the power can be activated within a certain amount of time.

Based on that and after an extensive inquiry of definitions and techniques from e.g. power engineering, information technology, and related domains [36], [37], [38], [23], [31] a definition of reliability in the context of the sub-project was derived:

- Reliability of a coalition with respect to the provision of an ancillary-service product is the probability with which this product is available within a product horizon under normal operational conditions.

As a next step, factors were identified that influence a coalition's reliability. Those are factors regarding the behaviour of units as well as their position. The behaviour is characterized by failures and forecasts with according forecast errors. The position of a unit can be distinguished between spatial and topological position. The first is according to the geographical position of a unit, which influences correlations between different units. The topological position relates to the grid node a unit is connected to and with that implicitly to the availability of operational equipment.

Those factors must be incorporated into the process model for assessing a coalition's reliability and is therefore part of the hierarchical model shown in Figure 6. Although those factors have influence on the reliability of a coalition, they are referred to as *non-influenceable factors*. The reason for this is that the model reflects the view point of a coalition-formation strategy that has no impact on those factors. However, there are some adjustments that can be used, termed as *influenceable factors*. Those are the lifespan of a coalition, the contribution of each unit, and the reliability level a coalition wants to fulfil.

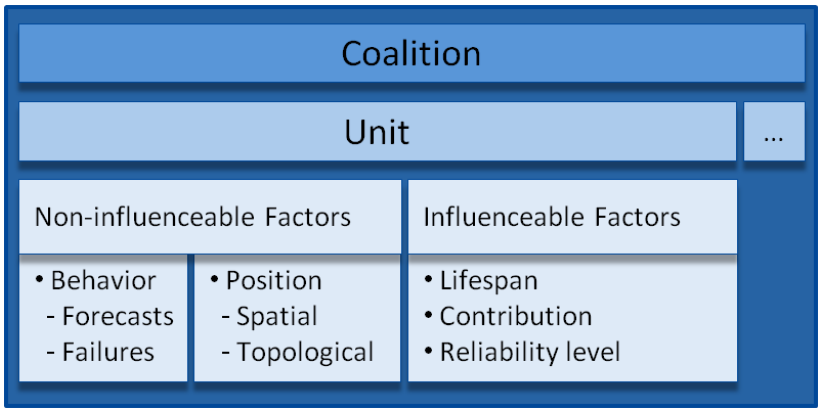

Figure 6: Hierarchical model for reliability assessment of a coordinated coalition

Furthermore, a model for risk assessment has been adapted from [31] (see Figure 7). Here, risk defined as the probability of the event that the needed amount of power of the ancillary-service product cannot be delivered – depending on the frequency of demand – together with the according amount of power. Additionally, the methods have been implemented and evaluated. During the whole project period, the models and results were published.

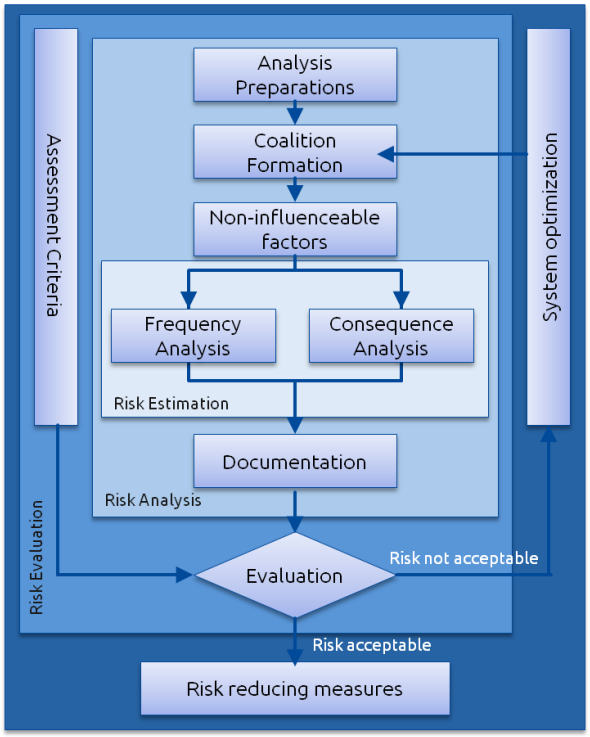

Figure 7: Model for risk assessment adapted from [31]

4 Main Results

The two main results of work package 2.2 are assessment models for both, reliability assessment and risk management for coordinated coalitions.

The model for reliability assessment is designed in a modular way, i.e. not all of its attributes must be taken into account at once. Additionally, more attributes can be added to the model. According to the model in Figure 6, for each member unit U of the coalition the failure rate must be known in order to compute the probability of a failure $\mathbb{P}(\text{fail}(U))$. Since the event of a failure of one unit is assumed to be independent of failures of other units, the according reliability of a coalition C amounts to

$$\rho_{\text{fail}}(C) = \prod\nolimits_{U \epsilon C} \big(1 - \mathbb{P}(\text{fail}(U))\big). \tag{4}$$

Furthermore, it is assumed that for each unit an error model of power predictions is known. This model gives a distribution of prediction errors for different prediction horizons. The knowledge about the error model is the foundation of reliability assessment of a unit with respect to its contribution to an ancillary-service product. The reliability is the probability that a deviation from the prediction, noted as X, does not exceed a certain amount x, i.e. $\rho(U) = \mathbb{P}(X \geq x)$. A specification of a unit's error model and the deduced reliability of a unit's contribution can be found in [35]. Furthermore, the effect of the influenceable factors (see Figure 6) on the reliability of a single unit is discussed in [35], too.

For reliability assessment of a whole coalition the dependencies between its member units must be taken into account. This can be derived by the positions of the units. As shown in Figure 6, it has to be distinguished between spatial and topological positions.

As mentioned earlier, the spatial position is reflected by the geographical position of units. According to the position of units they may be under the same external influences such as weather conditions. For the spatial consideration, the units within a coalition are classified according to

their technology (PV, wind) since it is assumed that the dependency of weather influences on different technologies is negligible (wind does not influence PV output as the sun has no impact on wind generation). However, the geographical coordinates of the units' positions are not enough information since this does not necessarily include knowledge about topographical traits. Hence, the dependency is directly inferred from the correlations between units. To this end, time series of power feed-in must be available of all units. In order to minimize computation time but include as much information as possible during reliability assessment of a coalition, an algorithm was developed for clustering the units within a coalition with respect of how strongly correlated they are; details can be found in [39].

From the knowledge about correlations between units together with their individual error models, a joint error model can be derived. The reliability is the probability that all units do not exceed a certain deviation from their prediction, i.e.

$$\rho_{\text{spatial}}(C) = \mathbb{P}(X_1 \geq x_1, \dots, X_n \geq x_n). \tag{5}$$

The statistical model of so-called copula functions provides flexible techniques to describe joint distribution models where no special assumptions on the single error models are necessary. From this joint error model a joint survival model can be derived. With this the reliability of a whole coalition with respect to a contribution can be estimated. A detailed presentation of this procedure is given in [40]. Furthermore, in [40] the effects on the reliability of a coalition were shown if correlations are included in the process of reliability assessment. Figure 8 shows a part of the result. Taking into account correlations for reliability assessment (compared to the assumption of uncorrelated behaviour) the reliability of a coalition is higher. This effect increases with higher correlation coefficient. Furthermore, the influence of correlations is higher if prediction errors are higher, but also if the contributions of units are similar shares compared to the prediction.

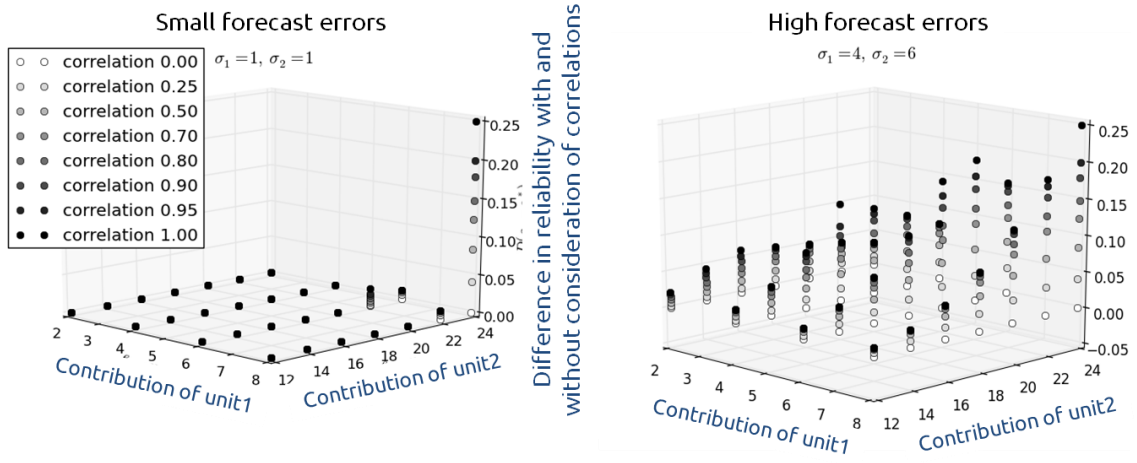

Figure 8: Influence of considering correlations within the reliability assessment process

For reliability assessment according to the topological position the grid topology of the sub-system the units are connected to must be known as well as the assignments of units to the nodes and the probability of failure $\mathbb{P}(\text{fail}(E))$ of operational equipment E. The topological reliability plays a major role in radial systems where the n-1 criterion does not hold. A coalition cannot provide an ancillary-service product to its full extent if one or more of its member units are disconnected from the system. With methods from graph theory, the minimal cuts of all units from the slack node of

the sub-system can be determined. Thereafter, the intersection of the cuts of all units K_C is computed. With this, the probability that at least one unit is disconnected from the system and hence the product cannot be delivered due to failures of operational equipment can be estimated. Based on that, the reliability with respect to grid topology can be computed

$$\rho_{\text{grid}}(C) = \prod\nolimits_{U \epsilon C} \big(1 - \mathbb{P}(\text{fail}(E))\big). \tag{6}$$

As mentioned before, the modules of units' failure rate, unit error model, spatial dependency (correlation between units), and topological dependency can be incorporated during coalition formation within the planning process to determine the contribution of a coalition's member units. Thereby, the modules can be considered separately, in an integrated way, or only some modules can be used in combination. Involving all components yields the overall reliability

$$\rho(C) = \rho_{\text{spatial}}(C) \cdot \rho_{\text{grid}}(C) \cdot \rho_{\text{fail}}(C). \tag{7}$$

For the task of risk management, the process for risk estimation, analysis and evaluation has been adapted from [31] and is shown in Figure 7. The system under investigation is the coalition formation process with its constraints and requirements (minimum contribution, minimum product horizon, minimum reliability level). The risk given by this is that power demanded for an ancillary-service product cannot be delivered and with that system stability is at stake. Since the amount of power needed depends on external measures, such as system frequency, this must be incorporated in the risk-estimation step, where the frequency of power not delivered and the amount of power are determined using simulations. Risk estimation for the case of primary frequency control is shown in Figure 9.

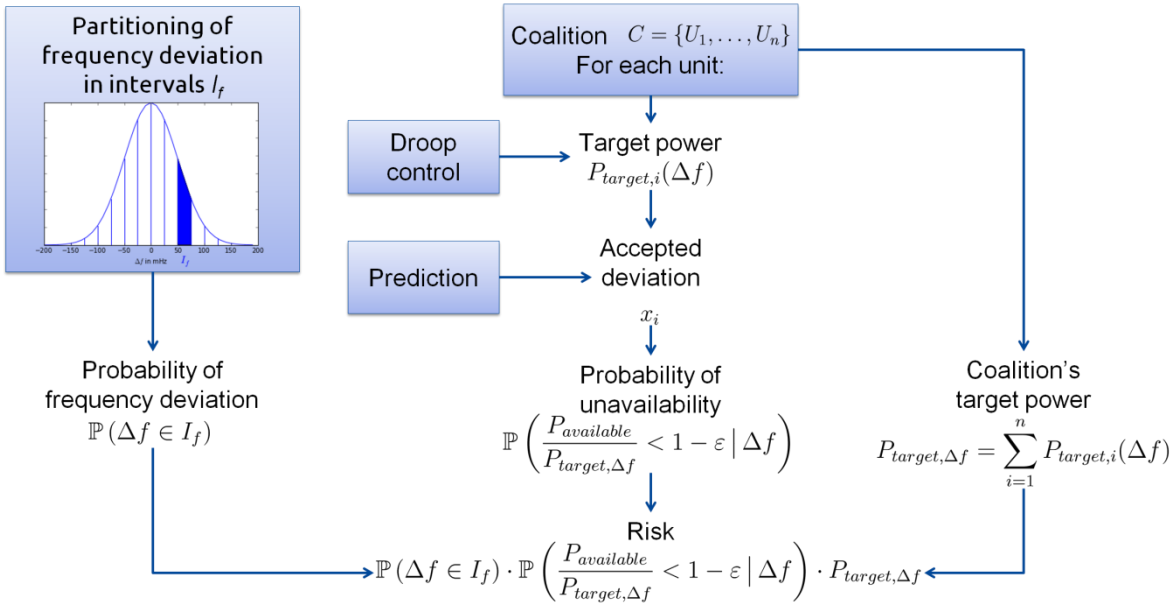

Figure 9: Steps of risk estimation of an ancillary-service coalition

The risk amounts to

$$\text{risk} = \sum\nolimits_{I_f} \mathbb{P}(\Delta f \epsilon I_f) \cdot \mathbb{P}\left(\frac{P_{available}}{P_{target,\Delta f}} < 1 - \varepsilon \,\middle|\, \Delta f\right) \cdot P_{targe,\Delta f}, \tag{8}$$

where I_f is one of equidistant intervals between the acceptable frequency deviation Δf of ±200 mHz, P_{target} is the power demanded for the given frequency deviation, and $P_{available}$ denotes the actual available amount of power that can be provided for the power product. Details on that case can be found in [41]. It is based on the joint survival model, but this can also be done using Monte-Carlo simulation. The results of the risk estimation must be prepared and visualized in order to evaluate the resulting risk against external criteria such as acceptable risk. If risk is not acceptable, the system must be optimized, e.g. the constraints for coalition formation can be relaxed.

5 Conclusion and Outlook

In work package 2.2, a method was developed to assess a coordinated coalition with respect to how reliable it can provide an ancillary-service product within a certain time horizon. It can be incorporated in the coalition formation process developed in work package 2.1. The reliability assessment incorporates uncertainties given by the volatile and stochastic character of DER as well as correlations between the units. Furthermore, the availability of units and operational equipment in power grids are integrated in the method. The method could be extended by taking account of availability of hardware-, ICT-components, and software systems, too. Moreover, the concepts can be used for assessment of active power products considered in sub-project one. However, the requirements are different and the method must be adapted accordingly.

Furthermore, a model for risk assessment has been developed to determine the risk resulting from providing ancillary services by coordinated coalitions of DER with regard to services that cannot be delivered and to identify possible adaptations to reduce the risk. The risk-estimation step in this model can also be the basis of simulative investigations using design of experiments where the requirements for coalition formation are parameterized differently in a structured way. This can be used for a Value-at-risk assessment in order to find the best combinations of requirements for coordinated coalitions.

Work Package 2.3: Interoperability and Performance Issues of Coalition Formation for Ancillary Services

Robert Bleiker[34], Sebastian Lehnhoff[34], Klaus Piech[34] and Mathias Uslar[34]

1 Goals and Integration in the Sub-Project

The main objective of work package 2.3 was supporting the overall project consortium by implementing a consistent and standardized infrastructure. Therefore international industrial standards, i.e. the Common Information Model (CIM), IEC 61850 and OPC Unified Architecture (OPC UA) were used to guarantee unified and vendor independent interfaces and standardized message handling within the multi-agent system (MAS) of Smart Nord. Advantages in using established standards are acceptance, exchangeability, reusability and portability. CIM and IEC 61850 are automated machine-to-machine (M2M) communication standards whereas OPC UA is a M2M communication-protocol (M2M communication standards define the syntax and sets of rules for the communication whereas M2M communication protocols are sets of predefined steps to communicate from machine to machine). To support the organization of coordinated coalitions within the multi agent-system a directory-service was required, to store and provide relevant information about active and available units within the system.

Out of these requirements the following main and sub-goals have emerged:

1) Providing the Smart Nord consortium with the means to rely on international automation standards.
2) Facilitate portability of the overall project results beyond the funding duration of Smart Nord.

2 Related Work

The current transition process in the electric utilities domain and power systems in general aims at establishing the so called Smart Grid combining different views, definitions, and aspects of existing concepts in the electric energy domain. One aspect appears to be a commonality between all existing definitions: the increasing use of Information and Communication Technologies (ICT) in order to support automation and energy distribution functionalities for Energy Management Systems (EMS) and Distribution Management Systems (DMS). The result of an integration of those two technological scopes will be an increasingly complex and highly dynamic power system with a multi-dimensional infrastructure.

Looking at other domains, e.g. commerce, manufacturing or logistics, the introduction of ICT-based technologies and mechanisms yield profound changes in the processes behind core services and businesses. When looking at industrial automation, strong parallels to the utility domain become apparent. Both application domains are characterized by monolithic software systems and their processes. In industrial automation, the introduction of reusable software components replaced this approach. Thus, standardized interfaces became more and more important to avoid costly and labour intensive integration work. Furthermore, the need for high performance Human Machine Interface (HMI) and Supervisory Control and Data Acquisition (SCADA) applications and their vendor-specific proprietary interfaces required the development of appropriate standards

[34] OFFIS – Institute for Information Technology, 26121 Oldenburg, Germany
{forename.surname}@offis.de, R&D Division Energy

in terms of both syntax and semantics. For this purpose, joined vendor-driven initiatives like the OPC Foundation established basic building blocks.

Initially, the OPC task force aimed at creating a standard for accessing real-time data based on Microsoft's OLE/DCOM technology for Windows operating systems. This work resulted in the creation of the OPC Classic, which is the prevailing standard in industrial automation, today [42]. OPC Classic covers aspects like data reading, writing and supervision of procedures (OPC Data Access), sending alarms (OPC Alarms & Events) and accessing saved historical process data (OPC Historical Data Access). Furthermore, extensions to those basic building blocks exist (OPC Complex Data, OPC Batch, OPC Data exchange) and some first platform-independent specifications for web service-based interaction (OPC XML-DA).

In [43], the ten most important drivers to create the new OPC Unified Architecture (UA) are discussed, among which the end-of-life cycle of COM/DCOM, the rising need for Internet-based communication, platform-independence, and using a common information model are listed as the most prominent factors. Future Smart Grids emphasize the (at least) partial coordination of a large number of stochastic appliances to balance consumption and generation of electrical energy. Due to the sheer number and complexity of the overall system automated means of measurement and (partially unsupervised) control are indispensable.

A vivid example of the need for automated monitoring and control is the supervision and operation of offshore wind farms using the example of the German "Alpha Ventus", which is the first German offshore installation that was constructed on the high seas. The pilot project is located some 45 km from the coast of Borkum and provides fundamental experience not only in the construction of an offshore wind farm but also on the operation of such a system that may not be directly accessible due to varying weather conditions. Twelve 5 MW class wind power turbines are operating at the Alpha Ventus test field: six AREVA Wind M5000 turbines and six REpower 5M turbines, resting on two different foundations. Whereas the AREVA wind turbines stand on tripods, the REpower turbines are mounted on jacket foundations in a water depth of 30 meters. In order to provide the required wind yield – which is considerably higher compared to its onshore counterpart – to compensate for the significantly higher investment and operational costs individual turbines have to be monitored in real-time and appropriate control actions optimizing turbine configuration (angle, speed etc.) have to be calculated and taken immediately.

3 Methodology

Figure 10 shows the overall communication and organization structure between agents and units in Smart Nord. Here the units have CIM- and IEC 61850-based interfaces. To communicate with the units OPC UA has been identified as a common interface for all agents who have to read and write values to their respective unit. To communicate through OPC UA with the units a domain-specific information-model for OPC UA Servers is needed. Creating CIM- and IEC-based information-models is very time-consuming and thus should be created automatically. To solve this automation issue two different kinds of mappings for CIM- and IEC 61850-based models to OPC UA have been created.

For creating coalitions within the multi-agent system a directory-service was implemented to support a high-performance coalition forming (see Figure 10). The directory-service stores topological data as well as unit parameters, which allows identifying units with specific properties within a specific (electric) distance through simple search requests.

In order to facilitate a unified communication within the multi-agent system a CIM-profile was created. Since the messages are XML-based, the CIM-objects have to be serialized to XML for creating the message and back again into CIM-objects by de-serializing the XML-message using an

XML Schema Definition (XSD). The XSD-file is generated from the CIM-profile and describes the structure of the XML-nodes. Utilizing a basic CIM-API agents can de- and serialize CIM-objects for standard-compliant communication.

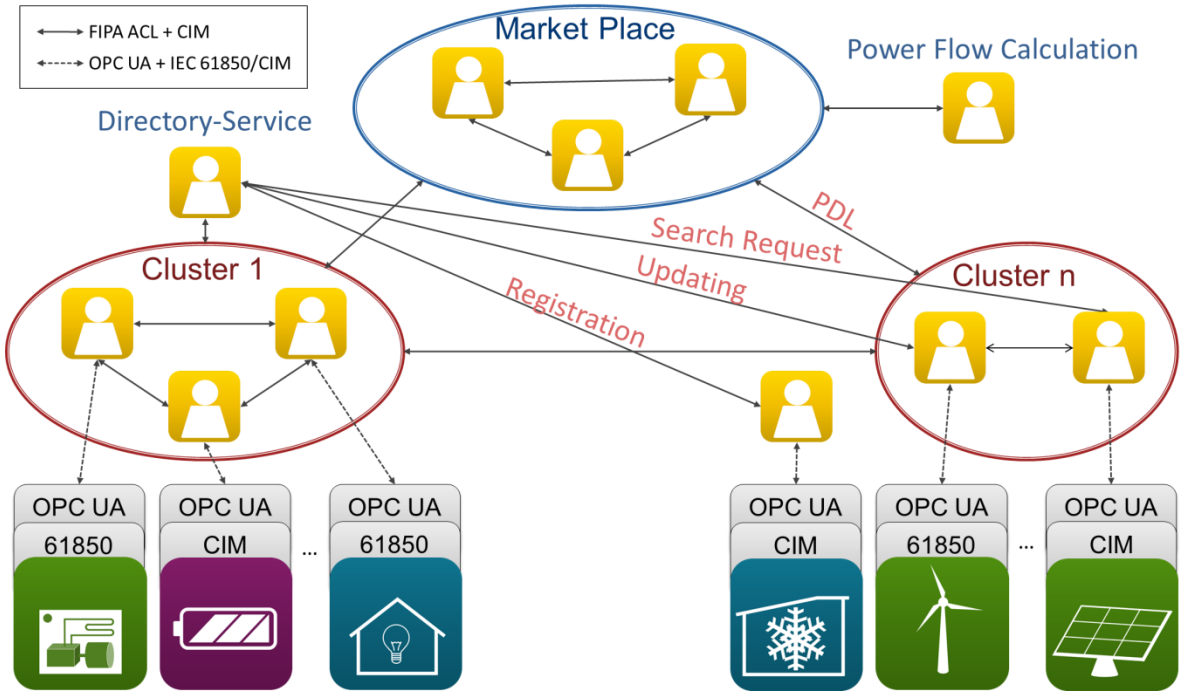

Figure 10: Communication and organization within Smart Nord

4 Main Results

In order to support the project consortium with international standards a software tool named UMLbaT[35], which stands for UML based Transformation, has been created to provide units with a common OPC UA interface. UMLbaT automatically creates domain-specific information models from IEC 61850 or UML data models for OPC UA Servers. It creates a so-called OPC UA NodeSet, which includes all the necessary nodes to represent the domain-specific model for building an OPC UA Server (see Figure 11). UMLbaT is based on CIMbaT – CIM based Transformation [42]. To achieve the project goals, CIMbaT has been redesigned in order to extend the CIM-based mapping to the context of Smart Nord. In addition, a mapping for creating IEC 61850-based information models has been created to support unit instances, which are based on IEC 61850. For more information about this NodeSet generation, please refer to [44] and [45]. After creating an OPC UA NodeSet file with UMLbaT, the file has to be loaded into an OPC UA Server for creating domain-specific unit-instances. These unit servers can now be used to establish communication between the units and their appropriate agents as well as for the purpose of setting up the simulation environment mosaik[36] (for establishing connections with all the instances of simulated units – please refer to the description of sub-project one for more details on Smart Nord's simulation environment). Finally, the multi-agent system will instantiate the agents for each unit-instance. For more information describing this process please refer to [46] and [47]. In order to support this generic and standard-compliant process, the UMLbaT-binaries have been made available as freeware online at www.umlbat.de.

[35] www.umlbat.de
[36] https://mosaik.offis.de/

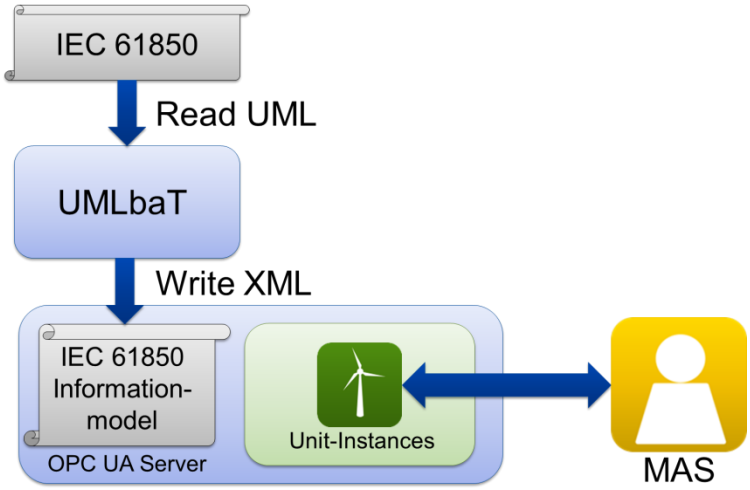

Figure 11: UMLbaT – workflow of creating an IEC 61850-based information model

For the communication within the multi-agent system as well as between the agents and the directory-service CIM was used. To create messages with all the needed information the CIM class-model has been extended to support generating appropriate CIM-profiles. Figure 12 shows the CIM-class as well as the created Smart Nord classes for describing market operations.

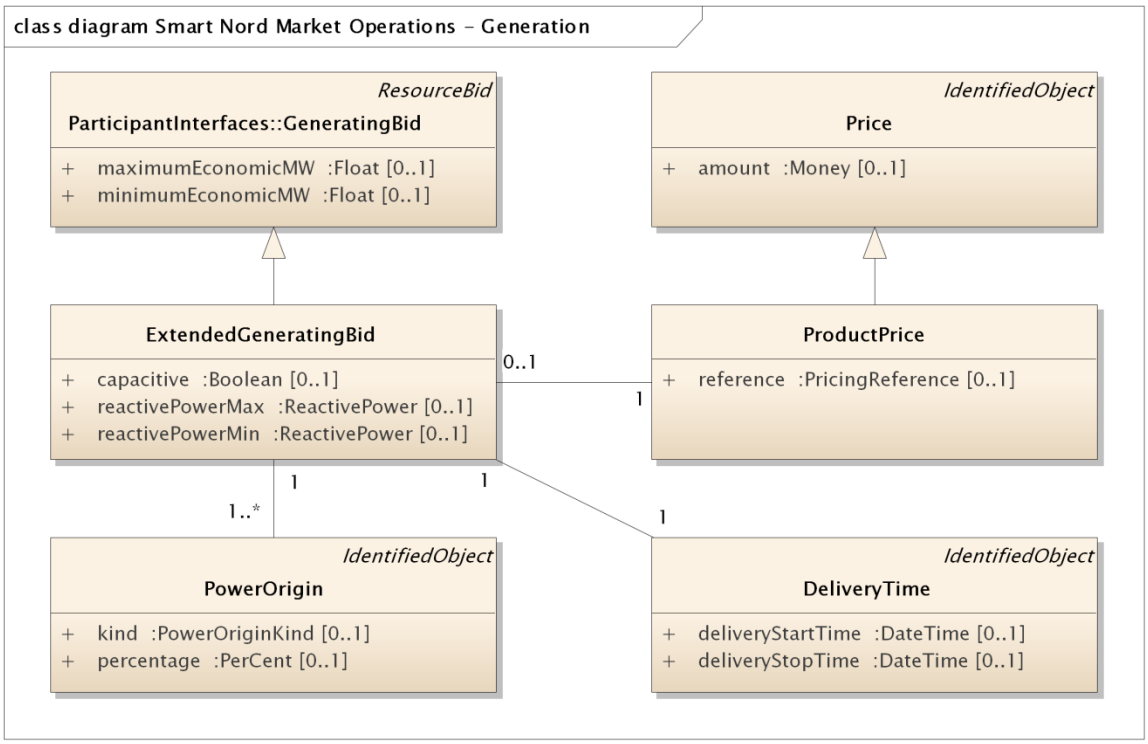

Figure 12: Class diagram – Market Operations

Four relevant packages have been added into the CIM class-model:

1) SmartNordAgents – Classes and parameters for describing an agent,
2) SmartNordDomain – Classes for describing data types, e.g. the AID (agent ID),
3) SmartNordMarketOperations – Classes for describing market-transactions, e.g. bidding,
4) SmartNordYellowPages – Classes for describing the search-requests to the directory-service.

For the Smart Nord CIM-profile these four packages and relevant CIM-classes have been combined to generate an XML Schema Definition (XSD), which is necessary to automatically generate all the necessary JAVA-classes for the de- and serialization of CIM-objects.

The directory-service is represented by a so-called "yellow-pages agent". This agent has the same parent-type as the other agents with the exception of an embedded database to store the information about the parameters, locations and distances between all registered units. The main purpose of the directory-service is to support the coalition formation by making available topological information to all agents within the Smart Nord system. The yellow-pages agent implements three main functions to make this possible:

1) Registration – An agent sends a request for registration with his identification, unit parameters and the distance values from the unit.
2) Sign-Out – When a unit stops its service (e.g. removal) the responsible agent will sign-out the unit and the stored data will be deleted.
3) Status-Response – In a specific interval the agents send a message about the state of their unit. If the unit is available the directory-service will create a new timestamp for its availability.
4) Search-Request – To get the information of units with specific properties, which are nearby an agent can send a unit type request stating the maximum distance receiving all agents' IDs, which are located within this range. The result may be used by the agent to send a message to the specific agent-ID for making a request for coalition forming.
5) Updating – If for instance a unit is unavailable (for a limited amount of time) for joining coalitions the agent in authority can update the state accordingly.

Security and data protection are important issues in data collection and M2M communication. Therefore a concept has been developed to identify the possible issues, which can occur in using a directory-service. It is described in work package 1.5 of sub-project one.

5 Conclusion and Outlook

With UMLbaT it is possible to create CIM and IEC 61850-compliant information models for OPC UA Servers automatically facilitating interoperable M2M communication and organization processes within Smart Node. This facilitates the usage and portability of concepts, models and algorithms developed in this project in ongoing (potentially third-party) projects and developments. While some steps, e.g. creating OPC UA servers, required manual loading and execution of appropriate data models and mapping tools, performing these tasks automatically for large numbers of devices will be the next step to automate more complex smart grid system instantiations, e.g. for the purpose of simulation.

Because of limited resources within this work package aspects for security and data protection for the directory-service have only been taken into account on a conceptual level. It is important to maintain data integrity and to integrate security measures for handling unauthorized data access into the Smart Nord System before taking the next step of putting these project results to practical tests.

Work Package 2.4: Small-Signal Stability of Frequency-Response Coalitions

Mauro Calabria[37] and Walter Schumacher[37]

1 Goals and Integration in the Sub-Project

The configuration derived in work package 2.1 delivers an optimal coalition which is able to provide frequency response reserve mimicking a large power plant. However, the actual injection of power in the low-voltage grid is done decentralized, based on local measurement of terminal quantities of the own power plant only, which could lead to instability caused by different synchronization phenomena between the power inverters present at each unit. This is caused by the internal control systems of the inverters, since each unit has to synchronize itself locally with the grid but also has a retroactive effect by injecting energy into the grid. The coupling of many inverters through the power grid hinders the synchronization, since each inverter tries both to estimate and modify the state of the grid at the same time. Improvements on the control algorithms of the inverters reduce these problems, but the electric coupling and the selection of the droop parameters are still decisive factors on the stability of the system.

The goal of work package 2.4 is to guarantee the small-signal stability of the optimal coalitions formed in work package 2.1, without modifying any of the parameters resulting from the optimization. The control algorithms of the inverters have to be adjusted in a way that the costs, reliability, and the system's response proportionally to the frequency deviation do not change, yet the interactions that arise from the synchronization of several generating units do not jeopardize the stability of the system.

Furthermore, a lumped model of the low-voltage grid with distributed generation must be derived, which encapsulates all significant attributes of the system with a simplified structure. This allows for a hierarchical integration of the behaviour of the low-voltage grid into simulations of the medium-voltage grid in sub-project three.

2 Related Work

The interaction of several distributed generators in a low-voltage grid and its effect on the small-signal stability of the system have been extensively studied for microgrids and other fixed systems with parallel inverters [48], [49], [50]. However, the stability analysis is usually done for given configurations, while few generalized models such as the one shown in [51] for a microgrid can be found in the literature.

Some authors consider stability constraints as part of the optimization problem when forming a coalition [52], [53], but this seriously restricts the parameter space, which limits the achievable coalitions.

Furthermore, there are none or very little references regarding the massive implementation of stable distributed generation and its participation on the provision of ancillary services. An integrated study of coalition-formation and small-signal stability in low-voltage grids such as the one presented here was missing up to date.

[37] Technische Universität Braunschweig, 38106 Braunschweig, Germany,
{first initial.surname}@ifr.ing.tu-bs.de, Institute of Control Engineering

3 Methodology

When studying the stability of a system with distributed generation, three factors are crucial in the analysis, namely the electrical coupling between generators, the chosen droop gains, and the dynamics of each power source.

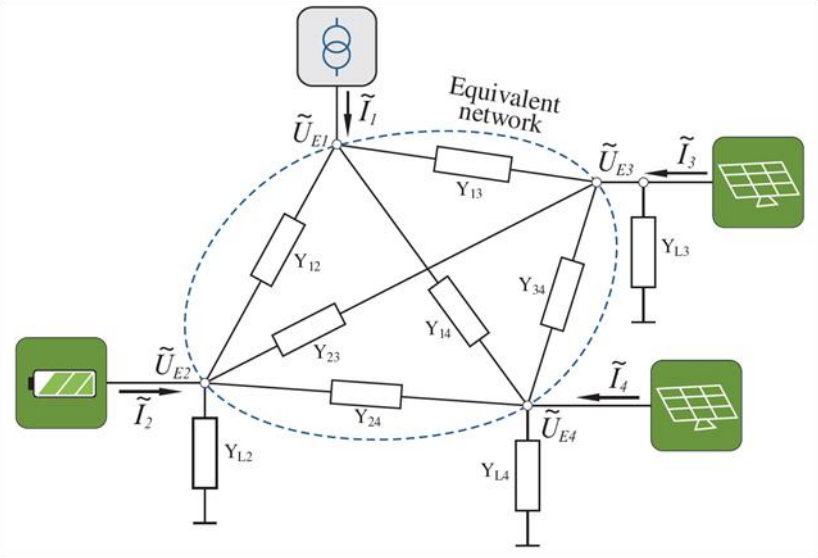

Figure 13: Equivalent representation of the grid with distributed generation

Although a valid grid model is in this sense of importance, modelling the whole network or even a detailed section of it comprises vast calculation power, while not gaining much insight into the functioning of the system itself. One way of simplifying a distribution network is by grouping sets of passive nodes and deriving equivalent admittance parameters. This method is essentially a Kron reduction of the network matrix and allows for a compact representation of the grid. Further mathematical details of this method applied to electrical networks can be found in [54]. An equivalent network is then derived using this approach, obtaining a reduced representation of the grid in form of an *n*-Port network which only considers those nodes where frequency response reserve is available, i.e. the nodes to which the units within the coalition are connected. A schematic diagram considering a coalition with only three units can be seen in Figure 13. The interface to the medium-voltage grid is represented by the transformer.

The resulting equivalent *n*-Port network is hence a function of the complete network model and the selection of the *n-1* units that form the coalition. The dynamics of the power flow between nodes can be modelled considering this equivalent coupling together with the dynamics of each unit and the chosen droops. A MATLAB script was written using this information, which implements a heuristic to analyse the stability of the coalition and an optimization algorithm which tunes the dynamic responses of the power units by means of an improved droop [55] in order to better damp the system or even stabilize it in case of instability.

This methodology can be better understood with the diagram shown in Figure 14. Note that a warning should be issued if a coalition results unstable even after tuning the improved droops, and the coalition-forming algorithm would have to be run again to find a different coalition. However, all the coalitions built and tested under the realistic scenarios within this project have been effectively stabilized with the approach developed in this work package, and hence no warning has ever been issued.

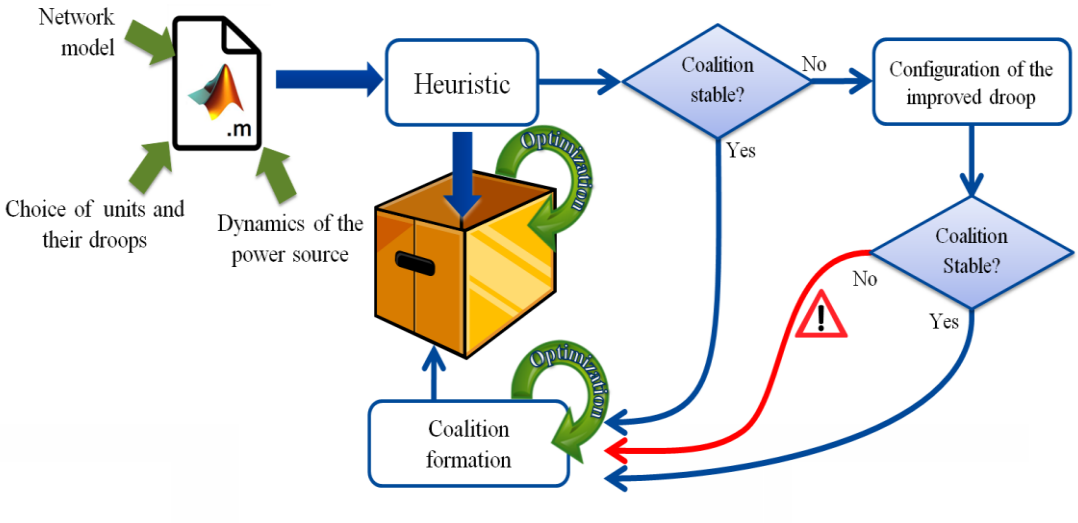

Figure 14: Methodology of the work package within the sub-project two

4 Main Results

The main results within this work package are threefold. On the first hand, a compact nonlinear model for the stability analysis of distributed generation was derived. Using this model, two algorithms enable the optimal configuration of the improved droops, which enhance the dynamics of the system. Finally, a reduced-order model reproduces the dynamic response of the low-voltage grid as seen from the medium-voltage grid in a simplified manner, which allows for the integration into higher-level simulations.

4.1 Nonlinear Model for Stability Analysis

In order to study the dynamic interaction between generating units in a low-voltage grid, it is necesary to model both the power units and the equivalent coupling between them. This coupling can easily be modelled by means of an equivalent *n*-Port network as discussed before, which yields an admittance matrix $\boldsymbol{Y_{eq}}$ of size $n \times n$. The dynamics of the power lines was disregarded, since a thorough investigation with the use of dynamic phasors [56] yielded no significant improvement when considering it.

Although modeling the dynamics of the power units could be done in great depth by considering detailed descriptions of the different blocks that it consists of, describing each inverter extensively does not necessarily provide further information on the stability of the system as a whole. This includes the nonlinearities and switching processes present inside the power electronics of the inverter, which are rarely detectable beyond the coupling point and can be safely disregarded [50]. Therefore, a simplified differential model as shown in [48] was considered, which includes all principal features of a power unit as a single-phase equivalent. The active and reactive power droops are described by the gains k_P and k_Q, while its dynamics are represented by first-order lag elements with time constants T_P and T_Q respectively. The offsets that determine the operating setpoint of the system are included through the variables P_s, Q_s, U_s, and f_s.

This model of a single inverter can easily be extended to contemplate several units by making use of vectorial notation. For example, the voltage phasors of all units can be integrated into an amplitude vector $\boldsymbol{U}$ and a phase vector $\boldsymbol{\theta}$.

Finally, the nonlinear relationships that couple all inverters are included through the phasor equation $\tilde{\boldsymbol{U}} = \boldsymbol{U}e^{j\boldsymbol{\theta}}$, the current equation $\tilde{\boldsymbol{I}} = \boldsymbol{Y_{eq}}\tilde{\boldsymbol{U}}$, and the power equation $\tilde{\boldsymbol{S}} = \boldsymbol{P} + j\boldsymbol{Q} = \tilde{\boldsymbol{U}}\tilde{\boldsymbol{I}}^*$.

The resulting model can be depicted by the block diagram shown in Figure 15.

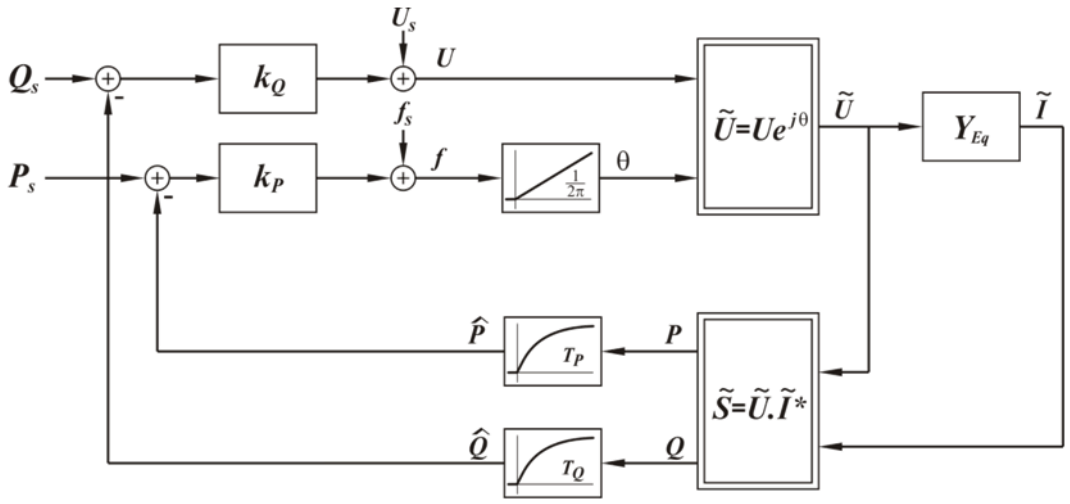

Figure 15: Proposed nonlinear model

Note that all variables on this diagram are vectors, while each element of a vector is related to a certain node on the system. This allows for a compact representation of the model and a simple implementation in MATLAB/Simulink. Accordingly, the gains $\boldsymbol{k_P}$ and $\boldsymbol{k_Q}$ are diagonal matrices of size $n \times n$.

This model has been validated comparing with other modelling approaches that can be found in the literature and documented in detail in [57].

4.2 Enhanced Dynamics of the System

Given its lagged response, a power unit behaves similar to a rotating generator, where its phase increases linearly and proportionaly to its frequency. However, distributed generators based on power electronics can implement a different behavior of the phase. For instance, a phase step can be implemented to enhance the dynamic response of the unit, whereas a sudden increment of the phase of a traditional rotating generator is rendered physically impossible.

Including not only a frequency but also a phase droop is referred to as angle droop control [49], improved droop control [55], phase-shift control [58], or transient droop control [59] in contrast to conventional droop control which governs merely the frequency of the power unit according to the injected active power. For a coalition with several inverters, this approach is a kind of distributed control, while the improved droop controller of each unit has to be tuned accordingly to assure a stable behavior. The advantage of this approach is that only the dynamic response of the power units has to be modified, while all other optimized features of the coalition regarding costs, reliability, and participation on load-following energy remain unaffected.

Experimental results have shown that this kind of controller can effectively damp and even stabilize a given coalition. However, a systematic approach to tuning it for a coalition with an arbitrary number of power units was missing.

The first step necessary to configure the improved droops is to study the small-signal dynamics of the coalition. This can be achieved by linearizing the nonlinear model proposed and studying the eigenvalues of the resulting system. By including an improved droop gain between active power P and the phase θ, the dynamics of the controlled system can be obtained.

The systematic tuning algorithms proposed in this work package are based on optimizing the improved-droop gains in a way that the resulting dynamics are suitably damped. The mathematical details needed to further comprehend in detail this process have to be left out of this text for matters of space. However, a detailed explanation has been documented in [60].

The algorithms proposed have been extensively tested with coalitions formed within the project. The simulation results for a coalition with ten units can be seen in Figure 16. The plot shows the active power injected by each unit after a frequency step on the medium-voltage grid triggers the injection of load-following energy. The response of the units before and after implementing the decentralized controller is shown in grey and blue respectively.

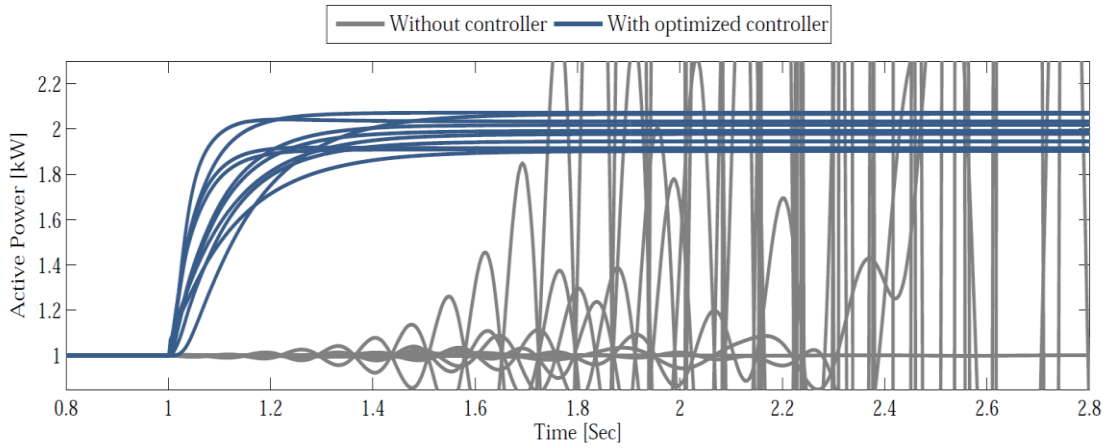

Figure 16: Active power response for a coalition before and after implementing the decentralized controller

Although the chosen coalition was originally unstable, depicted by the diverging active power of the units, the proposed decentralized controller yields a stable configuration, allowing all units to stably inject a fraction of load-following energy after a transient time of about half a second.

4.3 Reduced-Order Model

When studying the dynamics of distributed generation in a low-voltage grid, the medium-voltage grid to which the system is connected is usually considered stiff. Its dynamics and its power droops are entirely disregarded, and an ideal voltage source is used to model it instead. This helps study and enhance the behaviour of the low-voltage grid but disregards the dynamics and the droops of the distributed generators present in the medium-voltage grid and hence the interactions between both. In a similar manner, traditional power system stability analysis is carried out at high and medium-voltage levels, disregarding the behaviour of the low-voltage grids or considering them as mere loads. However, in a future scenario with larger amounts of distributed generation at the low-voltage level, the dynamics and the presence of power droops might play an important role in the stability of the power system. For instance, inter-area oscillations could appear between two low-voltage grids that interact over a medium-voltage grid, or the dynamics of one grid could affect the behaviour of the other. Running a complete simulation of a power system including details of the high, medium, and low-voltage grids would of course allow to study in detail the stability of the system, but the implementation of such a model is unrealistic, since the immense amount of nodes present in a power system such as the synchronous grid of continental Europe (ENTSO-E) would render any simulation impracticable.

A suitable approach to solving the problem of simulating such a large system is to build hierarchical models that can be integrated into higher-level simulations as needed. Although this is

usual practice in the power stability analysis, very little has been done up to date to include aggregated low-voltage models into higher-voltage grids.

The easiest way to derive a reduced-order model of a low-voltage system would be to apply order-reduction techniques to the linearized model of the grid. In this way, a state space representation of reduced order could easily be achieved. However, instead of making use of mathematical tools to derive systematically a reduced-order model of the system, a given model structure is followed. This aims to derive a set of parameters with physical meaning rather than to obtain some values that are correct in a mathematical sense but do not provide any further understanding on the functioning of the system.

The proposed structure of the reduced-order model consists of a single source connected to the medium-voltage grid through a single impedance, as shown in Figure 17. The power source is modelled similarly to the power units discussed before, including additional cross coupled droops that is a relationship between active power and voltage and reactive power and frequency. Although such droops are usually not found in distributed generators, nonzero cross coupled droops result in the lumped model given the resistive and inductive nature of the power lines in a low-voltage grid.

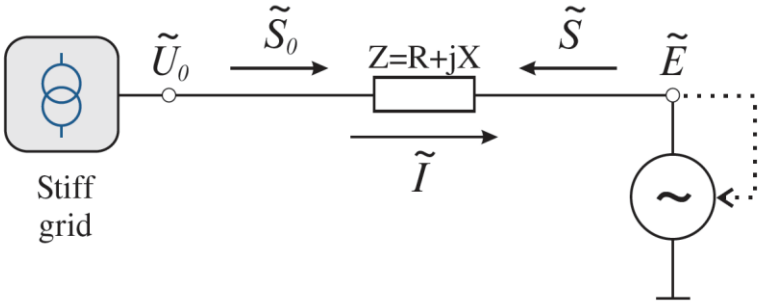

Figure 17: Proposed reduced-order model for a low-voltage grid

Based on this model structure, the parameters of the system are fitted considering steady-state values and the dynamic response of the system. A simulation for the same coalition as discussed before is shown in Figure 18.

Although the dynamic responses of the complete and the reduced-order models are not identical, a suitable fit can be achieved. The stationary values are nonetheless perfectly reproduced. Similar simulations were performed considering stiff and non-stiff medium-voltage grids, obtaining analogue results. Some minor differences proper of such an approximation arise, since the complete model of order 30 is reduced to a system of only third order. However, the reduced-order model can be used to fairly replicate the dynamics of a low-voltage grid with distributed generation without having to model each power source in detail. This sort of macro-model allows for the feasible integration of the dynamics of the low-voltage grid into medium-voltage models, such as those introduced in the sub-project four.

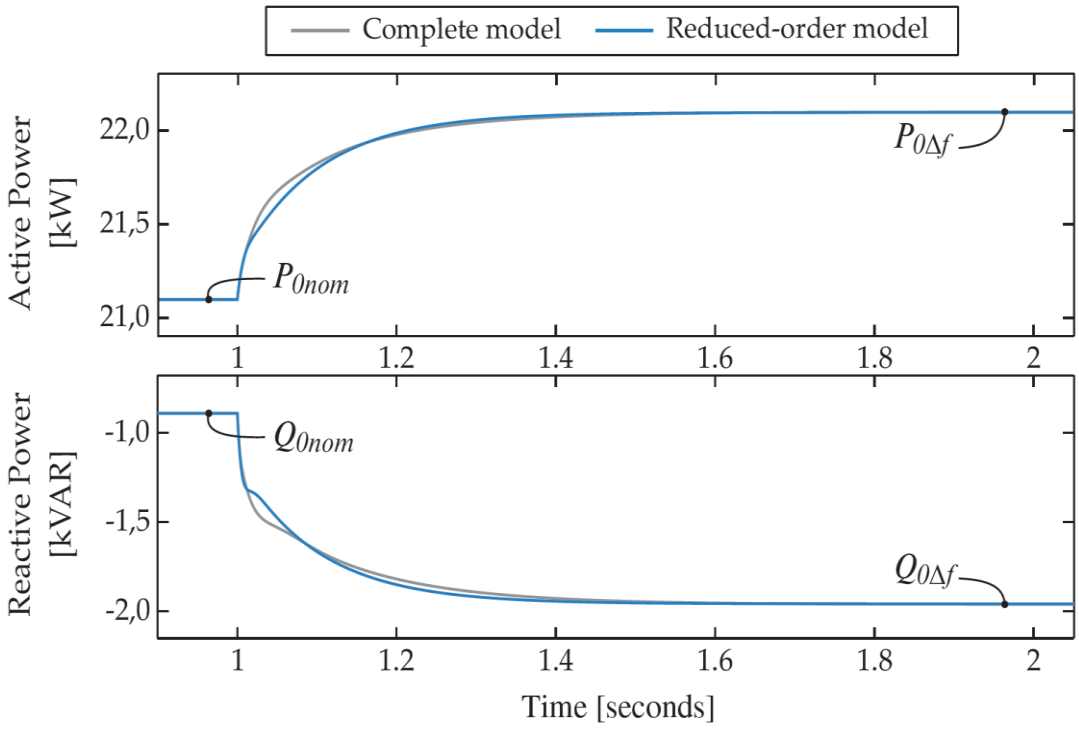

Figure 18: Response of the active and reactive power flow of the complete and reduced-order models

5 Conclusion and Outlook

When building coalitions for primary frequency control, an integrated stability analysis is possible and necessary, in order to guarantee the correct functioning of the grid, since some of the parameters of the coalition, such as the selection of units and their participation in the load-following product, affect the stability of the system.

An important consequence of the stability analysis performed is that only a single coalition might be formed on a given low-voltage grid, since the dynamic interactions between nodes of a power grid can turn the system unstable.

The stability of a given coalition in a known low-voltage grid can be studied and simulated with the nonlinear model proposed, which reproduces the behaviour of the grid in a way that is simple enough in order to reduce computational costs yet allows for the analysis of the fundamental dynamic interaction between different nodes on the system.

The implementation of a decentralized controller in the form of improved droop gains and the proposed algorithms derived to tune the controllers allow for a better damping of the system, and even the stabilization in case of an unstable coalition.

Finally, a reduced-order model makes it possible to describe the dynamic behaviour of the aggregated low-voltage grid, which can be integrated hierarchically into higher-level simulations.

The integrated investigation of coalition-forming and power inverter dynamics is an area of high importance for future power systems, since its complex nonlinear interactions shall not be further neglected in a system with larger amounts of distributed generation.

Further research should also be conducted regarding asymmetric-loaded grids, which are rather common in the low-voltage level, as well as studying the effect of nonlinear loads and devices that inject or consume constant power, which might have a destabilizing effect on the system.

Work Package 2.5: Grid-Supporting Services Through Inverters

René Dietz[38], Felix Fuchs[38] and Axel Mertens[38]

1 Goals and Integration in the Sub-Project

This work package examines in which way distributed generators can provide grid-supporting services through their converters. The main goal is to optimize the dynamics of the internal frequency and voltage control of the converter so that grid-supporting services can be optimized. Additionally, grid faults are considered in this context. Keeping this in mind, the overall grid stability in grids with highly distributed power generation may be improved. In this work package, the stability analysis is reduced to a local grid, for example a branch line connected to a medium-voltage grid.

The impact of the changed converter control in grids with a variety of distributed generators is analysed in cooperation with work package 2.4, especially by providing detailed converter models.

Another goal is to provide simplified converter simulation models for sub-project four. Specific electrical characteristics of distributed generators are provided for the coalition building in work package 2.1 (for example the assessment of active and reactive power domains for specific distributed generators and time constants for their control).

2 Related Work

Converters and their contribution to the stability of the electrical grid is a much discussed topic, since decentralisation of the electrical sources has become more evident [61].

Considering the current control of grid-connected converters, stability issues are also the topic of many publications. Problems in railway grids could be solved using impedance approaches [62]. Actual work in the field of renewable energies is dedicated to the influence of resonances within the grid on the operation and stability of current controllers [63], [64].

Considering power controllers, the conventional droop control method is based on the assumption of inductive line impedances [65]. This assumption was also extended to low-voltage grids, but here the resistance is in the range of the reactance [66]. This simple approach has been improved e.g. by implementing voltage sources with finite output impedances for supplying harmonic currents [67], and also by integrating adaptive control using an identification process [68]. The publications mentioned so far describe a coupled control of a multi-input multi-output system, since frequency and voltage can only be controlled in dependency on active and reactive power. Moreover, the coupling is related to – or caused by - the grid impedance, which is commonly unknown.

3 Methodology

The first part of this work deals with the modelling and dimensioning of regenerative power generation systems. Models of specific regenerative sources, solar and wind in particular, are developed and combined with switching converter models of different power classes.

The second part is about the converter control methods. The main work in this part can be split into two different domains regarding their dominating time behaviour. The first domain is the converter

[38] Leibniz Universität Hannover, 30167 Hanover, Germany,
{forename.surname}@ial.uni-hannover.de, Institut für Antriebssysteme und Leistungselektronik

current control where time constants from 1 ms to 5 ms are common. The second domain is the converter power control with time constants usually between 20 ms and 60 ms. These two domains are framed by other time domains, as can be seen in Table 1. On the time scale below 1 ms, there is usually the modulation unit as well as switching effects of the semiconductors. On a time scale above 60 ms, the converter behaviour is dominated by the primary power control, which is the connection to work package 2.1. However, this representation suggests a clear separation of these domains, and the interactions with other time domains are also part of this research.

> 30 s	~30 s – 15 min	~ 20 ms – 60 ms	~ 1 ms – 5 ms	> 1 ms	> 1 µs
...	Primary Power Control	Converter Power Control	Converter Current Control	Modulation	...

Table 1: Time line of dynamic behaviour

A combination of the regenerative power generation models, switched converter models and converter control models leads to complex system models which can be used for time-based simulation.

Based on these complex models, reduced analytical models are developed. These are suitable for analysis in the frequency domain, providing information for controller design and giving insight into parameter dependencies. At this point, first statements of the general converter's dynamic behaviour are possible. In time-based simulation, these statements and dependencies can be validated. Figure 19 illustrates a general view of the used methodology combined with the main goals.

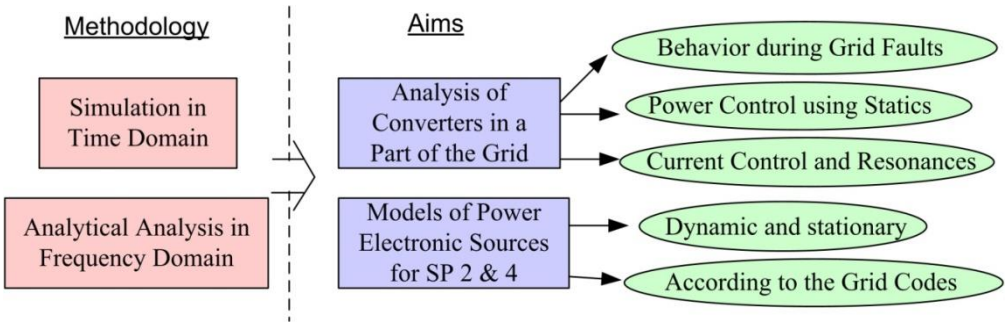

Figure 19: General view of the methodology

4 Main Results

4.1 Static Model

Based on a converter topology and the present grid situation, P/Q diagrams have been calculated providing access to possible reserves of active and reactive power as a function of the operating point. Inputs are the converter's nominal values and filter parameters, as well as the actual line voltage. This model is supposed to be used with the base load schedule from WP 2.1, which provides base load (active power) for all generators in a specific grid. A concept how the P/Q diagrams can be used considering market demands, stability analysis, current limitations and optimization has also been developed and made available on the project sharepoint.

4.2 Dynamic Model

As an input for the inverter models, time series models of the power of specific regenerative sources have been developed. The photovoltaic (PV) model uses sun radiation and atmospheric influences as input values and generates typical radiation input curves, which are calculated offline. Also an MPP tracker and a DC/DC converter (non-switching model) were modelled for a typical 30 kW PV source. Details of the implementation as well as a simulative validation are shown in [69].

Furthermore, simplified inverter models for low and medium voltage grids are provided. The converter ratings and its implemented control strategies are shown in Table 2. The topologies used can be seen in Figure 20 and Figure 21.

Low Voltage Grid (400 V)	Medium Voltage Grid (20 kV)
Current controlled 30 kW solar inverter with 2-level PWM and LCL filter	Current controlled 500 kW WEA with 2-level PWM and LCL filter
Direct power controlled 30 kW solar inverter with 2-level PWM and LCL filter	Current controlled 2 MW WEA with 2-level PWM and LCL filter
Indirect power controlled 30 kW solar inverter with 2-level PWM and LCL filter	Current controlled 5 MW WEA with 3-level PWM and LCL filter

Table 2: Provided converter models

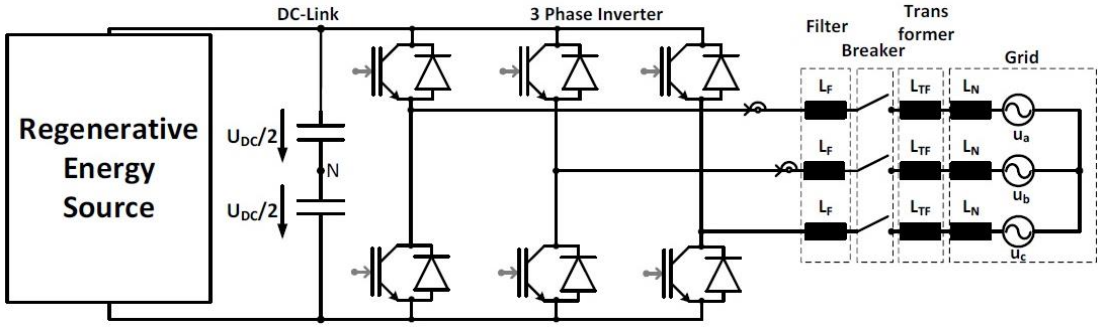

Figure 20: Two-level converter with simplified filter

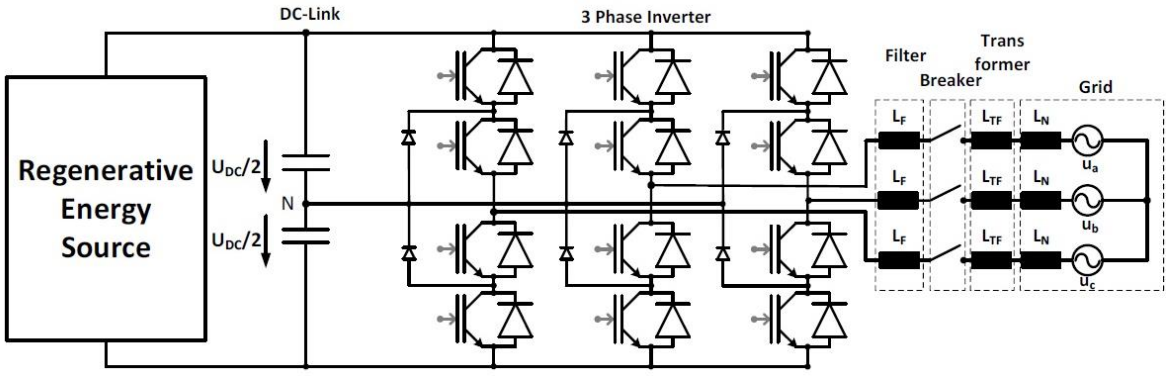

Figure 21: Three-level converter with LCL filter

Details of the inverter models, regarding dimensioning and implementation are given in the internal document "Modell von dezentralen Erzeugern – Projekt-Dokument Smart Nord, WP 2.5" on the Smart Nord share point. The integration of the developed models into the complete sub-project is documented in a joint publication [6]. The cooperation with the power engineering side of the project is documented in [8].

Besides developing detailed models to verify the coarse models used in other work packages, a major focus was on the stability of the control of grid-connected inverters. First, the stability of the current control of inverters in a variable grid situation was addressed.

For this purpose, the influence of a variable grid resonance on a standard inverter control was analysed. For the 2 MW wind turbine model the current control was designed (Figure 22).

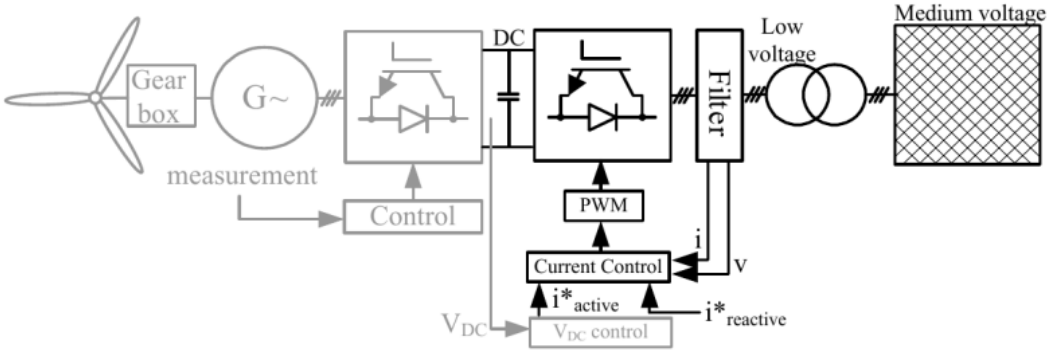

Figure 22: Grid-connected wind turbine
(all parts in black are considered, the dc link is considered as constant voltage source)

A grid resonance model with variable resonance frequency was developed. It could be found that current control with grid voltage feed forward (GVFF) in general is less sensitive to grid resonances than control without GVFF. This analysis was done using the control loop models shown in Figure 23.

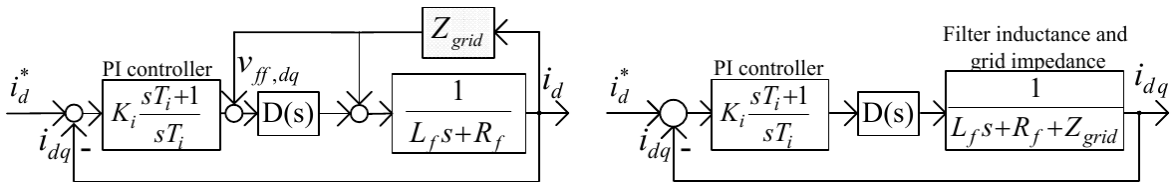

Figure 23: Control loop for stability analysis; left: control with GVFF; right: control without GVFF

Analysis regarding resonances caused by cable capacitances [70] and by power factor compensation capacitances [71] was done. It was found that specific resonances can bring the control without GVFF to instability, while the control with GVFF remains stable.

In Figure 24, simulation results for this case can be seen. This behaviour was also validated in laboratory [71].

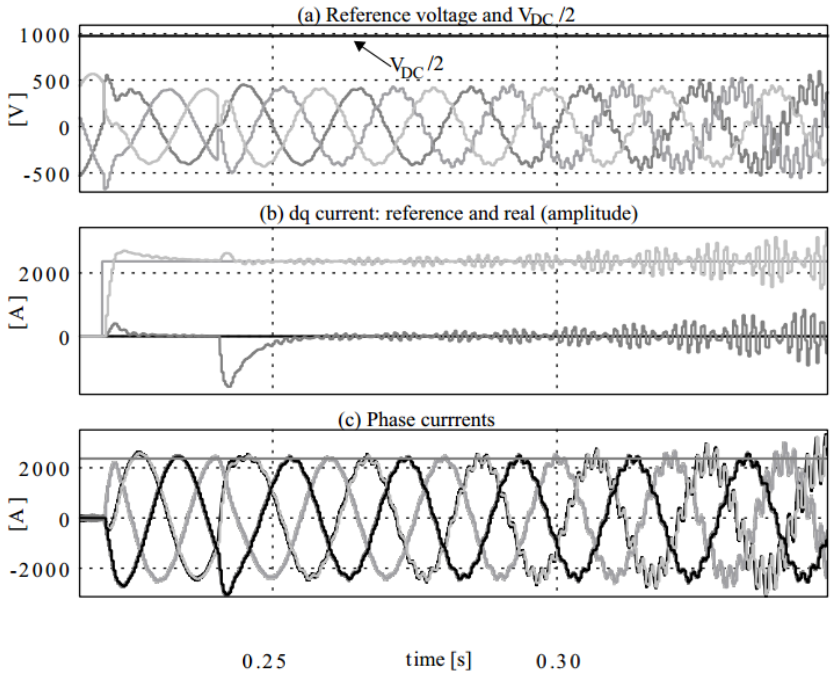

Figure 24: Instable control for critical grid resonance: switch from control with GVFF to without at t~0.24 s

Second, the behaviour of the power control was investigated. For the power controller, different approaches were made to optimize the internal converter control. The first step was the analysis of a direct and an indirect power controller with conventional droop control, using a specific branch line from the Smart Nord share point. This setup was then extended with a derivative term in the droop controller, offering more degrees of freedom. Since the resulting mathematical system description is of high order (four coupled transfer functions, each with a polynomial of 6^{th} order) even with a single converter connected to an ideal grid, the finding of optimal parameters requires a disproportional mathematical effort and global parameter knowledge. However, it is possible to achieve optimised step responses as can for example be seen in Figure 25. The left diagram shows normalised reactive power channel after a step in voltage, while the right diagram shows normalised reactive power after step in frequency appeared. Here a given PT1 behaviour is supposed to be optimal (green), while the pink curve is the optimised system response.

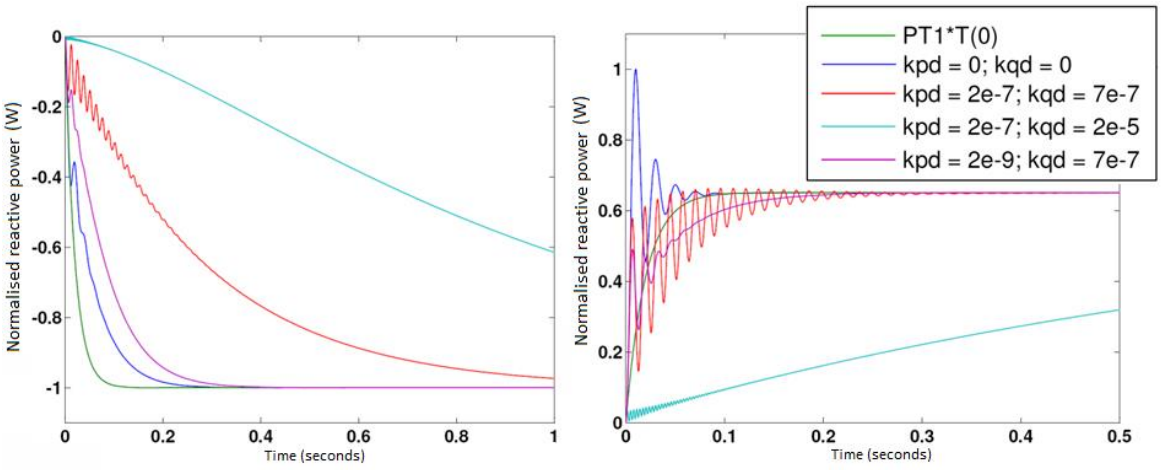

Figure 25: Step response (two channels normalised) of a grid-tied inverter with derivative droop control (green: optimal PT1 behaviour; pink: optimised behaviour; other colours: parameter variations)

The next step was to reduce the complexity of the system in a way that an easier controller parameter selection is possible with only a converter view of the grid. As it can be seen in Figure 26, the conventional direct droop controller (left) is extended with a decoupling matrix $M(s)$ (right). This matrix $M(s)$ consists of parameters selected according to the structure of the system $S_{sys}(s)$, which is composed of the subsystems shown in the system block (right). The parameters are known locally and can be estimated from the converter. Implementation details for a possible estimation process can be found in [72].

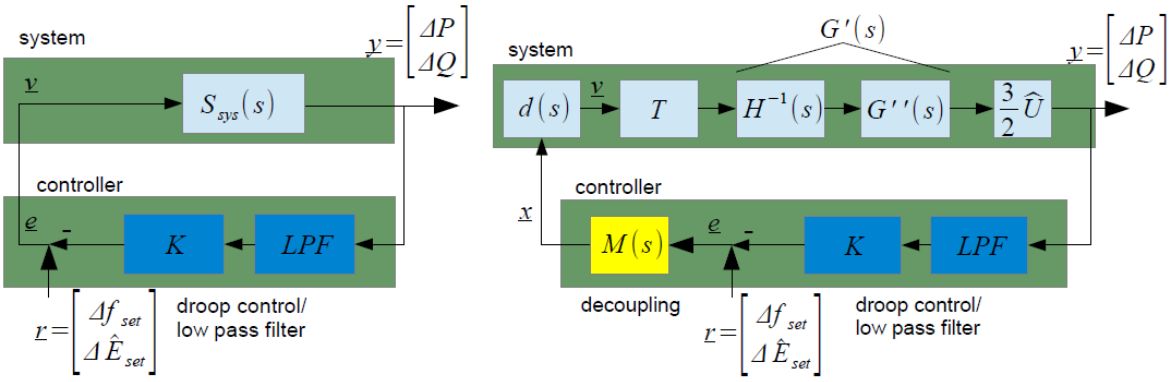

Figure 26: Conventional closed-loop system (left) and system with decoupling matrix (right)

With this decoupling, the overall converter system is reduced to a second order system. In Figure 27, the system step response for a single converter system can be seen. The upper and lower left diagrams show the step response of the conventional direct droop controller. It can be seen that the active and reactive power are coupled. The diagrams on the upper and lower right show the step response with the decoupling controller. Here, active and reactive power are independently controllable in each channel, leading to a decoupled system with optimised transient response. Details of the implementation have been submitted to an international conference in 2015 [73].

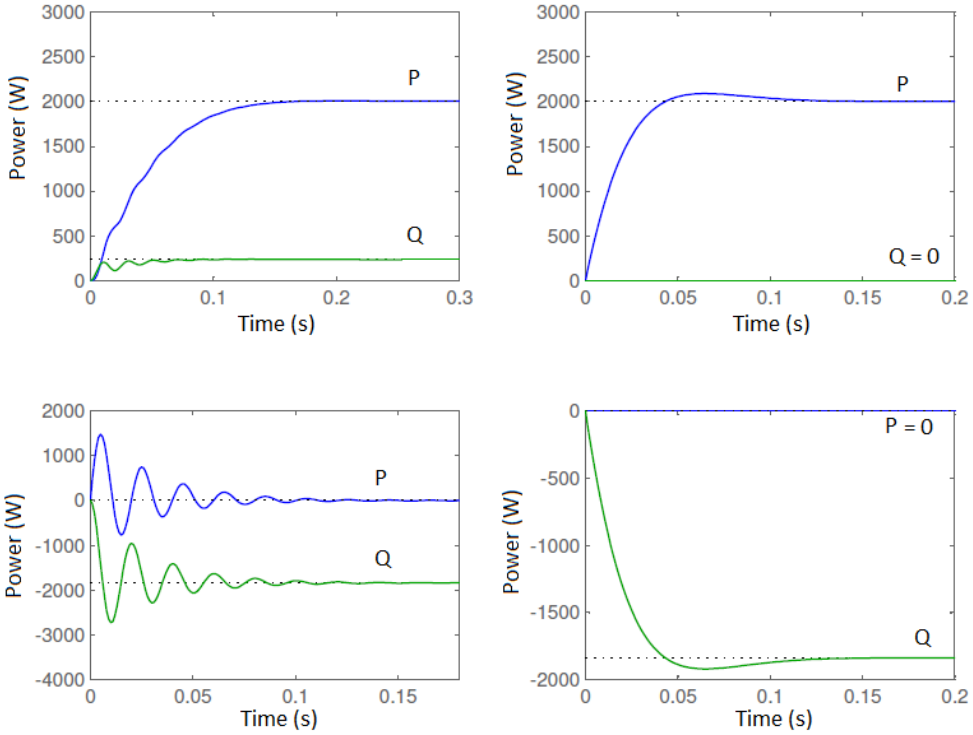

Figure 27: System response (blue: active power, green reactive power); upper-left: frequency step with classic droop lower-left: voltage step with classic droop; upper-right: for frequency step with ideal decoupling; lower-right: for voltage step with ideal decoupling

5 Conclusion and Outlook

In this work package, stationary and dynamic models for wind and solar energy sources were developed and analysed, and results were made available to all sub-projects on the Smart Nord share point. Moreover, the development process and application of these models were documented in two publications.

The current controller was analysed with respect to the influence of a variable grid resonance. This analysis was done considering cable capacitances and power factor compensation capacitances. It could be shown that controllers with voltage feed forward are in general is less sensitive to grid resonances.

The conventional power controller was analysed in direct and indirect configuration. Since a first extension with a derivative term did not lead to a simple model with locally known parameters, a new controller with a decoupling matrix was developed. With this improved extension, decoupled step responses could be achieved.

The analysis will be continued and intensified by the two authors in their doctoral thesis.

References

[1] A. Kamper, A. Eßer, “Strategies for Decentralised Balancing Power,” in Lewis, A. Mostaghim, M. and Randall, S. (eds.) Biologically-inspired Optimisation Methods - Parallel Algorithms, Systems and Applications, Studies in Computational Intelligence, Band 210, Springer 2009.

[2] R.-C. Mihailescu, M. Vasirani, S. Ossowski, “Dynamic Coalition Adaptation for Efficient Agent-Based Virtual Power Plants,” in Multiagent System Tech., LNCS, Vol. 6973, pp. 101-112 2011.

[3] S. Ramchurn, P. Vytelingum, A. Rogers, N. Jennings, “Agent-Based Control for Decentralised Demand Side Management in the Smart Grid,” in Int. Conf. on Auton. Agents and Multiagent Syst., Taiwan 2011.

[4] A. Nieße, S. Lehnhoff, et al., “Market-Based Self-Organized Provision of Active Power and Ancillary Services: An Agent-Based Approach for Smart Distribution Grids,” in Proc. of the 2012 IEEE Workshop on Complexity in Engineering (IEEE COMPENG 2012). Aachen, 2012.

[5] M. Calabria, W. Schumacher, “Stability optimization for distributed generation of load-following energy,” in s Energy Conference (ENERGYCON), 2014 IEEE International, 2014.

[6] M. Blank et al., “Agentenbasierte Vorhaltung und Erbringung von Primärregelleistung,” in at – Automatisierungstechnik, Band 62, Heft 5, pp. 347-363, April 2014.

[7] S. Lehnhoff et al., “Distributed Coalitions for Reliable and Stable Provision of Frequency Response Reserve – An Agent-based Approach for Smart Distribution Grids,” in proc. of IEEE International Workshop on Intelligent Energy Systems (IWIES), IEEE Press, 2013.

[8] F. Fuchs, R. Dietz, S. Garske, T. Breithaupt, A. Mertens, L. Hofmann, “Challenges of Grid Integration of Distributed Generation in the Interdisciplinary Research Project Smart Nord,” IEEE 5th International Symposium on Power Electronics for Distributed Generation Systems (PEDG), Galway, Ireland, 24.-27. June 2014.

[9] R. Bitsch, W. Feldmann, G. Aumayr, “Virtuelle Kraftwerke - Einbindung dezentraler Energieerzeugungsanlagen,” etz, vol 9, 2002.

[10] K. Rohrig, J. Heuer, F. Schlögl, “Renewable Model Region Harz : Climate Protection and Energy Efficiency by Modern ICT and Innovative Operation Strategies,” Wind Energy 2009.

[11] O. Abarrategui, J. Marti, A. Gonzalez, “Constructing the Active European Power Grid,” Proc. of WCPEE09 (pp. 1-4), Cairo 2009.

[12] J. C. Jansen, A. van der Welle, F. Nieuwenhout, “The Virtual Power Plant Concept from an Economic Perspective: updated final report,” Contract, vol. 31, 2008.

[13] M. C. Thoma, “Optimierte Betriebsführung von Niederspannungsnetzen mit einem hohen Anteil an dez. Erzeugung,” Thesis, ETH Zürich, 2007.

[14] European Union: Third package for electricity and gas markets

[15] H. F. Wedde, S. Lehnhoff, C. Rehtanz, O. Krause, “Bottom-up Self-Organization of unpredictable Demand and Supply under decentralized Power Management,” in Proc. of the 2nd IEEE International Conference on Self-Adaptive and Self-Organizing Systems, pp. 74-83, 2008.

[16] H. F. Wedde, S. Lehnhoff, K. M. Moritz, E. Handschin, O. Krause, “Distributed Learning Strategies for collaborative Agents in adaptive decentralized Power Systems,” in Proc. of the 15th Annual IEEE International Conference and Workshop on the Engineering of Computer Based Systems, pp. 26-35, 2008.

[17] R. Belhomme, R. Cerero, G. Valtorta, P. Eyrolles, “The ADDRESS project: Developing Active Demand in smart power systems integrating renewables,” 2011 IEEE PES General Meeting, 2011.

[18] C. Dänekas, A. König, et al., “Future Energy Grid. Future Energy Grid – Migration to the Internet of Energy,” acatech STUDY, Springer, 2012.

[19] A. Schnettler, “Verteilungsnetze der Zukunft – Anforderungen, Lösungsansätze und Systemdienstleistungen,” VDE Kongress 2008, München, 2008.

[20] H. Frey, “Bereitstellung von Systemdienstleistungen durch dezentrale Erzeugungsanlagen unter Einbeziehung von Lastmanagement und Smart Metering,” VDE Kongress 2008, München, (2008).

[21] “Operation Handbook,” ENTSO-E, 2010.

[22] R. Billinton, R.J. Ringlee, and A.J. Wood, “Power system reliability calculations,” Cambridge, MIT Press, 1973.

[23] K. W. Edwin, G. Traeder, “Zuverlässigkeitskenngrößen der elektrischen Energietechnik,” in ETZ-A 94, Heft 10, 1973, pp. 569-573.

[24] M. Schwan, "Aspekte der Zuverlässigkeitsberechnung elektrischer Energieversorgungsnetze im liberalisierten Markt," Ph.D. dissertation, Universität des Saarlandes, 2003.

[25] S. C. Krahl, "Berechnung der Wahrscheinlichkeitsverteilungen von Zuverlässigkeitskenngrößen in elektrischen Verteilungsnetzen," Ph.D. dissertation, in Aachener Beiträge zur Energieversorgung, Band 130, Klinkenberg, Aachen, 2010.

[26] Fraunhofer – Institut für Windenergie und Energiesystemtechnik (IWES, pub.), "Regelenergie durch Windkraftanlagen: Abschlussbericht," Kassel, März 2014.

[27] A. J. Gesino, "Power reserve provision with wind farms," Ph.D. dissertation, University of Kassel, 2010.

[28] J. Kays, et al., "Multidimensionales Verfahren zur Bestimmung des Regelleistungsbedarfes unter Berücksichtigung von Unsicherheiten," in *Energiewirtschaft 34*, Vieweg+Teubner, 2010, pp. 267-278.

[29] A. Ohsenbrügge, S. Lehnhoff, "Dynamic Dimensioning of Balancing Power with Flexible Feature Selection," to appear in proc. of 23rd International Conference on Electricity Distribution, CIRED, Lyon, 15-18 June 2015.

[30] R. Mock, A. Gheorghe, "Risk Engineering: Bridging Risk Analysis with Stakeholders Values," Dordrecht, Boston, Kluwer Academic Publishing, 1999.

[31] R. Mock, "Risiko, Sicherheit und Zuverlässigkeit – Analysemethoden in der Information and Communication Technology?," in Informatik Spektrum, Jun2 2003, pp. 167-172.

[32] K. Frauendorfer, A. Vinarski, "Risk Measurement in Electricity Markets," Universität St. Gallen, Technical Report, September 2007.

[33] C. Cornalba, P. Giudici, "Statistical Models for Operational Risk Management," in Physica A 338, Elsevier, 2004, pp. 166-172.

[34] M. Sadeghi and S. Shavvalpour, "Energy Risk Management and Value at Risk Modeling," in Energy Policy 34, Elsevier, 2006, pp. 3367-3373.

[35] M. Blank, S. Lehnhoff, "Assessing Reliability of Distributed Units with Respect to the Provision of Ancillary Services," in proc. of 11th IEEE Conference on Industrial Informatics (INDIN), Special Session on Industrial Informatics in Smart Grids, Bochum, Juli 2013.

[36] International Electrotechnical Vocabulary, International Electronical Comimission, IEC 60050.

[37] Distribution Study Committee Group of Experts, "Service Quality (DISQUAL): Availability of Supply Indices," 1997.

[38] M. Rausand, A. Høyland, "System Reliability Theory," John Wiley & Sons, Inc., 2004.

[39] M. Blank, S. Lehnhoff, "Considering Correlations for Reliable Distributed Ancillary Service Provision," in proc. of 5th IEEE PES Innovative Smart Grid Technologies (ISGT) Europe, October 12-14, 2014, Istanbul, Turkey.

[40] M. Blank, S. Lehnhoff, "Correlations in Reliability Assessment of Agent-based Ancillary-Service Coalitions," in proc. of 18th Power Systems Computation Conference (PSCC), August 18-22, Wroclaw, Poland, 2014

[41] A. Ohsenbrügge et al., "Efficient Provision of Ancillary Services by Decentralized, Volatile Generating Units," to appear in proc. of VDE/ETG Fachtagung Von Smart Grids zu Smart Markets, 25.-26. March 2015, Kassel.

[42] W. Mahnke, S.-H. Leitner, M. Damm, "OPC Unified Architecture," Springer, 2009.

[43] J. Lange, F. Iwanitz, T. J. Burke, "OPC: From Data Access to Unified Architecture," Huethig, 2010.

[44] J.-F. Cabadi, K. Piech, S. Rohjans, M. Uslar, "CIMbaT - Automated Generation of CIM-based OPC UA-Address Spaces," in Second IEEE International Conference on Smart Grid Communications, Brussels, Belgium, 2011.

[45] W. Mahnke, K. Piech, S. Rohjans, "Standardized Smart Grid Semantics using OPC UA for Communication," in IBIS – Interoperability in Business Information Systems, IBIS Issue 1 (6), 2011.

[46] R. Bleiker, S. Lehnhoff, C. Mayer, K. Piech, "Automatisierung heterogener, verteilter Energieanlagen mittels OPC UA," in Zukünftige Stromnetze für Erneuerbare Energien, Berlin, Germany, 2014.

[47] S. Lehnhoff, K. Piech, S. Rohjans, "UML-based Modeling of OPC UA Address Spaces for Power Systems," in IEEE International Workshop on Intelligent Energy Systems (IWIES 2013), Vienna, Austria, 2013.

[48] E. Coelho, P. Cortizo, P. Garcia, "Small-signal stability for parallel-connected inverters in stand-alone AC supply systems," Industry Applications, IEEE Transactions on, vol. 38, no. 2, pp. 533-542, 2002.

[49] R. Majumder, “Modeling, Stability Analysis and Control of Microgrid for Improved Power Sharing and Power Flow Management,” VDM Publishing, 2010.

[50] N. Pogaku, M. Prodanovic, T. Green, “Modeling, Analysis and Testing of Autonomous Operation of an Inverter-Based Microgrid,” Power Electronics, IEEE Transactions on, Bd. 22, Nr. 2, pp. 613-625, 2007.

[51] S. Iyer, M. Belur, M. Chandorkar, “A Generalized Computational Method to Determine Stability of a Multi-inverter Microgrid,” Power Electronics, IEEE Transactions on, Bd. 25, Nr. 9, pp. 2420-2432, Sept 2010.

[52] E. Barklund, N. Pogaku, M. Prodanovic, C. Hernandez-Aramburo, T. Green, “Energy Management in Autonomous Microgrid Using Stability-Constrained Droop Control of Inverters,” Power Electronics, IEEE Transactions on, Bd. 23, Nr. 5, pp. 2346-2352, 2008.

[53] P. Hasanpor Divshali, S. Hosseinian, M. Abedi, “A Novel Multi-Stage Fuel Cost Minimization in a VSC-Based Microgrid Considering Stability, Frequency, and Voltage Constraints,” Power Systems, IEEE Transactions on, Bd. 28, Nr. 2, pp. 931-939, 2013.

[54] F. Dörfler, F. Bullo, “Kron Reduction of Graphs With Applications to Electrical Networks,” Circuits and Systems I: Regular Papers, IEEE Transactions on, vol. 60, no. 1, pp. 150-163, 2013.

[55] G. Yajuan, W. Weiyang, G. Xiaoqiang, H. Wu, “An improved droop controller for grid-connected voltage source inverter in microgrid,” in s Power Electronics for Distributed Generation Systems (PEDG), 2010 2nd IEEE International Symposium on, 2010.

[56] L. Wang, X. Q. Guo, H. R. Gu, W. Wu, J. Guerrero, “Precise modeling based on dynamic phasors for droop-controlled parallel-connected inverters,” in s Industrial Electronics (ISIE), 2012 IEEE International Symposium on, 2012.

[57] M. Calabria, W. Schumacher, “Modeling power inverter interactions in a low voltage grid,” in s Control and Modeling for Power Electronics (COMPEL), 2014 IEEE 15th Workshop on, 2014.

[58] H. Avelar, W. Parreira, J. Vieira, L. de Freitas, E. Alves Coelho, “A State Equation Model of a Single-Phase Grid-Connected Inverter Using a Droop Control Scheme With Extra Phase Shift Control Action,” Industrial Electronics, IEEE Transactions on, Bd. 59, Nr. 3, pp. 1527-1537, March 2012.

[59] Y.-R. Mohamed, E. El-Saadany, “Adaptive Decentralized Droop Controller to Preserve Power Sharing Stability of Paralleled Inverters in Distributed Generation Microgrids,” Power Electronics, IEEE Transactions on, Bd. 23, Nr. 6, pp. 2806-2816, Nov 2008.

[60] M. Calabria, W. Schumacher, “Stability optimization for distributed generation of load-following energy,” in s Energy Conference (ENERGYCON), 2014 IEEE International, 2014.

[61] M. Liserre, R. Teodorescu, F. Blaabjerg, “Stability of photovoltaic and wind turbine grid-connected inverters for a large set of grid impedance values,” IEEE Transactions on Power Electronics, vol. 21, no. 1, pp. 263–272, Jan. 2006.

[62] M. Pröls, B. Strobl, “Stabilitätskriterien für Wechselwirkungen mit Umrichteranlagen in Bahnsystemen,” Elektrische Bahnen : EB ; Elektrotechnik im Verkehrswesen ; erste Fachzeitschrift für Elektrotechnik im öffentlichen Verkehr, vol. 104, no. 11, pp. 542–552, 2006.

[63] M. Cespedes, J. Sun, “Impedance Modeling and Analysis of Grid-Connected Voltage-Source Converters,” IEEE Transactions on Power Electronics, vol. 29, no. 3, pp. 1254–1261, Mar. 2014.

[64] X. Wang, F. Blaabjerg, M. Liserre, Z. Chen, J. He, Y. Li, “An Active Damper for Stabilizing Power-Electronics-Based AC Systems,” IEEE Transactions on Power Electronics, vol. 29, no. 7, pp. 3318–3329, Jul. 2014.

[65] M. C. Chandorkar, D. M. Divan, R. Adapa, “Control of parallel connected inverters in standalone AC supply systems,” IEEE Transactions on Industry Applications, Bd. 29, Nr. 1, S. 136-143, Jan. 1993.

[66] A. Engler, N. Soultanis, “Droop control in LV-grids,” in 2005 International Conference on Future Power Systems, 2005, S. 6 pp.-6.

[67] K. de Brabandere, B. Bolsens, J. van den Keybus, A. Woyte, J. Driesen, R. Belmans, K. U. Leuven, “A voltage and frequency droop control method for parallel inverters,” in Power Electronics Specialists Conference, 2004. PESC 04. 2004 IEEE 35th Annual, 2004, Bd. 4, S. 2501-2507 Vol.4.

[68] J. C. Vasquez, J. M. Guerrero, E. Gregorio, P. Rodriguez, R. Teodorescu, F. Blaabjerg, “Adaptive droop control applied to distributed generation inverters connected to the grid,” in IEEE International Symposium on Industrial Electronics, 2008. ISIE 2008, 2008, S. 2420-2425.

[69] M. Moriße, “Erstellung eines Programms zur Generierung reproduzierbarer Leistungsverläufe regenerativer Erzeuger sowie deren Implementierung in ein Labor zur Untersuchung von umrichterdominierten Netzen,” November 2012.

[70] F. Fuchs, D. V. Pham, A. Mertens, "Analysis of grid current control in consideration of voltage feed forward and cable capacitance demonstrated on a fully sized wind turbine installed in a wind park," Energy Conversion Congress and Exposition (ECCE), 2013 IEEE, pp.3325,3332, 15-19 Sept. 2013.

[71] F. Fuchs, A. Mertens, "Prediction and avoidance of grid-connected converter's instability caused by wind park typical, load-varying grid resonance," Energy Conversion Congress and Exposition (ECCE), 2014 IEEE, pp.2633,2640, 14-18 Sept. 2014.

[72] A. Vogel, "Schätzung der Netzimpedanz über Wirk- und Blindleistungsvariation," Bachelor Thesis, submitted for evaluation, 2015.

[73] R. Dietz, A. Mertens, "Extended Power Control for Distributed Generation Units," Power Electronics and Applications, 2015 European Conference on, 8-10 Sept., Geneva, Switzerland, 2015.

Sub-Project Three:
Integrated Market

Overview on Sub-Project Three: Integrated Market

Michael Kurrat[39], Carsten Wissing[40], Fridolin Muuß[39], Sören Meyer[41], Sabrina Schnabel[40]
Hans-Jörg von Mettenheim[41], Michael H. Breitner[41] and H.-Jürgen Appelrath[40]

1 Introduction

Through the transformation of the electrical energy system, a transformation of the generating structure has already been initiated. This transformation increasingly takes place in the decentralisation of power generating. While fluctuating renewable energy plants are being installed in the levels of low and medium voltage, and constructed as large scale farms even in high voltage level, conventional power plants are getting dismantled. In the upcoming years this trend is going to perpetuate. In addition, those conventional power plants (e.g., gas) are driven out of the market because of their higher generating costs. This is possible due to the German market model, which includes the so called "merit order effect". Until now the flexibility of conventional power plants usually allowed them to react to short-term shifts of the power demand and generation. Thus, the advantages resulting out of such a flexible generating structure are being waived. Alongside these advantages, conventional power plants provide energy system services comprising voltage and frequency stability, Versorgungswiederaufbau and production management. All of those services ensure a safe grid use and cannot be compensated. It is common ground that the key challenge of the transformation of the generating structure within Germany will be finding a way to provide those energy system services, without the major input of conventional power plants.

These system services, as well as the development of business models based on them, form the core within the sub-project three "Integrated Market". The difficulty of voltage stability is especially influenced by the volatility of the renewable energies power feed. As a result of this the occurrence of considerable voltage variation within the different voltage levels becomes more likely, which can cause a major voltage drop within the transmission grids. To counteract this phenomenon, reactive power is already being injected. Much of this reactive power is being injected in transmission level by conventional power plants. The minor remainder comes from small and medium sized facilities, which are integrated in the low voltage grid. Innovative concepts are required for the future to provide reactive power for the transmission and distribution grids.

In the event of a shortage of power within the transmission grids, the "redispatch" is currently being used to counter. Hence, the generating capacities are reallocated so that the impending bottleneck gets dissolved. The impact of the "redispatch mechanism" will decrease because of the upcoming lack of flexibility and the increasing amount of volatile and slightly regulated renewable energies. Currently, that type of system service, called operational management, is provided by the transmission grid operators. Decentralised, flexible generating units (e.g. combined heat and power units, storage, combined solar photovoltaic and storage systems) can be qualified to prevent such a shortage by smart redistribution in the lower gird levels.

Another difficulty resulting out of the German "Energiewende" (Transformation of the Energy System) and its economic and legal integration is the citizens' acceptance as well as the acceptance of the facility operators. While the citizens do not profit from lower electricity prices, charges for

[39] Technische Universität Braunschweig
[40] OFFIS – Institute for Information Technology
[41] Leibniz Universität Hannover

private and commercial facility operators rise. Since the “Energiewende” is driven by idealism the motivation of believing and participation remains a major factor. Creative and innovative marketing strategies are essential to maintain this motivation, so that the “Energiewende” will be supported any longer by facility operators, grid operators and electricity consumers. The definition and exploration of novel business models for facility operators, grid operators and citizens will be attempted within sub-project three by the development of new products, mechanisms and marketing options.

Like the following Figure 1 illustrates, those different topics will be approached in various voltage levels.

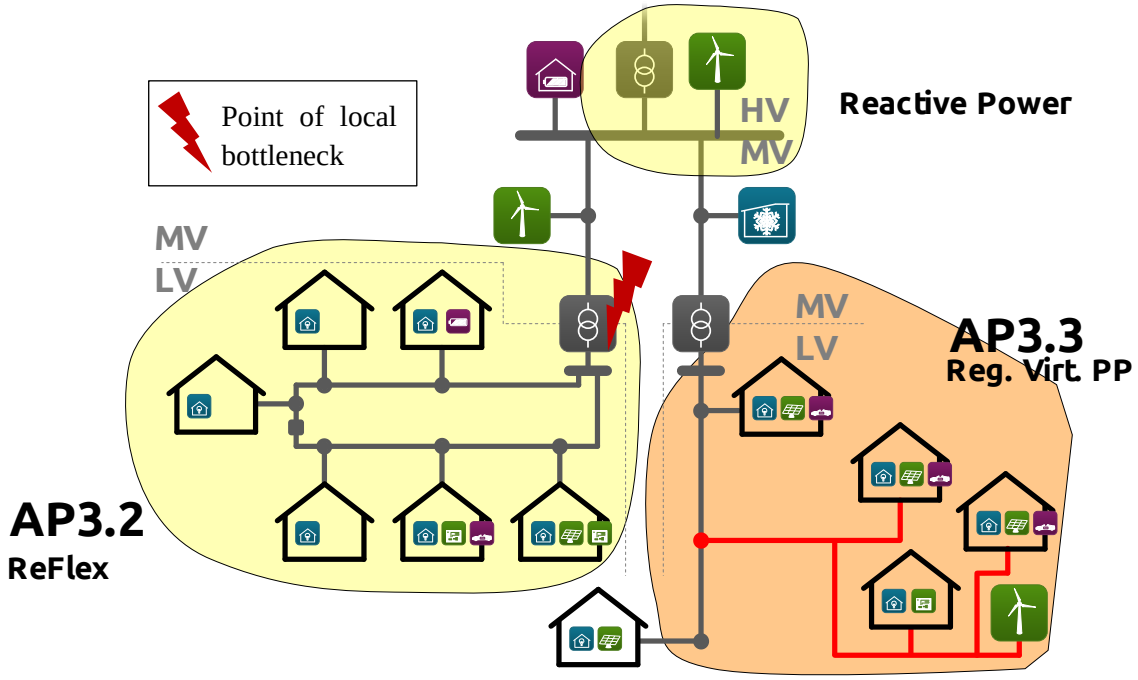

Figure 1: Overview of sub-project three

Work Package 3.1: Analysis and Development of Prospective System Services

Fridolin Muuß[42] and Michael Kurrat[42]

1 Introduction

Two varying aspects were covered within sub-project three "Integrated Market"- WP 3.1 "Analysis and Development of Prospective System Services". The complexity of grid regulation and marketing increases steadily through the progressive decentralisation of power generating and the slow deconstruction of central generating capacities for transmission grids. First, the possibilities of reactive power management in active distribution grids has been displayed, which can be used nowadays to optimize voltage stability, or to supply free reactive power for grids in future in case of progressive decentralisation of generating capacities. In this way, novel system services can be defined, which can be brought compounded as a virtual power plant. Second, simulation models of regional markets with functioning Demand-Side-Management (household and electrical vehicles), for minimal costs in effective power supply (low voltage grids) with a high autarky, has been acquired.

2 Reactive Power

Reactive Power emerges through phase shift between current and voltage, which is caused by components with capacitive and inductive characteristics. This report contains subsequent definitions:

If not specified, this report deals with inductive reactive power. It is consumed by engines for their running. Therefore inductive properties are always related to consumption, whereas capacitive properties result from reactive power output. Thus, inductive properties counteract capacitive properties.

For example, components with capacitive characteristics are cables and overhead lines with minor loading, while asynchronous engines, severe overloaded transmission components and LCC HVDC converter show inductive characteristics.

The deconstruction of central, the progressive constructions of decentralised generating capacities, as well as the rising challenges in the field of voltage stability, lead to a growing importance in reactive power management. Reactive power stresses grids and raises transmission losses. That is why it is reasonable to introduce reactive power at the point of consumption into the grid. To avoid excessive payments for the industries because of exceeding reactive power consumption, reactive power compensation facilities are being installed consumer-orientated. Therefore reactive power does no longer stress the grids; it only oscillates between industrial buildings and compensation facilities. This principle is being used within various grid levels to compensate the inductive or capacitive behaviour in case of heavy or weak loading. The objective is to maintain the voltage within the transmission distance and its designated band.

Many reactive power compensation facilities are already located in Germany along the existing distribution grid structures, since converter based decentralised generating facilities within the 20 kV and 110 kV voltage level can potentially be used for that. Converter based systems are being

[42] Technische Universität Braunschweig, 38106 Braunschweig, Germany,
{first initial.surname}@tu-braunschweig.de, elenia

utilized for local voltage stability at the point of feed by integrating reactive power characteristics into the converter. These characteristics lift the voltage by output of reactive power, respectively, reduce the voltage by reactive power consumption. The voltage stability is elucidated in the following chapter.

3 Voltage Stability Within the Distribution Grid

Today, characteristic curves of reactive power consumption and output within converter systems are requested and implemented in subject to apparent power and grid level. Figure 2 displays those characteristic curves for voltage stability exemplarily.

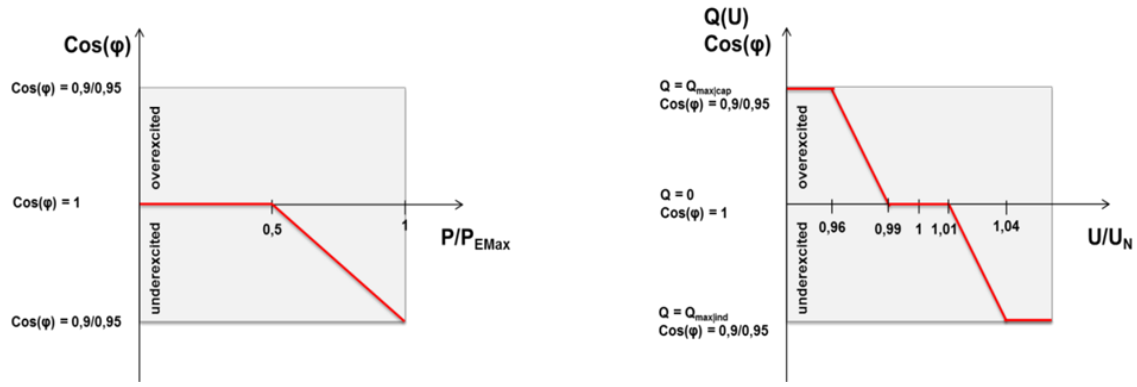

Figure 2: $\cos(\varphi)\,(P)$ and $Q(U)$ as local reactive power control methods

While the reactive power consumption is orientated in objective to the power input $\cos(\varphi)\,(P)$ regulation; inductive behavior of generator), the reactive power behavior with $Q(U)$ regulation correlates to the voltage at the access point. Thereby, the voltage can be raised through reactive power output (capacitive behaviour of generator), if it comes below a critical value. In the other case, the voltage can be reduced through reactive power consumption (inductive behaviour of generator), if it exceeds a critical value. Depending on the facility capacity, the amount of maximum reactive power, approximated by $\cos(\varphi)$, varies. Facilities bigger than 13.6 kVA need a $\cos(\varphi)$ of 0.9. Facilities beneath that capacity need a $\cos(\varphi)$ of 0.95. In general, $\cos(\varphi)$ is defined as the ratio between effective power P and apparent power S.

These facilities can contribute to voltage stability in that way. Through ameliorated satisfaction of voltage values, by applying $\cos(\varphi)\,(P)$ and $Q(U)$ characteristic curves, grid connection capacity has been increased. No further voltage increase was noted although a solar photovoltaic and combined power and heat facility with applied characteristic curves were added. Caused by higher resulting reactive power consumption and partially increased reactive current, losses may emerge. But usually that is the cost-effective manner of grid expansion. Within the simulation of low and middle level voltage grids, it is shown, that an extension of the previous characteristic curves from Figure 2 does not lead to any advantages. Actually they are adequate to compensate voltage instabilities, even short-term induced by clouds or gusts. Therefore, there is no need for higher converter investments with greater apparent power, within the low level grids.

The resulting reactive power fluxes lead, as noted earlier, to higher losses and also to increased reactive power import at the LV|MV or even MV|HV transformer. The required reactive power payment to the responsible grid operator may rise, due to extra effort for the reactive power balance compensation.

For that reason, it may be reasonable to apply the free reactive power management already within the middle level grids.

Figure 3 demonstrates the intended prospective condition of reactive power supply by a virtual reactive power plant within the medium voltage distribution level.

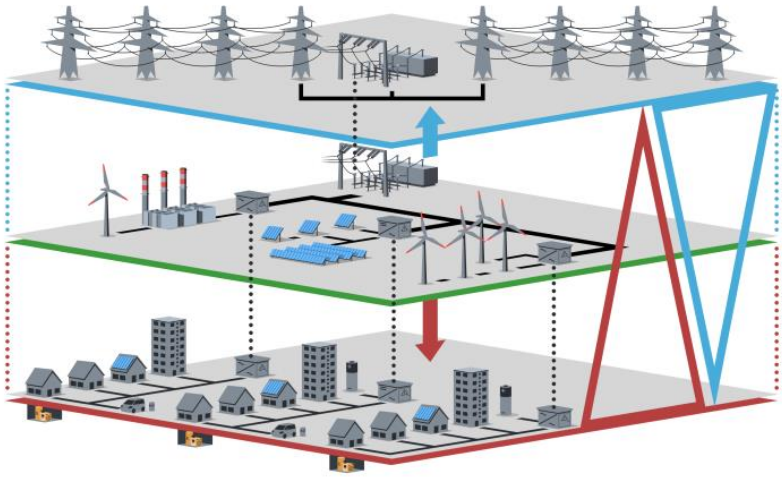

Figure 3: Virtual reactive power plant

Within the low voltage level, reactive power is being used for local voltage stability, whereas within the upper grid levels reactive power guarantees safe system management.

4 System Management and System Services

Large-scale additional construction of generating capacities within the distribution grids (up to 110 kV) increases the responsibility of distribution grid operators concerning the security of supply and grid management. The future impact of different voltage levels and system management is shown in Figure 4. All tasks within the system management subdivide onto different grid operators.

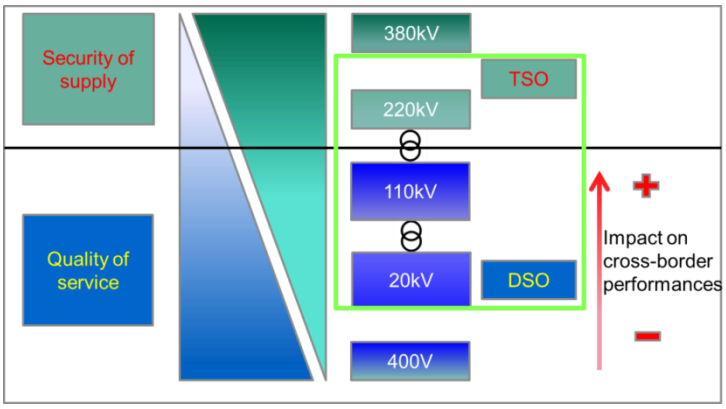

Figure 4: Influence of the DSO in future power grids

While the transmission grid operators guarantee the security of supply, the other grid operators orientate to the quality of service. In that field the voltage stability, as well as the processing and grid integration of generating facilities and their access conditions have priority. Table 1 shows the benefits of advanced reactive power management for DSO and TSO.

Benefits	
DSO	**TSO**
reducing reactive power import (economic)	lower reactive power load (technical and economic)
selling reactive power as ancillary service (economic)	additional reactive power supplier (economical)
possibility of reducing losses (economic)	less need for compensation systems could be possible
voltage control (technical)	-

Table 1: Benefits of Reactive Power Management for System Operators

DSO and TSO have both advantages of a reactive power management.

As noted earlier, the voltage levels of 20 kV and 110 kV with a high rate of penetration by renewable energies will play a leading role in terms of reactive power management (compare Figure 2 and Figure 4). Within work package 3.1 it was examined whether the prospective necessary reactive power for system management, within the upper voltage levels, can be supplied by the distribution grid.

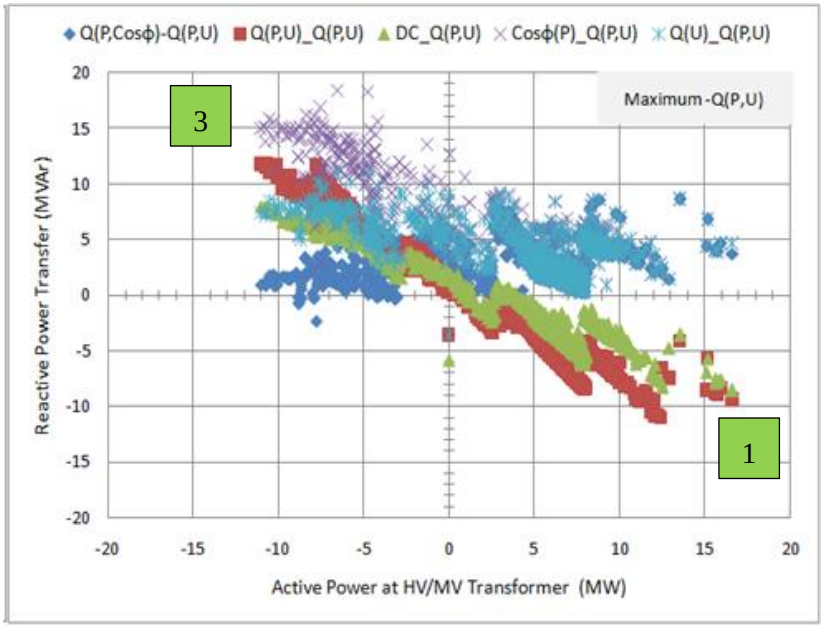

Figure 5: Different voltage control methods in medium-and low voltage networks

Figure 5 shows different combinations of reactive power regulation, which are integrated directly into the facilities of low and medium voltage level. The simulation results base on a "Cigre-Benchmark" medium voltage grid, including 12 coupled low voltage grids. The results are worked off in the "Load Counting System". This paragraph focuses on the effects of reactive power management methods within the medium voltage level.

The outcome of active reactive power management, with extended voltage stability orientated converter characteristics, points out the possibility of reactive power transfer between middle and high voltage grids. By choosing various regulation methods within the middle voltage grids (Q(P,U) or DC), reactive power can be transferred into the next higher grid in case of high effective

power consumption of the middle voltage grid. This leads to a decrease of voltage within the middle voltage grid and an increase of voltage within the next higher grid (quadrant 1). In case of an effective power flow from the lower to the higher grid it behaves vice versa (quadrant 3). Because of the static voltage stability, voltage criteria of the middle and low voltage grids are fulfilled anytime. More detailed information provides the publication [2].

5 Free Reactive Power Supply

Moreover, to supply a much higher rate of reactive power, grid connection conditions of many grid operators have been adjusted. Thus, the grid operator keeps the possibility to equip the facilities with different characteristic curves, than shown in section 1 of this chapter, or to influence them. As a consequence of that the opportunity of free reactive power management emerges which is provided by renewable energies, coupled as virtual power plants.

The "elenia" developed various algorithms to realize virtual power plants within the work package 3.1. They are written in the programming language DPL (by DIgSILENT) within the simulation environment PowerFactory.

The algorithms are designed to achieve a central goal, using different secondary constraints. They can be divided into three main groups.

- Cost reduction for reactive power
- Reactive power supply
- Optimized grid management

Main group 1- "Cost reduction for reactive power" contains two different goals. First, smart use of reactive power capacities shall supply the required reactive power fort the own grid territory as well as the grid territory beneath that level by the DA. The reactive power import and its costs decline thereby for the transmission grid operator. That approach is called "**Q-Neutrality**". Second, the limit violation at the transfer point shall be reduced or avoided. To avoid fines, caused through high reactive power, the individual facilities of a virtual power plant have to preserve the reactive power transfer within specified limits. That approached is called "Setpoint Value based Q-supply".

Main group 2- "Reactive power supply" is built on intelligent designed reactive power supply by the DEA, based on a defined profile. That profile complies either to a specified capacity of the DVRPP or to the requested demand of the transmission grid operator. In that way, the operator of a virtual dynamic reactive power plant can offer a system service. It is insignificant whether the reactive power supply profile is constant or volatile. That approach is called "**Q-Profile-Based**".

Main group 3- "Optimized grid management" also contains two different goals. First, reactive power shall be used to reach optimal voltage stability at the connection point. Second, DEA's with their reactive power capability within network clusters to compensate reactive power.

With those different algorithms and goals various grids of the 20 kV level have been simulated and evaluated according to the goals. That evaluation was focused on technical effects of free reactive power management, the grid voltage behaviour, the burdens on grid components, and losses. Because of the fact, that every network is different the results can not be generalized for every network. But the tendency demonstrates the greater impact on the network if there are several distributed decentralized generation unit pools which are providing reactive power. Within the economic analysis the focus lied on the financial effects of reactive power management, regarding the costs as well as proceeds. To quantify the financial effects, costs for STATCOM and converter systems of various producers have been compared and the mean was calculated. The price of reactive power, which must be paid to the responsible grid operator, was attained 10.6 €/Mvarh.

Within the minimal costs for reactive power there is no way to implement a reactive power market. Furthermore the fact that reactive power need to be provided nearby the load leads to a minimal offer of suitable decentralized generation units.

The upper proceeds limits orientate towards the efficiency, respectively, the efficiency improvements of grid operation. Due to this, the grid operators are interested to ameliorate their grid operations. Consequently, reactive power management can be used as a determining factor to accomplish the efficiency goals. Thereby, grid operators get the chance to achieve an increase in earnings. The integration of these facilities into the control systems can be financed with the grid fees. This opportunity of apportionment based financing represents, at the same time, a serious obstacle for business model development within the sector or reactive power management. Hence, there is no need in integrating renewable energy facilities into free reactive power management because of the grid fees, which include the financing of reactive power compensation facilities. The difference to grid operator owned compensation facilities is that grid operator must pay a monthly apportionment for reactive power supply instead of a one-time financing of the compensation facility.

The results demonstrate the technical impact of an advanced reactive power management. The algorithm helps to identify best strategies for different network, network conditions and network cluster.

The importance of reactive power management will steadily increase in the future. The effects of volatile renewable energy feed will imply a dynamic grid operation, which can be implemented more efficient and easier through reactive power management.

Work Package 3.2: Market Design

Sabrina Schnabel[43], Carsten Wissing[43], H.-Jürgen Appelrath[44] and Michael Kurrat[45]

1 Goals and Integration in the Sub-project 3.2

The participants of the SP 3 developed a trading system for system services. Based on a model of the currently existing electricity market new products in the field of system services are defined in connection with network analysis. On the development of business models, the studies on the integration of an increasingly high energy conversion are completed. Smart Nord developed a previously non-existing market for ancillary service providing, which unified an economic participation of operators with the stability of supply. With the analysis of system service providing and the definition of new market products, Smart Nord has extended the quantitative compensation system with essential components.

In order to develop a comprehensive modelling of the trading platform for current and future products in the electricity market, the working package 3.2 for "Market Design" has been developed. The goal of the work package 3.2 was the study and adaptation of the energy economic and energy market frame conditions for a power supply system with a very high percentage of distributed and renewable energy sources. The focus of this work package was the development of an integrated market design, to resolve the conflicting goals between the supply of active power and the provision of ancillary services providing. Therefore, several possibilities were investigated to reduce the grid expansion by using market-based mechanisms and economic incentives existing energy infrastructures.

2 Requirements

The energy revolution leads to a lasting transformation within the structure of the power generation in Germany and also to a very different kind of utilization of the power grids. The structure of the electric power supply sometimes transforms from a top-down structure to a bottom-up structure, whereby the current flow direction is partially reversed. Planning and expansion of the distribution grid therefore can no longer be operated purely load-oriented, but must take particular account of distributed generation for the network expansion.

Due to the Merit-Order-Effect, big thermal power plants fade out of the markets. That leads to a totally different type of task for the transmission grid. The decentralized produced energy has to be transported from different parts of Germany to the electrical load centres. Therefore in the future the operational management of the electrical grid must provide a high flexibility.

This impact of the energy revolution will lead to an increase of capacity congestions in the transmission and distribution grid. For the transmission grid, the conventional way to eliminate capacity congestions is to expand the electrical grid. An extension of the transmission grid is necessary to avoid wide-ranging blackouts. The great economic importance of a comprehensive power failure leads to a cost-benefit calculation, which ends in an inevitable extension of the transmission network.

[43] OFFIS – Institute for Information Technology, 26121 Oldenburg, Germany, {forename.surname}@offis.de, R&D Division Energy
[44] OFFIS – Institute for Information Technology, 26121 Oldenburg, Germany appelrath@offis.de, R&D Division Energy
[45] Technische Universität Braunschweig, 38106 Braunschweig, Germany, m.kurrat@tu-braunschweig.de, elenia

However, a cost-benefit calculation for an expansion of the distribution grid ends in a different way: In contrast to the transmission grid the capacity congestions in the distribution grid regularly originate in distributed generation units, because the distribution grid was designed to provide sufficient capacity only for the electrical load. Taking the costs and the efforts of the distribution grid expansion into account, an expansion of the distribution grid is not acceptable. Capacity congestions in the distribution grid usually lead to a powering down of responsible generation units. It would not be efficient to extend the distribution grid to every possible feed in of distributed generation units which is why the occurrences of the capacity congestions should be considered for the expansion planning.

This is why the ReFlex concept has been created. ReFlex takes smart market opportunities and provides them to be used within the smart grid. The ReFlex concept aims to increase the amount of decentralized generation units in distribution grids. This concept furthermore allows the distribution system operator (DSO) to deal with capacity congestions in the grid through flexibilities of network users.

3 Methodology

For the work package 3.2 several methodologies were used and will be explained in this chapter. On the basis of literature review and discussions within the project's internal interdisciplinary working group for market design, different future specifications of the energy-economic framework have been developed. In cooperation with the German Academy of Science and Engineering (acatech), the representative of the Ministry of Economy and Energy, the Federal Network Agency, the Bremen Energy Institute (Prof. Brunekreeft), Offenburg University (Prof. Dr. Weidlich), the Agora energy turn (Dr. Graichen), from energy suppliers (EWE AG) and energy company (RWE) the expert workshop "Future Energy Markets" was carried out. Their discussion focuses the main essential question if a market, which includes both energy supply and ancillary service providing, will be able to ensure a stable system operation even without a central coordinating actor. During this workshop the challenges of the market design were discussed and led to the publication "Future Energy Markets" which handles the structured challenges and problems.

Another methodology was the "Market Engineering" methodology by Neumann [4]. This methodology describes a possibility for the development and introduction of a market design (as shown in Figure 6). The process model starts with a requirement analysis. The goal is to identify all important requirements for the implementation of the market design. Based on the main requirements, the market design development occurred. This is an iterative development process which generates a market model to identify the requirements as good as possible. For the evaluation of the market model, individual components were investigated in function tests and plausibility tests. After a successful evaluation of the individual components, the market model can be implemented completely and introduced as a market system.

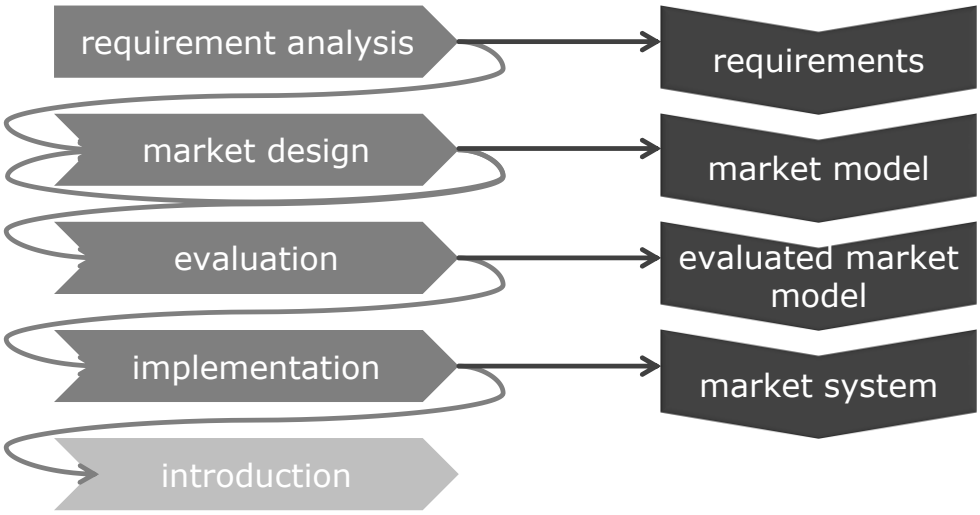

Figure 6: Methodology for Market Engineering

In order to achieve an efficient mains operation, the network operator should have an opportunity to provide short-term resolution of network congestions through a market-based method (market-based redispatch). It is easy to integrate the resulting market design into the current intraday market and allows the network operator to influence the regulatory and the economical restrictions of energy trade.

The process of market design focused on the development of the existing market model to implement new requirements. Therefore the workgroup "Market Design" was established within the project Smart Nord. This group consists of the scientific staff of the disciplines of power engineering, computer science and industrial engineering from the Universities of Oldenburg, Hanover and Brunswick. In this group, variations and evolutions of the current market design were discussed in general and in particular for Smart Nord on the basis of requirements analysis.

The evaluation of the final market model and the concept of ReFlex were made by several functional tests of the individual components as suggested in the methodology by Neumann. The components include the calculation of the grid, the identification of critical grid-areas and the resulting definition of the product. The evaluated market model was implemented and integrated into the Smart Nord system.

4 ReFlex Concept and Evaluation Scenario

The aim of the ReFlex concept is to promote the integration of distributed energy systems into the power grid. It is intended to give a DSO the option to take a market-based impact on the supply situation in the network. Therefore, an assignment of products required from grid areas is needed. In contrast to the auction, trading the intraday market can be characterized as continuous and combinatorial. Bids of the market participants are placed in an order book and are visible to other market participants. These can be asks or bids of power products. Set bids in the order book will be continuously assessed by the market and matched with other orders if it is possible. For the contribution of a bid, the following properties must be provided: buy or sell (bid / ask), validity period of the bid (expiry), quantity, price limit and delivery. In addition, other restrictions can be made. Execution conditions are restricted to the marketplace operator and are focused on the market matching. They connect the market matching with the conditions of the bid. To implement the ReFlex approach, two execution conditions have been added: Restricted-To-Grid (RTG) and Restricted-out-of-Grid (ROG). Both execution restrictions need additional information to identify the grid topological areas. In a simple scenario it is a set of network nodes. In a complex scenario

area of a power grid, the utilization of appropriate keys is preferred. The execution conditions RTG and ROG allow a market matching only for offers that are within (RTG) or outside (ROG) of the defined grid topological area. With these design conditions it is possible to set bids in the intraday market as a network operator which have a grid topological reference. A network operator is able to set specific products in the market that counteract capacity congestions within the power supply. The network operator is able to perform a redispatch within the distribution network while using this product. For this reason two AND-linked bids need to be set in the market: the first bid (RTG) to resolve the capacity congestion in the distribution grid itself and the second bid (ROG) for the balance sheet of the first bid. Therefore the financial balance does not counteract against the redispatch measure, the second bid should be located within the inverse grid area of the first bid.

The timing of the scenarios for evaluation is as follows: At first the units trade energy at the Day-Ahead Auction of the Epex Spot market. On the basis of the trading results the unit schedules are generated and transmitted to the DSO. Then the DSO performs a network state estimation of the distribution grid and identifies possible capacity congestions within the electrical network. Thereupon the DSO discovers the electrical grid zone (RTG) and defines corresponding ReFlex products that are able to counteract on the capacity congestion. The corresponding ReFlex product for the balance sheet (ROG) is also set up and both products are set on the intraday continuous market with an AND-link. After the intraday trading, the DSO again can estimate a network state estimation for the distribution grid with updated unit schedules and can take further action if the capacity congestion was not solved completely.

The evaluation scenario includes one medium voltage grid with 71 underlain low-voltage grid that contains 7808 grid nodes. It also includes 11,951 households, 789 heat pumps, 122 cogeneration plants, 1048 photovoltaic modules and 30 wind turbines. Models of white goods (fridges/freezer) as well as models of electric cars at first were an integral part of the evaluation scenario but had to be removed due to hardware limitations of the simulation server.

5 Main Results

The main results are split into results of the simulation and general results. The following section describes the simulation model and its results at first and ends with the general outcomes.

For the used simulation models, statistical parameters were calculated and visualized in the behaviour diagrams. In each case, a power plant capacity of five units per simulation model has been simulated over the year. The combined heat and power plant (CHP) is used in this section as an example to describe the simulation model. Figure 7 shows a differentiated analysis of day profile of a CHP within five diagrams. The diagrams show the daytime for one day with 1440 minutes on the horizontal axis and the power in watts on the vertical axis. The curves shown represent the electrical power (blue), the thermal power (green) and the thermal demand (red) of the unit. The first diagram “average day profile” shows the yearly average value for every minute as a characteristic curve. The red curve clearly figures the daily rhythm of the thermal demand, which is characterized by a high rise in the morning and by a peak in the evening and relative low demand during the night. The thermal power of the CHP (green curve) follows the run of the red line very well in the average. Deviations between the red and green curve can be explained by the thermal maximum power of the CHP and by taking advantage of the thermal buffer memory. The average value shows that the thermal buffer is loaded during the night time by the operation of the CHP, because the green curve is largely above the red curve. The peak of the thermal demand in the morning and in the evening will be covered by the collaboration of thermal buffer memory and peak load boiler, because the characteristic of the thermal power of the CHP is below the thermal requirements. The course of the electric (blue) and thermal (green) performance is very similar,

since these quantities are directly related. Ordinarily from minute 400 (equivalent to 6.40 clock) to minute 1300 (equivalent to 21.40 clock) an increased average performance by the CHP is provided.

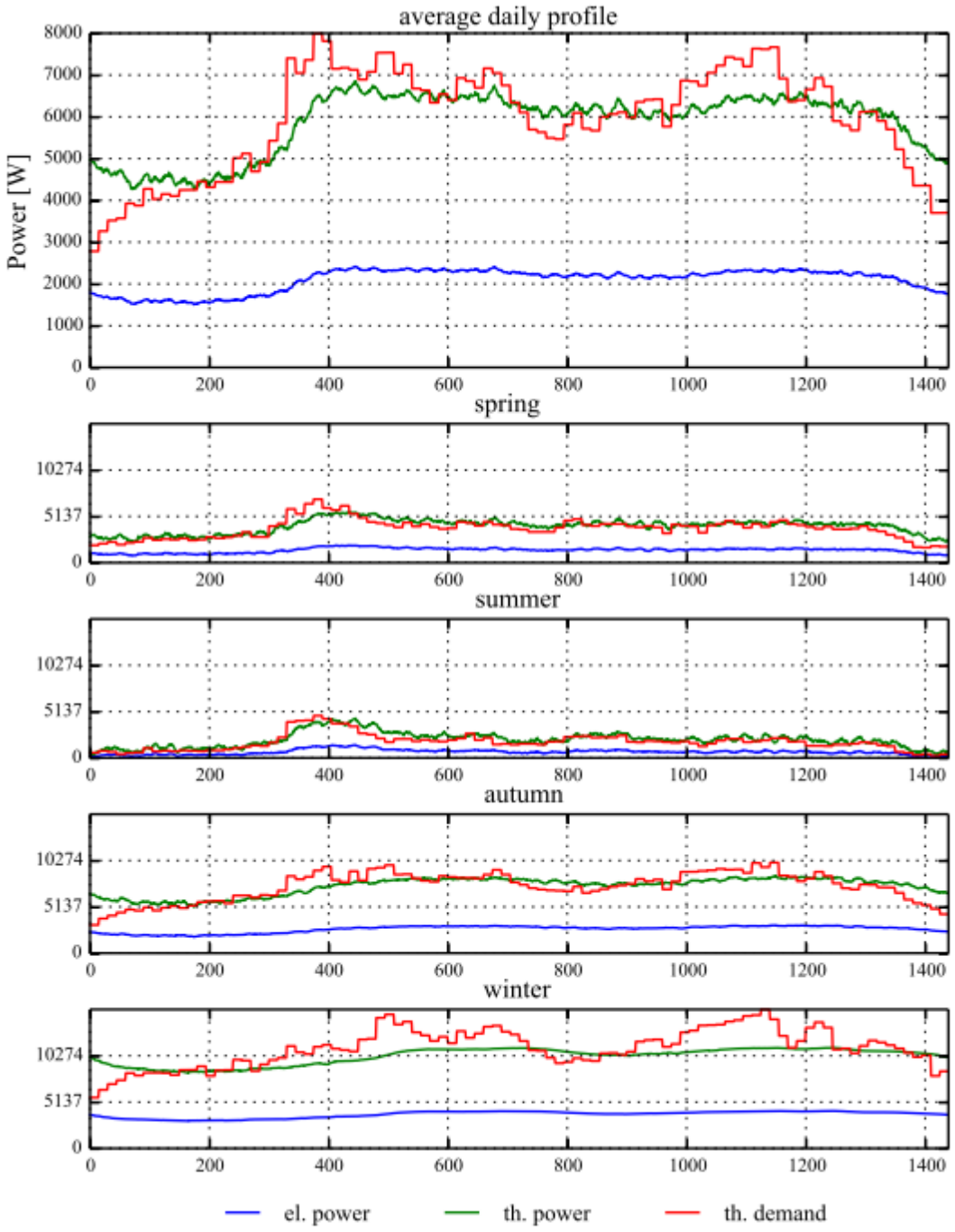

Figure 7: Differentiated analysis of day profile of a CHP

The simulation results of each day type were summed according to the advertised and successfully traded energy quantities of ReFlex products of one day. This makes it possible to determine the daily amount of energy, which was also picked up by the ReFlex concept from the grid. The difference between the tendered amount of energy and the actually traded energy produced an amount of energy, which threatened the state of the power system and has to be shut down. These operating numbers will be compared and contrasted in Figure 8. For each day the percentage of successfully traded amount of ReFlex bids is shown. The figure shows the results for typical days

during the transition period between summer and winter in the first four bars, followed by four winter-type days and two summer type days. The abbreviations mean the following (first character): transition (Ü); winter (W); summer (S). The second character differentiates between working days (W) and Sundays (S). The last character of the coverage means Clear (H) or Cloudy (B).

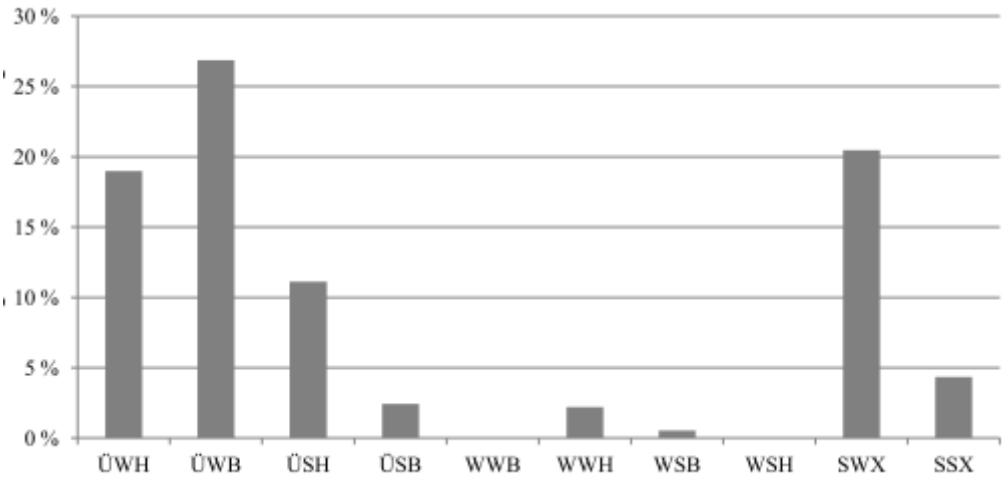

Figure 8: Seasonal evaluation to the percentage share of traded reflex amounts of energy

The proportion of traded ReFlex bids is subject to a significant seasonal variation. During the transition days, as well as during the summer days, a proportion up to 26 % of the advertised performance was sold. During the winter days there was no significant success. One reason for those negative results during the winter days is based on the simulation models used, which cover up those flexibilities. Both simulation models (heat pump and CHP) consider flexibilities for evaluation. For that reason, the results reflect flexibility potentials reduced during the winter months, because both systems refer to the thermal requirement of a connected object as well as they must cover up their primary demand.

Another significant criterion is whether the day is a weekday or Sunday / holiday. This is clearly reflected in the transitional and summer-type days, because the percentage of the amount of traded ReFlex energy is significantly less on Sundays / holidays than on working days. The differences regarding the transition type days are about 8 % (ÜH) respectively about 25 % (ÜB). Even during the summer type days a high difference about 16 % is given. The third criterion describes a cloudy / unclouded scenario, which does not give a concrete statement. For it seems not to be possible as the proportion of successfully traded ReFlex energy levels do not correlate.

The evaluation of the results on an annual basis shows how the results strongly depend on the flexibilities. The reduction of the flexible simulation models (white goods, electric cars) has a significant negative effect on the quality of the results. The analysis of each type day shows a frequently violation of the voltage band of the upper voltage band in the middle of the day, which results into the intensive electricity from the PV. The flexible consumers (heat pumps) cannot work against the violation of the voltage band, particularly not within the winter months. The reason behind is the design of the heat pumps. They can rarely provide their connected objects during the winter with thermal power. Therefore heat pumps will permanently be in operation on cold days and have no flexibility to obtain additional power. The thermal demand of households for preparation was rather insignificant on warm days, whereby the heat pumps cannot handle the additional heat power from the charge of the operation of the PV. The other flexible units are the

CHP, which are very similar to the thermal coupling to the supplied objects in their behavior. During the summer, the low thermal requirement prevents the operation. During the winter, a shutdown due to the high thermal demand of the supplying object is not possible. Overall, there are some type days which produce an overload within the MV network. This leads to correspondingly high ReFlex bids by the network agents.

The magnitude of the required compensation is currently so high that the units behind the gird overload are not able to provide sufficient flexibility. The scenario was defined in this study as part of the project Smart Nord. The simulation results of this work repeatedly show that for the MV network line expansion is necessary.

By the following assumptions (the ReFlex reduced voltage band violations, reduced line overloads, transformer overloads and also increased the capacity for integration of RES) in particular the possibilities of the network operator have been restricted to resolve capacity congestions. Moreover, the results represent the potential of the ReFlex concept, which can be used in combination with other measures for the network operator to increase the capacity of the current electricity networks for renewable energy. It became also evident in the simulations that a network expansion in the MV network is required. The concept could not solve the network problems. However, a network expansion in the distribution network would require 3-5 years what can lead to voltage band violations and grid overloads. During the transitional period until this network expansion, the concept has the opportunity to implement a forthcoming network expansion, or to use the time to expand efficiently for the energy revolution.

6 Conclusion and Outlook

In this sub project a market-based approach for the development of flexibilities was engineered. This approach can serve as another possibility for a power company to increase the renewable energy integration of the electricity grid. For this purpose, new requirements for a market design were identified within a requirements analysis:

- The compensation of lost revenue from the renewable energy due to the isolation will not be sustainable with the increasing development of renewable energy. The renewable power plants have to be traded directly on the energy market to respond on the price signals.

A precondition for an effective input to the energy transition is the practical relevance and the compatibility to the existing market design. Therefore only market models with a possible transition of the current market design will be developed.

The simulation study has shown that the potential of operators' flexibility through the ReFlex concept can be utilized. These potentials are visible, especially in the transitional period. Furthermore they are about 20 % of the tendered amount of energy in the simulation studies. Localizable products are characterized by an additional condition of completion of a market matching. This only allows trading on the market when the market participants are located in the defined grid area of the DSO. Therefore only a slight change in the current market design is necessary, what is reflected in an additional execution condition for intraday products. The qualities of results based on the scenario, in particular due to the transition time by the use of thermally coupled systems as the only flexibility option. The limitation of these systems depends on the complexity of the simulation environment, the resulting computation time and the memory requirements.

The ReFlex concept was not always capable to counteract grid problems within the simulation study. This is due to the scenario, which is based on a network state in 2011 and covering the development of renewable energy with a time horizon to 2030. Although it leads to significant

reverse power flow in the medium voltage grid and associated overload. Within the illustrated scale a grid expansion in the range of medium voltage network is not averted by the ReFlex approach.

The evaluation was based on the evaluation scenarios of the research project Smart Nord and with mosaic-simulation framework which was developed at OFFIS. This market design of today's energy market is modelled in the simulation framework and implemented enhancements are based on the ReFlex concept.

Overall, the developed market model has a non-massive intervention to the existing market design. It merely extends the existing market design to an additional execution condition for Intraday-market products, so that a transition from the current market design to the proposed market model is possible.

Work Package 3.3: Business Models for Energy Producer and Price Sensitive Consumer

Sören Christian Meyer[46], Hans-Jörg von Mettenheim[46] and Michael H. Breitner[46]

1 Current Market Situation on the German Electricity Market

The German electricity market is divided into areas with strong market regulation and fixed taxes and levies as well as market driven segments. Examples for market driven participants are large scale fossil power plants and large scale electricity consumer.

Those fossil power plants actively base their production on EEX-market prices and as additional revenue on auction based controlling power compensation. Assumed that the marginal cost (the merit order) are price setting on both markets, a cost effective behaviour for effective and balancing power supply can be assumed.

Large electricity consumer (above 1 GWh) profit as well from 85 %-99 % reduced EEG apportionment (§64 EEG 2014) as from reduced grid tariffs due to their connection to the medium or high voltage grid and options like the atypical grid usage. (§19 StromNev).

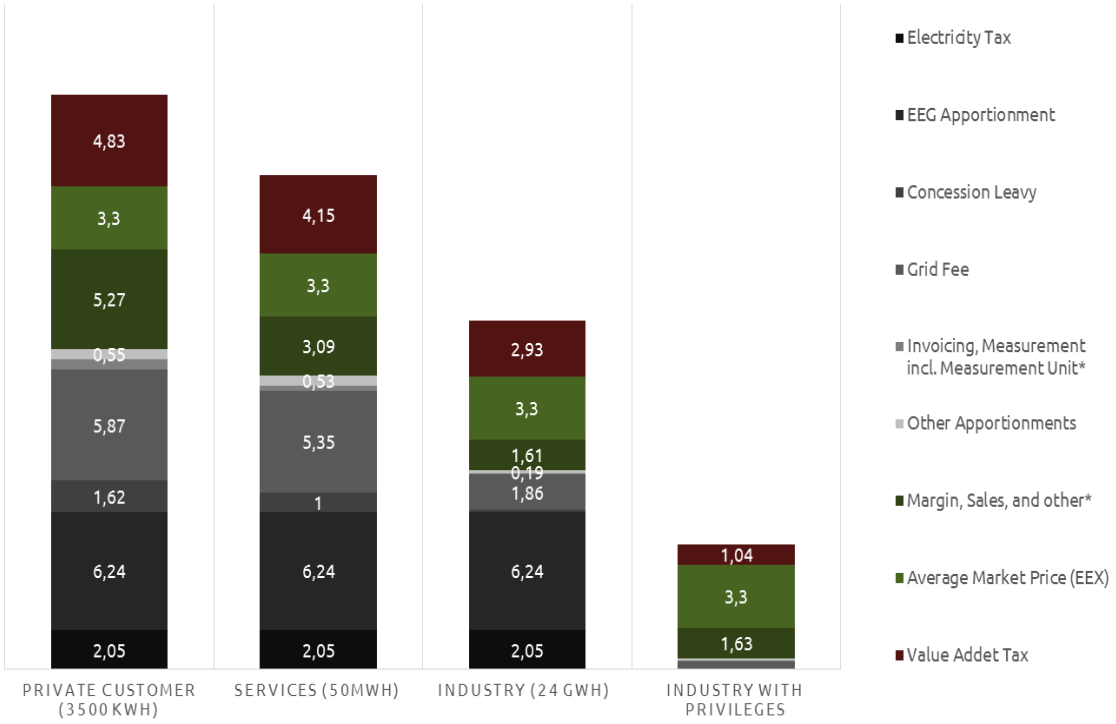

Figure 9: Tax and levy burden on electricity consumption in eurocent per kWh

In contrast small scale decentralized producer are either dependent on weather conditions (Wind, PV) or on heat demand (CHP). For all three exist with the market premium model the option to participate in the market, but the investment in steering infrastructure needs to be set in relation to

[46] Leibniz Universität Hannover, 30167 Hanover, Germany,
{surname}@iwi.uni-hannover.de, Institute for Information System Research

the generation capacity. For large electricity customers the price is mainly based on fixed taxes and levies, as well as administrative cost and margins. For those customers no incentives for grid friendly usage change exist.

From the economic perspective, it is efficient, to supply grid services with lowest overall cost as possible. As long as large scale electricity generator and consumer are able to supply these services with low cost for steering infrastructure, this is indeed the best option.

With the Transformation of the Energy System (TES) and the substitution of centralized fossil power plants by decentralized renewable power plants, grid services are no longer minor products from effective power generation but have to be actively supplied by small, decentralized agents. In general the decrease of steerable producing units already results in a higher volatility and increasing price spread in the effective power market. With further progress of the TES and decreasing costs of steerable units small customer and producer are going to have an incentive to invest in measurements enabling them actively to benefit from volatile prices for effective and balancing power.

Therefore in the long run the current high liquidity on the market for balancing power will decrease resulting in an increase of the overall price level as well as the volatility of balancing power prices. In consideration of a highly legislative regulated market and long investment live times in the electricity sector, it is necessary to develop solutions in advance of the expected shortage.

2 Tax and Duty Burden on Electricity in Germany

Figure 9 illustrates that fixed taxes and levies are the main price component and solutions for reducing this burden needs to be found first to create an economic feasible business model for flexible pricing. The taxes add up to 17 eurocent per kWh. Most important factors are the EEG apportionment with 6.24 eurocent per kWh and the grid fee (dependent on area) with an average of 5.87 eurocent per kWh. Connected to the grid usage is the concession levy, which differs dependent on the city size, increasing for larger cities and having an average of 1.62 eurocent per kWh. The energy tax of 2.05 eurocent per kWh is dependent on extracting electricity from the public grid and the sales tax is an addition of 19 % on the electricity price and is also raised on the taxes included in the electricity prices. Furthermore with such a tax burden the consumer price of 17 eurocent per kWh only for refinancing taxes and levies it is nearly impossible to develop flexible electricity tariffs. Therefore the business model needs an essential step to reduce the tax burden.

Due to the nature of the different taxes the grid fee can be saved if no public grid is used. If a public grid is used, only the actual usage needs to be paid. Therefore the usage of only the low voltage grid, saves the grid fees for high voltage usage. The EEG apportionment can be saved if electricity from renewable sources is used by its proprietary and the maximum power is below 10 kWp. If the maximum power is above 10 kWp 40 % of the EEG apportionment has to be paid. Furthermore the power generation units have to be in the same low voltage grid. The grid fee is dependent on the usage of a low voltage grid, therefore it has to be paid if electricity is transported from one household to another. The assessment basis of the electricity tax is the usage of power from the public grid, but can be avoided if the electricity is used in direct local connection to its generation. The sales tax can only be reduced if other taxes and levies are reduced.

3 Future Renewable Electricity Generation Cost

The second essential part for future business models is the knowledge about the development of renewable electricity prime cost. Therefore production based experience curves were used, due to

the fact that they have proven to be robust for long time price predictions and they are widely used in policy scenarios. Experience curves are based on statistical derived learning rates. Learning rates describe the percentaged price decrease of a product, each time the amount ever produced is doubled. Learning rates are statistical derived from market data.

The learning rates were retrieved from a literature review of 100 scientific high ranked paper dealing with the research area. This data were combined with market forecasts from the IEA. Those predictions can be included in cost calculations. The shown prices are examples for the conditions in the Hanover region. The resulting experience curves are shown in Figure 10. The forecast shows that for onshore wind energy a further price decrease by 50 % can be expected and electricity from photovoltaic rooftop installations can reach price levels of 7.5 eurocents per kWh until 2030.

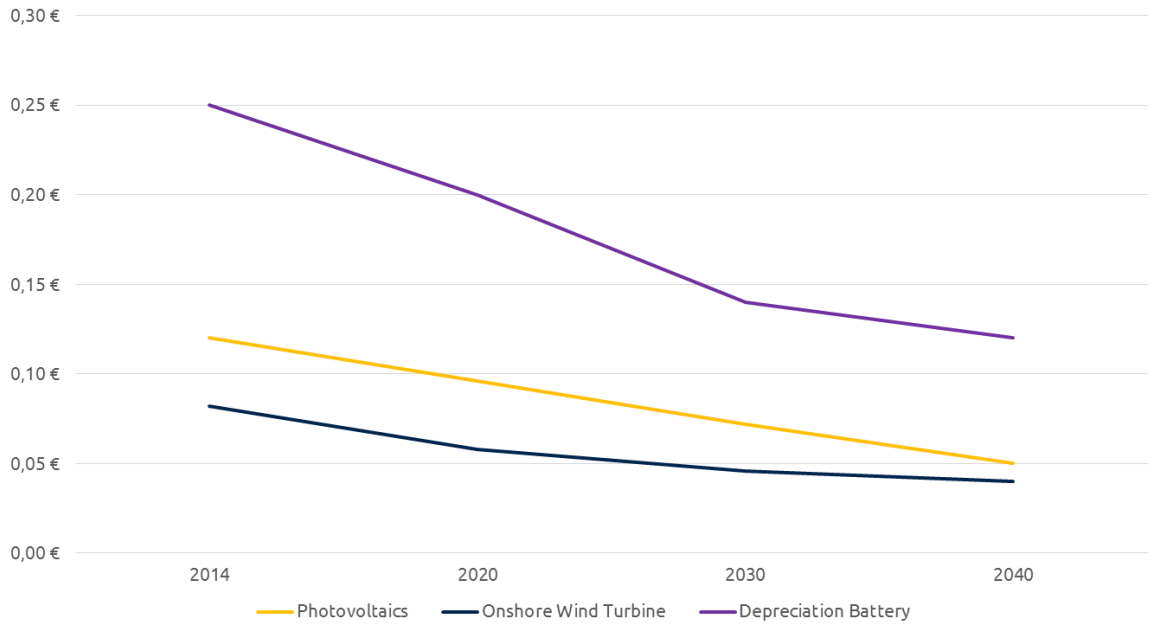

Figure 10: Expericene curve based prediction of renewable electricity generation cost per kWh

4 Description of the Developed Business Model

The business model was designed as iterative process using the methodology of Wirtz [2] and combined with design science research. The resulting business model was simulated with the environment "MATLAB" and the result was used to optimize the business model which was finally tested in the simulation.

The developed business model combines the described tax and duty burden criteria with the price forecasts. As result mainly for the EEG apportionment and the grid fee a "Customer Installation" would be the most inclusive solution. Using a construct consisting of an energy association as owner of the installation and customer being member in the association [5].[47] The needs for the a customer installation as actually being owned by the association as well as the untypical grid topology with wind power and free field-PV connected to the distribution grid mainly limits the business model to newly developed area. Furthermore the economic feasibility of CHP is better if the heat distribution network can be built together with for example the water supply.

[47] The author wishes to appoint to unsettled lawsuits in close relation to the legal construct. For use in actual projects waiting for a cleared legal situation after settlement of those trials is advised.

The project calculation is based on a fictive example project with 86 accommodation units distributed in mixed apartment and detached houses.

For keeping the amount of other supplier minimal, it is necessary to offer electricity with a cost competitive pricing. In the Hanover region the reference price for an renewable electricity supplier is a value added tax cleared net price of 19.6 eurocent per kWh and an annual base price of 68 €.

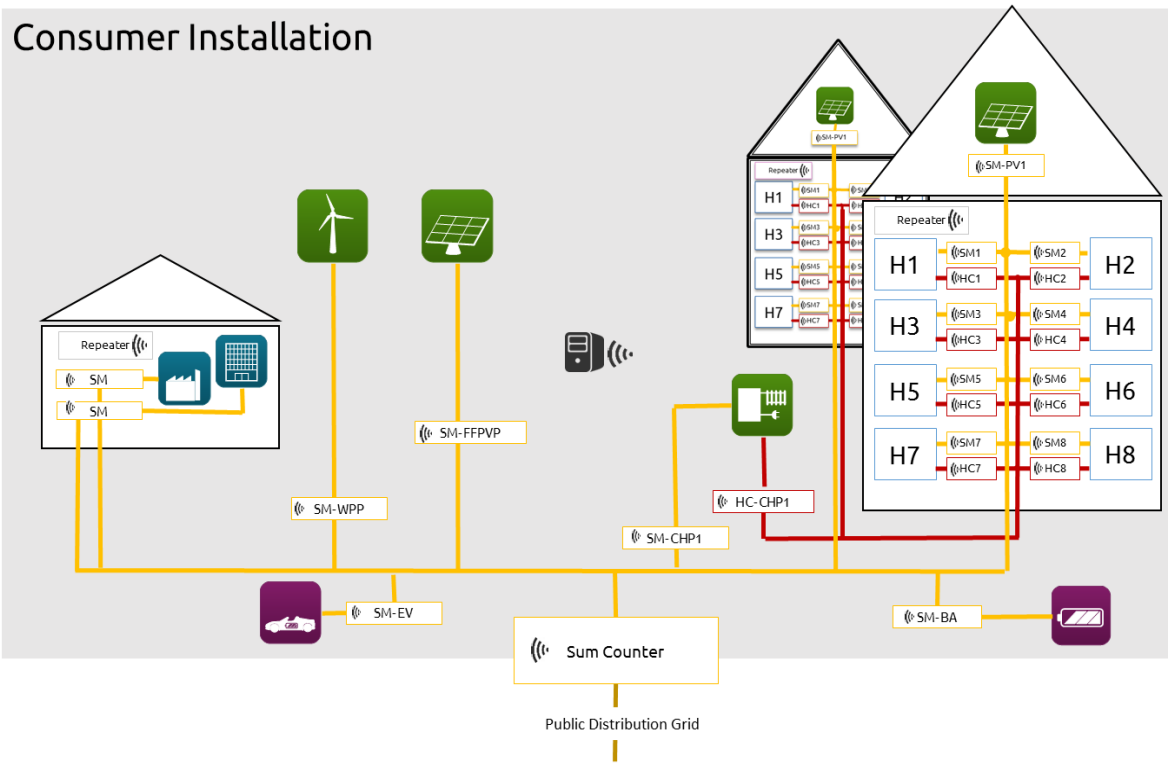

Figure 11: Schematic diagram of the consumer installation

The needed IT infrastructure for optimization and billing can be used as hosted solution priced with 3250 € p.a. or about 40 € p.a. per customer. The overall electricity consumption from the public grid or feed in into it from the customer installation is measured by the sum counter model. Therefore the electricity demand or feed in at the connection point to the public grid, the power generation within customer installation, and the electricity consumption of all customer is measured using a 15 min resolution. This is necessary, for being able to subtract customer within the customer installation, receiving electricity from other suppliers and deliver by calculation electricity from the public grid. This additional effort is needed, due to the regulatory necessity to allow the customer to choose their supplier without restriction. Furthermore a smart meter is obligatory for flexible electricity tariffs resulting in investment related cost of about 18 €. Therefore the net pricing is sufficient for maintaining the optimization and data collection infrastructure.

Hence the competitive average price of 19.3 eurocent per kWh needs to cover the remaining tax and levy burden, the consumer installation, the generation cost and the producer and consumer incentive for grid stabilizing demand shift.

The electricity generated and carried within the customer installation is freed of 60 % EEG apportionment, grid fees and electricity tax. The resulting subsystem therefore only needs to pay 2.5 eurocent per kWh EEG apportionment, 1.79 eurocent per kWh concessions levy if public

ground is crossed and the value added tax of 19 % on the overall price. For the residual load from the public grid a peak load based basic charge needs to be paid. The customer installation can be financed by about 3.5 eurocents. With 11.71 eurocent as remaining factor, the most suitable electricity sources are gas powered CHP with electricity generation after CHP-subsidies (5.41 eurocent) or wind power in the same price range. Simulations have shown the option to allow a price range low to high about 18-28 Eurocent. Therefore the administrative cost needs to remain about 2 eurocent per kWh or 8000 € for the subsystem. This is only possible if the billing takes place automated and in relatively large scale. So either the administration has to take place for a larger group of customer installations or by a service supplier.

In 2030 as described a higher volatility of the electricity prices can be assumed. Those lower renewable electricity prices and higher price fluctuations as well as existents of smart metering increases the cost competitiveness of the customer installation. Furthermore in general fixed electricity prices might vanish, due to those higher price fluctuations and the existents of smart meter. Also the existence of smart home components might progress driven by additional functionality if hardware can be controlled by smartphones. Under those conditions combined with lower prices the simulation was able to economically run a self-balancing system shown in Figure 11. It consists of batteries, electric vehicles, wash-dryer as steerable consumer and the central CHP-Unit as steerable supplier. As non-steerable the residual household load and wind power and PV is used.

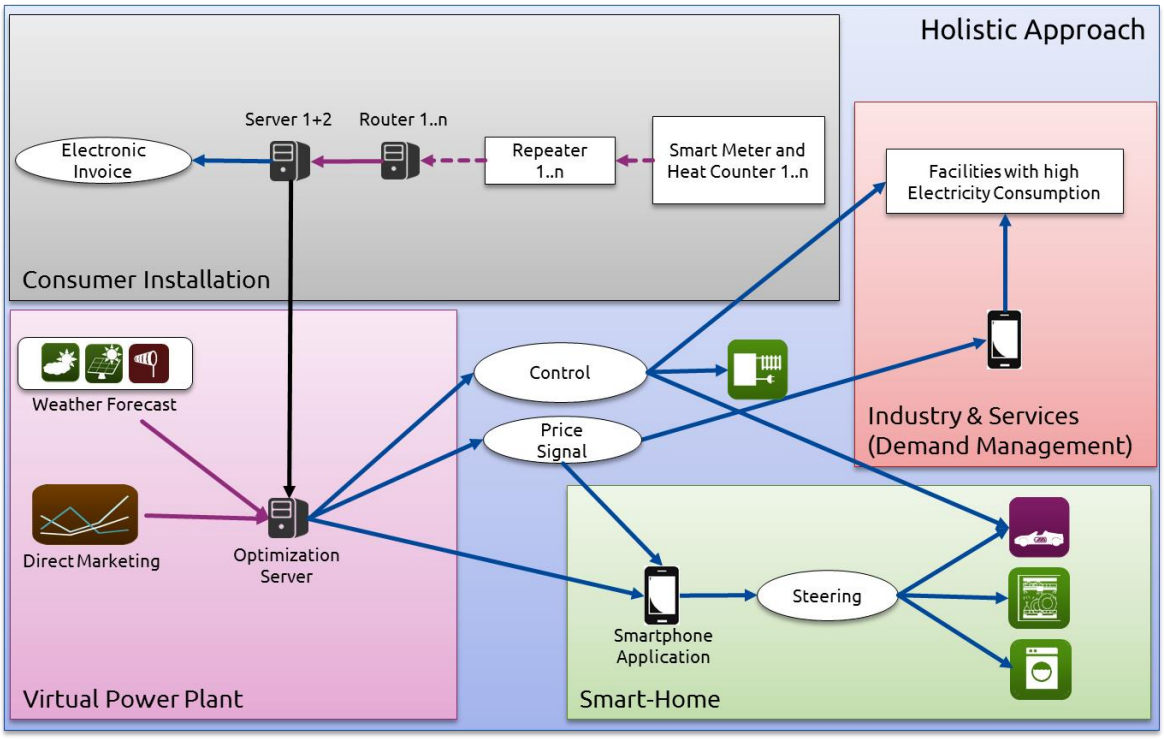

Figure 12: Interaction between the business model components

Figure 12 illustrates the modular business model. In the best case scenario heating and electricity are automatically billed together with smart metering and smart heat counter. The collected data can be used as well for billing as for forecasting purposes. The optimization server optimises the CHP-scheduling based on weather prognosis. This can be done in a local solution aiming to reach self-sufficiency, or optimized for benefit from high price timeslots on the EEX thereby smoothing the electricity prices. When economic feasible, Smart-Home solutions are able to use price signals

for steering of the household units. Large consumption units in households like EV or air conditioning in commercial units can be directly controlled by the optimisation server. The four segments of the holistic approach are interconnected and reach the maximum efficiency when joined. Due to the long lifetimes of the related goods and infrastructure of 15-40 years the approach was developed to be able to work with partial solutions. For example is the CHP unit joint with its billing infrastructure is already today available and in the described newly developed area scenario economic feasible. It can be run grid stabilizing and is flexible enough to smooth supply and demand peaks on an hourly base. With the direct marketing model sufficient market incentives for this steering exists. From the technological perspective it can also contribute minute grid reserve capacities which will become attractive if those is lesser contributed by large fossil power plants. Furthermore the CHP in the solution is able to contribute a significant CO_2 reduction compared with a solutions based on local gas powered heating.

Overall the sub-project was able to show, that at least in the 2030 scenario VPP solutions combined with Smart-Home components are able and economic feasible to actively contribute grid services, secured power and controlling power compensation. Furthermore it can reduce the volatility in EEX-electricity prices. Thereby VPP are able to fill part of the gap left by the reduction of large fossil power plants. The sub-project was able to show, that if enough steerable consumer exist, a price based supply-demand balancing is economic feasible in newly developed areas and can be combined with CHP. The legislative situation thereby forces difficult solutions. It would be preferable and lead to less market distortion, if the amount based tax and levy burden was changed towards a price based percentual system. This would allow to give easier price incentives also to non-privileged small commercial and private customers.

References

[1] N. G. A. Hemdan, F. Muuß, D. Unger, M. Kurrat, "Reactive Power as an Ancillary Service Provision into Transmission Networks through Decentralized Generation," Cigre Belgium 2914.

[2] M. Kurrat, N. G. A. Hemdan, B. Engel, R. Canders, M Henke, "Technical challenges for ancillary services provided by decentralized power generation in active distribution systems," ETG Kongress Berlin 2013

[3] F. Muuß, N. G. A. Hemdan, M. Kurrat, D. Unger, B. Engel, "Dynamic Virtual Reactive Power Plant in Active Distribution Networks," Powertec, Eindhoven 2015

[4] D. Neumann, "Market Engineering - A Structured Design Process for Electronic Markets Faculty of Economics Karlsruhe," University of Karlsruhe (TH), 2004.

[5] B. W. Wirtz, "Business Model Management : Design - Instrumente - Erfolgsfaktoren von Geschäftsmodellen," 3. akt. u. überarb. Aufl. 2013. Wiesbaden: Gabler Verlag, 2013.

[6] C. Köpp, H.-J. von Mettenheim, M. H. Breitner, "Decision Analytics mit Heatmap-Visualisierung von mehrschrittigen Ensembledaten." Wirtschaftsinformatik: 147. doi:10.1007/s11576-014-0417-3., 2014.

[7] B. Küster, A. Koukal, M. H. Breitner, "Towards an Allocation of Revenues in Virtual Clusters within Smart Grids" IWI Diskussionsbeiträge 60 (September), 2013.

[8] S. C. Meyer, M. H. Breitner, "Electricity Associations as Marked - Based Steering Mechanism and Alternative to Fixed Feed - in Tariffs," Proceedings of the 28th EnviroInfo 2014 Conference: 729–734, 2014.

Sub-Project Four:
Distribution and Transmission System

Overview on Sub-Project Four: Distribution and Transmission System

Lutz Hofmann[48], Timo Breithaupt[48], Steffen Garske[48], Torsten Rendel[48], Bernd Engel[49], Stefanie Koch[49] and Marco Zobel[50]

1 Introduction

Within the ongoing transformation of the electric energy supply system several questions of grid integration and overall system stability occur. With the decreasing feed-in of conventional thermal power plants, the ancillary services formerly provided by conventional power plants have to be taken over by distributed generation (DG) mainly using renewable energy sources (RES). For future energy supply systems, the possibilities and the boundaries of power system states with a high share of DG units, which – in opposite of the conventional generation – are connected to the distribution grid have to be analysed. Hence this is a matter of transmission and distribution grids, both system levels have to be analysed in one integrated simulation model. Therefore an overall system model is developed to evaluate the two evaluation scenarios of this research project – the reference scenario 2011 and the future outlook scenario 2030. The integration of DG units within these scenarios into the distribution grid as well as micro combined heat and power (CHP) units in particular are analysed in detail within this sub-project.

The research questions of this sub-project cover the provision of two essential ancillary services. These are reactive power provision to support stationary voltage stability in all voltage levels and provision of control reserve to ensure frequency stability. The reactive power provision is managed within the integrated grid and market simulation model (INES) to secure valid power system states. The frequency stability studies are done for characteristic points in time based on characteristic system states and incidents. In this way the need and the amount of primary control reserve provided by DG units are determined. Furthermore the possible capabilities and also the limitations of grid states with high shares of DG can be analysed and evaluated. This is accompanied with simulations and laboratory experiments of micro-CHP systems and detailed analyses of the grid integration of DG within the medium and low-voltage distribution grid.

2 Goals

The main goals of the sub-project four: Distribution and Transmission System are:

- Setting up a system model for integrated simulations of transmission and distribution grid (work package 4.1) based on the integrated grid and market simulation
- Integration of the evaluation scenarios 2011 and 2030 into the system model (work package 4.1)
- Simulations of the evaluation scenarios 2011 and 2030 in the system model and the distribution grids (work package 4.1 and 4.2)
- Analyses of stationary system states and provision of reactive power by DG units in the underlying voltage levels to the transmission system (work package 4.1)

[48] Leibniz Universität Hannover
[49] Technische Universität Braunschweig
[50] EWE-Forschungszentrum für Energietechnologie e.V.

- Frequency stability studies within the system model for characteristic points in time to determine the required provision of primary control reserve by DG (work package 4.1)
- Evaluating the supply of active power using micro-CHP systems (work package 4.2)
- Assessment of the integration of DG units in the medium and low-voltage distribution grid (work package 4.2)

3 Main results

The work package 4.1 developed an overall system model as extension of the integrated grid and market simulation model in cooperation with the work package 4.2 and the work group Scenario Design. This system model is suitable for simulations of stationary power system states and for frequency stability studies within the evaluation scenarios 2011 and 2030 of this research project. The provision of reactive power by DG units was evaluated for different reactive power management approaches. The frequency stability studies were done for four characteristic points in time based on an incident referring to the ENSTO-E reference incident. The simulations show that a secure system operation regarding frequency stability in the future scenario is possible and that within the simulation model the provision and management of reactive power is essential. To ensure stable operation, RES generation has to participate in a fastened primary control at some points in time.

Furthermore it was shown that the ongoing installation of DG units leads to a high grid reinforcement demand. Within the evaluation scenarios for the distribution grid section and the increased amount of DG a reinforcement of 32 % of all cables and 58 % of all transformers at the MV-level was needed. Similarly, at the LV-level 11 % of the cables and 7 % of the transformers had to be supplanted. It was shown that the simulated and measured data of the micro-CHP within laboratory validations are consistent. The evaluated CHP system matches the requirements for a controlled active power supply, but its high potential can only be used if a high number of systems are installed in the local grid.

Work Package 4.1: Interconnected System

Timo Breithaupt[51], Steffen Garske[51], Torsten Rendel[51] and Lutz Hofmann[51]

Abstract

The ongoing transformation of the energy supply system from a classical design with large scale fossil power plants and power flows directed from ultra-high voltage to low voltage levels to a generation mainly realised using renewable energy sources (RES) leads to several questions of grid integration and overall system stability. Conventional thermal power plants are more and more displaced by distributed RES generation which is mainly connected to the distribution grid. With this changed power plant dispatch the ancillary services formerly provided by conventional power plants have to be taken over by RES generation. As the provision of ancillary services is a matter of overall system stability within the transmission system, not only the possibilities, but also the boundaries of future energy supply systems with a high share of RES generation have to be analysed. Since this topic is a matter of both, transmission and distribution grid, a system model has been developed to analyse both system levels. These analyses have been done for a reference and a future outlook scenario developed within this project. The system model comprises the European electricity wholesale markets, the Continental European Transmission grid and single distribution grid sections modelled in detail at selected transmission grid nodes. By means of this system model mainly two ancillary services have been investigated: reactive power provision to support stationary voltage stability and control reserve provision to ensure frequency stability. The reactive power provision is analysed in both scenarios and implemented as new optimisation approaches for the transmission system model as well as the extended model with underlying distribution grid sections. The provision of reactive power has been analysed within the voltage bands deviations of the transmission system model. Several approaches have been examined to attain valid and stable system states and to quantify the reactive power exchange between the two system levels. The frequency stability studies show, that a secure system operation regarding frequency stability in the future scenario is possible. To ensure this stable operation, RES generation has to participate in a fastened primary control at some points in time.

1 Introduction

The analysis of the contribution of underlying voltage levels for ancillary services to the transmission system is a matter of both distribution and transmission grid. Hence, both system levels have to be evaluated in one overall system model. A detailed model of the ENTSO-E[52] Continental Europe transmission system (see Figure 1) is given by an integrated grid and power market simulation (INES) developed by the Institute of Electric Power Systems (IEH) [1] [2] [3].

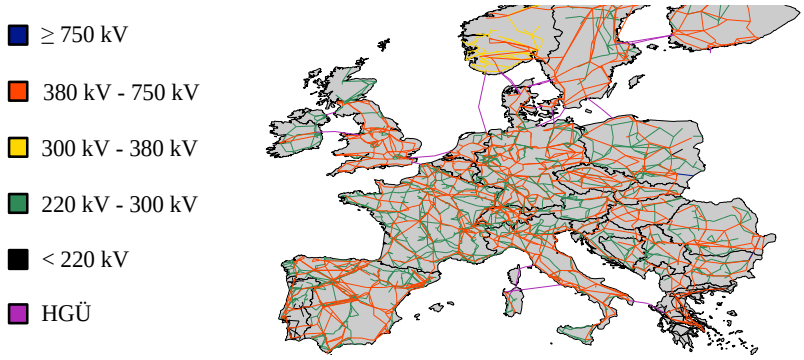

Figure 1: Integrated grid and power market simulation

[51] Leibniz Universität Hannover, 30167 Hanover, Germany,
{surname}@iee.uni-hannover.de, Institute of Electric Power Systems
[52] European Network of Transmission System Operators for Electricity, https://www.entsoe.eu/

The INES system model is parametrised on basis of several databases, e.g. power plant allocation, regional characteristics as well as various input parameters like e.g. grid and economic data. With this simulation environment a wide foundation for different analysis of stationary processes like transnational transmission grid calculations is given and a fundamental data basis can be used for this project.

The answering of the research questions of the work package (WP) 4.1 are based on the analyses of stationary as well as dynamic processes (see Figure 2) carried out by example of the two evaluation scenarios which were prepared by the work group Scenario Design (see report of the Work Group Scenario Design) for this research project. Firstly, the year 2011 (reference) and secondly, the year 2030 (future outlook) have been implemented into the simulation model and have been evaluated and compared in respect to stationary system state and frequency stability. With this methodology the need and the amount of contribution of distributed generation (DG) units, which basically use renewable energy sources (RES), to ancillary services, esp. provision of reactive power and control reserve, in the transmission system can be analysed and estimated.

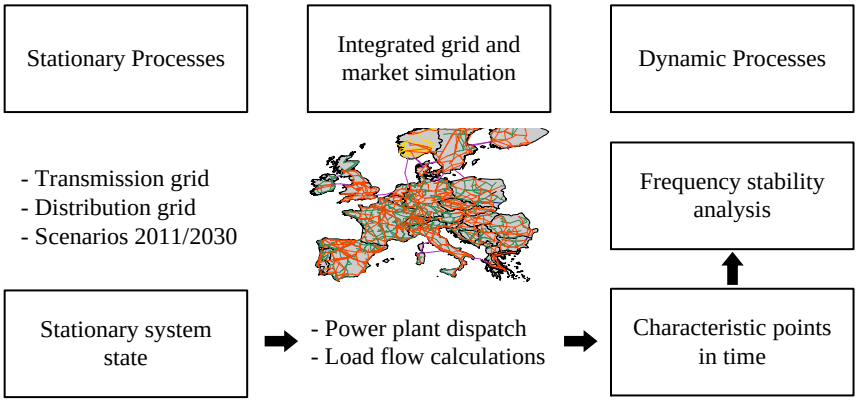

Figure 2: Methodology of the work package 4.1

Therefore the WP 4.1 in cooperation with the WP 4.2 and the work group Scenario Design has developed an integrated system model as extension of the INES simulation environment covering all voltage levels with coherent growth forecasts for power generation in both scenarios. This can be used for the analysis of stationary processes (see chapter 3) and with extensions made within this project also for the evaluation of frequency stability (see chapter 4).

2 Overall System Model

Because of the spatial expanse of the ENTSO-E transmission system and the expanse of distribution grids from the ultra-high voltage (UHV) to high voltage (HV) transformation down to the single households in the low voltage (LV)-level a simulation of the entire transmission system with all underlying voltage levels is not feasible. Thus only at single UHV nodes a distribution grid section is integrated into the INES simulation framework of the transmission system. Hence, as presented in [4], one challenge was to integrate the underlying voltage levels with detailed grid, load and generation data (see work group Scenario Design) for the medium voltage (MV) and LV level into the existing system model of the transmission grid. Therefore, the UHV nodal load and generation data was partitioned in distributed models of high voltage and medium voltage load and decentralised generation. Herewith the given aggregated data of one UHV node was substituted with an equivalent share of the underlying voltage levels and with a coherent consideration of the two scenarios for the years 2011 and 2030 in one system model. The HV level is modelled with

synthetic grids for each considered UHV node similar to the MV grid, which is based on a common MV benchmark grid [6]. For further description please refer to [4] and the report of the work group Scenario Design.

With this approach it is possible to analyse the two evaluation scenarios of the research project Smart Nord for both transmission and distribution grids in one coherent and detailed simulation framework and to determine the contribution of underlying voltage levels to ancillary services for the transmission system.

3 Analyses of Stationary Power System States

3.1 Power Plant Dispatch and Market Simulation

As a first result of the simulation of the overall power system using the integrated power system and power market model INES a power plant dispatch is determined with a market simulation based on a merit order of marginal costs, including the priority feed-in of RES with zero marginal costs [8]. Depending on the current load, which is partitioned in discrete load blocks (see [2]), all available power plants are arranged according to their current marginal costs

$$C_{\mathrm{m}} = \frac{C_{\mathrm{fu}}}{\eta_{\mathrm{el}}} + \frac{C_{\mathrm{CO2}}}{\eta_{\mathrm{el}}} EF + \frac{t_{\mathrm{su}}}{t_{\mathrm{op}}} \left(\frac{C_{\mathrm{fu}}}{\eta_{\mathrm{el}}} + \frac{C_{\mathrm{CO2}}}{\eta_{\mathrm{el}}} EF \right) \left(1 - \mathrm{e}^{-\frac{t_{\mathrm{down}}}{\tau}} \right) \tag{1}$$

which leads to a load and time depending power plant dispatch (see Figure 3 for the scenarios 2011 and 2030 for the German transmission system within the INES simulation model).

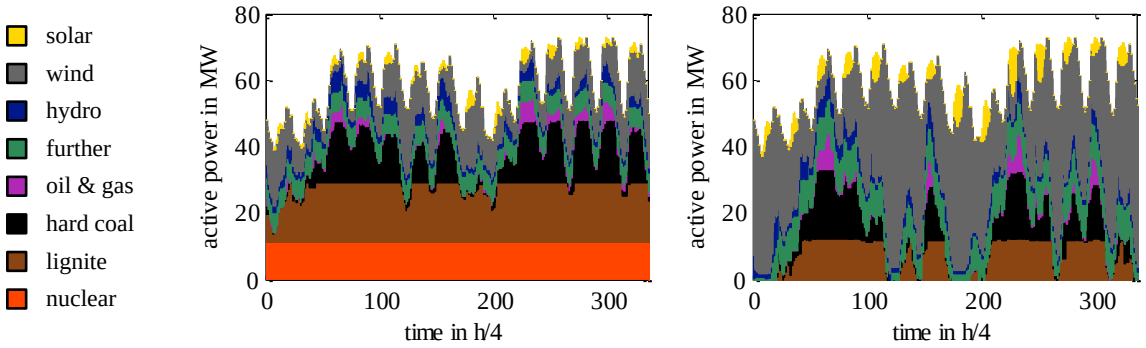

Figure 3: Power plant dispatch in the simulation model for two weeks in January in the scenarios 2011 and 2030

In the scenario 2011 (left figure in Figure 3) with two weeks of high load in January), the base load is mainly provided by nuclear and coal-fired power plants while the share of DG fluctuates between 5 GW and 20 GW. In comparison with the scenario 2030 (right figure in Figure 3 with two weeks of high load in January) including the withdrawal from the nuclear energy programme, a high ratio of the energy is provided by the RES (in this case mainly wind energy generation), which is mostly complemented in times of peak load or low wind generation with coal-fired or gas-fired power plants. These results for the power plant dispatch, generation by RES and load time series are the input data for the subsequent power system calculations.

3.2 Load Flow Calculations and Grid Expansion

The simulation environment INES combines the power plant dispatch for the different scenarios with geographical generation and grid data, which allows load flow calculations [11] for the transmission grid model. Including all electrical equipment models, current load and generation data regarding to the power plant dispatch and further input parameters such as high-voltage-direct-

current (HVDC)-transmission or inter transmission system operator transit data for all utilities within the simulation model the grid equation is compiled as

$$3\underline{\boldsymbol{U}}_{\mathrm{N}}\underline{\boldsymbol{Y}}^{*}_{\mathbf{NN}}\underline{\boldsymbol{u}}^{*}_{\mathbf{N}} - \underline{\boldsymbol{s}}_{\mathrm{N}}\left(\underline{\boldsymbol{u}}_{\mathrm{N}}\right) = \Delta\underline{\boldsymbol{s}}_{\mathrm{N}}(\boldsymbol{x}) \tag{2}$$

This equation is separated in a real and an imaginary part and approximated by a Taylor expansion [2] with

$$\frac{\partial\Delta\boldsymbol{p}(\boldsymbol{x}_v)}{\partial\boldsymbol{x}^{\mathrm{T}}}\boldsymbol{x}_{\boldsymbol{v+1}} = -\Delta\boldsymbol{p}(\boldsymbol{x}_v) \tag{3}$$

$$\frac{\partial\Delta\boldsymbol{q}(\boldsymbol{x}_v)}{\partial\boldsymbol{x}^{\mathrm{T}}}\boldsymbol{x}_{\boldsymbol{v+1}} = -\Delta\boldsymbol{q}(\boldsymbol{x}_v) \tag{4}$$

The equations (3) and (4) can be summarised with the Jacobi-Matrix which depends on the choice of the state vector, where Cartesian and Polar coordinates are possible. For further description especially for the implementation within the INES simulation model please refer to [11] [8] [2] and [3].

Because of the extensive transformation of the energy supply system with the scenario 2030 the transmission grid model of the reference scenario 2011 used in the simulation framework is not sufficiently dimensioned (see Figure 4). Thus, the expansion of the transmission grid had to be considered in the transmission system model (cf. work group Scenario Design report). This was realised by implementing the concluded grid expansion projects from the ENTSO-E ten years network development plan (TYNDP) [6] and the German *Netzentwicklungsplan* (NEP) 2012 [22].

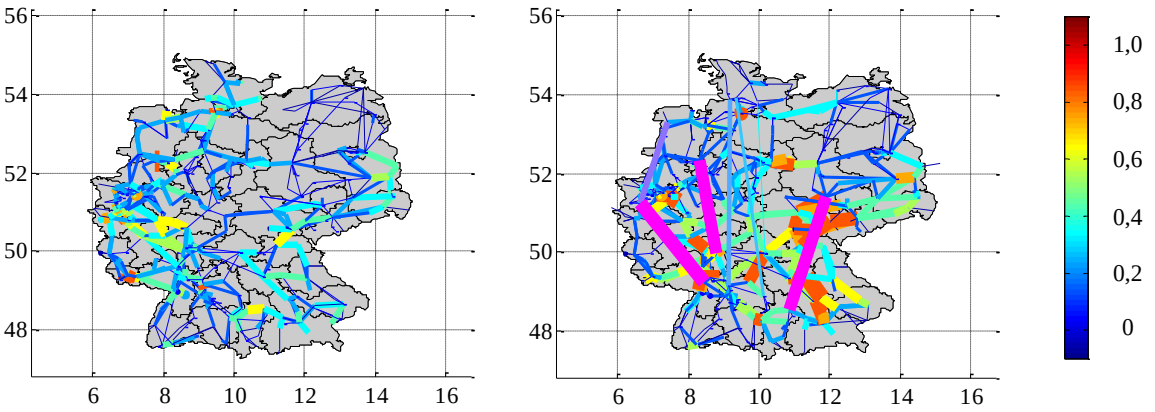

Figure 4: Load flow analysis of the transmission system with the average load of all power lines in relation to nominal load in the scenarios 2011 and 2030 (January)

These plans cover an outlook of transmission grid expansion for the next ten years and are implemented into the transmission system model. Hence, these plans do not cover the total growth forecast up to the year 2030, the further need of grid expansion is integrated into the grid models based on load flow analyses. This led to a high amount of additional grid expansion measures. This can be attributed firstly to the gap of ten years in the official grid expansion plans and secondly to the growth forecast of the power plant distribution. This forecast was modelled with an algorithm to allocate the power plants for the year 2030 which is based on the data of the simulation model of the year 2011 and not on actual future forecasts for each single power plant (see Work Group Scenario Design). With varied load flow analyses all affected power lines have been improved to secure a valid system state.

3.3 Voltage Bands and Reactive Power Management

In addition to the load flows on all power lines, one main challenge within the stationary system model and simulations for both scenarios has been the compliance of the node voltages to the voltage bands and therefore the reactive power management in the transmission system simulation. Depending on regional grid connection and allocation of power plants, DG and their feed-in of active and reactive power, the voltage bands differ widely in the grid model (see Figure 5).

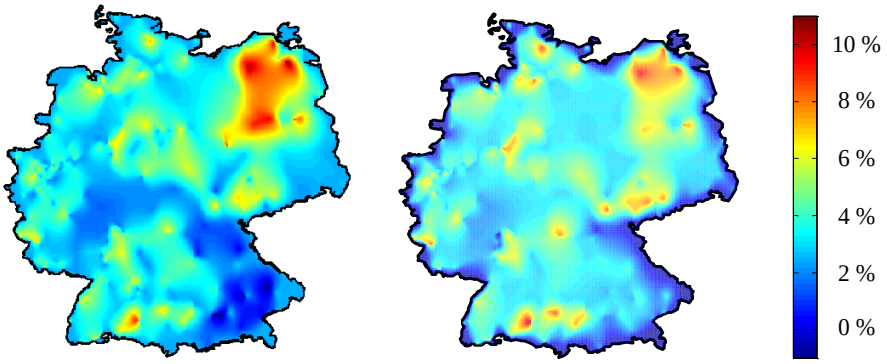

Figure 5: Average voltage band deviation in relation to nominal voltage in the transmission system model with and without reactive power management

In the INES model within the reference scenario 2011 the DG units originally feed in with a power factor of $\cos(\varphi) = 1$. This would lead to extensive voltage band violations and a high need of reactive power provision of remaining generation units or reactive power compensation in simulations of the scenario 2030. Stationary reactive power compensations are currently not considered as asset data within this simulation model and the high share of DG units would not provide the required reactive power. Hence, a reactive power management was developed to ensure the voltage bands for each node and a reasonable distribution of reactive power for both conventional power plants and DG within their operation boundaries. As a first approach to generate a valid system state, this optimisation identifies in several iterations all violations of voltage bands and reactive power boundaries by setting the nodal reactive power or the node voltage to its maximum allowed value. Afterwards a load flow calculation is executed and the optimisation is executed as long as violations of voltage bands or reactive power boundaries are identified. Thus all node voltages are optimised in order of their grade of voltage band violation to ensure a reliable system state in all calculations (see Figure 5).

3.4 Reactive Power Provision of Underlying Voltage Levels

In this context one main research question was the contribution of underlying voltage levels to the provision of ancillary services like e.g. reactive power provision. Thus, in several scenarios the provision of reactive power by DG units located in the HV and MV level was analysed with the overall system model including the distribution grid sections at different single UHV nodes. For a fundamental estimation of the range of possible reactive power contribution, a basic optimisation was developed to identify the range of reactive power demand within the transmission grid model. For one node with a high share of DG the nodal data was substituted with a distribution grid section. As a first approach the usage of discrete inductive or capacitive power factors for the distributed generation units (wind and solar)

$$\cos(\varphi) = \begin{cases} \cos(\varphi_{\mathrm{ind}}) \; \forall \left\{ u_{\mathrm{K}} > u_{\mathrm{K,r}} \right\} \\ \cos\left(\varphi_{\mathrm{kap}}\right) \; \forall \left\{ u_{\mathrm{K}} < u_{\mathrm{K,r}} \right\} \end{cases} \tag{5}$$

in dependence on upward and downward voltage band violations was used to quantify the reactive power demand of the transmission grid model. In this way the dependence of the reactive power provision on the current active power contribution within the distributed DG units in the distribution grid section (see diagram on the left side in Figure 6) can be analysed.

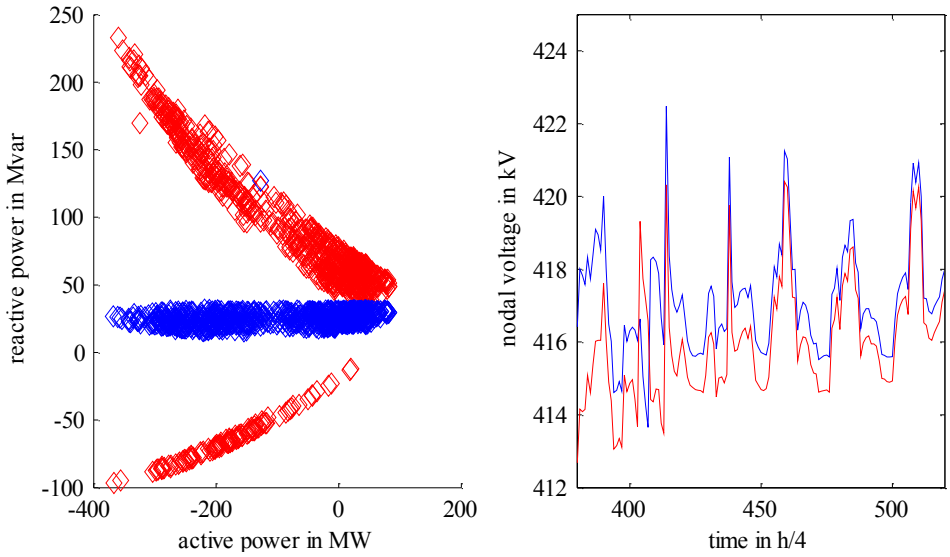

Figure 6: Reactive power optimisation and the corresponding nodal voltage

The node voltage calculated for the reference scenario 2011 for a node with a high share of DG in the node region could be improved up to several kV depending on the overall grid state. With the time depending contribution of the RES, the overall power plant dispatch fluctuates time-dependent and consequently the overall grid state of nodal voltages and load flows. This leads to diverging feasibility for voltage optimisation of the reactive power contribution of the DG in the distribution grid section due to the diversity of the transmission grid model states. With the use of discrete power factors the demanded range of reactive power provision can be quantified for single UHV nodes. Hence, this methodology is only suitable for single UHV-nodes, a reactive power management for the overall transmission grid is required for an optimisation of the entire system.

Based on [7] an optimisation approach was implemented to minimise the deviation of all node voltages in relation to reference voltages for each UHV node. In this way the reactive power demand and the potential of voltage optimisation for the entire grid model can be analysed. Without reliable reference voltages for all nodes as a first approach all voltages were optimised in reference to their nominal voltage. From the Jacobian matrix of the Newton-Raphson-method in polar coordinates

$$\begin{bmatrix} \frac{\partial \Delta p}{\partial \Delta \delta} & \frac{\partial \Delta p}{\partial \Delta u} \\ \frac{\partial \Delta q}{\partial \Delta \delta} & \frac{\partial \Delta q}{\partial \Delta u} \end{bmatrix} \begin{bmatrix} \Delta \delta \\ \Delta u \end{bmatrix} = - \begin{bmatrix} \Delta p \\ \Delta q \end{bmatrix} \tag{6}$$

the correlation of voltage alterations regarding reactive power variations can be received through inverting as

$$\begin{bmatrix} \Delta \delta \\ \Delta u \end{bmatrix} = - \begin{bmatrix} \frac{\partial \Delta \delta}{\partial \Delta p} & \frac{\partial \Delta \delta}{\partial \Delta q} \\ \frac{\partial \Delta u}{\partial \Delta p} & \frac{\partial \Delta u}{\partial \Delta q} \end{bmatrix} \begin{bmatrix} \Delta p \\ \Delta q \end{bmatrix} \tag{7}$$

which is valid for minor changes of the operating point. The requested coherence of nodal voltage and reactive power provision results in

$$[\Delta u] = -\left[\frac{\partial \Delta u}{\partial \Delta q}\right] = -[V][\Delta q] \tag{8}$$

With the parameters of the integrated grid and market simulation for each operating point aggregated reactive power constraints for each node can be determined in dependence of current provision of DG units (maximum and minimum power factor), generator power limits and voltage bands. The minimum deviations can be solved with the Gauss-Newton-algorithm [7] to calculate the optimal reactive power Δq_{red} of all nodes which can provide reactive power. After this optimisation load flow calculations with the optimised voltages as new reference voltages and the resulting reactive power provision are performed within iterative optimisations, because the results depend on the operating point [7]. The results of this optimisation can be used to analyse the regional reactive power demand and the overall potential of reactive power provision of the underlying voltage levels within the transmission system model and as an approach to gain valid system states (Figure 7). The calculated demand and the possible provision are time dependent and differ strongly within the INES model. These facts complicate a summarising evaluation, especially because of the size and calculation time of the simulation environment.

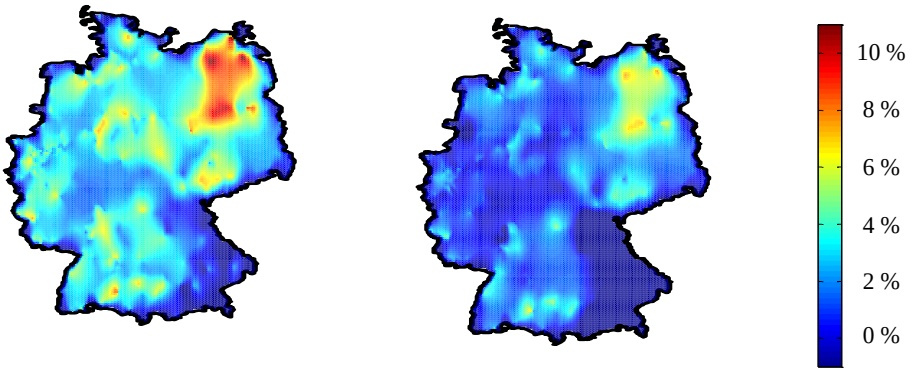

Figure 7: Average node voltages in the transmission system model with and without minimisation of voltage band deviations

For further analyses with this approach reliable reference voltages are needed and stationary reactive power compensators should be included within the grid model to improve the results of the reactive power management approaches in the simulation model. This approach is used as optimisation after the "standard" load flow calculation of the INES model. Further research is needed for a reactive power optimisation integrated within the INES model and load flow calculations. Main challenges for the analyses of stationary system states have been the implementation of the future outlook scenario 2030 and the determination of valid system states, which could not be realised for all points in time. This can be attributed to various challenges within the architecture of the INES model in combination with the key data of the scenario 2030, as e.g. the uncertain forecasts data (grid expansion and future power plants allocation).

The transfer project "iQ-Regler"[53] will develop further approaches to analyse the reactive power contribution of underlying voltage levels in more detailed scenarios and the results of the reactive power adjusting ranges can be used within the transfer project.

[53] http://smartnord.de/downloads/Praesentationen_Abschlusstagung/iQ-Regler.pdf

4 Frequency Stability Studies

In order to carry out frequency stability studies, the stationary system model described above is extended. Regarding the time frame of the relevant transient phenomena a quasi-stationary approach is chosen: grid, load, decentralised generation, primary control and stators of synchronous machines are described with algebraic equations using phasors while rotors, motion, excitation systems and power system stabilisers of synchronous machines as well as secondary control are depicted by state space equations. The system is calculated by solving the state space differential equations with numerical integration using the classical Runge-Kutta method and the algebraic equations by turns every integration time step [13]. The start values of the state variables are calculated from the results of the market and load flow simulation (see chapter 3).

As the resulting model and thus the calculations are very extensive and time-consuming, it is common practice to identify single points in time with characteristic properties and to analyse them in detail. In the past, these characteristic points in time have been times of low load and therefore low generation of conventional power plants. As conventional power plants provide most of the inertia which decelerates the frequency deviation resulting from a difference between load and generation, these points in time had the highest dynamic frequency drop. To regard the displacement of conventional generation with its inertia by RES dominated DG, four characteristic points in time are identified: high load/high DG; high load/low DG; low load/high DG; low load/low DG. These four points in time are simulated in detail for the scenario 2030 and are then compared to the corresponding points in time of the reference scenario 2011.

4.1 Grid and Load Modelling

The chosen quasi-stationary approach neglects transients in grid and stator windings of generators. This allows a representation of grid and stator voltage with phasors for steady-state relationships. Basis is the standard grid equation

$$\underline{\boldsymbol{Y}}_{\mathbf{NN}}\underline{\boldsymbol{u}}_{\mathbf{N}} = \underline{\boldsymbol{i}}_{\mathbf{N}} = \underline{\boldsymbol{i}}_{\mathbf{G}} + \underline{\boldsymbol{i}}_{\mathbf{Dez}} + \underline{\boldsymbol{i}}_{\mathbf{L}} \tag{9}$$

where $\underline{\boldsymbol{Y}}_{\mathbf{NN}}$ is the complex node-admittance matrix, $\underline{\boldsymbol{u}}_{\mathbf{N}}$ the vector of complex node voltages and $\underline{\boldsymbol{i}}_{\mathbf{N}}$ the vector of complex node currents, which can also be expressed as sum of synchronous generator current $\underline{\boldsymbol{i}}_{\mathbf{G}}$, decentralised generation current $\underline{\boldsymbol{i}}_{\mathbf{Dez}}$ and load current $\underline{\boldsymbol{i}}_{\mathbf{L}}$. These variables are known as a result of stationary analyses [11].

In order to include the load into the node-admittance matrix, it is expressed as diagonal matrix of admittances $\underline{\boldsymbol{Y}}_{\mathbf{L}}$ [11]:

$$\left(\underline{\boldsymbol{Y}}_{\mathbf{NN}} - \underline{\boldsymbol{Y}}_{\mathbf{L}}\right)\underline{\boldsymbol{u}}_{\mathbf{N}} = \underline{\boldsymbol{i}}_{\mathbf{G}} + \underline{\boldsymbol{i}}_{\mathbf{Dez}} \tag{10}$$

The voltage dependence of load is modelled by an exponential approach and the frequency dependence by a linear approach for each node i [13], [14]:

$$\underline{S}_{\mathrm{L}i} = P_{0i}\left(\frac{U_i}{U_{\mathrm{r}i}}\right)^{p_{\mathrm{exp}}} \cdot (1 + K_{\mathrm{f}})\Delta f_i + \mathrm{j}Q_{0i}\left(\frac{U_i}{U_{\mathrm{r}i}}\right)^{q_{\mathrm{exp}}} \tag{11}$$

The voltage dependence exponents are parameterised with literature values [14], [20], K_{f} is derived from the worst-case assumption in ENTSO-E Operation Handbook of 1 %/Hz static frequency dependence of loads [10]. Voltage and frequency dependence are integrated into the model by a recalculation of $\underline{\boldsymbol{Y}}_{\mathbf{L}} = \mathrm{diag}(\underline{Y}_1, \ldots, \underline{Y}_i, \ldots, \underline{Y}_n)$ in every numerical integration time step using actualised values of voltage and frequency for every n nodes [11].

Decentralised generation is integrated the same way but with constant feed-in power:

$$\left(\underline{\boldsymbol{Y}}_{\mathbf{NN}} - \underline{\boldsymbol{Y}}_{\mathbf{L}} - \underline{\boldsymbol{Y}}_{\mathbf{Dez}}\right)\underline{\boldsymbol{u}}_{\mathbf{N}} = \underline{\boldsymbol{i}}_{\mathbf{G}} \tag{12}$$

4.2 Synchronous Generator Modelling

Synchronous generators are modelled in d-q-coordinates with the above mentioned neglect of stator transients. The sets of differential equations for each synchronous generator are built by rotor (13) and motion equations (14) [11].

$$\begin{bmatrix} k_\mathrm{f}\dot{\Psi}_\mathrm{f} \\ k_\mathrm{D}\dot{\Psi}_\mathrm{D} \\ k_\mathrm{Q}\dot{\Psi}_\mathrm{Q} \end{bmatrix} = \begin{bmatrix} -1/T_\mathrm{ff} & k_\mathrm{f}/T_\mathrm{fD}k_\mathrm{D} & 0 \\ k_\mathrm{D}/T_\mathrm{Df}k_\mathrm{f} & -1/T_\mathrm{DD} & 0 \\ 0 & 0 & -1/T_\mathrm{Q} \end{bmatrix} \begin{bmatrix} k_\mathrm{f}\Psi_\mathrm{f} \\ k_\mathrm{D}\Psi_\mathrm{D} \\ k_\mathrm{Q}\Psi_\mathrm{Q} \end{bmatrix} + \begin{bmatrix} k_\mathrm{f} & k_\mathrm{f}^2 R_\mathrm{f} & 0 \\ 0 & k_\mathrm{D}^2 R_\mathrm{D} & 0 \\ 0 & 0 & k_\mathrm{Q}^2 R_\mathrm{Q} \end{bmatrix} \begin{bmatrix} U_\mathrm{f} \\ I_\mathrm{d} \\ I_\mathrm{q} \end{bmatrix} \tag{13}$$

$$\begin{bmatrix} \Delta\dot{\omega}_\mathrm{L} \\ \Delta\dot{\delta}_\mathrm{L} \end{bmatrix} = \begin{bmatrix} 0 & 0 \\ 1 & 0 \end{bmatrix} \begin{bmatrix} \Delta\omega_\mathrm{L} \\ \Delta\delta_\mathrm{L} \end{bmatrix} + \begin{bmatrix} k_\mathrm{m}(T_\mathrm{m} + T_\mathrm{e}) \\ 0 \end{bmatrix} \tag{14}$$

In the equations above index L represents rotor, m mechanical, e electrical, f field winding, D the d-axis amortisseur circuit and Q the q-axis amortisseur circuit. The angle δ_L describes the rotor position, ω_L its angular velocity, Ψ the different flux linkages, U_f the excitation voltage and I_d, I_q the d- and q-component of generator current. As this set of equations can be found in this or a similar depiction in literature, the factors k and time constants T are not explained any further [11], [13].

Under neglect of subtransient saliency, the terminal voltage of the generator can be expressed as

$$\underline{U}_\mathrm{G} = (R_\mathrm{a} + \mathrm{j}X''_\mathrm{d})\underline{I}_\mathrm{G} + \underline{U}'' \tag{15}$$

with the subtransient voltage

$$\underline{U}'' = \left(U''_\mathrm{d} + \mathrm{j}U''_\mathrm{q}\right)\mathrm{e}^{\mathrm{j}\delta_\mathrm{L}} = \mathrm{j}\omega_0\left(k_\mathrm{f}\Psi_\mathrm{f} + k_\mathrm{D}\Psi_\mathrm{D} + \mathrm{j}\omega_0 k_\mathrm{Q}\Psi_\mathrm{Q}\right)\mathrm{e}^{\mathrm{j}\delta_\mathrm{L}}. \tag{16}$$

For integration into the grid equation, synchronous generators are treated as current sources with source current $\boldsymbol{i}_{\mathbf{qG}}$, generator-node incidence matrix $\boldsymbol{K}_{\mathbf{GN}}$ and $\underline{\boldsymbol{Y}}''_{\mathbf{G}} = \mathbf{diag}(\boldsymbol{R}_\mathbf{a} + \mathbf{j}\boldsymbol{X}''_\mathbf{d})^{-\mathbf{1}}$ [11]:

$$\underline{\boldsymbol{i}}_{\mathbf{G}} = \boldsymbol{i}_{\mathbf{qG}} + \boldsymbol{K}_{\mathbf{GN}}^{\mathrm{T}}\underline{\boldsymbol{Y}}''_{\mathbf{G}}\boldsymbol{K}_{\mathbf{GN}}\underline{\boldsymbol{u}}_{\mathbf{N}} \tag{17}$$

Finally, (17) is inserted into (12):

$$\left(\underline{\boldsymbol{Y}}_{\mathbf{NN}} - \underline{\boldsymbol{Y}}_{\mathbf{L}} - \underline{\boldsymbol{Y}}_{\mathbf{Dez}} - \boldsymbol{K}_{\mathbf{GN}}^{\mathrm{T}}\underline{\boldsymbol{Y}}''_{\mathbf{G}}\boldsymbol{K}_{\mathbf{GN}}\right)\underline{\boldsymbol{u}}_{\mathbf{N}} = \underline{\boldsymbol{i}}_{\mathbf{qG}} \tag{18}$$

with

$$\underline{\boldsymbol{i}}_{\mathbf{qG}} = -\boldsymbol{K}_{\mathbf{GN}}\underline{\boldsymbol{Y}}''_{\mathbf{G}}\underline{\boldsymbol{u}}'' \tag{19}$$

Synchronous generator parameterisation is done by literature values of different sized generators [12].

4.3 Excitation System and Power System Stabiliser Modelling

Excitation systems and power system stabilisers (PSS) are modelled using IEEE Std. 421.5-2005 [15]. Each synchronous generator is provided with a ST1A exciter and a PSS1A power system stabiliser (Figure 8) using the sample parameterisation given in Annex H of [15].

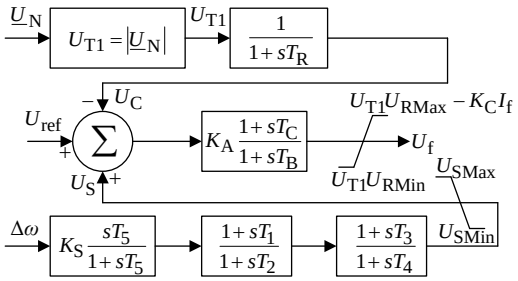

Figure 8: Voltage transducer, power system stabiliser PSS1A and excitation system ST1A with applied sample parameterisation

Inputs are the complex node voltage $\underline{U}_N$, the voltage reference for the respective node U_{ref} and the speed deviation of the rotor $\Delta\omega$. The output variable of the whole system is U_f. As these components are modelled in per unit system, input and output variables are converted appropriately.

4.4 Primary Control Modelling

Turbine regulation of conventional power plants and the resulting provision of primary control reserve (PCR) are modelled as a linear function representing the minimum standard defined in [9]. This means a linear activation of PCR within at least 30 s. As the reaction of power plants on frequency deviations is strongly dependent on their specific construction type [13] and this type is not represented in the INES data base, this simple approach can represent every conventional power plant providing PCR. Furthermore, this is a worst-case assumption and therefore leads to a conservative assessment which is common in power system planning. The droop of each power plant is defined by the results of PCR market simulation, which is an extension of the INES wholesale market simulation [16]. The maximum PCR provision of each conventional power plant is set to the minimum requirement of 2 % of their nominal power output defined in [9]. The controller input Δf is limited to steady-state frequency deviation of ± 200 mHz where maximum PCR has to be supplied [10].

The same approach is used to identify a possibly required contribution of DG in PCR provision. This contribution is assumed to be linear within 5 s for wind generation and within 1 s for solar generation. These rates are taken from literature and in case of solar generation have been adapted due to the results of WP 2.4 [17]. As it is principally possible for these units to provide PCR, e.g. in case of wind generation by intentionally operating in a worse operating point [18] and in case of solar generation by using additional battery storage [19], a concrete method of provision and the units themselves are not modelled in detail. Further, it is assumed that the units described provide this fastened PCR with a droop identified as described in the following section. The reason for the PCR provision, e.g. market based or as a consequence of an altered grid code is out of focus of this work package.

4.5 Methodology

The simulations are based on the ENTSO-E reference incident for PCR for the Continental European transmission grid. This incident assumes a sudden loss of generation or load of 3000 MW at minimum load with worst-case assumptions for frequency dependence of loads [10]. Since, due to the high modelling effort, the simulated grid area comprises Germany and all its neighbouring countries and therefore varies from the ENTSO-E grid area Continental Europe, the incident has been respectively adjusted. The incident is scaled the same way the PCR of 3000 MW for the

whole grid area is distributed to the single control areas. This is done by (20) with the primary control reserve PCR_i and the yearly generated energy $E_{\mathrm{gen},i}$ of control area i [10].

$$PCR_i = \frac{E_{\mathrm{gen},i}}{\sum_i E_{\mathrm{gen},i}} 3000\ \mathrm{MW} \tag{20}$$

This results in an adjusted reference incident of 1866 MW (in this project only loss of generation is regarded) for the simulated grid area. The incident is located in the region with the highest generation density in Germany – the "Ruhrgebiet". There, a well-integrated node is chosen – "Rommerskirchen".

To evaluate the frequency stability and possibly required measures to ensure a secure system state the adjusted reference incident is simulated for the four characteristic points in time for both scenarios 2011 and 2030. Frequency stability is ensured if the frequency at each grid node does not decrease below the minimum instantaneous frequency of 49.2 Hz defined by ENTSO-E at any time. If frequency stability cannot be ensured with PCR of conventional power plants, the fastened PCR described above is gradually increased until frequency stability is ensured. This approach determines the minimum required contribution of DG in providing PCR in the scenario 2030.

Key figures of the simulated characteristic points in time are given in Table 1. As the points in time have been selected according to the residual load as difference between load and DG, the individual values for load and DG do not necessarily match their individual extremes.

		scenario 2011		**scenario 2030**	
load	**DG**	**load total/Germany**	**DG total/Germany**	**load total/Germany**	**DG total/Germany**
high	high	183 GW/53 GW	33 GW/22 GW	183 GW/53 GW	85 GW/53 GW
high	low	226 GW/70 GW	25 GW/1 GW	226 GW/70 GW	56 GW/27 GW
low	high	109 GW/35 GW	33 GW/25 GW	109 GW/35 GW	69 GW/35 GW
low	low	147 GW/46 GW	15 GW/9 GW	147 GW/46 GW	36 GW/15 GW

Table 1: Key figures of characteristic points in time

5 Results

The essential results of the different simulation runs are the frequencies over time for each generator node. As an example Figure 9 shows the frequencies over time for the low load/high DG 2011 scenario. Within the first few seconds after the incident the frequency at the generator nodes is significantly different. After these transients, among others damped by the PSS, the frequency is virtually identical at each node. The minimum instantaneous frequency lies above 49.2 Hz; hence the simulated characteristic point in time is stable in respect to frequency stability. For reasons of clarity in further depiction the weighted mean frequency $\overline{f}$ is used to describe frequency over time for stable points in time [13]:

$$\overline{f} = \frac{\sum_{i=1}^{n} S_{\mathrm{rG}i} T_{\mathrm{m}i} f_i}{\sum_{i=1}^{n} S_{\mathrm{rG}i} T_{\mathrm{m}i}} \tag{21}$$

It is defined as arithmetic average of generator node frequency weighted with the rated power $S_{\mathrm{rG}i}$ and the mechanical time constant $T_{\mathrm{m}i}$ of generator i.

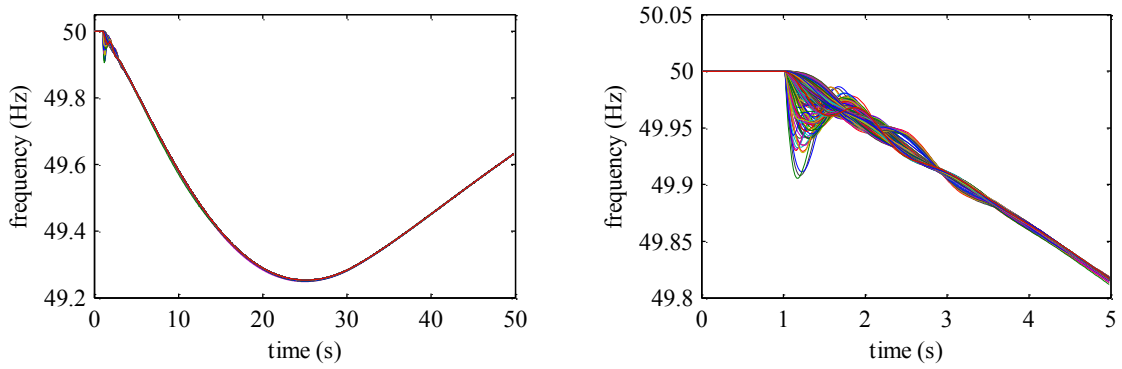

Figure 9: Frequency over time at each generator node in low load/high DG 2011 scenario (incident after 1 s)

The results for all high load points in time (left side) and low load points in time (right side) with respectively high and low DG are shown in Figure 10. The high load points in time are stable in both scenarios 2011 and 2030 without additional fastened PCR provided by DG. Three out of four low load points in time are also stable without further measures; the only exception is the low load/high DG point in time in scenario 2030. In this point in time a provision of fastened PCR by DG in the amount of 1.6 % of their actual power feed-in is required to stabilise the system (the situation without provision of fastened PCR is not depicted for this point in time, because it is not stable). In comparison to the simulation results for the other points in time it shows a different behaviour. The decrease of the frequency is faster due to the reduced inertia, the increase likewise because of the fastened PCR.

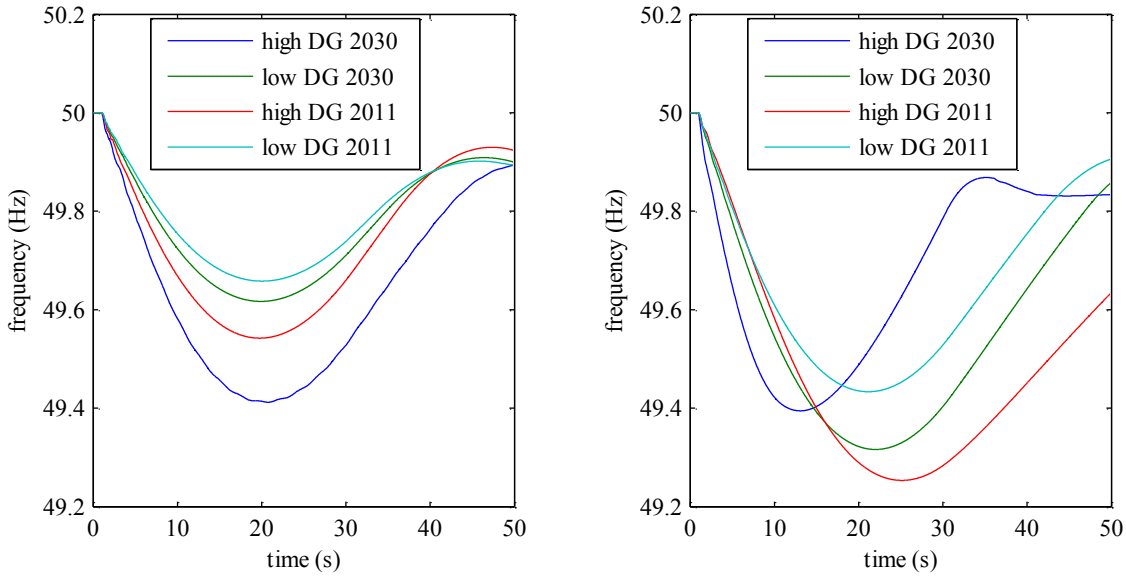

Figure 10: Mean frequency over time in high load (left) and low load (right) points in time (incident after 1 s)

This basic correlation between rate of frequency decrease and inertia is not obvious for the other points in time, because it is overlaid by another effect. In the chosen modelling approach at high DG points in time the voltage decrease at grid nodes after the incident is relatively greater that at low DG points in time. This can be explained first with the constant power feed-in modelling of DG. A reduction of voltage at a grid node immediately leads to a greater current. Due to the subsequent greater current on the connecting transmission lines the voltage drops on this

transmission lines also increase and consequently the voltages at neighbouring nodes are reduced. If DG is installed at these nodes as well, the described effect can also be observed there. The second reason is that an active voltage regulation is only modelled in detail for conventional power plants and as a consequence of this less conventional power plants lead to a slower return to the reference voltages. Finally the greater voltage decrease leads to a greater influence of the voltage dependence of load and therefore to a greater deceleration of frequency decrease. As an example Figure 11 shows the described effect for a high DG and a low DG point in time (low load 2011).

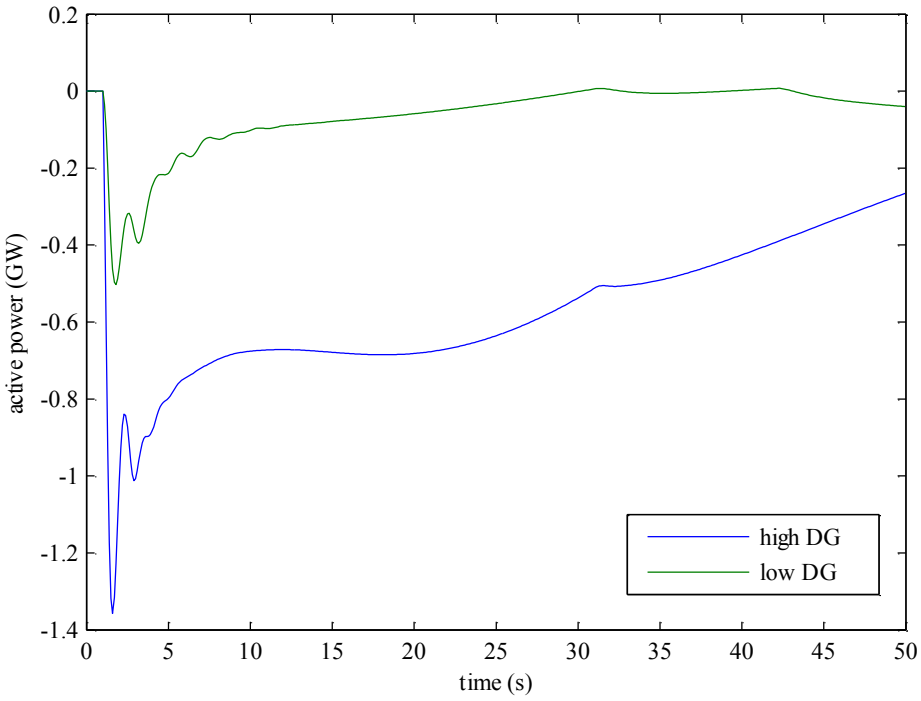

Figure 11: Alteration of load due to voltage dependence in high DG and low DG point in time (incident after 1 s)

As due to the described effects frequency stability and voltage regulation of DG have a close relation, parameterisation of voltage regulation of DG may offer potentialities to support frequency stability. These potentialities are strongly dependent on further implementation and analyses of voltage dependence of the loads, which are both subject of further research.

6 Conclusion

Within the research project Smart Nord the work package 4.1 developed an overall system model. This model is an extension of the integrated grid and power market model INES and comprises the transmission system, underlying distribution grid sections at selected UHV nodes, the wholesale electricity market as well as the primary control reserve market and enables integrated analyses of stationary and dynamic processes. The two evaluation scenarios 2011 and 2030, which have been defined by the interdisciplinary working group Scenario Design, were implemented into this simulation environment. For this, the existing integrated grid and power market model INES was extended by generation forecasts and grid expansions for the future outlook and several new approaches as for instance a reactive power management. Beyond that, models required for the frequency stability studies were added. Consequently, the stationary analyses as well as the frequency stability studies can be carried out based on the same asset data and simulation models and within one process from market simulation over stationary system states to stability studies that uses the results from one step as start value for the next step.

The simulation environment has been originally developed to represent the year 2011. Grid and market model were evaluated and optimised for the characteristics and the given public data for this specific year. The integration of the future outlook scenario 2030 into the system model was a major task within this research project. The current discussions about grid expansion and possibilities of future grid operation show the uncertainties and challenges for the future energy supply system. In order to gain valid stationary system states for the scenario 2030 within the system model several new developments for the transmission system and market model were needed, because stable and valid grid states were rarely given without further measures. The grid model had to be extended far above the discussed grid expansion plans (because these plans only look forward to the year 2020). The alternated power plant allocation and dimensioning (see Work Group Scenario Design), and the changed power plant dispatch led to entirely new load flow situations.

It was shown, that the future outlook 2030 within the simulation model leads to high loads of power lines and a high demand of reactive power provision of the underlying voltage levels. At many points in time the conventional power plants, which normally provided the reactive power within the simulation model, were displaced by distributed generation units. Hence, the reactive power provision had to be rearranged within the simulation model. The high voltage band violations in the simulation model were minimised with reactive power management approaches for the German transmission system model. These approaches were evaluated considering the DG units in the distribution grid section to quantify the provision of DG in the underlying voltage levels within the German transmission system model. For further analyses these approaches have to be evaluated in the overall transmission system model and within more detailed distribution grid sections, as e.g. in the transfer project “iQ-Regler”[54]. With the new challenges of the future outlook for the year 2030 within the simulation model, including the high load of power lines and the high demand of reactive power, more advanced solutions are needed to improve the permissibility of stationary system states, as e.g. optimal power flow solutions, which have not been part of the research project Smart Nord.

To evaluate the frequency stability four characteristic points in time were identified and simulated in detail: high load/high DG; high load/low DG; low load/high DG; low load/low DG. For all characteristic points in time the same incident was assumed: the loss of generation of about 1866 MW. This incident corresponds to the primary control reserve reference incident for the grid

[54] http://smartnord.de/downloads/Praesentationen_Abschlusstagung/iQ-Regler.pdf

area Continental Europe defined by ENTSO-E though was adapted because of the different size of the regarded grid area. Within the developed model the frequency stability could be ensured for the reference scenario as well as the future scenario. Nevertheless, temporarily a contribution of DG in frequency control was necessary. For this purpose wind generation had to provide fastened PCR linearly within 5 s, solar generation within 1 s. The characteristic point in time, which required this contribution, was low load/high DG in the scenario 2030 with a required amount of fastened PCR at the high of 1.6 % of the current feed-in power of wind and solar generation.

The developed model does not consider active voltage control by DG after the incident. Therefore a high share of DG in interaction with the voltage dependence of loads has a decelerating influence on the frequency over time after an incident. The usability of this effect for active voltage control design of DG and its actual height as well as the future development of voltage dependence of loads are subject of current research. For this, the developed model will be extended by more detailed models for aggregated DG as well as its active power and voltage control, the turbine control of power plants, a secondary reserve market and the above mentioned optimal power flow approach to gain control reference values.

Work Package 4.2: Low-Voltage Grid Modelling and Grid Compatibility Assessment

Stefanie Koch[56], Marco Zobel[55] and Bernd Engel[56]

Abstract

It is possible to manage the supply of active power with small decentralized power generators within a defined distribution grid. To get a feeling for the real and effective capability of decentralized power suppliers, micro combined heat and power (CHP) systems have been evaluated. Variances and restrictions that are specific to the system have been validated through simulation and lab tests. Such systems would typically be used to supply single-family homes. The electrical power is between 0.2 and 1.5 kW_{el}. To compare different systems with another reference, load profiles as defined in VDI 4655 [23] were used. Numerous scenarios have therefore been calculated using MATLAB-Simulink models as well as test devices. All systems are restricted by the quantity of heat, that is, all heat must be used or buffered. Because of this requirement, it is possible that the CHP system will be shut down in months with lower or no heat demand. The BlueGEN system is an exception. Because of its technical characteristics, heat limitation is only marginal with this kind of system, and it is thus ideal as a decentralized power generator. To achieve critical or relevant influence, it is necessary to have high penetration of these systems within the distribution grid.

Furthermore, the Smart North scenarios in the form of holistic network models have been analysed. For this purpose, several rural and an urban low-voltage (LV) networks were implemented in the grid calculation software PowerFactory and linked to a medium-voltage (MV) benchmark-network. In a first step, these networks have been equipped with consumer loads and supplemented by production units from other work packages. With this model, a comprehensive analysis of the grid status in 2011 (reference) and 2030 was possible. It can be concluded that the ongoing integration of decentralized generation units in distribution grids will entail reasonable reinforcements of the networks.

1 Supply of Active Power Using Micro-CHP Systems

It is possible to use micro-CHP systems to meet the energy demand of single-family houses. Typically, CHP systems cover the base load of power and heat. Additional heat requirements can be covered using a peak heater in an efficient manner, while surplus of power is fed into the grid. The required fuel can be taken continuously out of the natural gas grid. That allows a predictable as well as specific active power supply. The variances and restrictions of micro-CHP systems are evaluated and the service capacities of targeted active power supply are validated within the following sections.

1.1 Pre-Evaluation of Micro-CHP Systems

Only commercial CHP systems for single-family houses were considered for pre-evaluation. Despite this restriction, there is sufficiently high potential for installing high numbers of micro-CHP systems within the supply grid. Examples of commercial CHP systems are shown in Figure 12. With the exception of the BlueGEN system, which is based on a solid oxide fuel cell generator, all other systems are generically referred to as power-generating heating systems. That means that these systems will always generate heat that must be buffered or used. If no heat is required, these systems must be shut down at a certain temperature limit.

[55] EWE-Forschungszentrum für Energietechnologie e.V., 26129 Oldenburg, Germany, marco.zobel@next-energy.de, Bereich Brennstoffzellen / KWK-Systeme
[56] Technische Universität Braunschweig, 38106 Braunschweig, Germany, {forename.surname}@tu-braunschweig.de, elenia

Stirling engine: Dachs Stirling SE [24]	Engine: Vaillant ecopower 1.0 [25]	SOFC fuel cell: HEXIS Galileo 1000N [26]	PEM fuel cell: Viessmann Vitovalor 300-P [27]	SOFC fuel cell: CFCL BlueGEN [28]
				

Figure 12: Commercial micro-CHP systems with different cogeneration technologies in the power range of up to 1.5 kW_{el}

In order to identify suitable micro-CHP systems with a high potential for active power supply, the heat or, rather, temperature dependence must be given particular consideration. To classify CHP systems, the ratio between generated power and useful heat – the power to heat ratio – is used. The higher this value, the lower the generated amount of heat. High power to heat ratios result in longer operating times for a power supply, while low numbers result in shorter operating times that are limited by an overcapacity of generated heat. Systems based on electrochemical energy transformation, such as fuel cells, have higher efficiencies and power to heat ratios than conventional combustion engines.

To compare and evaluate different systems, a representative scenario was defined using the standard load profiles from the guideline VDI 4655 [23]. These include heat and power demand sets for single-family houses and apartments with typical daily demands to a resolution of one minute. For Germany, fifteen climate zones are defined with typical ambient temperature profiles based on values from the Deutscher Wetterdienst (German Meteorological Service). As shown in Table 2, a year is divided into seasons, such as winter, summer and transition, as well as working days and Sundays. To cover heat transmission by solar radiation, there is also a subdivision for cloudiness during the heating period. For every day type there exists a typical heat demand profile with standardized energy factors for heating, hot water and power. The heat demand depends on the year of construction of the building and the insulation level. The hot water and power demand depends on the number of inhabitants and quantity of equipment. The distribution and frequency of day type depends on the climate zone.

Season	**Weekday W**		**Sunday S**	
	Clear H	**Cloudy B**	**Clear H**	**Cloudy B**
Transition Period Ü	ÜWH	ÜWB	ÜSH	ÜSB
Summer S	SWX		SSX	
Winter W	WWH	WWB	WSH	WSB

Table 2: Standard reference days based on VDI 4655

For a single family house in Oldenburg (climate zone TRY03), these values result from annual base demands for heat of 15,000 kWh/a, hot water of 2,000 kWh/a and power of 4,000 kWh/a, as can be seen in Table 3.

Reference Days	SWX	SSX	ÜSH	ÜWH	ÜSB	ÜWB	WSH	WWH	WSB	WWB	$\sum_{year}$
Days per year	71	10	8	33	19	87	5	28	21	83	365
Power [kWh/d]	8.8	9.7	12.2	9.9	13.3	10.9	12.6	10.9	14.2	11.9	4,000
Heat [kWh/d]	0	0	37.2	25.8	33.8	36.1	85.3	75.6	63.8	74.5	15,000
Hot Water [kWh/d]	3.8	6.6	7.9	4.4	8.3	4.9	11.4	6.0	8.6	5.6	2,000

Table 3: Overview of the energy demand of a single-family house (climate zone TRY03/Oldenburg) on different VDI reference days

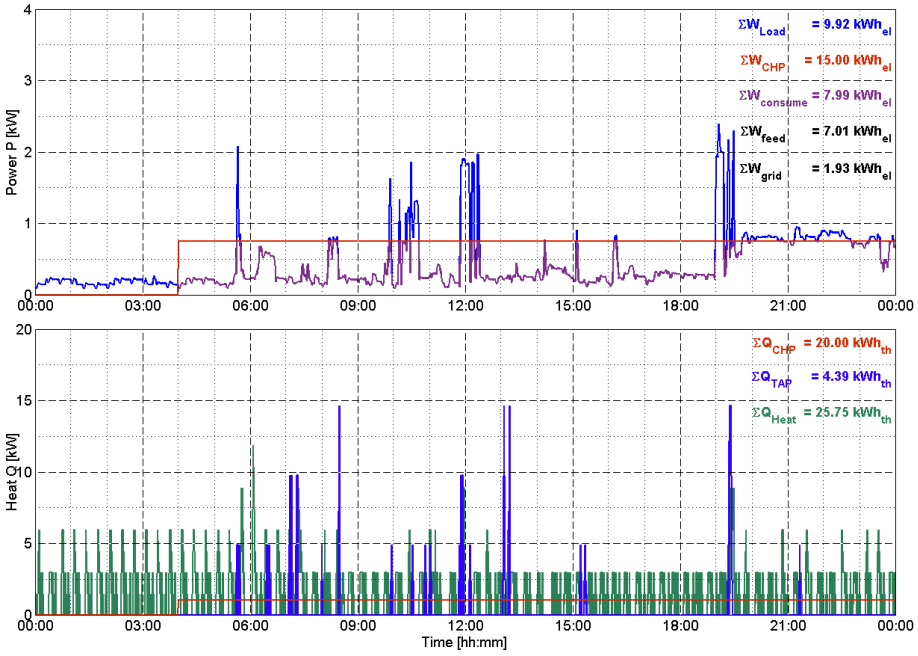

Figure 13: Power and heat load profiles for a single-family house on a VDI ÜWH-day and PEMFC-CHP profiles with 0.75 kW_{el} and 1 kW_{th}

By using those available load profiles, the achievable cover ratios and system characteristics can be evaluated. Shown in Figure 13 are power and heat load profiles for a single-family house on a ÜWH-day. The generator profile is given with electrical power of 0.75 kW_{el} and thermal power of 1 kW_{th}, representing a PEMFC-CHP system. In addition, the specific power demand for that day is 9.92 kW_{el}, heat demand is 25.75 kW_{th} and domestic hot water demand is 4.39 kWh_{th}. The low overnight heat demand causes the CHP system to start at 4:00 pm. If no heat is required, it is possible to reduce electrical and thermal power by modulation. Lower numbers for active power are expected for summer days. The minimum active power level would be 0.25 kW_{el}. The technical concept of the CHP system combined with the high electrical efficiency of 60 % at 1.5 kW_{el} and the low amount of heat of 0.6 kW_{th} allows almost continuous operation of the BlueGEN system. The laboratory evaluation therefore focussed on that system.

1.2 Laboratory Validation of the CHP System

The required load profiles can be simulated using an autonomous test environment with integrated control loops developed by NEXT ENERGY. The BlueGEN system has therefore been connected electrically and hydraulically to this system. All input and output flows can be calculated exactly from sensor readings. Day profiles have been combined in such a manner that a year can be simulated in a time lapse test. Figure 14 shows the entire system consisting of the CHP unit, the heat buffer and an additional peak burner (condensing boiler).

Figure 14: NEXT ENERGY test environment for CHP and heating systems

1.3 Determined Potentials of Micro-CHP Systems

The total amount of active power is defined by the difference between the electrical load demand and the energy supplied by the CHP unit. To reduce the necessary measuring time and to get a better understanding of the process, a model of the system was developed on a MATLAB-Simulink basis and validated using characteristics that had already been measured. All real components or, rather, sub-systems have been implemented, as have control procedures and the temperature dependency of flow temperature.

Using the standardized load profiles, measured and simulated results can be compared in an easy and transparent way. The characteristics and temperature levels within the thermal buffer store in the simulation fit the measurements very well. An important quality requirement is thus fulfilled. In Figure 15, the seasonally dependent heat demand (red) for different day types is shown. As expected, the heat demand decreases to hot water demand only in summer time (red line). The green line represents the daily power demand. Simulated and measured surplus power fed into the grid also fit very well (dotted blue, blue line). In summary, the evaluated BlueGEN CHP system matches the requirements for a controlled active power supply. Nevertheless, its high potential can only be used if a high number of systems are installed in the local grid.

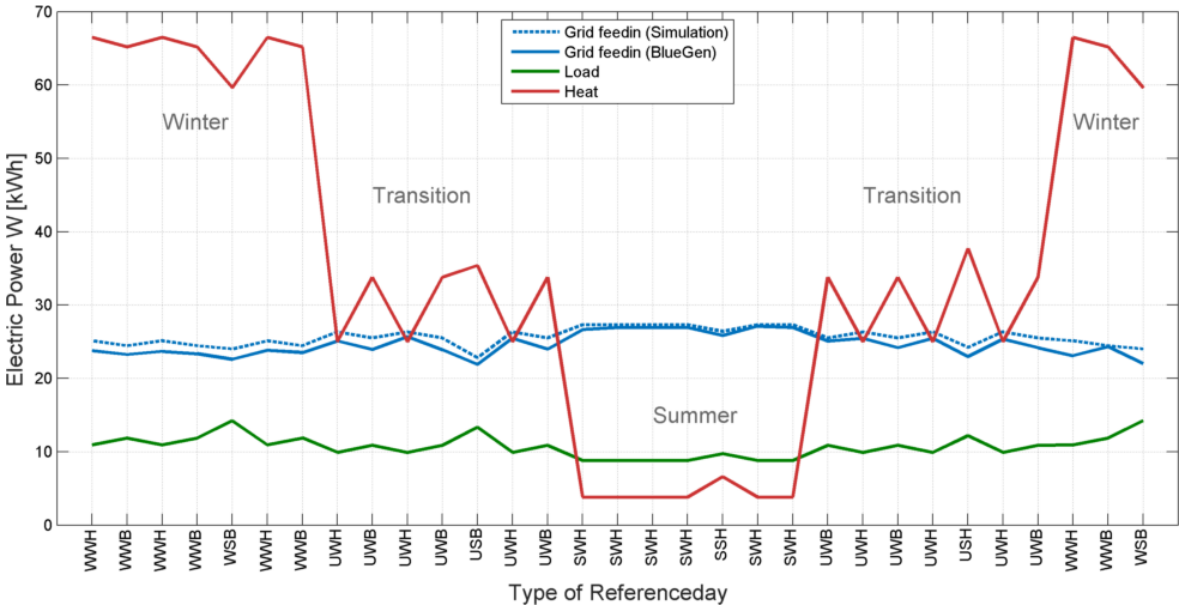

Figure 15: Power feed to the grid according to seasonal heat demand

2 Assessment of the Integration of Decentralized Generators in the Distribution Grid

The objective of this subsection is to determine whether the increasing penetration of decentralized generating units has an adverse effect on the power quality.

2.1 Methodology

Two scenarios have been implemented to achieve the aforementioned objective. The first scenario takes into account the situation prevailing in 2011, the latter scenario the situation expected to be the case in 2030. For both scenarios a power grid model involving the medium- and low-voltage-level has been developed. The power grid model is based on the Cigre-Benchmark Grid for the medium-voltage level and has been augmented using 71 low-voltage-grids being based on real grids existing in Germany. The power grid model is illustrated in Figure 16. In total, the model comprises 12,000 loads representing single residential buildings. For the scenario 2011 and 2030, 700 and 2,750 decentralized generators, respectively, have been integrated.

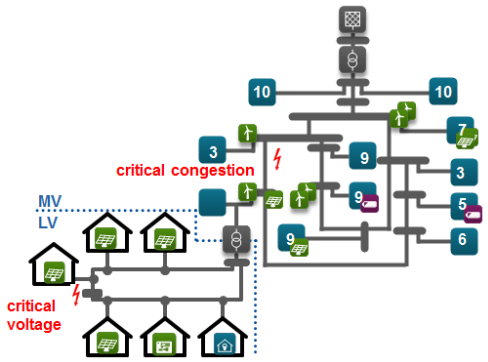

Figure 16: Implemented power grid model

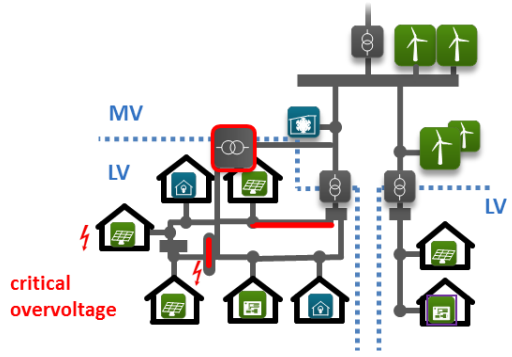

Figure 17: Grid reinforcement measures

Two key issues, being common when integrating decentralized units, are depicted in Figure 16. At the medium-voltage-level it is likely that critical congestions occur at single feeders, bus bars, or substations. Many transformer stations include an in-built overload capability. Consequently, they

can cope with temporary overload periods, affecting merely their aging behaviour. In terms of cables, predominantly underground cables are deployed in MV and LV power grids. The permissible wiring ampacity must not be exceeded by any means. Critical situations can especially occur during temporary reversals of the power flow.

The second key issue is the occurrence of critical overvoltages at the low-voltage-level. Small photovoltaic modules are connected at the point of common coupling of residential buildings. Particularly at the end of feeders the voltage can exceed the admissible range.

Several simulations were carried out with a view to observing differences in the individual scenarios. As can be seen from Table 4, two calculations per scenario have been conducted, i.e. high load condition and load flow reversal condition.

Scaling factor	Low-Voltage		Medium-Voltage	
	High load	Load flow reversal	High load	Load flow reversal
Load	1	0.25	-	-
Wind power	-	-	0	1
Solar power	0	0.85	0	0.85
CHP units	0	1	0	1

Table 4: Scaling factor of load and generating units for the high load and load flow reversal case

The results have been assessed taking the following requirements into account. The maximum capacity utilization factor of MV-transformer substations and MV-cables is at 60 % for the high load and at 100 % for the load flow reversal calculation. Distribution transformers and LV-cables can be loaded up to 100 % in both cases. The maximum magnitude of the voltage change is ±10 % of the nominal voltage. In addition, the maximum voltage rise at grid nodes, where generating units are coupled, is 2 % and 3 % at the MS- and LV-level, respectively.

In case of an overvoltage at one of the nodes or a congestion of the network equipment, grid reinforcement measures have been implemented for the ensuing calculations. As remedial actions we take into account the following grid reinforcement measures. These measures are implemented into the grid as depicted in Figure 17:

- Optimization of disconnection points in cable distribution cabinets
- Implementing a parallel cable
- Separating the LV-grid and installing a second distribution transformer
- Supplanting the distribution transformer with a new one with a higher rated power

2.2 Scenario 2011

The first scenario under investigation is the high-load scenario. The relevant input parameter can be seen in Table 4. The findings reveal that all voltages occurring in the power grid are within the permissible range (Figure 18). Moreover, the capacity utilization of all cables and transformer stations are below the determined load limit. This result was to be expected as the high load scenario is commonly used by grid operators to design and construct the grid.

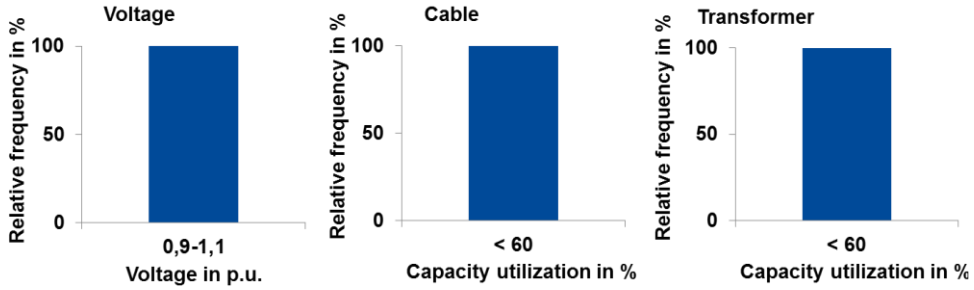

Figure 18: Grid reinforcement measures (High load scenario 2011)

The second case analysed is the load flow reversal scenario of 2011. As can be seen from Figure 19, the average photovoltaic power installed in this grid is still below the average maximum load per PCC in this case. However, as this is the case only in the low-voltage-grid, in the medium-voltage-grid also wind power has been taken into account. The results of the simulations clearly show that the voltages of virtually all nodes are within the permissible range. Still, a small fraction (1 %) of all nodes exhibits voltages exceeding the limit of 1.1 p.u. Thus, a preliminary conclusion might be that the design of power grids based solely on the high load scenarios is no longer sufficient to resemble the real situation prevailing in power grids.

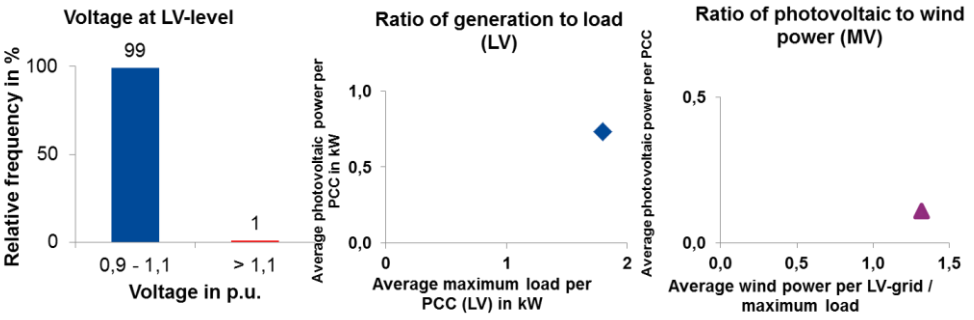

Figure 19: Characteristics of load flow reversal scenario 2011

For a more thorough investigation, Figure 20 illustrates the voltage increase both at LV-level and MV-level. It is obvious that particularly at the MV-level the voltage of a significant amount of nodes exceeds the 2 %-limit. At the LV-level the proportion of voltages exceeding the 3 % limit is less but still at 11 %.

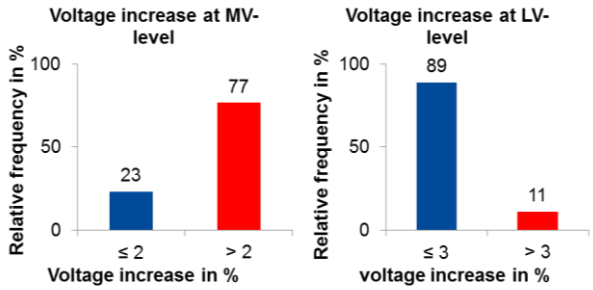

Figure 20: Calculation results (Load flow reversal scenario 2011)

In the second calculation all cables and transformers have been within the limits of the determined maximum capacity utilization factor. However, to mitigate the increase of the voltage at the nodes we proposed and implemented several grid reinforcement measures (Figure 21). These measures are commensurate to increase in voltage, thus the majority of the measures have been proposed for the MV-level. At the MV-level 16 % of the grid length is subject to reinforcement. An additional amount of three transformer stations have to be supplanted with more powerful ones.

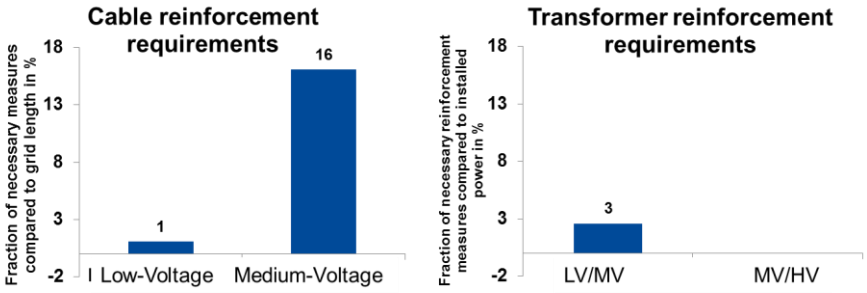

Figure 21: Requirement for grid reinforcement measures (Load flow reversal scenario 2011)

2.3 Scenario 2030

The simulation data for the year 2030 was obtained by increasing the penetration of decentralized generators (see Figure 22). In total the amount the installed power increased by the factor 2.7. As the scenario of 2011 clearly revealed, the simulation for the load flow reversal is more suitable to identify critical grid congestions. Consequently, in for the scenario 2030 we omitted the high load scenario.

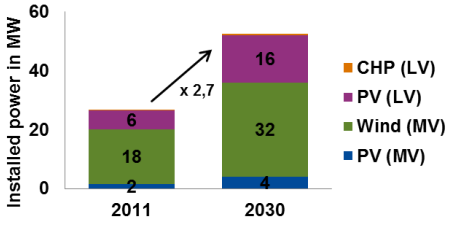

Figure 22: Installed generating capacity (Load flow reversal scenario 2030)

As can be seen from the two bar charts in Figure 23, the voltage at the majority of MV-nodes exceeds the required limits. Only 23 % of the voltages are within the admissible range. At 10 % of the nodes the voltage is 11 % higher than the nominal voltage which could entail adverse effects on the power quality. In terms of the voltage increase at the connection points of generating units it can be derived that only 23 % of the nodes meet the voltage requirements. The same conclusion also applies for the condition in the LV-level of the power grid (Figure 24). The maximum magnitude of the voltage change was calculated as an increase of 14 %. However, 76 % of the nodes exhibit voltages within the admissible range, but a more detailed view reveals that especially at nodes with attached generating units the voltage is significantly too high (Figure 24, right-hand side).

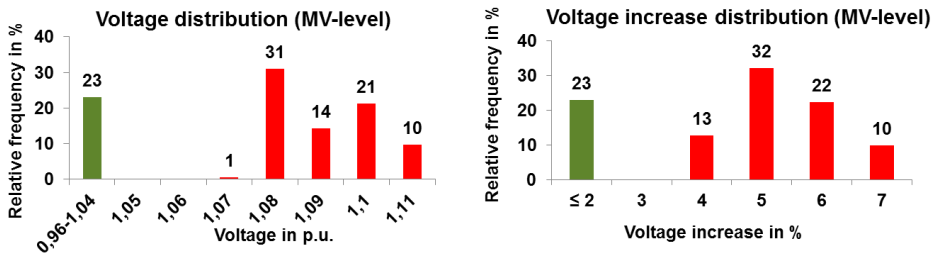

Figure 23: Calculation results in terms of voltage at MV-level (Load flow reversal scenario 2030)

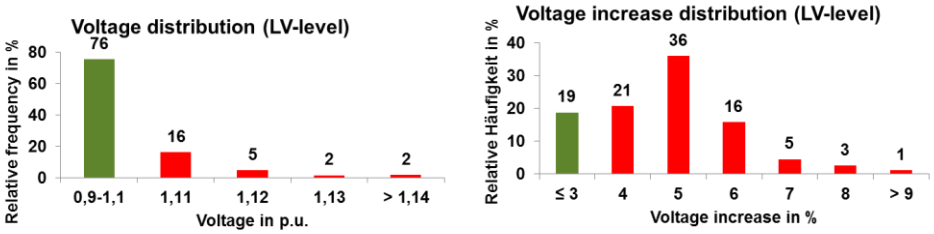

Figure 24: Calculation results in terms of voltage at LV-level (Load flow reversal scenario 2030)

Based on the simulation results we applied the same pattern as in the scenario 2011 to identify relevant grid reinforcement measures. Both results are compared in Figure 25. Whereas the reinforcement requirement in the LV-level in terms of cables significantly increased, the amount slightly decreased at the MV-level. In contrast, the situation regarding the necessary replacements of transformers is striking. Particularly at the MV-level 58 % of the installed transformer capacity has to be supplanted with more powerful ones. On the LV-level only a slight increase of 1 % was found.

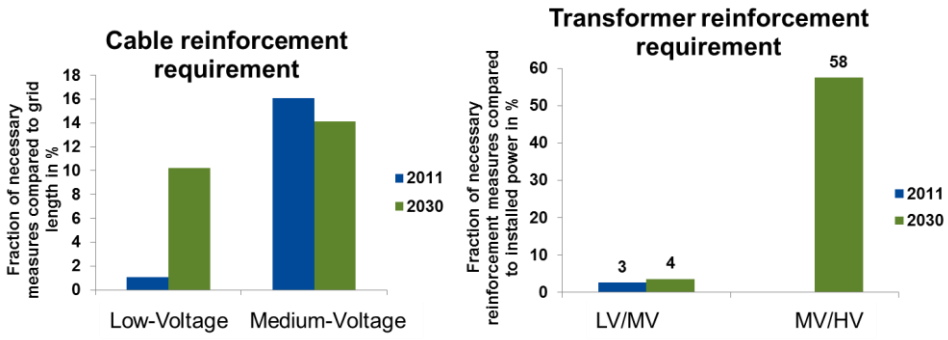

Figure 25: Total grid reinforcement requirement (Load flow reversal scenario 2030)

2.4 Conclusion

In conclusion, it can be noted that the ongoing installation of decentralized generators will entail a tremendous grid reinforcement demand. In the present grid we increased the amount of decentralized units by a factor of 2.7. This will lead to the requirement of reinforcing 32 % of all cables and 58 % of all transformers at the MV-level. Similarly, at the LV-level 11 % of the cables and 7 % of the transformers have to be supplanted until 2030.

References

[1] T. Breithaupt, T. Rendel, C. Rathke, L. Hofmann, “Modeling the Reliability of Large Thermal Power Plants in an Integrated Grid and Market Model,” 2012 IEEE International Conference on Power System Technology (Powercon), Auckland, New Zealand, 2012.

[2] T. Rendel, C. Rathke, T. Breithaupt, L. Hofmann, “Integrated Grid and Power Market Simulation,” IEEE PES General Meeting, San Diego, CA, USA, 2012.

[3] T. Rendel, C. Rathke, L. Hofmann, “Integrated Grid and Power Market Simulator,” in: ew - das Magazin für die Energiewirtschaft, no. 20, pp. 20-23, 2012.

[4] T. Breithaupt, S. Garske, T. Rendel, L. Hofmann, “Methodological Approach for Integrated Grid and Market Simulation of Coherent Distribution and Transmission Systems,” EnviroInfo 2013, Hamburg, Germany, 02.-04. September 2013.

[5] F. Fuchs, R. Dietz, S. Garske, T. Breithaupt, A. Mertens, L. Hofmann, “Challenges of Grid Integration of Distributed Generation in the Interdisciplinary Research Project Smart Nord,” IEEE 5th International Symposium on Power Electronics for Distributed Generation Systems (PEDG), Galway, Ireland, 24.-27. June 2014.

[6] K. Rudion, A. Orths, Z. A. Styczynski, K. Strunz, “Design of Benchmark of Medium Voltage Distribution Network for Investigation of DG Integration,” IEEE Power Engineering Society General Meeting.

[7] T. Leveringhaus, L. Hofmann, “Optimized voltage and reactive power adjustment in power grids using the least-squares-method: Optimization of highly utilized power grids with stochastic renewable energy-sources,” IEEE International Conference on Power and Energy Systems (ICPS), Chennai, Indien, 22.12 – 24.12. 2011.

[8] C. Rathke, “Entwicklung eines Modells für die integrierte Simulation der europäischen Übertragungsnetze und Strommärkte,” Aachen, Shaker Verlag, 2013.

[9] European Network of Transmission System Operators (2009). “Continental Europe Operation Handbook – P 1: Load-Frequency Control and Performance,” Brussels, Belgium, 2009.

[10] European Network of Transmission System Operators. “Continental Europe Operation Handbook – Appendix 1: Load-Frequency Control and Performance,” Brussels, Belgium, 2004.

[11] B. R. Oswald, “Berechnung von Drehstromnetzen,” vol. I. Wiesbaden: Vieweg+Teubner, 2009.

[12] K.-D. Weßnigk, “Kraftwerkselektrotechnik,” vol. I. Berlin: vde-verlag, 1993.

[13] P. Kundur, “Power System Stability and Control,” vol I. New York: McGraw-Hill, 1994.

[14] IEEE Task Force on Load Representation for Dynamic Performance, “Load representation for dynamic performance analysis,” IEEE Transactions on Power Systems, Vol. 8, No. 2, pp.472-482, May 1993.

[15] IEEE Recommended Practice for Excitation System Models for Power System Stability Studies, IEEE Std. 421.5-2005, April 2006.

[16] T. Breithaupt, T. Rendel, L. Hofmann, “INES - Integrierte Netz- und Energiemarktsimulation,” 15. Dresdener Kreis 2014, Fachtagung der TU-Dresden, der Universität Hannover, der Universität Magdeburg und der Gesamthochschule Duisburg: Elektroenergieversorgung, Leipzig, Deutschland, 19.-20. März 2014.

[17] K. Knorr, B. Zimmermann, D. Kirchner, M. Speckmann, R. Spieckermann, M. Widdel, M. Wunderlich, R. Mackensen, K. Rohrig, F. Steinke, P. Wolfrum, T. Leveringhaus, T. Lager, L. Hofmann, D. Filzek, T. Göbel, B. Kusserow, L. Nicklaus, P. Ritter, “Kombikraftwerk 2 / RegenerativKraftwerk 2050: Wege zu einer 100%-Versorgung mit erneuerbaren Energien - Abschlussbericht,” Pilotprojekt unter Förderung des Bundesministeriums für Umwelt, Naturschutz und Reaktorsicherheit, August 2014.

[18] CIGRE Technical Brochure, Modeling and Dynamic Behavior of Wind Generation as it Relates to Power System Control and Dynamic Performance, prepared by CIGRE Working Group C4.601 on Power System Security Assesment, August 2007.

[19] R. Hollinger, L. Engesser, T. Erge, “Frequenzhaltung als Serviceleistung dezentraler Solarstromspeicher,” R. Hollinger, M. Llerena Engesser, L. M. Diazgranados, T. Erge, VDE-Kongress 2014, Frankfurt am Main, Deutschland, 20.-21.10.2014.

[20] IEEE Technical Report PES-TR13, “Interconnected Power System Response to Generation Governing: Present Practice and Outstanding Concerns”.

[21] “Ten Years Network Development Plan,” ENTSO-E, 2014.

[22] “Netzentwicklungsplan Strom,” 50Hertz Transmission GmbH, Amprion GmbH, TenneT TSO GmbH, TransnetBW GmbH, 2012.

[23] Reference load profiles of single-family and multi-family houses for the use of CHP systems, Technical guideline VDI 4655, 2008-5.

[24] Micro-CHP system Senertec Dachs SE (stirling engine), 2015.

[25] Micro-CHP system Vaillant ecopower 1.0 (gas engine), 2015.

[26] Micro-CHP system HEXIS Galileo 1000N (Solid Oxide Fuel Cell), 2015.

[27] Micro-CHP system Viessmann Vitovalor 300-P (Polymere Electrolyte Membran Fuel Cell), 2015.

[28] Micro-CHP system CFCL BlueGEN (Solid Oxid Fuel Cell), 2015.

Sub-Project Five:
System Theory for Active Distribution Grids

Overview on Sub-Project Five: System Theory for Active Distribution Grids

Hans-Peter Beck[57], Mehrnaz Anvari[58], Christian Bohn[57], Timo Dewenter[58], Alexander Hartmann[58], Detlev Heinemann[58], Wiebke Heins[57], Gerald Lohmann[58], Joachim Peinke[58], Florian Pöschke[57], Mohammad Reza Rahimi Tabar[58] and Benjamin Werther[57]

1 Work Package 5.1

In this sub-project we focus on the system theory of distribution grids and MicroGrids. In work package 5.1 MicroGrids in different settings are investigated. Parameters of a virtual synchronous machine that mimics the behaviour of a synchronous machine are optimized with respect to a cost functional. Simulations as well as experiments to validate the obtained time series have been done to achieve a realistic result. A MicroGrid consisting of inverters, such a special machine and a load is also numerically optimized. A distributed frequency control for a MicroGrid was applied and parameters adjusted such that with the help of communication the original load sharing of the machines in the grid could be restored via a secondary control. Different models like a simple transport model on various random networks have been investigated to characterize very resilient network topologies.

2 Work Package 5.2

Work package 5.2 deals with the short-term stochastic dynamics of wind and solar power in order to assess their effects on the stability of distribution grids. By means of power spectrum analyses and increment statistics, frequent high magnitude fluctuations (flickering) are documented in both wind power and solar irradiance. To help mitigate the risk of MicroGrid instability in the future, a time delayed feedback method is proposed that is capable of suppressing some of the most extreme flickering events in aggregated decentralized power production from wind turbines and photovoltaic systems.

3 Work Package 5.3

Work package 5.3 has two main focuses. Part one improves a given experimental setup to a demonstration plant for MicroGrids. The purpose of this demonstration plant is to validate the theoretical results of the work packages WP 5.1 and WP 5.2. Furthermore, this work package deals with the detection of islanding situations in MicroGrids. Due to the on-going increase of distributed energy generation in the distribution grid a safe and sufficient fast detection of the transition from the grid-connected to the islanding mode of the MicroGrid has to be ensured. Several islanding detection methods and there applicability are tested and validated in the demonstration plant.

[57] Clausthal University of Technology
[58] University of Oldenburg

Work Package 5.1: System Theory for MicroGrids

Wiebke Heins[59], Timo Dewenter[60], Benjamin Werther[59], Alexander Hartmann[60], Christian Bohn[61] and Hans-Peter Beck[62]

1 Introduction

This work package focuses on the design and optimization of control strategies for MicroGrids, as well as on the characterization of resilient network topologies. Section 2 introduces the models of a MicroGrid and a so-called virtual synchronous machine which are used later for the parameter optimization in sections 3 and 4. Section 5 describes the distributed frequency control of a MicroGrid, where the virtual synchronous machines used in the grid are able to communicate with each other. The characterization of resilient network topologies for different models is done in section 6 of this chapter.

2 Model and Setup for MicroGrid Optimization

Objective of the optimization is to find a parameter setup for the virtual synchronous machine (see below section "Principle and Model of the Virtual Synchronous Machine") with a droop controller for frequency (P(f)) and an integral controller for secondary frequency control. The VISMA is acting as the grid-building component in a MicroGrid. The MicroGrid contains two decentralized energy sources which are interfaced to the grid via inverters and equipped with droop frequency (P(f)) and droop voltage control (Q(U)) [46]. A load is connected to the grid at the central point of the radial topology.

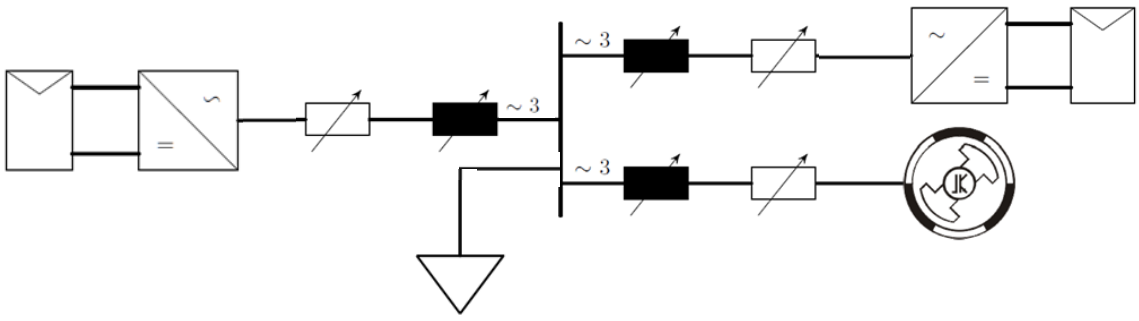

Figure 1: MicroGrid in island mode containing two inverters, one VISMA and one load

[59] Clausthal University of Technology, 38678 Clausthal-Zellerfeld, Germany, {forename.surname}@tu-clausthal.de, Institute of Electrical Information Technology
[60] University of Oldenburg, 26111 Oldenburg, Germany, {forename.surname}@uni-oldenburg.de, Institute for Physics
[61] Clausthal University of Technology, 38678 Clausthal-Zellerfeld, Germany, bohn@iei.tu-clausthal.de, Institute of Electrical Information Technology
[62] Clausthal University of Technology, 38678 Clausthal-Zellerfeld, Germany, vorsitzender@efzn.de, Institute of Electrical Power Engineering and Energy Systems

2.1 Principle and Model of the Virtual Synchronous Machine (VISMA)

The VISMA concept aims to set up the static and dynamic performance of the electromechanical synchronous machine to a three phase hysteresis controlled inverter. Figure 2 shows the basic structure of the VISMA.

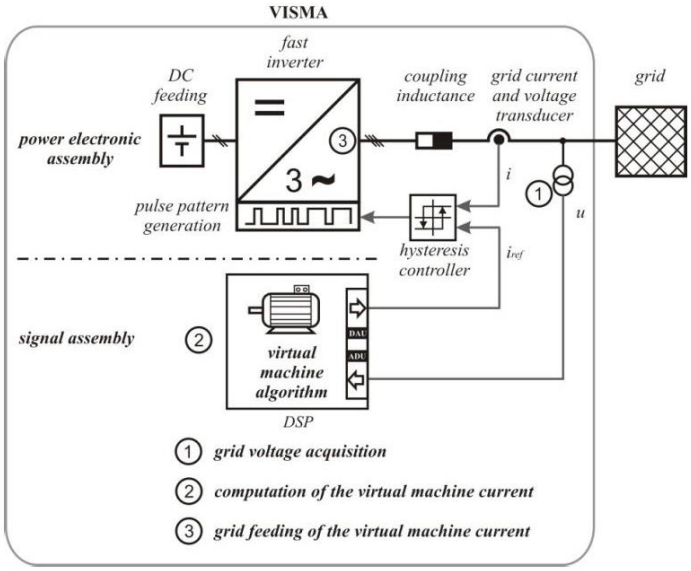

Figure 2: Functional scheme of the VISMA [4]

The complete VISMA functional chain contains three sub-processes, the real-time measurement of, the process computer and the hysteresis controlled inverter. The grid voltage is measured to feed the virtual synchronous machine algorithm, which calculated the resulting stator currents of the mathematical model of a synchronous machine. These stator currents are used as reference current signals to drive fast hysteresis controlled inverter.

Figure 3 shows the equivalent circuit diagram of a synchronous machine stator

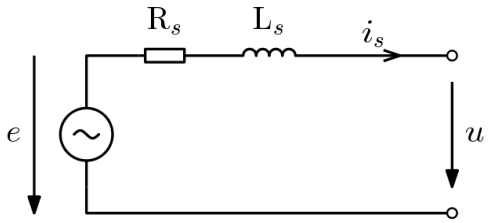

Figure 3: Equivalent circuit diagram of a synchronous machine stator (only one phase is shown)

The differential equation of the stator circuit is given in equation

$$\dot{\boldsymbol{i}}_{\boldsymbol{s}} = \frac{\mathbf{1}}{\mathbf{L}_{\boldsymbol{s}}} \cdot (-\mathbf{R}_{\boldsymbol{s}} \cdot \boldsymbol{i}_{\boldsymbol{s}} - \boldsymbol{u} + \boldsymbol{e}) \tag{1}$$

The parameter $\boldsymbol{i}_s$, $\boldsymbol{u}$ and $\boldsymbol{e}$ are state variables in the form $\boldsymbol{x}^T = [x_1 \quad x_2 \quad x_3]$, where $\boldsymbol{i}_s$ is the stator current, $\boldsymbol{u}$ embodies the grid voltage, and $\boldsymbol{e}$ equates to the induced EMF (electromotive force) in the stator windings.

$$\boldsymbol{e} = E_p \cdot \begin{pmatrix} \sin(\varphi) \\ \sin(\varphi - 120°) \\ \sin(\varphi + 120°) \end{pmatrix} \tag{2}$$

With the voltage $\boldsymbol{u}$ and the current $\boldsymbol{i}_s$ the electrical power is calculated by equation

$$P_{el} = \sum_{i=1}^{3} (u_i \cdot i_{s,i}) \tag{3}$$

The interconnection between the virtual electrical and virtual mechanical part of the machine is specified by the polar wheel angle φ.

$$\dot{\varphi} = \omega \tag{4}$$

$$\dot{\omega} = \frac{1}{\mathrm{J}} \left(M_{mech} - \frac{P_{el}}{\omega} - M_D \right) \tag{5}$$

The damping torque M_D is defined by equation

$$\dot{M}_D = \frac{1}{\mathrm{T_d}} (\mathrm{k_d} \cdot \dot{\omega} - M_D) \tag{6}$$

The differential equations (1) and (4) - (6) descripted the in the process computer used mathematical of synchronous machine.

2.2 Model and Setup for MicroGrid Optimization

Line resistances in the grid are chosen as $1.67\ \Omega$, line inductances as 1.514 mH. The nominal frequency is 50 Hz, nominal voltage is 230 V. This mimics a typical low voltage grid in Germany [2]. The load is constantly consuming active power at a level of 1.5 kW until at a certain point in time, when it increases in a step-like way to a level of 3 kW. Objective of the optimization is to find a set of parameters for the VISMA that enables the MicroGrid to overcome this disturbance in a stable and beneficial way.

The model used for simulation is a system of differential-algebraic equations. Assuming small frequency variations in the grid, the active power $P_i(t)$ and reactive power $Q_i(t)$ injected to or drawn from the grid at node i are approximated by algebraic grid equations (see e.g. [47])

$$\begin{aligned} P_i\big(\boldsymbol{U}(t), \Delta\boldsymbol{\theta}(t)\big) &= G_{ii} U_i^2(t) \\ &\quad - \sum_{k \in N(i)} U_i(t) U_k(t) \big(G_{ik} \cos\big(\Delta\theta_i(t) - \Delta\theta_k(t)\big) + B_{ik} \sin\big(\Delta\theta_i(t) - \Delta\theta_k(t)\big) \big), \\ Q_i\big(\boldsymbol{U}(t), \Delta\boldsymbol{\theta}(t)\big) &= -B_{ii} U_i^2(t) \\ &\quad - \sum_{k \in N(i)} U_i(t) U_k(t) \big(G_{ik} \sin\big(\Delta\theta_i(t) - \Delta\theta_k(t)\big) - B_{ik} \cos\big(\Delta\theta_i(t) - \Delta\theta_k(t)\big) \big). \end{aligned}$$

Here, $N(i)$ means the indices of all nodes in the grid that are neighbours to node i (excluding index i itself), $G_{ik} + \mathrm{j}B_{ik}$ denotes the admittance of the line between nodes i and k, $U_i(t)$ resp. $U_k(t)$ are the root mean square values of the voltages at nodes i resp. k, and $\Delta\theta_i(t)$ resp. $\Delta\theta_k(t)$ denote the phase difference between nodes i resp. k and a reference node. The values G_{ii} and B_{ii} are given as

$$G_{ii} = \hat{G}_{ii} + \sum_{k \in N(i)} G_{ik}\,, \quad B_{ii} = \hat{B}_{ii} + \sum_{k \in N(i)} B_{ik},$$

where $\hat{G}_{ii} + \mathrm{j}\hat{B}_{ii}$ is the shunt admittance at node i.

As reference node, the node is used where the VISMA is connected. Without loss of generality, this node is labelled as node no. 1. The simplified differential equations describing the VISMA which are used for the simulation are

$$\Delta\theta_1(t) = 0,\ \Delta\dot{\theta}_1(t) = 0,$$

$$J\dot{\omega}_1(t) = -\frac{k_\mathrm{d}}{T_\mathrm{d}}\,\omega_1(t) - \frac{k_\mathrm{d}}{T_\mathrm{d}}\,d(t) + \frac{1}{\omega_1(t)}\left(\frac{1}{k_{\mathrm{P},1}}\left(\omega_\mathrm{nom} - \omega_1(t)\right) + P_{\mathrm{sec},1}(t) - P_1\left(\boldsymbol{U}(t), \Delta\boldsymbol{\theta}(t)\right)\right),$$

$$T_\mathrm{d}\dot{d}(t) = -\,\omega_1(t) - \,d(t),$$

$$T_1\dot{U}_1(t) = -U_1(t) + U_{1,\mathrm{nom}} + K_\mathrm{U}\left(U_{1,\mathrm{nom}} - U_1(t)\right),$$

where $U_{1,\mathrm{nom}}$ is the nominal voltage setpoint for the VISMA, ω_nom is the nominal angular frequency setpoint, $\omega_1(t)$ the virtual frequency of the VISMA, $d(t)$ a virtual damping term, and T_1 and K_U parameters of proportional voltage control. The parameters J, k_d and T_d are design parameters for the dynamic behaviour of the VISMA. The secondary control $P_{\mathrm{sec},1}(t)$ is realized as a simple integral controller governed by

$$P_{\mathrm{sec},1}(t) = x_\mathrm{I}(t),$$

$$\dot{x}_\mathrm{I}(t) = K_\mathrm{I}\left(\omega_\mathrm{nom} - \omega_1(t)\right).$$

with nominal angular frequency setpoint $\omega_\mathrm{nom} = 2 \cdot 50 \cdot \pi$.

The inverters are approximated as third-order systems of the form

$$\Delta\dot{\theta}_i(t) = \omega_i(t) - \omega_1(t),$$

$$T_i\dot{\omega}_i(t) = -\,\omega_i(t) + \omega_\mathrm{nom} + k_{\mathrm{P},i}\left(P_{\mathrm{nom},i} - P_i\left(\boldsymbol{U}(t), \Delta\boldsymbol{\theta}(t)\right)\right),$$

$$T_\mathrm{i}\dot{U}_i(t) = -U_1(t) + U_{i,\mathrm{nom}} + k_{\mathrm{Q},i}\left(Q_{\mathrm{nom},i} - Q_i\left(\boldsymbol{U}(t), \Delta\boldsymbol{\theta}(t)\right)\right).$$

The parameters $k_{\mathrm{Q},i}$ are the droops of the Q(U)-droop control used in the inverters. In both VISMA and inverter equations, $k_{\mathrm{P},i}$ denotes the droop of P(f)-droop-control.

The load is modelled as time series of active power.

3 Optimization of the Dynamical Behaviour of a Virtual Synchronous Machine

We examine both numerical and experimental the response of a Virtual Synchronous Machine (see section “Principle and Model of the Virtual Synchronous Machine”) to a perturbation caused by a jump in the virtual torque of the machine. This jump triggers the VISMA to provide output power, which is taken from an DC energy storage. In the DEQs of a VISMA (cf., Eqs. (1)-(6)) are two parameters which can be chosen freely and both influence the damping behaviour: The damping factor k_d and the damping time constant T_d. These parameters should be chosen such that the temporal development of the output power of the VISMA follows an exponential, i.e. we look for minima of the cost functional

$$E = \int_{t_0}^{t_0+T} \lambda(t) \cdot \|\bar{P} - P_{\mathrm{Soll}}\|_2^2 \, \mathrm{d}t \tag{7}$$

where t_0 is the time of the step of the torque, T the measurement time, $\bar{P}(t)$ the active power, $P_{\mathrm{Soll}}(t)$ the desired exponential behaviour and

$$\lambda(t) = \begin{cases} 1, & t \leq (T/2 + t_0) \\ 2, & t > (T/2 + t_0) \end{cases} \tag{8}$$

a weighting parameter. We numerically solve the DEQs of a VISMA connected with a stiff grid for different parameter settings (k_d,T_d) and search for minima of Eq.(7) with the Downhill-Simplex algorithm [5]. Here, we show exemplarily a result for a minimum of the cost functional for a time constant $\tau = 0.4$ s which determines the steepness of $P_{Soll}(t)$ (see Figure 4(a)). More details can be found in [9].

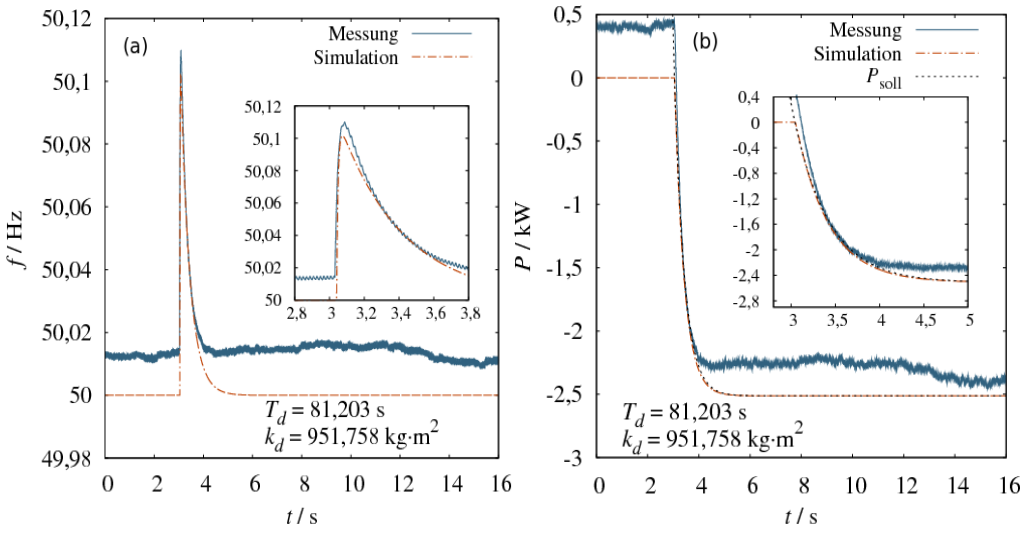

Figure 4: (a) Comparison of measured and simulated VISMA frequency for $\boldsymbol{\tau = 0.4}$ s and a minimum of the cost functional for the given parameter values [9]. (b) The same for the active power feed-in of the VISMA [5]. Shown are measured, simulated, and desired output power. Inset: Region close to step in virtual torque at time $\boldsymbol{t_0 \approx 3}$ **s**

4 MicroGrid Optimization

The set-up of the MicroGrid is depicted in Figure 1 and the corresponding equations are described in section "Model and setup for MicroGrid optimization". Like in the parameter optimization of the VISMA (see section "Principle and Model of the Virtual Synchronous Machine") we are looking for minima of a cost functional defined by

$$S = t_\mathrm{R} + \sum_i^3 \lambda(i) \cdot \int_{t_0}^{t_0+t_\mathrm{R}} |P_i(t) - P_{\mathrm{Soll},i}| \, \mathrm{d}t + \beta \cdot (J + k_d) \tag{9}$$

where t_R is the maximum of the relaxation times of frequency and voltage of all nodes after the step-like increase at time t_0 of the power demand of the load, the sum runs over the VISMA and the two inverters (nodes 2 and 3), $P_{\mathrm{Soll},i}(t)$ is the desired active power output of the corresponding node, and the weighting parameter is

$$\lambda(i) = \begin{cases} \alpha/100, & \text{for } i = 1 \text{ (VISMA)} \\ \alpha, & \text{for } i \neq 1 \end{cases} \tag{10}$$

The parameters α and β determine the focus of the optimization, e.g., choosing a large α results in focusing on minimizing the area between output and desired power. In addition to this cost functional we use constraints for the parameters to ensure that we get a realistic result. Therefore, we apply bounds on parameters to ensure that the secondary control is slower than the VISMA itself, and that the VISMA is not faster than a regular inverter corresponding to a bounded energy feed-in.

We search for minima of Eq. (9) with the Downhill-Simplex algorithm [5]. Figure 5 shows two results for different values of α and β.

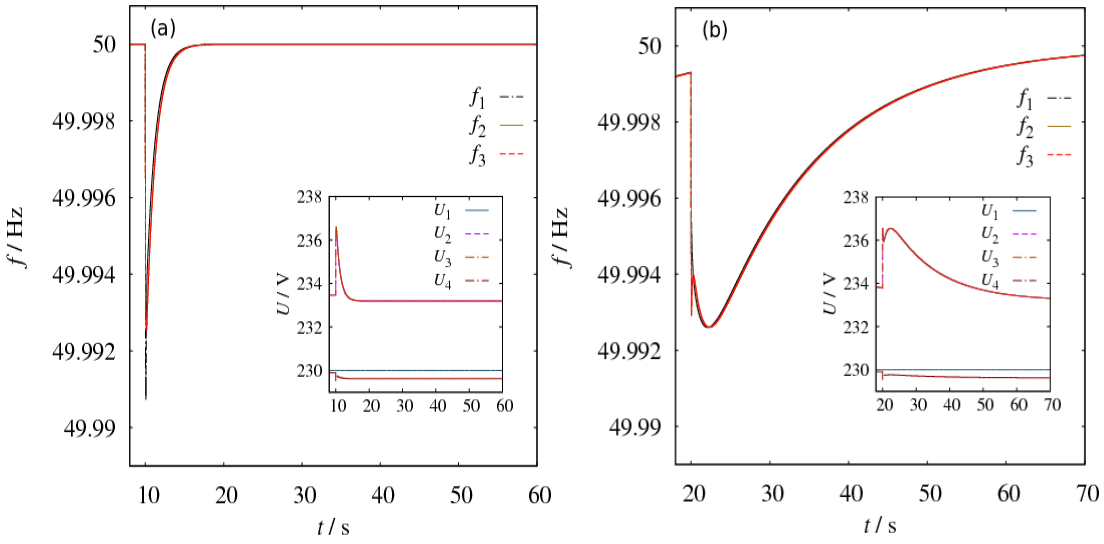

Figure 5: (a) Frequencies of the VISMA and the two inverters for a minimum of the cost functional for parameters $\boldsymbol{\alpha = 2.5 \cdot 10^{-7}}$, $\boldsymbol{\beta = 1}$, $\boldsymbol{J = 0.827}$, $\boldsymbol{k_d = 1.94 \cdot 10^{-3}}$, $\boldsymbol{T_d = 9.32 \cdot 10^{-7}}$, $\boldsymbol{K_I = 2.72 \cdot 10^4}$, and $\boldsymbol{K_P = 0}$. Step in the load at time $\boldsymbol{t_0 = 10\ s}$. Inset: The same for the voltages of the four nodes. (b) The same for parameters $\boldsymbol{\alpha = 5 \cdot 10^{-7}}$, $\boldsymbol{\beta = 0.01}$, $\boldsymbol{J = 5.12 \cdot 10^{-3}}$, $\boldsymbol{k_d = 50.83}$, $\boldsymbol{T_d = 0.78}$, $\boldsymbol{K_I = 2.07 \cdot 10^3}$, and $\boldsymbol{K_P = 0}$. Inset: Behavior of the voltages for the same scenario

4.1 Outlook

In addition, one could use "Parallel Tempering" [6] for searching minima [7] of the cost functional. In this statistical physics method simple Monte Carlo simulations at different temperatures are performed simultaneously while allowing for swaps of systems belonging to "neighbouring" temperatures. With this procedure it is possible to overcome high barriers in the energy landscape defined by the cost functional and therefore it is very likely to find a global optimum as possibly the whole parameter space can be sampled.

5 Distributed Frequency Control for VISMA-Based MicroGrids

5.1 Objectives and Example Setup

A concept for distributed frequency control for MicroGrids is presented that is based on the virtual-synchronous machine (VISMA). The control has to be robust against disturbances, communication failures and sudden islanding. The key concept applied here is based on the "distributed-averaging proportional-integral" (DAPI) controller presented in [8].

A simulation example is presented here that illustrates the performance of the distributed control strategy. A MicroGrid with three VISMA-controlled inverters of equal power rating, four loads and a power source (for example a photovoltaic source without storage) is considered. Loads and power source are not controlled, but act within known bounds. In grid-connected mode, the three VISMA-controlled inverters are acting as grid-supporting units by supplying active power according to a P(f) droop. When an islanding event occurs, they are able to perform primary control tasks, i.e. to manage the transient and afterwards act as grid-building components, providing a constant voltage and a common frequency. The level of the frequency is defined by the P(f) droops, as well as is load sharing among the three VISMAs, e.g. by choosing the droops according to the power rating of each VISMA.

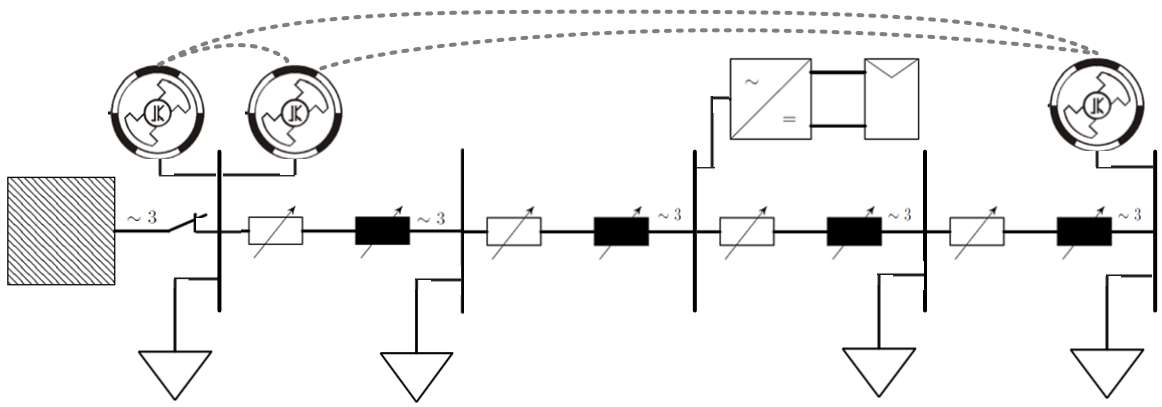

Figure 6: MicroGrid with three VISMA-controlled inverters, four loads and one power source (e.g. a PV source without storage). For distributed secondary control, the three VISMAs are able to communicate among each other as indicated by the grey dotted line

After islanding, the grid frequency is usually not equal to the desired nominal frequency. Therefore, a secondary frequency control is used to restore the nominal frequency.

5.2 Model Used for Design and Simulation

The model used for design and simulation is a system of differential-algebraic equations. Assuming small frequency variations in the grid, the active power $P_i(t)$ and reactive power $Q_i(t)$ injected to or drawn from the grid at node i are approximated by algebraic grid equations (see e.g.[47])

$$\begin{aligned} P_i\big(\boldsymbol{U}(t), \Delta\boldsymbol{\theta}(t)\big) &= G_{ii}U_i^2(t) \\ &\quad - \sum_{k\in N(i)} U_i(t)U_k(t)\big(G_{ik}\cos\big(\Delta\theta_i(t)-\Delta\theta_k(t)\big) + B_{ik}\sin\big(\Delta\theta_i(t)-\Delta\theta_k(t)\big)\big), \\ Q_i\big(\boldsymbol{U}(t), \Delta\boldsymbol{\theta}(t)\big) &= -B_{ii}U_i^2(t) \\ &\quad - \sum_{k\in N(i)} U_i(t)U_k(t)\big(G_{ik}\sin\big(\Delta\theta_i(t)-\Delta\theta_k(t)\big) - B_{ik}\cos\big(\Delta\theta_i(t)-\Delta\theta_k(t)\big)\big). \end{aligned}$$

Here, $N(i)$ means the indices of all nodes in the grid that are neighbors to node i (excluding index i itself), $G_{ik} + \mathrm{j}B_{ik}$ denotes the admittance of the line between nodes i and k, $U_i(t)$ resp. $U_k(t)$ are the root mean square values of the voltages at nodes i resp. k, and $\Delta\theta_i(t)$ resp. $\Delta\theta_k(t)$ denote the phase difference between nodes i resp. k and a reference node. The values G_{ii} and B_{ii} are given as

$$G_{ii} = \hat{G}_{ii} + \sum_{k\in N(i)} G_{ik}\,, \quad B_{ii} = \hat{B}_{ii} + \sum_{k\in N(i)} B_{ik},$$

where $\hat{G}_{ii} + \mathrm{j}\hat{B}_{ii}$ is the shunt admittance at node i.

The differential equations describing the VISMA

$$\Delta\dot{\theta}_i(t) = \omega_i(t),$$

$$J\dot{\omega}_i(t) = -\frac{k_\mathrm{d}}{T_\mathrm{d}}\,\omega_i(t) - \frac{k_\mathrm{d}}{T_\mathrm{d}}\,d_i(t) + \frac{1}{\omega_i(t)}\left(\frac{1}{k_{\mathrm{P},i}}\big(\omega_\mathrm{nom} - \omega_i(t)\big) + P_{\mathrm{sec},i}(t) - P_i\big(\boldsymbol{U}(t), \Delta\boldsymbol{\theta}(t)\big)\right),$$

$$T_{\mathrm{d},i}\dot{d}_i(t) = -\,\omega_i(t) - d_i(t),$$

where $U_{i,\mathrm{nom}}$ is the nominal voltage setpoint for the VISMA, ω_nom is the nominal angular frequency setpoint, $\omega_1(t)$ the virtual frequency of the VISMA, $d(t)$ a virtual damping term. The parameters J, k_d and T_d are design parameters for the dynamic behaviour of the VISMA. The secondary control $P_{\mathrm{sec},1}(t)$ is realized in different ways as described below.

The loads and power sources are modelled as timeseries of active and reactive power. They are realized by algebraic constraints at the grid nodes.

5.3 Simulation Results for Secondary Frequency Control Strategies

Often, secondary frequency control is done by individual simple PI-controllers that are slow in comparison to the primary droop control [8]. This means that in the VISMA equations the value $P_{\mathrm{sec},i}(t)$ for secondary control is governed by

$$P_{\mathrm{sec},i}(t) = x_{\mathrm{I},i}(t),$$

$$\dot{x}_{\mathrm{I},i}(t) = k_{\mathrm{I},i}\big(\omega_\mathrm{nom} - \omega_i(t)\big), \qquad i = 1,2,3,$$

where $x_{\mathrm{I},i}(t)$ is an auxiliary state, and $k_{\mathrm{I},i}$ is the integral control constant. However, this does not generally maintain the original load sharing. Especially in MicroGrids with storage units of limited capacity, this can lead to undesirable behaviour. Figure 7 illustrates this effect: A disturbance causes the secondary control to start not at the same time, but one after the other in timesteps of 0.1 second. Although all VISMAs have the same power rating, the control does not manage to restore the power sharing. Nonetheless, the frequency is restored quickly. This effect cannot be overcome by a completely decentralized control strategy.

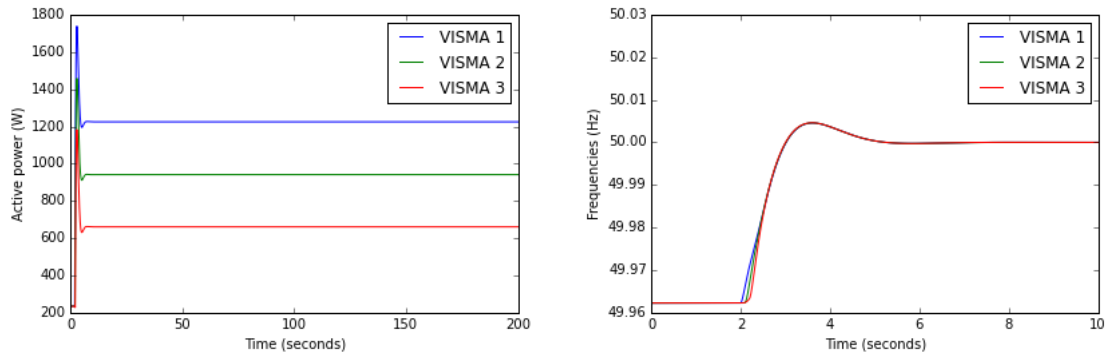

Figure 7: Simulation result for decentralized PI-control: Injected active power (left) and VISMA frequencies (right)

The distributed control requires a communication link between all components that take part in secondary control (Figure 7). The control law then reads in this example (see [8])

$$P_{\mathrm{sec},i}(t) = x_{\mathrm{I},i}(t),$$

$$T_{\mathrm{I},i}\dot{x}_{\mathrm{I},i}(t) = k_{\mathrm{I},i}\big(\omega_{\mathrm{nom}} - \omega_i(t)\big) - \sum_{\substack{j=1,2,3,\\ j\neq i}} \left(\frac{x_{\mathrm{I},i}(t)}{k_{\mathrm{I},i}} - \frac{x_{\mathrm{I},i}(t)}{k_{\mathrm{I},i}}\right), \quad i = 1,2,3,$$

where $T_{\mathrm{I},i}$ is a time constant.

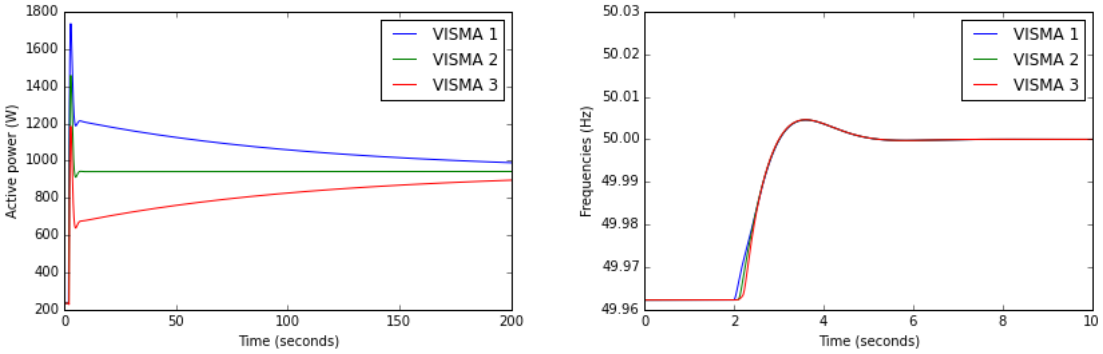

Figure 8: Simulation result for distributed secondary VISMA-based control: Injected active power (left) and VISMA frequencies (right)

In the same setup as above, this control is able to restore the original load sharing, as can be seen in Figure 8.

An anti-windup strategy was included in the control in the case of limited control power. Figure 9 shows that the control works well. Even though the limits are met for a while, the control is able to restore the frequency and power sharing as long as the power balance in the grid is feasible. Details can be found in [48].

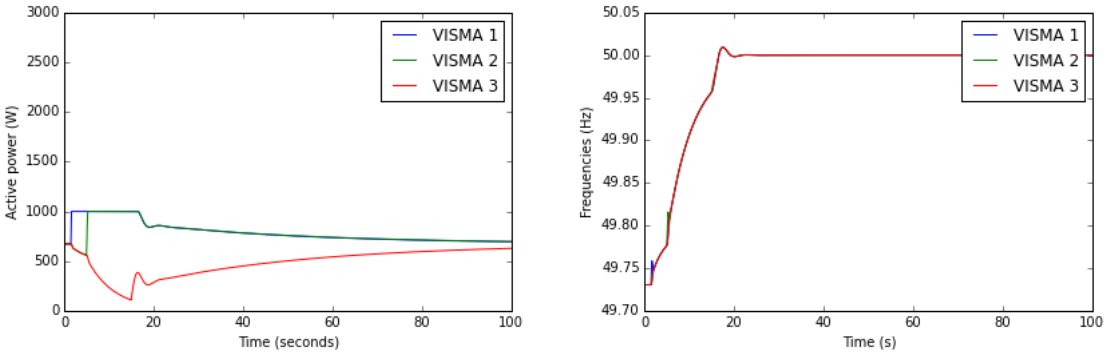

Figure 9: Simulation result for distributed secondary VISMA-based control with limited control power and anti-windup

6 Optimal Network Topologies

Two different models have been investigated with the so-called “large-deviation method” [10] and a third model [13] is currently put under scrutiny. This first one is a simple transportation model based on shortest paths, the second one is based on a linearized, static power flow and the third one deals with the calculation of attraction areas of fixed points of a dynamical power grid model. The first two models are about resilience of networks, while the third one is about the effect of topology changes on the stability. The large-deviation method is used to study tails of distributions of a so-called “backup capacity” which is a measure for resilience of a certain network.

6.1 Transport Model

Distributions of the resilience of transport networks are studied numerically, in particular the large-deviation tails. Thus, not only typical quantities like average or variance but the distributions over the (almost) full support can be studied. For a proof of principle, a simple transport model based on the edge-betweenness and three abstract yet widely studied random network ensembles are considered here: Erdős-Rényi random networks (ER) with finite connectivity, small world networks (SW) and spatial networks embedded in a two-dimensional plane. Using specific numerical large-deviation techniques, probability densities as small as 10^{-80} are obtained here. This allows to study typical but also the most and the least resilient networks. The resulting distributions full the mathematical large-deviation principle, i.e., can be well described by rate functions in the thermodynamic limit. The analysis of the limiting rate function reveals that the resilience follows an exponential distribution almost everywhere. An analysis of the structure of the network shows that the most-resilient networks can be obtained, as a rule of thumb, by minimizing the diameter of a network (see Figure 10(b). Note that a small backup capacity corresponds to the most resilient networks). Also, trivially, by including more links a network can typically be made more resilient (see Figure 10(a)). On the other hand, the least-resilient networks are very rare and characterized by one (or few) small core(s) to which all other nodes are connected. In total, the spatial network ensemble turns out to be most suitable for obtaining and studying resilience of real mostly finite-dimensional networks. Studying this ensemble in combination with the presented large-deviation approach for more realistic, in particular dynamic transport networks appears to be very promising. A more detailed description and more results can be found in [11].

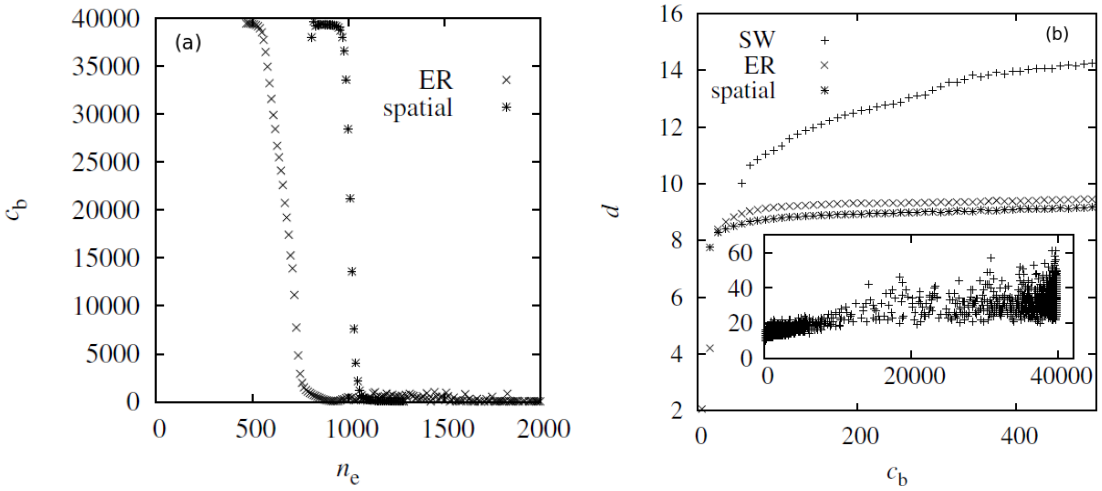

Figure 10: (a) The average resilience c_b as a function of the number n_e of links for ER and spatial networks of size $N = 400$ [11]. (b) The average diameter d as a function of the resilience c_b for SW, ER and spatial networks of size $N = 400$, in the range of small value of c_b. The inset shows a scatter plot of the data for the entire range of backup capacities for the SW case [11]

6.2 Power Flow Model

Distributions of the resilience of a power flow model against transmission line failures are studied via a so-called backup capacity. In this linearized DC power flow model only active power is investigated, where nodes in the network can either produce or consume active power. This power is transported via lossless lines (edges in the graph) between the nodes, where the amount depends on the phase angle difference between the two neighbouring nodes. We consider three ensembles of random networks, and in addition, the topology of the British transmission power grid. The three

ensembles are Erdős-Rényi random graphs, Erdős-Rényi random graphs with a fixed number of links, and spatial networks where the nodes are embedded in a two-dimensional plane. We numerically investigate the probability density functions (pdfs) down to the tails to gain insight into very resilient and very vulnerable networks. This is achieved via large-deviation techniques, which allow us to study very rare values that occur with probability densities below 10^{-160}. We find that the right tail of the pdfs towards larger backup capacities follows an exponential with a strong curvature. This is confirmed by the rate function, which approaches a limiting curve for increasing network sizes. Very resilient networks are basically characterized by a small diameter and a large power sign ratio (c.f., Figure 11). The diameter of a network is the longest of all shortest paths in the graph. The so-called "power sign ratio" is the fraction of edges that directly connect a producer with a consumer of power. In addition, networks can be made typically more resilient by adding more links. More details can be found in [12].

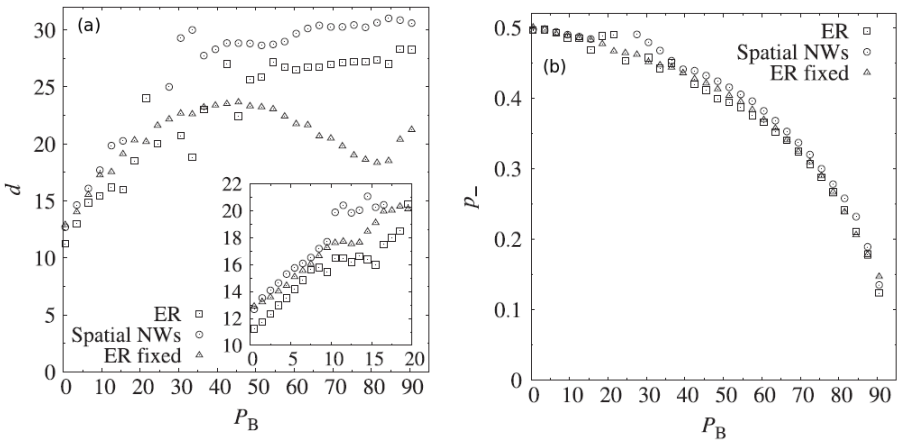

Figure 11: Average diameter $\boldsymbol{d}$ (a) and power sign ratio $\boldsymbol{p_-}$ (b) as functions of the backup capacity $\boldsymbol{P_B}$ for all studied network ensembles with size $\boldsymbol{N = 400}$. Note that because of the gap in the data for ER and spatial networks, some intermediate values of $\boldsymbol{P_B}$ are not present [12]. Inset in (a) enlarges region for small $\boldsymbol{P_B}$

6.3 Outlook

Numerical studies of the distribution of "maximum-disturbance" stability of power grids could also be investigated [13]. The model is based on networks of oscillators. Here, we consider different ensembles of random networks, like standard Erdös-Renyi and two dimensional spacial networks. To access the distribution down to very small probabilities, we use specific large deviation techniques [10]. The stability is given by a conservative estimation of an asymptotic stability boundary, which is well known in stability theory. The starting point is the matrix A defined by $\mathbf{J^T \cdot A + A \cdot J = E}$, $\mathbf{J}$ being the Jacobean Matrix. By calculating the maximum disturbance of $\mathbf{x}$, which results in the quadratic form $V = \mathbf{x^T \cdot A \cdot x} = \epsilon(\mathbf{x})$ not being a Lyapunov-function [14] of the system any longer, the boundaries for the stability can be found. For comparison, for the given networks also simple stability measures based on shortest paths [11], on the eigenvalues of the Jacobi matrix and on a linearized power-flow model [12] are obtained.

Work Package 5.2: System Theory of Generation and Loads

Gerald Lohmann[63], Mohammad Reza Rahimi Tabar[63], Mehrnaz Anvari[63], Detlev Heinemann[63] and Joachim Peinke[64]

1 Introduction

With the decided exit from nuclear and fossil-fuel energy, and shares of wind and solar energy on the rise, German power grids face increasing challenges regarding the integration and management of said renewable sources [15]. Amongst others, issues of decentralized grid topology and the maintenance of voltage and frequency stability is expected to become more and more difficult in distribution grids with a high share of wind and solar power. Both renewable resources vary considerably on virtually all time scales, with seasonal variations being in the order of months, while weather-induced variations range from days to hours to minutes, and even seconds. Changes in the magnitude of wind speed or solar irradiance are almost immediately translated into variations in the output power of wind energy converters and photovoltaic (PV) systems [16].

Especially on very short time scales, these variations are stochastic in nature and thus difficult or nearly impossible to predict. If more and more distributed generation from renewables is simply integrated in existing power grids, thereby replacing conventional technologies such as hydro, gas, coal, and nuclear power plants, system instabilities will be likely to occur [22]. Instead, to handle this kind of volatile power production from decentralized renewables, and in order to contribute to resilient power grids, a revision of traditional power grids becomes necessary [23], [24]. In particular,

- a reduction of correlation of variations may be aimed for by increased spatial dispersion and diversification of sources (e.g. mix of solar and wind power),
- flexible generators may be held available as back-up production capacity, which can be ramped up and down quickly for balancing the load and generated power,
- energy storage may be progressively introduced to the grid (although the cost of advanced storage technologies, such as batteries, is often considered their main limitation),
- trade and transfer of electricity across long distances may be increased, and finally
- flexibility and grid management (including smart grid technologies) may be enhanced.

In the context of the last point, positive ramps caused by a sudden increase in renewable production can, in principal, be limited very quickly at any time using power electronics. For negative increments (ramp down), expensive energy storage systems are needed to help smooth out sudden power decreases [17], [18], [19].

However, simply using electronics technology is not enough. It's rather the interplay with the intrinsic dynamics of the various interconnected conventional and renewable power systems that determines the feasibility and effectiveness of any measure. For the best grid integration of wind and solar energies, the physics of the wind and solar power fluctuations and their stochastic behaviours must thus be understood in details. It's mainly this aspect that the analyses presented in

[63] University of Oldenburg, 26111 Oldenburg, Germany,
{forename.surname}@uni-oldenburg.de, Institute of Physics and ForWind
[64] University of Oldenburg, 26111 Oldenburg, Germany,
peinke@uni-oldenburg.de, Institute of Physics and ForWind

this report aim to contribute to, by documenting certain key characteristics of local high frequency fluctuations in wind and solar power production.

As any power grid may be viewed as a complex system of systems, in which each sub-system is comprised of a diverse set of passive and active components, the increasing share of intermittent renewable energy links this complex network of power grids with the equally complex weather system. Understanding the constituents of interaction of two complex systems, in this case power grids and weather, and simulating their collective presence form the necessary basis from which an efficient design of resilient power grids can emerge.

2 Material and Methods

The present work is based on relatively high frequency measurements from operating wind turbines and continuous solar irradiance observations. Time series of wind speed, wind power, and global horizontal irradiance (GHI) have been collected from several regions around the world (the United States, Germany, Algeria, and Spain) with sampling rates ranging from 1 min^{-1} to 1 Hz. General information on all datasets is presented in Table 1.

Dataset	Variables	Frequency	Number of observations
Wind farm, Germany (12 turbines with a total of ~ 25 MW rated power)	Wind speed [ms^{-1}], wind power [W]	1 Hz	$15.3 * 10^6$
Solar campaign, Germany	GHI [Wm^{-2}]	1 Hz	$12 * 10^6$
Solar campaign, Hawaii, USA	GHI [Wm^{-2}]	1 Hz	$14 * 10^6$
BSRN, Algeria	GHI [Wm^{-2}]	1/60 Hz	$3.7 * 10^6$
BSRN, Spain	GHI [Wm^{-2}]	1/60 Hz	$1.3 * 10^6$

Table 1: Details of available data

In order to facilitate comparisons between datasets, the wind power time series $P(t)$ are normalized to the rated power P_r of their respective turbines, hence scaled power

$$P_s(t) = \frac{P(t)}{P_r} \tag{11}$$

is used. Similarly, and also to eliminate deterministic trends of diurnal and seasonal variations, all $GHI(t)$ time series are related to their respective theoretical clear-sky values $GHI_{clear}(t)$. The resulting time series of clear-sky index

$$k^* = \frac{GHI}{GHI_{clear}} \tag{12}$$

is thus dimensionless. Figure 12 shows an example of single-point measurements of GHI for a typical summer day with variable cloud cover in Northern Germany, measured with 1 Hz temporal resolution, along with the corresponding k^* time series.

As for obtaining the theoretical clear-sky irradiance, the clear-sky model presented in [20] is used to derive time series of clear-sky irradiance for all available datasets. To ensure conservative results when calculating k^*, only those times with solar elevation angles > 10° are considered for processing. At lower angles (after sunrise; before sunset), the relatively low values of GHI, in conjunction with path prolongation and the problem of small denominators, can result in unrealistic

clear-sky index values [21]. Moreover, shadows from the surroundings frequently distort irradiance measurements at times of low solar elevation angles.

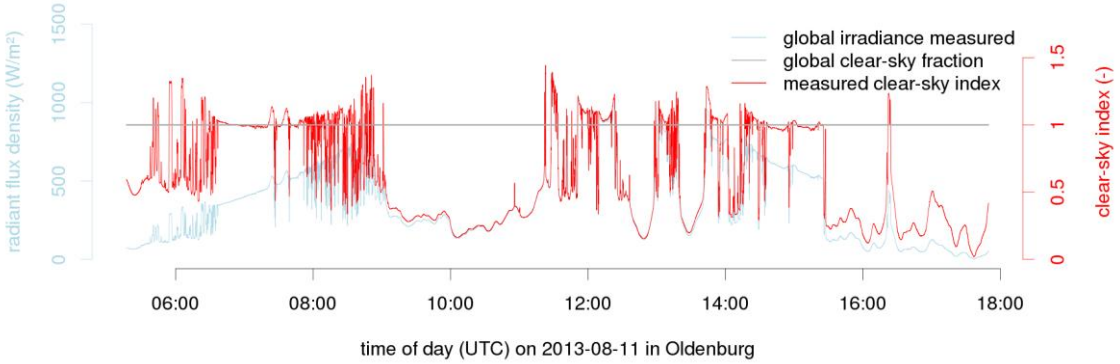

Figure 12: Single-point measurements of global horizontal irradiance (GHI) for a typical summer day in Northern Germany measured with 1 Hz temporal resolution (light blue). By means of the theoretical irradiance at clear sky conditions (gray), deterministic patterns, such as diurnal variations may be removed effectively. The resulting clear-sky index reduces variability to its atmospheric origin, without accounting for influences due to the time of day, or the time of year. Note that measured irradiance frequently exceeds its theoretical clear-sky counterpart during times of high variability, because solar irradiance is reflected by proximate clouds.

The first approach to describe the high-frequency characteristics of the aforementioned normalized wind and solar time series is to analyse the power spectrum of wind turbine output power and solar irradiance. By comparing the behaviour of a spectrum $S(f)$ with the well-known Kolmogorov-law of turbulence, i.e. $S(f) \sim f^{-5/3}$, conclusions regarding the nature of variations may be inferred. Turbulent time series typically exhibit stochastic fluctuations at various time scales.

As these kinds of variations are of special interest to various stakeholders involved with decentralized renewable power production, e.g. distribution system operators, a key aspect of this work package is to further quantify and compare short-term fluctuations in wind and solar power for different time intervals. In this context, the intermittency of a time series $X(t)$ can be described by means of probability density functions (pdf) of the time series' increments

$$\Delta X(t,\tau) = X(t+\tau) - X(t) \tag{13}$$

for different time lags τ.

Furthermore, a time-delayed feedback method is proposed for suppressing the short-term intermittency of wind and solar power of multiple renewable generators. When considering such a time dependent, spatially aggregated, cumulative power

$$P^*(t) = N^{-1} \sum_{i=1}^{N} P_i(t), \tag{14}$$

based on N intermittent power systems, each of which supplies an output power $P_i(t)$, the time-delayed feedback method proposes to save a fraction α of each generator's power at time t. After T seconds, this power is then fed into the grid in a delayed fashion, while only a fraction of $(1-\alpha)$ of the original power had been input to the grid at time t.

Thus, the new time delayed feedback power feed-in of each system is

$$P_i(t)^{new} = (1-\alpha)P_i(t) + \epsilon P^*(t-T), \tag{15}$$

where, in general, $\epsilon \leq \alpha$. The cumulative power output $\sum_{i=1}^{N} P_i(t)^{new}$ depends on the delay lag T and amplification α, and the method enables the assessment of operation strategies for power

systems. It can be a complementary method for energy storage, on the existence of which it obviously depends, and ramp-rate control. The effectiveness of this approach could even be increased by using multiple energy storage systems, each with a different time lag T.

3 Results

Since the power spectrum of a time series reveals the contributions of different time scales to the variations in the signal, the spectral analysis of wind velocity, scaled wind turbine power output, and GHI in Figure 13 allows drawing conclusions on the nature of their respective variability. In general, both wind turbines and photovoltaic cells convert wind velocity and solar irradiance fluctuations into power fluctuations quickly. In case of wind power, the conversion dynamics take place at short time scales in the order of seconds, while photovoltaic power conversion happens almost instantaneously.

Both wind speed and wind power output of a single turbine have similar spectral behaviour at low frequencies $f < 0.1$ Hz, and both adhere to the Kolmogorov-law of turbulence, i.e. $S(f) \sim f^{-5/3}$ [23]. While the spectrum of wind speed fluctuations does not significantly differ from the Kolmogorov-spectrum at higher frequencies, the spectrum of wind turbine power fluctuations does, as is shown in Figure 12a. This is due to the finiteness of the reaction time scale of wind turbines: the fast wind fluctuations are partly filtered, and slower wind fluctuations are adiabatically converted into power output fluctuations. For cumulative power fluctuations of a wind park, the filtering in the high frequency domain ($f > 0.1$ Hz) is even more emphasized, by the way. Hence, the power output of an entire wind park has even weaker high frequency fluctuations than that of a single turbine (not shown here).

In contrast to wind turbines, there is no considerable instrumental filtering in the conversion of irradiance to power at 1 Hz sampling, and the turbulence-type spectrum of the Kolmogorov-law is present in irradiance fluctuations of a single sensor for frequencies $0.001 < f < 0.05$ Hz (more than one order of magnitude). This is shown in Figure 12b. The spectrum of the spatial average of 17 sensors shows some filtering in the higher frequency region, but already starting around 0.005 Hz, the reason of which is similar to the spectrum of total wind farm power that has been mentioned above. Spatial aggregation thus dampens high frequency fluctuations in wind and solar power to some degree.

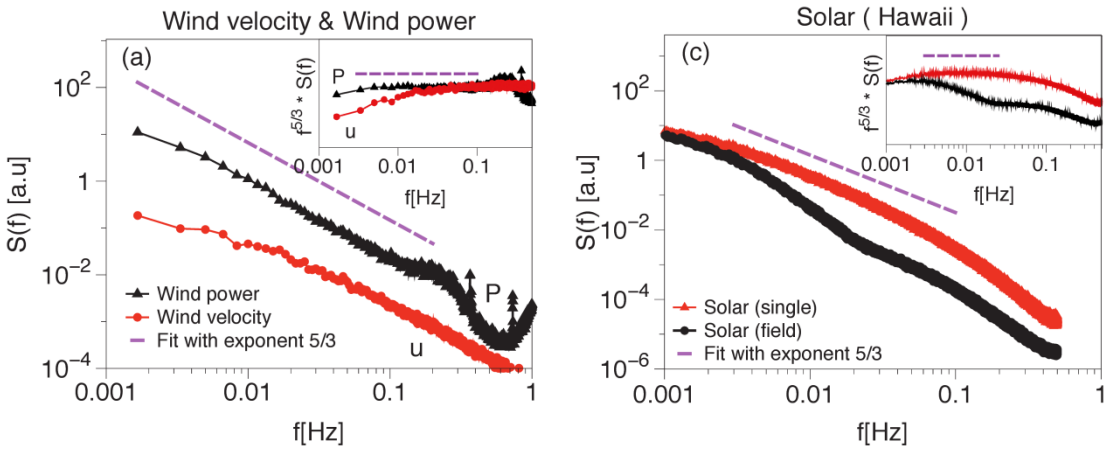

Figure 13: Power spectra of (a) wind velocity (red) and wind power output of a single turbine (black) from high frequency measurements in a wind park, and (b) irradiance fluctuations from high frequency measurements in Hawaii for a single sensor (red) and the mean of 17 sensors (black) in log-log scale. The Kolmogorov-spectrum with an exponent of 5/3 is represented by dashed lines in each plot. The insets of (a) and (b) show log-log plots of the compensated energy spectra $f^{5/3}S(f)$ as a function of frequency f.

To further analyse the characteristics of short-term wind and solar power fluctuations, increment statistics of the aforementioned 1 Hz measurements of wind turbine power and GHI are shown in Figure 15 for time lags $\tau = 1, 10, 1000\, s$. Every distribution is normalized to the respective standard deviation of its increment time series, and they all depart largely from the normal (Gaussian) distribution, as they possess exponential-like fat tails. These tails extend to extreme values, corresponding to a higher-than-normal probability to record an extreme ramp event (flickering).

When averaged (irradiance) or aggregated (wind power) over several sensors and turbines, respectively, the probability of extreme fluctuations decreases and overall flatness of the increment distributions decreases. In general, the flatter an increment distribution, the more will its corresponding time series exhibit flickering characteristics, which are dangerous for e.g. power system stability. However, the pronounced tails are still present in the distributions of averages and aggregates and pose challenges to the wide integration of renewables into the power grid.

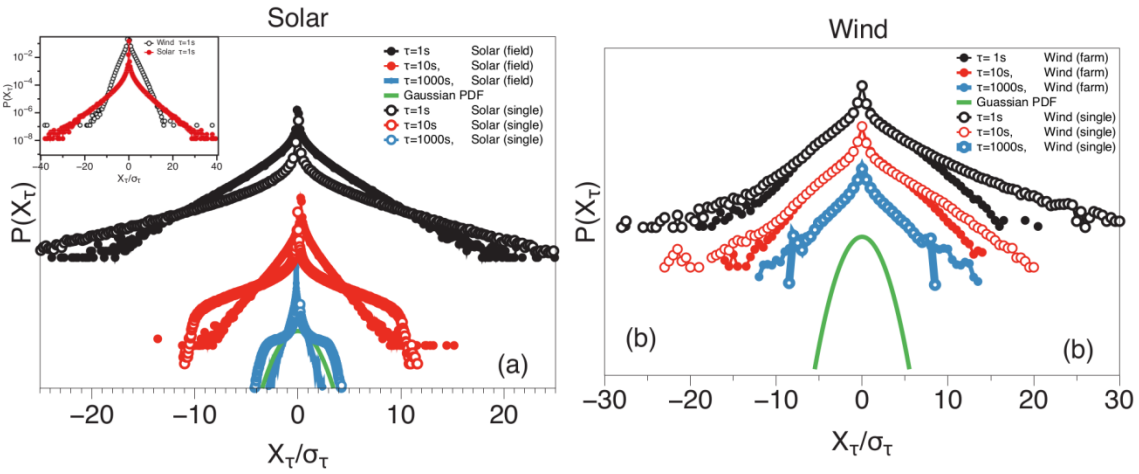

Figure 14: Probability distributions of increment statistics for (a) solar irradiance and (b) wind turbine power fluctuations for time lags τ = 1, 10, 1000 s in log.-lin. Scale. Both single sensor irradiance and single turbine power are contrasted with averaged irradiance of 17 sensors in a field and aggregated power output of 12 wind turbines, respectively. The distributions are vertically shifted for clarity, and increments X_τ are normalized to their respective standard deviations σ_τ. A Gaussian distribution with unit variance is plotted for reference. The inset of (a) compares the increments of wind and solar power time series with similar rated power and time lag of 1 s.

The fat-tailed characteristics of increment statistics for solar irradiance are also still evident in minute-averaged measurements of GHI, as shown in Figure 15. As minute-averaged data is much more readily available around the world, it can be shown that the dynamics on this time scale are generally similar in several regions around the world, including Hawaii, Algeria, Spain, and Germany. Though the range of extreme flickering values is reduced in units of its respective time series' standard deviation when compared to 1 Hz data, the distributions are still fat-tailed and non-Gaussian in nature.

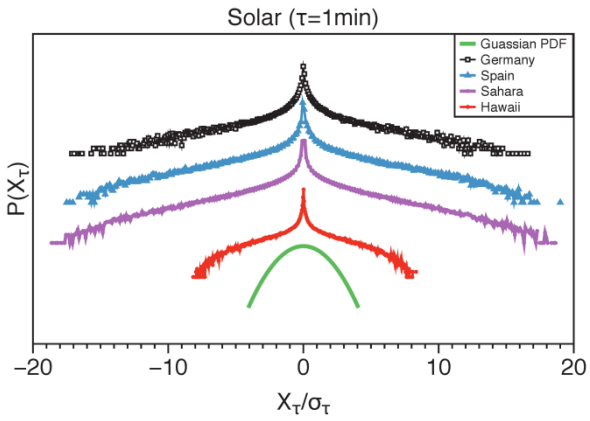

Figure 15: Probability distribution functions (PDF) of increment statistics for one minute averages of solar irradiance in several regions around the world (Hawaii, Algeria (Sahara), Spain, Germany) for an increment time lag of 1 minute. The distributions are vertically shifted for clarity, and increments X_τ are normalized to their respective standard deviations σ_τ. A Gaussian distribution with unit variance is plotted for reference. Extreme events of up to 20 σ are recorded.

To dampen the high frequency flickering from multiple distributed wind and solar power systems, we propose a time-delayed feedback method, which leads to a power feed-in time series of each system according to equation $P_i(t)^{new} = (1-\alpha)P_i(t) + \epsilon P^*(t-T)$,(15 (see Material and Methods).

The optimal parameter values can be determined from minimization of, for example, the aforementioned increment flatness. For the datasets analysed in this study, best increment flatness is obtained for time delay lags $2\,s < T < 5\,s$, while increment flatness decreases strongly with increasing α. The optimal amplification coefficient is therefore considered to be around $\alpha \approx 0.5$.

Figure 16a and b show how the flatness of increment statistics decreases from about 12.5 to about 6.5 for a wind park and an increment lag $\tau = 1\,s$, while that of 17 averaged irradiance sensors decreases from more than 120 to about 80 for the same increment lag. The larger the increment time lag, the less pronounced the effect of time delayed feedback in general becomes for both wind and solar power. The probability distributions of power increments for the aggregated wind turbines and the averaged solar sensors are plotted in Figure 16c and d, respectively, for different exemplary increment time lags. The positive suppression of strong non-Gaussian increment statistics is evident, as the time-delayed distributions are both less flat, and both possess less pronounced tails compared to their original counterparts.

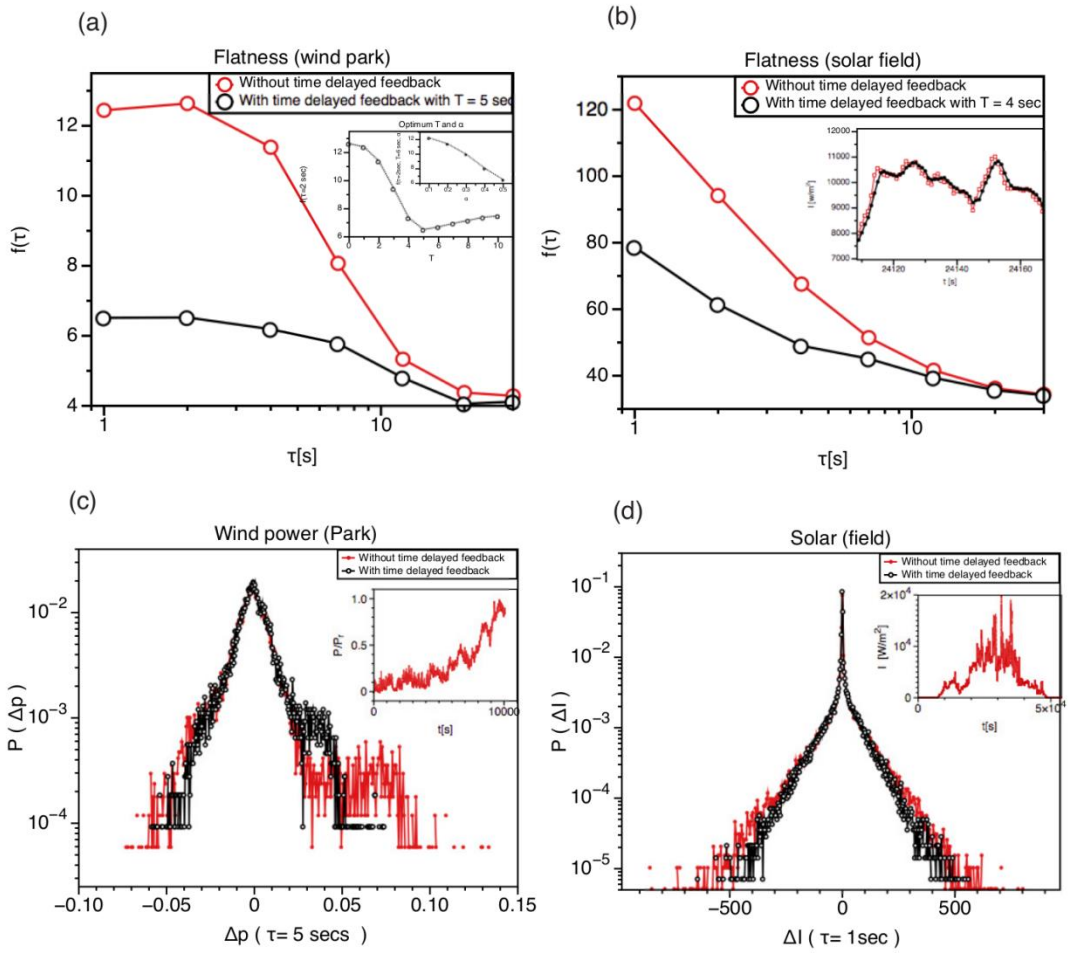

Figure 16: The results of time delayed feedback to suppress the short term flickering of wind and solar power. Panels (a-d) show characteristic changes in stochastic dynamics of aggregated wind turbines and averaged solar sensors when applying the time delayed feedback method: increment flatness (a, b) and probability distribution function of increments (c, d). The suppression of extreme fluctuations are evident in all panels. The inset of panel (a) shows the optimum values of delay lag T and amplification coefficient α of the time delayed feedback method with minimizing the flatness of a 12 turbine wind farm for an increment lag $\tau = 2\ s$. The inset of (b) shows typical variations in the average irradiance of 17 sensors deployed in a field. The time delayed output is seen to exhibit smoother dynamics than the untouched original data. The results presented in panels (a, c) are derived from 10000 s of 1 Hz data during a time interval of strong intermittent fluctuations, as shown in inset of panel (c). Panels (b, d) are based on 1 Hz data of a day with very variable cloud cover in Hawaii (03.03.2011), as shown in inset of panel (d).

4 Conclusion

In this work package, the characteristics of high frequency fluctuations in renewable power production from wind turbines and photovoltaic systems have been analysed. First, a close adherence to the well-known Kolmogorov-spectrum $S(f) \sim f^{-5/3}$ has been documented for more than an order of magnitude in the power spectra of wind velocity, wind turbine power, and solar irradiance. Then, the intermittent, non-Gaussian nature of solar irradiance and wind power fluctuations has further been proven, by means of increment statistics, to feature strong stochastic fluctuations (flickering) on time scales of seconds. Finally, a time delayed feedback method has been proposed to help suppress this very flickering in distributed power generation.

These results imply that any distribution grid with local renewable power production is essentially being fed with turbulent-like generation. The typical time scales for the associated stochastic fluctuations in wind and solar power are in the range of seconds to minutes, and the more decentralized wind or solar power systems are introduced to such a grid, the higher the magnitude

of power fluctuations will become on these critical time scales. Despite a smoothing effect when averaging, for example, several wind turbines, high frequency flickering still continues to occur with a slightly reduced probability, but a higher magnitude in absolute numbers, of course.

Therefore, statistical analyses of the kind that have been presented here yield important information that must be considered in order to guarantee an optimal design of resilient power grids. The challenge will be to fine tune the intelligent management tools, as well as technological possibilities, to achieve a stable and low cost power system that can handle the intermittent renewable sources of power efficiently. The proposed time delayed feedback method aims to contribute to reaching this goal by providing a means to suppress the most extreme short-term flickering events in wind and solar power production at source.

As a consequence of the increased complexity in the power dynamics, any central management of power grids is likely to become more and more difficult as the shares of wind and solar power increase. Any means to accommodate intermittent renewable energy sources, and to mitigate risk of grid instabilities will further increase the complexity of the existing systems, and thus, future actions have to be based on the detailed knowledge of the dynamics of the variable power feed-in. This type of research on power grid stability in the presence of stochastic renewable sources, including their extreme events, is an emerging field of science. It forms a conjunction of several, thus far disconnected fields of work and will allow for many more exciting results to come.

Work Package 5.3: Demonstration Plant for MicroGrids under Consideration of Islanding Detection

Benjamin Werther[65], Florian Pöschke[65] and Hans-Peter Beck[66]

1 Introduction

Work package 5.3 has two main focuses. Part one improves a given experimental setup to a demonstration plant for MicroGrids. The purpose of this demonstration plant is to validate the theoretical results of the work packages of WP 5.1 and WP 5.2.

Furthermore this work package deals with the detection of islanding situations in MicroGrids. This issue evolves from the on-going increase of distributed energy generation in the distribution grid. This, from the islanding point of view, can be considered as threat for the safety since the disconnectedness to the overlaid grid does not automatically ensure the volt-free state of the operating devices. On the other hand this circumstance can be considered as chance to increase the availableness of the devices in the distribution grid. Anyhow, in both of the mentioned aspects a safe and sufficient fast detection of the transition from the grid-connected to the islanding mode of the MicroGrid has to be ensured.

This work package considers several islanding detection methods, which are tested in the described demonstration plant. The effectiveness of the different methods are compared in relation to real measurements, where an islanding situation is enforced in the laboratory.

In addition different parameters for the identification of islanding situations in MicroGrids are presented. Based on the measurement of the voltage in the grid, the frequency is obtained by a phase-lock-loop. The frequency signal then is analysed with respect to the noise, which can provide information of the state of the observed grid.

2 Demonstration Plant

The task in this part of the work package, is to improve the “FEN-Multi-VISMA-GRID”, a given demonstration plant from the “Forschungsverbund Energie Niedersachsen (FEN)” [3]. In this demonstration plant (cf. Figure 17) every device is connected on one single busbar. To analyse the effect of decentralized power generation on power grids, a grid with line-elements is necessary. These line-elements have to be scalable and combinable.

[65] Clausthal University of Technology, 38678 Clausthal-Zellerfeld, Germany,
{forname.surname}@tu-clausthal.de, Institute of Electrical Power Engineering and Energy Systems
[66] Clausthal University of Technology, 38678 Clausthal-Zellerfeld, Germany,
vorsitzender@efzn.de, Institute of Electrical Power Engineering and Energy Systems

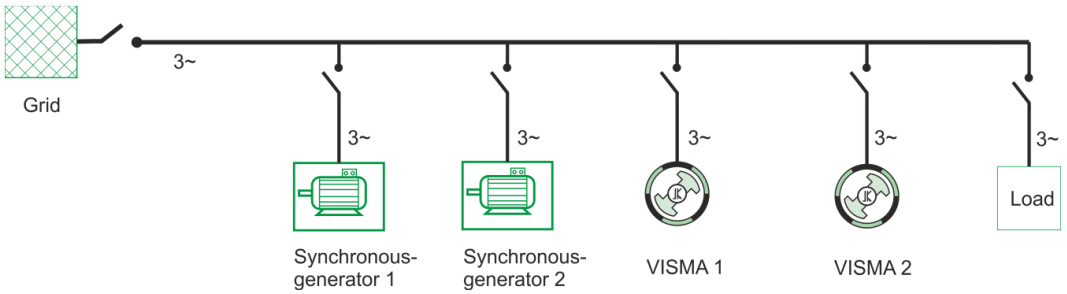

Figure 17: realisation of the "FEN-Multi-VISMA-GRID"

It has been also added a central measurement system, to measure every line current and node voltage with the same timestamp.

Figure 18 shows a possible example realization, in description from WP 5.1 and WP 5.2 can be other realizations of the micro grid found.

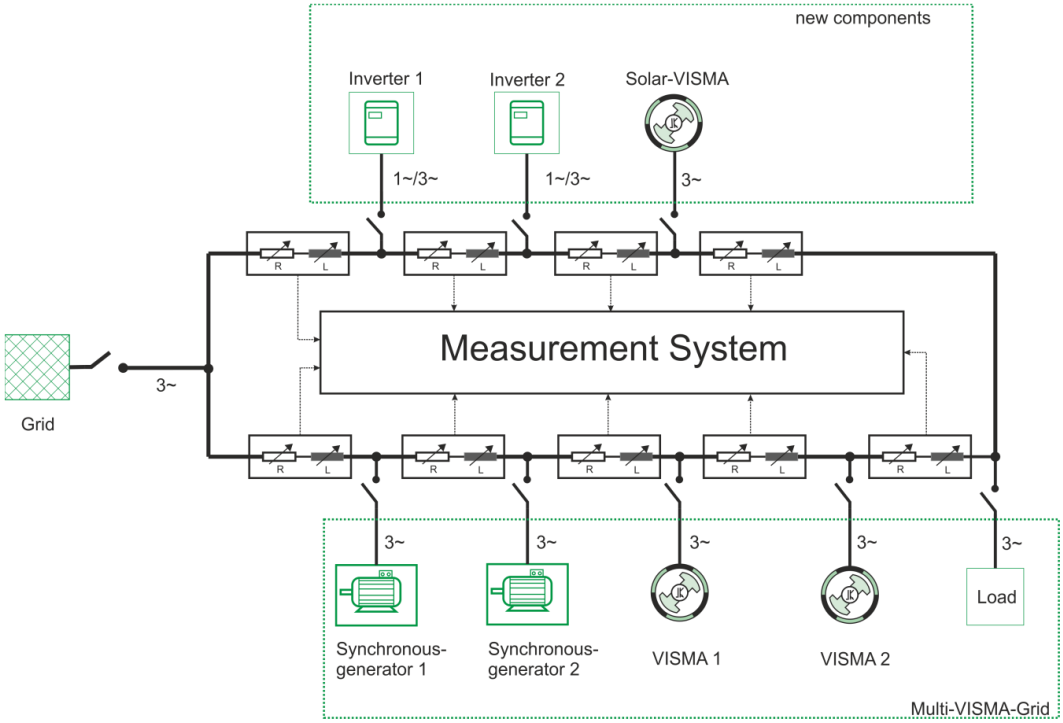

Figure 18: Scheme of a possible realisation of the demonstration Plant

A schematic circut diagram of the line elements, is shown inFigure 19. Every line element is a four-wire system, each wire has three switchable resistive and three switchable inductive elements.

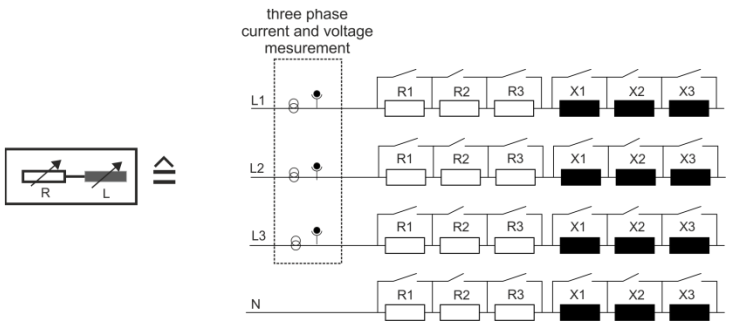

Figure 19: circuit diagram of a line element

3 Parameter of the Line Elements

The choice of the line elements is based on real data of typical cables, which are used in low voltage distribution grids. In Table 2 parameter for different typical used cable of the low voltage grid are shown. The line-elements should have a R/X-ratio between 1- 15. In low voltage grids the typical line length is below 1 km and typical impedances are below 0.1 Ω. For an effect on the voltage over the line elements, by small impedances like this, big currents are necessary. For this reason every current is scaled by 1:10, by a voltage scaling factor 1:1. As a result the power is ten times smaller compared to real distribution grids having the same voltage droop in the demonstration plan.

Type	**R' in Ω/km**	**X' in Ω/km**	**R/X**
16 mm² CU	1.15	0.077	14.9
150 mm² AL	0.206	0.068	3.0
240 mm² CU	0.078	0.067	1.2

Table 2: Parameter of typical lines in low voltage grids

This is realized with the following parameters (see Table 2). In Figure 20 is the voltage droop over an in lab-scale ectypal 150 mm² AL line shown.

R_1	0.50 Ω	**L_1**	433 µH
R_2	0.24 Ω	**L_2**	216 µH
R_3	0.10 Ω	**L_3**	108 µH

Table 3: Parameter of typical lines in low voltage grids

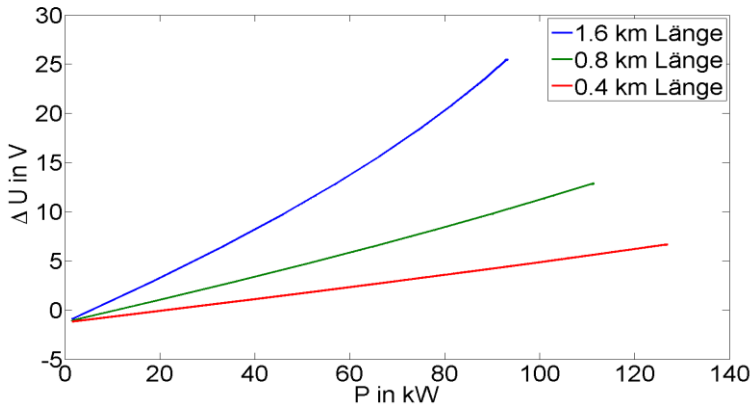

Figure 20: Voltage droop over line elements with represented a 150 mm² AL line with different length

4 Measurement System

The choice of the measurement system is based on the identified requirements.

Resolution in Bit	Resolution in V
8	3.125
12	0.2
16	12.2 m
18	3.05 m

Table 4: Voltage resolution in dependency of the ADC resolution

Each line element requires six measurements, and with eight elements, that implies that minimum 48 channels are needed for a full measurement. In the EN 61000-2-2 are compatibility levels to the 50th harmonic (2.5 kHz) specified. To analyse up to this harmonic level is from theoretical point of view a sampling rate more than 5 kHz per channel necessary. From a practical point of view, 25 kHz per channel are necessary. The maximum ratings of the instantaneous voltage are ±400 V, with a voltage converter with this maximum rating the voltage resolution in dependency of the resolution of the ADC-card (Analog Digital Converter) can be found in Table 4. In this table it can be seen that a resolution of 16 bit at least, because a discretisation error of 0.2 volts (at 12 bit) not being acceptable.

A measurement system which was chosen and fulfils this specification is a NI-PXe-1073 chassis with three NI PXIe-6363 ADC-cards. A NI PXIe-6363 is a 16 bit ADC-Card with 16 differential channels and cumulative sampling rate of 2 MS/s. This involve that the maximum resolution with 48 channels is 128 kHz, if a higher resolution is needed the number of the used channels has to be reduced, till the maximum sampling rate is 2 MHz.

5 Islanding Detection

The steadily increasing percentage of decentralized energy generation in distribution grids leads to new challenges concerning safety issues. Protection concepts of humans and operating devices have to be reviewed. This tendency evolves from the fact of a change in the direction of the power flow in electrical grids, cf. Figure 22. In the past massive power plants, which are connected to the high voltage level of the electric transmission system, delivered the energy for the underlying parts

of the electrical grid. Furthermore the power plants were responsible for the stable operation of the grid, achieved by spinning reserve, primary and secondary control of the plants. Since the decentralized energy resources (DER) have to contribute to the global stability of the grid, control mechanism are included in the design of decentralized energy conversion systems. Thus the likeliness of a formation of a stable grid without connection to the overlying high voltages level is increased.

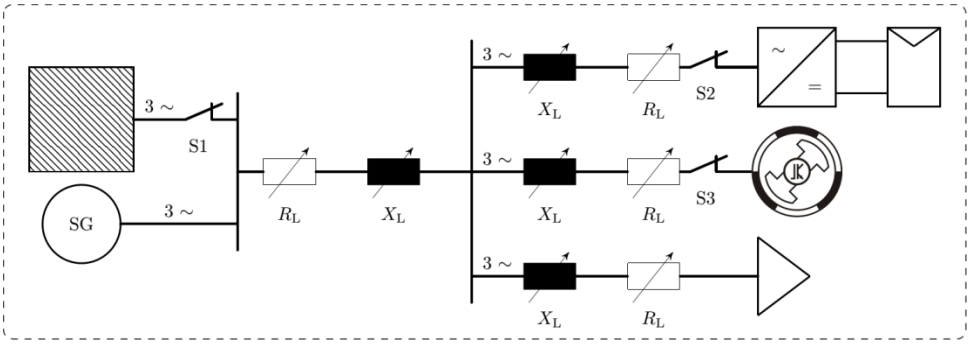

Figure 21: Grid structure islanding

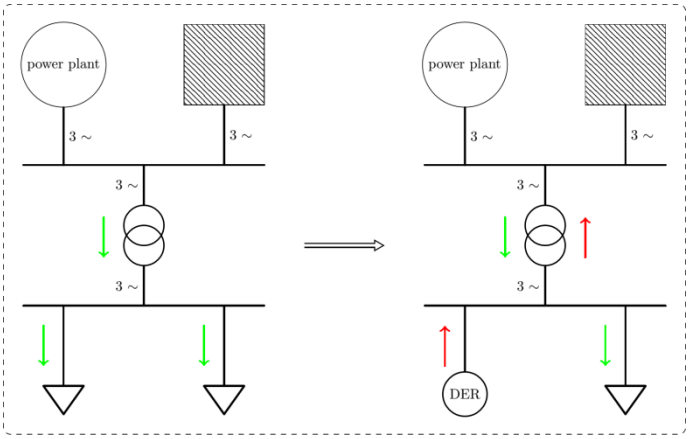

Figure 22: Changing direction of the powerflow resulting from DER

On the other hand the high percentage of energy delivered by decentralized resources leads to the possibility of increasing the availability in MicroGrids, especially in combination with energy storage systems. In case of an islanding situation, the control strategy of the conversion systems, either the ones for the decentralized resources or the ones for the storage systems, have to be adjusted to the new MircoGrid situation, accordingly.

However, in any of the described cases the detection of an islanding situation has to be achieved safe and sufficiently fast. There exist different concepts of the islanding detection in literature, which can be divided into passive and active methods [1]. Since the tested islanding detection methods will be compared to the here presented method based on the noise of the frequency signal and passive methods have no influence on the quality of the electrical power supply of loads, only passive methods are considered in this report.

6 Testing Islanding Detection Methods in the Demonstration Plant

Active components in MicroGrids usually watch over the frequency and voltage in the MicroGrid. The acceptable bounds for the condition of the grid are defined in [2]. The frequency range has to

fulfil $f = 50\,Hz + 4\,\%\,/{-6}\,\%$ for 100 % of the time. The 10-minute average root mean square value of the voltage has to remain in the bounds of $U = U_N + 10\,\%/{-15}\,\%$ for all the time. So the violation of these bounds (especially the frequency violation) would automatically imply an islanding condition – or at least a problem of the grid itself – leading to a sage shutdown of the active components or a change in the control scheme. Especially the frequency is compared to the voltage, a global quantity being very stiff because of the wide spread leverage of the frequency all over the transmission grid. The voltage can be altered depending on the point of measurement throughout the considered MicroGrid and the power consumption/generation of the concerned operating device. Since there can be active components in the MicroGrid, which are parameterised to support the stable operation of the grid, the detection of a stable MicroGrid can become quiet challenging and might not be separated from the grid-connected operation.

Figure 21 shows the structure of the demonstration plant for the islanding measurements. The active components on the grid are represented by the virtual synchronous machine (VISMA) connected to the grid by the switch S3, an inverter fed by a battery stack connected by S2 and a synchronous machine (SG), which is directly mounted to the bus of the overlying grid. Opening the switch S1 leads to an islanding of the MicroGrid. Depending on the structure of the grid, the chosen parameters of the active components and the load a stable - in terms of voltage/frequency limitations - MicroGrid in islanding mode can be achieved.

The synchronous generator is driven by an asynchronous machine fed by a frequency inverter. The inverter can be parameterized, so a frequency dependent control is achieved. The possibly alterable control properties are the proportional gain k_P and the integration time constant T_i. The behaviour of VISMA can be – as described in WP 5.1 – be altered through the quantities of k_d, T_d and J. The inverter used in the islanding experiment has a droop speed control k_f to support the necessary power generation to stabilize the grid.

In Figure 23 a measurement for the islanding of the presented MicroGrid can be seen. The measurement of the three voltages and currents are captured in three different locations in the grid. The black lines represent the measurement at the load, the green line shows the measurement at the inverter and the black line considers the state at the bus with the overlying grid (until islanding occurs) and the synchronous machine. As can be seen in Figure 23 a violation of the boundaries of frequency and voltage did not occur, even though the islanding operation was enforced at $t \approx 7\,s$. The inverter with speed droop control starts feeding in power as a result from the decrease of frequency, leading to a stabilisation of the grid. As can be seen in Figure 23 the frequency and the root mean square voltage remain in the defined bounds. Consequently the monitoring of these quantities are not sufficient to identify an islanding situation. The measurements can be used to create other signals indicating an islanding condition. Figure 23 takes the distortion, which includes all frequencies with a magnitude above 2 V (to exclude the measurement noise), the rate of change of Voltage $\frac{dU_{eff}}{dt}$ and the rate of change of power $\frac{dP}{dt}$ into account. The voltage can be viewed as a vector with phase, magnitude and frequency. The islanding results in a change of this vector, which can be seen in the frequency, magnitude (here rms-value), angular acceleration (rate of change of frequency) and the phase. Anyhow this event occurs only once and might not be distinguished from a change of load, whereas the distortion shows a permanent change and thus indicates the islanding situation.

Parameter	Quantity
k_P	3
T_i	0.5 s
k_f	1000 W/Hz
load	3400 W

Table 5: Parameter for stable islanding

Table 5 shows the Parameters used for this stable operation of the MicroGrid. The switch S3 was opened in this particular measurement; anyhow a stable islanding operation can also achieved by the use of the VISMA in different experiments.

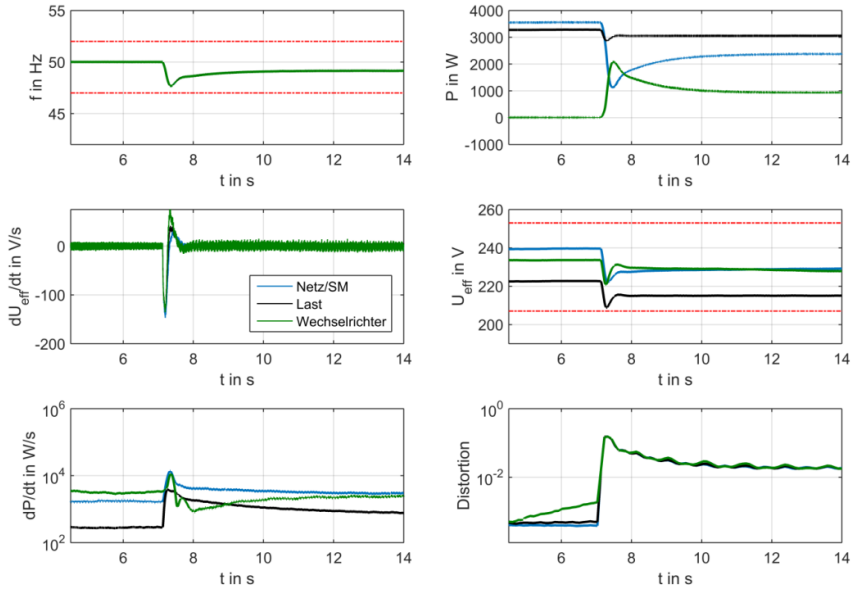

Figure 23: Measurement Islanding of the MicroGrid

7 Islanding Detection Based on the Frequency Dynamics

As shown in Figure 23, the dynamics of the voltage vector change due to the altered operation in islanding mode. Through the use of a phase locked loop the frequency signal can be obtained. It can be observed, that in islanding situation the statistical parameters of the frequency signal changes. One of the parameters, which showed a good level of identification of the grid situation, was the sum of the squares of differences in the frequency signal, defined by equation (16).

$$\boldsymbol{SQD}(\mathbf{n}) = \sum_{\boldsymbol{i=1}}^{\mathbf{n-1}} (\boldsymbol{f}(\boldsymbol{i}) - \boldsymbol{f}(\boldsymbol{i}+\mathbf{1}))^{\mathbf{2}} \tag{16}$$

This identification is based on the idea of a very large amount of switching loads and generators in the global grid, which directly influences the frequency in a very short time scale. Thus the frequency signal is used to generate the SQD for n discrete measured points. The number of the measured points in combination with the sample time defines the identification time.

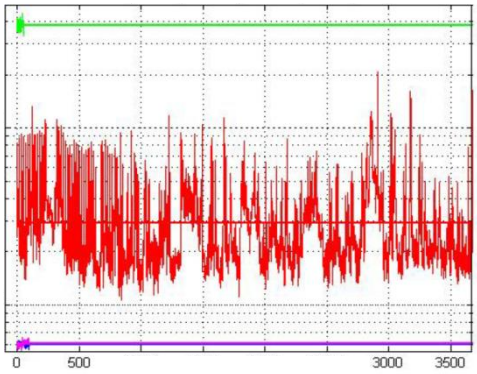

Figure 24: SQD of different devices, green: VISMA, red: grid; purple/blue: synchronous machine

Especially the possibility of identification of the participating utilities leads to the islanding detection. It can be shown, that different participants show a very unique level of SQD, when being active in the MicroGrid. When the overlying grid is considered as a component, cf. Figure 21, the high number of loads of the overall grid affect the frequency signal in a unique way, compared to other devices like the synchronous machine or the VISMA. In Figure 24 the measurement of the SQD for different devices are shown. The green line shows the SQD for a grid, where only the VISMA is active. The red lines represent the grid connected operation of the MicroGrid, whereas the purple/blue lines show a grid driven by synchronous machines.

Some facts are important for the design of SQD generation. First of all the dynamics of the frequency signal depends on the parameters of the used phase-locked-loop (PLL). On the other hand the frequency is filtered through a high pass before forwarded to the PLL, since the slowly changing components (ca. seconds - minutes) do not the affect the SQD signal, which has a high dependence on the sample time of the measurement.

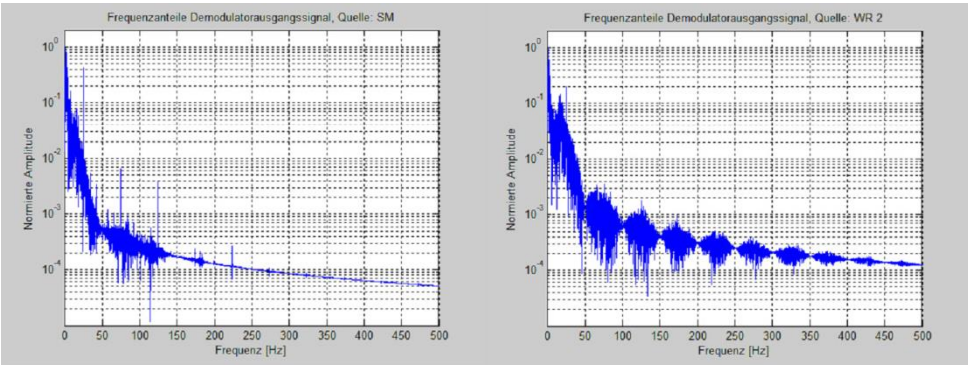

Figure 25: Frequency dependent magnitude of different generators

Furthermore this method can be improved by the use of frequency dependent analysis. It can be shown, that the frequency demodulated signal (by the use of a PLL) behaves unique dependent on the investigated frequency bounds. Figure 25 shows the frequency dependent magnitudes of a synchronous machine (SM) on the left side and 3-phase inverter (WR2) on the right side of the figure. Using this knowledge, the generation of the SQD can be specified in certain bounds, cf

Figure 26. It shows the analysed SQD for different generators (SM=synchronous machine, Netz=grid, WR1/2/3=inverter) from a frequency of f=400 Hz upwards.

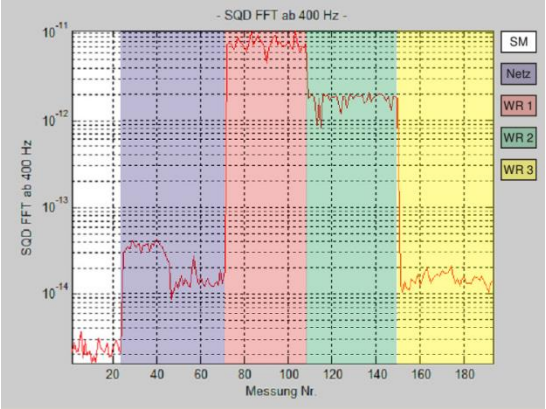

Figure 26: SQD, frequency sensitive from a frequency f=400 Hz

8 Conclusion

Parameters of a VISMA have been optimized to get a desired behaviour of the output power. The simulated and the measured results from the laboratory agree well for an optimal parameter setting. In an extension, a MicroGrid has been optimized with respect to the parameters of a VISMA which is part of the MicroGrid. First results show that with the change of the two free parameters in the cost functional the focus of the optimization can be changed. In the future, one should think of a optimization method from statistical physics to find global minima more likely than with the simple Downhill-Simplex method. A concept for distributed frequency control for MicroGrids has been presented and validated via simulations. In this set-up, three VISMA-controlled inverters communicate with each other to restore an original load sharing. This works well and also the frequencies of the VISMAs could be harmonized. The characterization of very resilient network topologies has been done for two different models. For these models, resilient networks have many edges and a small diameter. A third model which deals with the "maximum-disturbance" stability could be considered for investigation.

An optimization method to use less free parameters of the decentralize devices to get in sum the desired behaviour in the grid is confirmed. Also a method to investigate the influence of topologies of grids on different stability measures was developing.

A decentralized frequency controller for island mode with a zero steady-state error and projectable load sharing was elaborated. In case of a stable island mode, it's important to detect the situation. Because the control strategies has to change or for safety reasons devices had to been shut down.

As the characteristics of high frequency variability in decentralized power production from wind turbines and photovoltaic systems are shown to be turbulent-like, with non-Gaussian increment statistics, distribution grids need to be prepared for an increasing amount of intermittent power feed-in. The frequent occurrence of strong stochastic fluctuations (flickering) in the renewables calls for new measures, like the proposed time delayed feedback method, to be developed and implemented in future MicroGrids in order to ensure stability in voltage and frequency, and to guarantee the meeting of power demand. These tasks will become more urgent and more challenging, the higher the shares of decentralized wind and solar power become.

Islanding detection methods and their applicability in MicroGrids was tested. It could be shown that methods which are based on off-limit conditions had no reliable results. The procedures which carry out a continuous assessment of the state variables seem more useful.

A demonstration plant for MicroGrids was build up. The purpose of this demonstration plant was to validate the theoretical results of the work, and it is available for further research activities.

References

[1] W. Bower, M. Ropp, "Evaluation of Islanding Detection Methods for Utility-Interactive Inverters in Photovoltaic Systems," Sandia National Laboratories, Albuquerque, New Mexico 87185, 2002.

[2] Voltage characteristics of electricity supplied by public distribution networks; German version EN 50160:2010+Cor.:2010.

[3] Y. Chen, R. Hesse, D. Turschner, H.-P. Beck, "Untersuchungen an der VISMA (TP 11), Forschungsverbund Energie Niedersachsen Abschlussbericht," Braunschweig 2012. ISBN: 978-3-925268-45-8.

[4] Y. Chen, R. Hesse, D. Turschner, H.-P. Beck, "Investigation of the Virtual Synchronous Machine in the Island Mode," 3rd IEEE PES Innovative Smart Grid Technologies Europe (ISGT Europe), Berlin, 2012.

[5] J. Nelder, R. Mead, "A Simplex method for function minimization," Computer Journal 7, 308 (1965)

[6] K. Hukushima, K. Nemoto, "Exchange monte carlo method and application to spin glass simulations," J. Phys. Soc. Jpn., 65:1604 (1996).

[7] W. Heins, T. Dewenter, A. K. Hartmann, C. Bohn, "Parameter optimization of a virtual synchronous machine in a MicroGrid," in preparation.

[8] J. W. Simpson-Porco, F. Dörfler, F. Bullo, "Synchronization and power sharing for droop-controlled inverters in islanded microgrids," in Automatica 49 (2013), Nr. 9, pp. 2603–2611.

[9] T. Dewenter, B. Werther, A. K. Hartmann, H.-P. Beck, "Optimierung des dynamischen Verhaltens netzstützender Anlagen am Beispiel der Virtuellen Synchronmaschine," Graz/Austria, 12.-14. Februar 2014, 13. Symposium Energieinnovation.

[10] A. K. Hartmann, "Sampling rare events: Statistics of local sequence alignments," Phys. Rev. E, 65, 056102 (2002).

[11] A. K. Hartmann, "Large-deviation properties of resilience of transportation networks," Eur. Phys. J B 87, 114 (2014).

[12] T. Dewenter, A. K. Hartmann, "Large-deviation properties of resilience of power grids," New J. Phys. 17, 015005 (2015).

[13] A. K. Hartmann, B. Werther, W. Heins, T. Dewenter, "Large-deviation study of the maximum-disturbance stability of power grids," in preparation.

[14] E. J. Davison, E. M. Kurak, "A Computational Method for Determining Quadratic Lyapunov Functions for Non-linear Systems," Automatica, Vol. 7, pp. 627-636. Pergamon Press, 1971.

[15] J. Carrasco, L. Franquelo, J. Bialasiewicz, E. Galvan, R. Guisado, M. Prats, J. Leon, N. Moreno-Alfonso, "Power-electronic systems for the grid integration of renewable energy sources: A survey," Industrial Electronics, IEEE Transactions on, vol. 53, no. 4, pp. 1002–1016, Jun. 2006.

[16] L. von Bremen, "Large-scale variability of weather dependent renewable energy sources," in Management of weather and climate risk in the energy industry. Springer, 2010, pp. 189–206.

[17] F. Blaabjerg, Z. Chen and S. B. Kjaer, "Power electronics as efficient interface in dispersed power generation systems," Power Electronics, IEEE Transactions on 19 1184, 2004.

[18] J. Marcos, O. Storkel, L. Marroyo, M. Garcia, E. Lorenzo, "Storage requirements for PV power ramp-rate control," Solar Energy 99, 28, 2014.

[19] J. Marcos, I. de la Parra, M. Garcia, L. Marroyo, "Control Strategies to Smooth Short-Term Power Fluctuations in Large Photovoltaic Plants Using Battery Storage Systems," Energies 7, 6593, 2014.

[20] M. Fontoynont, et al., "Satellight: a WWW server which provides high quality daylight and solar radiation data for Western and Central Europe." Proceedings of the 9th Conference on Satellite Meteorology and Oceanography. No. 2, 1998.

[21] A. Woyte, R. Belmans, J. Nijs, "Fluctuations in instantaneous clearness index: Analysis and statistics," Solar Energy 81, 195, 2007.

[22] M. Amin, "Energy: The smart-grid solution," Nature, 499, 145, 2013.

[23] P. Milan, M. Wächter, J. Peinke, "Turbulent Character of Wind Energy," Phys. Rev. Lett., 110, 138701, 2013.

[24] A. Nieße, M. Tröschel, M. Sonnenschein, "Designing dependable and sustainable Smart Grids -How to apply Algorithm Engineering to distributed control in power systems," Environmental Modelling & Software 56, 37, 2014.

[25] R. Baldick, et al., "Initial review of methods for cascading failure analysis in electric power transmission systems," IEEE PES CAMS task force on understanding, prediction, mitigation and restoration of cascading failures, IEEE Power Engineering Society General Meeting, 10142341, 1, 2008.

[26] B. A. Carreras, V. E. Lynch, M. L. Sachtjen, I. Dobson, D. E. Newman, "Modeling Blackout Dynamics in Power Transmission Networks," Hawaii International Conference on System Sciences, January 3-6, Maui, Hawaii, 2001.

[27] I. Dobson, B. A. Carreras, V. E. Lynch, D. E. Newman, "Complex systems analysis of series of blackouts: cascading failure, critical points, and self organization," Chaos, 17(2), 026103, 2007.

[28] G. Nicolis, I. Prigogine, "Exploring Complexity," W. H. Freeman, San Francisco, 1989.

[29] B. A. Carreras, D. E. Newman, I. Dobson, A. B. Poole, "Evidence for self-organized criticality in a time series of electric power system blackouts," IEEE Trans. Circuits & Systems I 51, 1733, 2004.

[30] M. Rohden, A. Sorge, M. Timme and D. Witthaut (2012) Self-Organized Synchronization in Decentralized Power Grids, Phys. Rev. Lett. 109, 064101.

[31] D. Witthaut, M. Timme, "Braess's paradox in oscillator networks, desynchronization and power outage," New J. Phys. 14, 083036, 2012.

[32] M. Chertkov, M. Stepanov, F. Pan, R. Baldick, "Exact and Efficient Algorithm to Discover Extreme Stochastic Events in Wind Generation over Transmission Power Grids," 2011.

[33] J. Heitzig, N. Fujiwara, K. Aihara, J. Kurths, "Interdisciplinary challenges in the study of power grid resilience and stability and their relation to extreme weather events," in Eur. Phys. J. Special Topics 223(12), 2281, 2014.

[34] C. Kamath, "Understanding wind ramp events through analysis of historical data," in Transmission and Distribution Conference and Exposition, IEEE PES,1, 2010.

[35] H. Haken, "Advanced Synergetics, Instability hierarchies and self-organizing systems and devices," Springer, Berlin, 1983.

[36] R. Friedrich, J. Peinke, M. Sahimi, M. R. Rahimi Tabar, "Approaching complexity by stochastic methods: From biological systems to turbulence," Phys. Rep. 506, 87, 2011.

[37] C. Nicolis, V. Balakrishnan, G. Nicolis, "Extreme Events in Deterministic Dynamical Systems," Phys. Rev. Lett. 97, 210602, 2006.

[38] Extreme Events in Nature and Society, Edited by: S. Albeverio, V. Jentsch & H. Kantz (2006) Springer, Berlin.

[39] H. Farhangi, "The Path of the Smart Grid," IEEE Power and Energy Magazine 8, 18, 2010.

[40] H. Kanchev, D. Lu, F. Colas, V. Lazarov, B. Francois, "Energy Management and Operational Planning of a Microgrid With a PV-Based Active Generator for Smart Grid Applications," IEEE Transactions on Industrial Electronics 58, 4583, 2011.

[41] H. Haken, "Synergetics: Introduction and Advanced Topics," Springer, Berlin, 2004.

[42] S. V. Buldyrev, R. Parshani, G. Paul, H. E. Stanley, S. Havlin, "Catastrophic cascade of failures in interdependent networks," Nature 464, 1025, 2010.

[43] P. J. Menck, J. Heitzig, N. Marwan, J. Kurths, "How basin stability complements the linear-stability paradigm," Nature Physics 9, 89, 2013.

[44] P. Menck, J. Heitzig, J. Kurths, H. J. Schellnhuber, "How dead ends undermine power grid stability," Nat. Commun. 5, 3969, 2014.

[45] R. Perez, T. Hoff, J. Dise, D. Chalmers, S. Kivalov, "The cost of mitigating short-term PV output variability," Energy Procedia 57 755, 2014.

[46] A. Engler, "Applicability of droops in low voltage grids," International Journal of Distributed Energy Resources, Vol 1, No 1, 2005.

[47] P. Kundur, N. J. Balu, M. G. Lauby, "Power system stability and control," McGraw-Hill: New York, 1994.

[48] W. Heins, C. Bohn, "Distributed frequency control in MicroGrids based on the virtual synchronous machine," in preparation.

Sub-Project Six:
SmartSpatial

SmartSpatial

Claudia Palmas[67], Almut Siewert[67], Francesca Dossola[67], Christina von Haaren[67] and Michael Rode[67]

Abstract

In the context of energy transition, Germany's political agenda on renewable power usage aims at further expansion of decentralized energy production, in a large scale. However, the large-scale installation and utilization of decentralized renewable energy technologies necessitates relevant changes of all sectors of energy use and the transformation of the energy system. These changes can lead to negative impacts on the landscape and such expansion is often accompanied by land use conflicts and environmental sensitivity due to disturbance. Moreover, a chaotic development of renewable energy (RE) can exacerbate conflicts with residents, nature conservation, tourism interests, and food production. Therefore, rational approaches to spatial planning are needed for a sustainable allocation of renewable energy systems. In SP 6 we develop a smart and spatial model (SmartSpatial) in order to identify the most suitable areas for decentralized RE generation, which can be integrated into smart and in particular into micro grids [SP 1-5]. SmartSpatial is based on a spatial multi-criterial methodological framework for RE siting. It follows the objectives of sustainability by simultaneously maximizing spatial efficiency and minimizing the environmental impacts of RE production. The model supports decisions on regional RE target setting and siting by combining the spatial efficiency of using the RE potential and projected environmental impacts. Methodologically, the model combines RE-potential analysis with an ecological impact analysis, which is specified for different RE specific pressure factors. Firstly, we estimate different GIS-based theoretical energy potentials (wind, solar, and biomass), whereby the mapping estimation depends only on the geophysical properties of the landscape. Accordingly, we develop a raster data-set to estimate the technical energy potentials by including the technical requirements of the different power plants [WP 6.1]. In order to exclude unsuitable areas, we identify institutional based (legally) and recommended (in the practice considered) restriction areas. In parallel, on the basis of regional data about environmental values and sensitivities to typical pressures caused by RE-production, a map of spatially differentiated degrees of environmental trade-offs is produced for a region [WP 6.2]. Finally, we overlay the three GIS-based outcomes (layers) in order to compare the specific and combined energy production by developing different scenarios for identifying suitable and conflict areas for RE-development [WP 6.3]. These outcomes are compared with the actual decision-space for RE-development and the political RE energy targets. This approach supports participative and more transparent regional planning and decision processes in order to find the most environmental sustainable options of RE-development with the highest energy potentials in a given region. Furthermore, due to the high model's feasibility, local preferences can be integrated into site selections for RE expansions. The possibility to test different scenarios as well as the transparency of trade-offs between energy output and the environment, make the model a suitable instrument for decision processes of municipalities and the public on the regional or higher decision levels. The model is tested in the Hanover region in Lower Saxony, but could be also applicable in other German or European regions if it were to be slightly adjusted according to the availability of local data.

1 Introduction

In the context of energy transition, the political agenda in Germany regarding renewable power usage intends to increase the share of renewable energy (RE) in final electricity consumption to at least 80 % by 2050 [1]. However, the large-scale installation and utilization of decentralized renewable energy technologies compels relevant changes be made to all sectors of energy use and the transformation of the energy system. The energy system is currently changing from "energy for

[67] Leibniz Universität Hannover, 30149 Hanover, Germany,
{surname}@umwelt.uni-hannover.de, Institute of Environmental Planning

space" to "energy from space" [2]. These changes can lead to negative impacts on the landscape as expansion is often accompanied by land use conflicts and environmental sensitivities to disturbance [3], [4], [5], [6], [7]. Moreover, a chaotic development of renewable energy (RE), especially due to the initial largely unregulated implementation of the different types of RE facilities, can exacerbate conflicts with residents, nature conservation, tourism interest and food production [8], [9], [10]. Consequently, public protests against wind power plants, electricity grids, or increases in maize cultivation are, in spite of the German public, largely supported Transformation of the Energy System ("Energiewende") and have become common in many regions [11], [12], [13], [14]. Even though many regions have set themselves ambitious RE production targets, current planning practice do not yet include an integrated analysis of RE production and an effective evaluation of energy-related land-use issues. However, sectorial approaches are not sufficient when dealing with the aforementioned issues [8], [10], [15], [16]. Instead, it is necessary to estimate GIS-based RE-potentials, as input data for decentralized RE generation [17], [18], and to minimize the land consumption for RE production on the regional and local scale [10], [15], [16], [19]. This can be achieved by the optimal exploitation of combined RE potentials together with a simultaneous minimization of environmental trade-offs [6], [10], [16]. Therefore, rational approaches to spatial planning are needed for decentralized RE-generation. Approaches, which can be integrated into smart and in particular, into micro grids for an intelligent energy supply by different sources [SP 1-5]. A spatial methodological framework should be further developed to integrate the objectives of decentralized energy generation, spatial energy efficiency, and sustainable landscape planning and development [16], [17], [18], [20].

2 Research Questions

In order to support regions in achieving their energy targets and an environmentally friendly way to attain decentralized RE-production in the future, we aim to answer the following research questions:

- How can the geographic distribution of different energy potentials (wind, solar, and biomass energy) be calculated on the regional scale? Which criteria and algorithms are needed for identifying the theoretical and technical energy potentials? How can RE energy mix combinations be identified? [WP 6.1]
- How can environmental values and sensitivities, opposed RE production, be integrated on the regional scale? Which methods are suitable for modelling the value of natural resources and their environmental sensitivity to disturbance? [WP 6.2]
- According to energy potential estimations and environmental assessments, how can suitable areas for RE-production be identified? Which kind of scenarios can be developed in order to support political decisions by optimizing the space energy efficiency and minimizing environmental trade-offs? [WP 6.3]
- Do the results increase the scope for decision making for RE generation in comparison to the current formal approach that is based on legal and planning standards? Do the results help to achieve the RE political regional targets by 2050? [WP 6.3]

3 Methods and Materials

We sought to solve the above research questions by developing the SmartSpatial model as a system for analysing and optimizing different RE scenarios. SmartSpatial is based on a spatial multi-criterial methodological framework for RE siting. It follows the objectives of sustainability by simultaneously maximizing the spatial efficiency and minimizing the environmental impacts of RE

production (Figure 1). Methodologically, the model combines RE-potential analysis with an ecological impact analysis, which is specified for different RE pressure factors. The model consists of three modules: a first raster data-set of GIS-based theoretical energy potentials (wind, solar, and biomass), whereby the mapping estimation depends only on geophysical properties of the landscape; and a second raster data-set of GIS-based technical energy potentials, whereby technical requirements of the different power plants are included [WP 6.1]. The second module makes assessments based on regional data environmental values and sensitivities against typical pressures caused by RE-production. Accordingly, we produce a map of spatially differentiated degrees of environmental trade-offs. In order to exclude unsuitable areas, institutional established (legally) and recommended (in the practice considered) restriction areas are identified [WP 6.2]. The third module is obtained by overlaying the three GIS-based outcomes (layers) in order to compare the specific and combined energy production. Different scenarios are developed for identifying suitable and conflict areas for RE-development [WP 6.3]. These outcomes are compared with the actual decision-space for RE-development and the political RE energy targets.

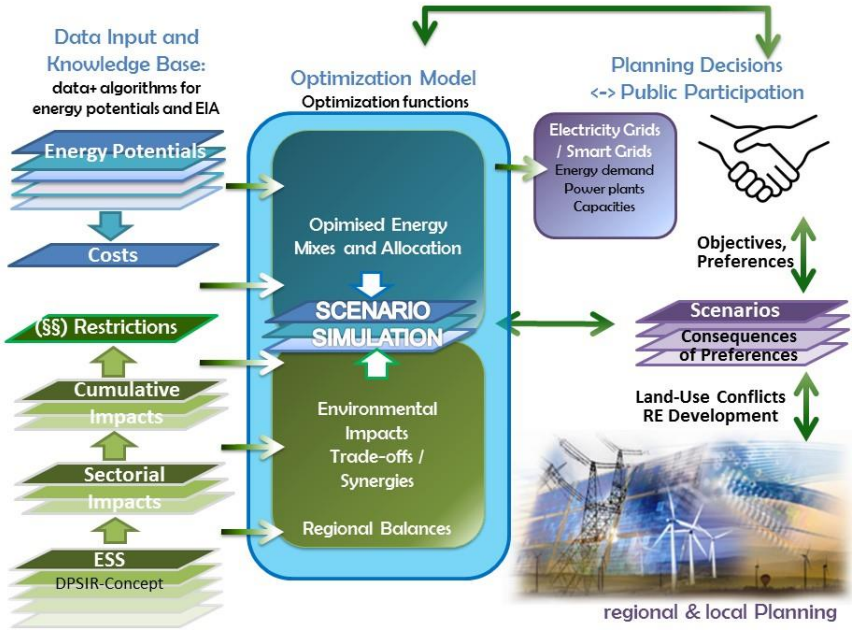

Figure 1: Methodological framework of SmartSpatial

In order to test the modules with respect to plausibility of results and their applicability under actual spatial data conditions, SmartSpatial is applied in the region of Hanover in Lower Saxony. This region is chosen as a case study area for the project, on account of the high interest and engagement in RE-development in the areas and because of the comparatively comprehensive digital geo-data attached to its recently updated regional landscape plan [21], [22].

Administratively, the region of Hanover is composed of 21 municipalities and townships spreading across 2,290 km². With Lower Saxony's capital city Hanover situated at its centre, the region is the most densely populated (496 inhabitants per km²) area within the federal state (166 inhabitants per km²) [23]. The complexity associated with the increasing urban sprawl of suburbanization, includes traffic growth and road expansions, the interests of nature conservation, agriculture and tourism, and growing RE-development. Dealing with each of these various issues contributes to the ambitious challenges facing regional planning. In fact, as a 100 % RES Region, Hanover aims to reduce GHG emissions by 95 % while cutting down on 50 % of final energy consumption [24].

3.1 Energy Potential Estimations [Work Package 6.1]

The energy potential modules refer to established methodologies [15], [18], [25], which are adapted to the information available for the regional scale [17], [18]. In order to locate and quantify the RE potential, geographical distribution potentials are modelled according to geophysical properties, for instance solar irradiation [kWh/m^2*d], wind speeds [m/s], biomass availability and distribution [t/ha]. These variables are site-specific and related to land use, latitude, altitude, climate, and terrain properties (ibid.). Furthermore, other site-specific characteristics, such as the slope, were considered to best identify suitable areas for RE-development (i.e. photovoltaics). The technical potentials are expressed as the energy yield per unit area, calculated for a year [MWh/ha*a] as well as the technical energy mix potentials.

3.2 Environmental Analysis and Restrictions [Work Package 6.2]

In addition to geographical and technical constraints, spatial, legal and in the planning practice considered restrictions are necessary to prevent an overestimation of energy potentials. For the environmental impact assessment module an extensive literature review was conducted [3], [4], [5], [6], [7], [10], [16], [20]. The results are used as a basis for the selection of different indicators and for the development of evaluation standards. These are applied in the module in order to assess sensitivity and value of objects of environmental protection. The resulting indicators and algorithms for aggregation are discussed concerning their validity in view of their foundation in literature. The environmental sensitivity analysis is compared with the current methodological approach of regional planning for locating areas for wind power plants.

3.3 Energy Scenarios Design and Modelling [Work Package 6.3]

Based on the spatial methodological framework of the described SmartSpatial model, we constructed one reference scenario and two RE-development scenarios according to different environmental trade-offs. Testing the scenarios in the Hanover region, we calculate possible RE energy yields per year [GWh/a] and the installable power [GW], which are then compared with the actual decision-space for RE-development and the political RE energy targets. The essential input data for the conducted spatial analyses were obtained from the Hanover region, the ATKIS Basis-DLM for Lower Saxony [26]. The spatial analyses were processed by ESRI ArcMap 10.2.2 and included the integrated ModelBuilder (ESRI Inc. 1999-2014). In accordance with the analyses from the other SP within the Smart Nord joint research project and the RE production targets of the test region, the presented results focus mainly on large onshore wind power plants and open-space PV power plant developments.

Table 1 shows an overview on the main data used in the sub-project SmartSpatial.

Energy potentials			
	Inputs	**Scale/unit/format**	**Sources**
Solar	Digital Terrain Model (DTM)	50 m x 50 m	State Office of geographic information and land development ("Landesamt für Geoinformation und Landentwicklung", LGLN)
	Aspect (azimuth of the solar panel)	180°	Geographic Resources Analysis Support System (GRASS GIS) manual, 2012
	Slope (solar panel inclination)	37°	GRASS GIS manual, 2012
	Linke atmospheric turbidity coefficient	3.0 - 4.2	GRASS GIS manual, 2012
	Albedo coefficient	0.2	GRASS GIS manual, 2012
	Real-sky beam radiation coefficient	0.118 - 0.62	GRASS GIS manual, 2012
	Real-sky diffuse radiation coefficient	0.86 - 5.49	GRASS GIS manual, 2012
	Day of the year	1 - 365 [d]	GRASS GIS manual, 2012
	PVGIS Database	[kWh/m²]	Photovoltaic Geographical Information System Interactive Maps (Joint Research Center of the European Commission, JRC, 2010).
Wind	Digital Terrain Model (DTM)	50 m x 50 m	State Office of geographic information and land development ("Landesamt für Geoinformation und Landentwicklung", LGLN)
	Wind speeds	[dm/s]	German Weather Service ("Deutscher Wetterdienst", DWD), 1981-2000
Biomass	Biomass (maize) yields	[t/ha]	Bauböck, Kapas, Uni Göttingen, 2012
Environmental sensitivities and values			
RE	Basic geodata	1:25,000	State Office of geographic information and land development ("Landesamt für Geoinformation und Landentwicklung", LGLN)
	Information for environmental indicators	1:50,000	Regional planning programme ("Regionales Raumordnungsprogramm", RROP), Hanover region, 2005
	Geodata on abiotic and biotic environment	1:50,000	Landscape structure plan ("Ladschaftsrahmenplan",LRP), Hanover region, 2013
	Geodata on soil charateristics	1:25,000	State Office of Mining, Energy and Geology, "Landesamt für Bergbau, Energie und Geologie", LBEG, 2015
	Environmental protected areas	1:50,000	Department for environment, energy and climate protection of Lower Saxony ("Niedersächsisches Ministeriums für Umwelt, Energie und Klimaschutz", MU)
	Priority areas for wind development and recreation areas	1:50,000	Regional plan ("Regional Plan", RP), Hanover region, 2005

Table 1: Input data for the energy potential estimation and the environmental analysis

The current restrictions for RE-development are derived from either legally binding regulations such as laws (e.g. Germany's Federal Nature Conservation Act, BNatSchG) that are referred to as hard restriction areas, or from different recommendations by official planning institutions and are referred to as soft restriction areas (Table 2 and Table 3). In the case of regulations on wind power development, we refer to the latest draft of the Wind Energy Decree, produced by the federal state of Lower Saxony ("Windenergieerlass") [28].

Area Categories		Wind Power	PV Plants	Energy Maize	Legal Basis
Building areas	Residential areas	hard	-	hard	§5 BlmSchG; §35 BauGB
	400 m residential area's buffer zone	hard	-	-	§5 BlmSchG; §35 BauGB
	Commercial and industrial areas	hard	-	-	§5 BlmSchG; §35 BauGB
	400 m commercial and industrial area's buffer zone	hard	-	-	§5 BlmSchG; §35 BauGB
Infrastructures	Motorways, 30 m		hard	-	§35 BauGB
	40 m motorway's buffer zone	hard	-	-	§9 FStrG; §24 NStrG
	Federal roads, 16 m		hard	-	§35 BauGB
	20 m federal road's buffer zone	hard	-	-	§9 FStrG; §24 NStrG
	Overhead power lines, 31m	hard	-	-	DIN EN 50341-3-5
	82 m overhead power line's buffer zone	hard	-	-	DIN EN 50341-3-5
Water and soil	(all) Water surfaces	-	-	hard	-
	Main watercourses, 50 m buffer zone	hard	-	-	§61 BNatSchG
	Flood hazard areas	hard	hard	-	§78 WHG; §35 BauGB
	Slopes >21 %	-	soft	-	-
	Areas of high water erosion pot.	-	-	soft	-
	Areas of high wind erosion pot.	-	-	soft	-

Table 2: A general overview on the restriction areas for RE-development; - = no restrictions and legal basis [16], [27] - [30]

Area Categories		Wind Power	PV Plants	Energy Maize	Legal Basis
Protected areas	Nature conservation areas	hard	hard	hard	§23 BNatSchG
	EU-Special Protection Areas (SPA)	hard	soft	soft	§31 BNatSchG
	Protected biotopes	hard	hard	hard	§30 BNatSchG
	Protected landscape units	hard	hard	hard	§28, §29 BNatSchG
	Drinking water protection areas (zone I and II)	hard	-	hard	§51 WHG
	Drinking water protection areas (zone III)	-	-	soft	-
	Landscape conservation areas	soft	soft	-	-
	Special areas of conservation (FFH)	soft	soft	soft	-
Biodiversity, flora and fauna	Faunisic habitats (values 4 and 5)	-	soft	soft	-
	Migratory bird resting areas (values 3-5)	soft	soft	soft	-
	Wetlands of international importance	soft	soft	soft	-
	Breeding bird habitats (values 3-5)	soft	-	-	-
	Bat habitats	soft	-	-	-
	Areas of special importance für species and ecosystems	-	soft	-	-
	Forests	soft	soft	soft	-
	Green belts and infrastructures	-	soft	-	-
Landscape	Landscape units of special importance	soft	soft	soft	-
	Landscape of special structural diversity	-	soft	-	-
	Areas of historical-cultural importance	-	soft	-	-

Table 3: A general overview on the restriction areas for RE-development; - = no restrictions and legal basis [16], [27] - [30]

4 Renewable Energy Potentials [Work Package 6.1]

Based on the geo-physical properties, we estimate theoretical RE potentials for wind power, solar power, and biomass cultivation for the production of biogas. Subsequently, by taking into account the technical requirements, we develop different GIS-based raster data-sets in order to compare and combine different energy yields (Figure 2). These results are used as input-data to model energy RE-development scenarios for the Hanover region.

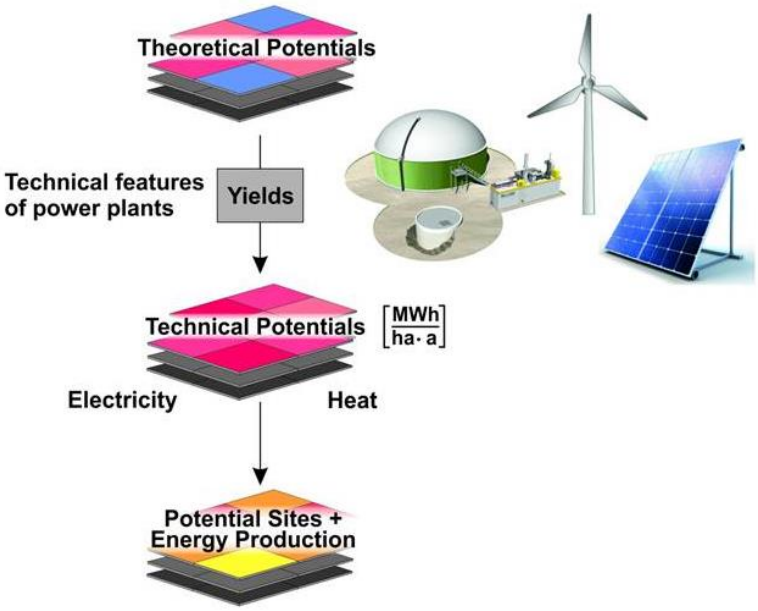

Figure 2: General methodological procedure for identifying preliminary scenarios for RE-development according to GIS-based RE-potentials

5 Spatial Wind Energy Potential

Theoretical wind energy potentials are estimated by processing data on average annual wind speeds derived from the German Weather Service ("Deutscher Wetterdienst", DWD). These input data from DWD for the reference period 1981 to 2000 exhibit wind speeds at 10m height above ground at a 200m resolution. These data were already processed taking into account roughness (from relief and land characteristics), height above sea level, as well as geographical location. Differences between calculated and measured wind speeds are quoted ± 0.15. We further processed these input data by firstly downscaling on a Digital Terrain Model, DTM (50), and secondly calculating wind speeds at the heights of 65, 100, 140, and 180 m. For the further analyses, we used a wind speed at the height of 100 m, accounting for wind power plants of current technical standard. The increases of wind speed at the different heights are calculated by equation 1 (Eq.1). Underlying assumption is that the atmosphere thermic condition is stable, which is expressed by the empirically derived coefficient α at a value of α = 0.143 [31], [32].

(Eq.1) $$v = v_{ref} (z / z_{ref})^{\alpha}$$

Where:

v: wind speed at height z above ground level;

v_{ref}: reference speed, i.e. a wind speed we already know at height z_{ref};

z: height above ground level for the desired velocity, v;

z_{ref}: reference height, i.e. the height where the wind speed is measured v_{ref}.

In order to obtain the wind technical energy potential expressed in energy yields per unit area, calculated for a year [MWh/ha], we take into account a "standard" wind turbine with an installable power of 3 MW. For each installed turbine, an average distance of about 300 m is needed. Therefore, we consider for the calculation, a grid of 300 m × 300 m. The fundament of each turbine occupies a raster cell of approximately 20 m × 20 m. We excluded a buffer zone of about 90,000 m^2 around each wind turbine which cannot be occupied by other wind turbines. Energy

yields vary according to average wind speeds distribution for each cell throughout the region. Due to data unavailability, we do not take into account the wind speeds variability on the region.

5.1 Spatial Solar Energy Potential

Theoretical solar energy potentials are estimated on the basis of a DTM (50) in raster map format. For this purpose, the open-source solar radiation tools *r.sun* solar radiation model, implemented in GRASS GIS (6.4.2) and the PVGIS CM-SAF estimation utility are used [33]. The calculation of the solar radiation for specific sites is based on data taken from the PVGIS database, which includes the crucial influencing factor of sky cloud coverage, with a stated overall error of approximately 5 % for an entire year [18]. Clear sky indexes are estimated by the JRC [34]. As an approximation, the assumption was made that albedo and Linke turbidity are constant during each month for the entire Hanover region. The output raster map expresses the annual average of global irradiation daily sums estimated for optimized angle [kWh/m^2*d].

Defining the solar technical potentials we consider large-scale PV on agricultural areas (open space). When considering terrain suitable for PV installations, we excluded north-facing slopes, defined as terrain for which the aspect is less than 60° from north (more than 30° from east/west in the direction of north), and the slope of the terrain is more than 5°. The terrain affected by this exclusion amounts to about 2 % of the total area of the region (0.5 % if slope > 10°). The average power density according to pvgis database is about 22 m^2 for producing 1 kW.

5.2 Spatial Biomass Energy Potential

The biomass energy potential estimation for maize cultivation was executed by the carbon based Java software tool Biomass Simulation Tool for Agricultural Resources (BioSTAR) [35]. For computing biomass potentials, the model uses the input data soil texture, precipitation, solar radiation, temperature, humidity, wind speeds and soil texture. Currently, BioSTAR is tested and validated for several energy crops grown in Lower Saxony [36]. The biomass theoretical potential is expressed in [t/ha]. For use in the SmartSpatial model, the biomass polygon map was transformed into a 50 x 50 m raster. The estimation of the energy yields calculated for a year [MWh/ha], we assume as basis for the calculation according to in the practice considered rules of thumb, while 1 ha Silomais is equal to 8,000-12,000 m³ Biogas and 1 m³ Biogas produce 5.0-7.0 kWh (1.8-1.5 electricity production) [37].

5.3 Energy Potential Combinations

To combine different technical energy potentials, we use the raster data-set, developed for summing the specific energy yield. We consider the following RE-combinations: wind and solar power; wind and biomass (maize) cultivation. PV installations on the ground around wind turbines may be affected by the shadow of the wind turbine. For this reason we have excluded a rectangular area stretching 25 m east and west of the turbine and 30 m north, for a total of (30 (25 + 25)) = 1500 m^2.

Taking into account land-use conflicts, i.e. food production and nature conservation, we assume a maize cultivation covers approximately 20 % of the agricultural areas. This estimation has resulted by other at the Department of Environmental Planning developed projects [38], [39]. According to the abovementioned assumptions, we overlay and sum the specific energy yields in order to obtain the respectively cumulative yields of each energy combination, expressed in [MWh/ha]. A part from the calculation, it is also possible to visualize simultaneously the specific energy contribution and the sum of the energy yields. This information is really useful for the RE-development scenarios [WP 6.3].

6 Spatial Environmental Analysis

In order to identify sub-regional units which are ecologically suitable or unsuitable to be opened up for RE-development, we follow the Driver-Pressure-State-Impact-Response (DPSIR) framework [40], which is largely used by conducting environmental impact assessment [40], [41]. We assume that pressures have to be specified into a concrete planning case. Basically, we conduct an extended sensitivity analysis under consideration of combined sensitivities and values specified to the general pressures to be expected from the development of wind power plants, open-space PV power plants as well as energy maize cultivation (steps 1 to 4). Accordingly, site-specific pressures (5) derived by RE-development are relevant mainly as background information, since sensitivities are by definition dependent on a certain pressure. Together, the state (2) of the landscape units and the corresponding pressures (5) constitute the predicted impacts (6) of RE-development. The general methodology of the conducted environmental analysis is illustrated in a flow chart in Figure 3.

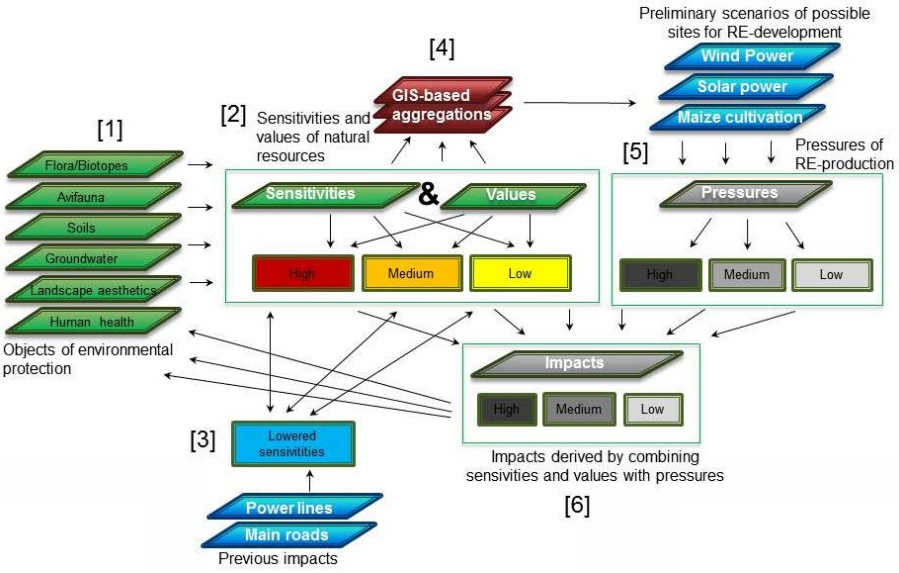

Figure 3: General environmental analysis methodology

In a stepwise analysis process, we select the most relevant objects of environmental protection (1) which are assessed for each RE-production, respectively. Then, we define indicators of their specific sensitivities and consider their environmental values, if available, against the typical-RE pressures. Together, values and sensitivities account for the state (2) of the environment according to the DPSIR concept. While the sensitivities characterize the changes of the environment which are expected, if pressure is exerted, the values of the natural resources and the biodiversity are defined as a measure for the relevance of potential changes of the environment by RE-production. Therefore, they express the scarceness and endangerment of the natural capital and are derived by the regional landscape plan ("Regional Plan", RP), or by evaluation scales in state directives (values of habitats), in certain cases adapted to the specific local situation. Often values of natural resources are coherent with their sensitivities. In the case of previous environmental impacts, caused by previously implemented infrastructures like roads or power lines, environmental qualities are reduced, which we refer in this case to as new category defined by "lowered sensitivities" (3). The indicators per RE source and objects of environmental protection are shown in more detail in Table 4 and Table 5.

	Objects of environmental protection	Pressures	Sensitivities	Values	Previous impacts
Wind	Flora and biotopes	ground clearing (removal of vegetative cover) and micro-climate changes caused by wind turbines	Flora and biotope sensitivity to microclimate changes on plant–soil carbon cycling and biotope values (Landscape structure plan, "Landschaftsrahmenplan", LRP)		------
	Avifauna	wind turbine's noise emissions	bird's sensitivity to sound pressure levels on mapped and potential bird habitat conservation areas including their respectively buffer zones (Landscape structure plan, LRP)	habitat and biotope values (LRP)	noise emissions from roads > 10,000 vehicles per day
		wind turbine's mechanical rotation speeds	bird's sensitivity to collision and mortality on mapped and potential bird habitat conservation areas including their respectively buffer zones (Landscape structure plan, LRP)	habitat and biotope values (LRP)	------
	Human health and visual landscape	wind turbine's noise emissions	human sensitivity to sound pressure levels, specifically for visual landscape on recreation areas (Regional planning programme ,"Regionales Raumordnungsprogramm", RROP)	------	noise emissions from roads > 5,000 vehicles per day
		mechanisation of the visual landscape caused by wind turbines	human sensitivity (visual perception) to wind turbines on recreation areas (Regional planning programme,"Regionales Raumordnungsprogramm", RROP)	------	high-voltage power lines (LRP)

Table 4: Definition of environmental indicators on RE-development [21], [42] - [55]

	Objects of environmental protection		Pressures	Sensitivities	Values	Previous impacts
Solar	Flora and biotopes	land-use requirements and micro-climate changes caused by open-space photovoltaics	ground vegetation sensitivity to microclimate changes on plant–soil carbon cycling and biotope values (Landscape structure plan, LRP)			------
	Fauna		fauna sensitivity to the ground-level microclimates changes and habitat values (Landscape structure plan, LRP)			------
	Soil		soil sensitivity to microclimate changes on plant–soil carbon cycling and soil erosion sensitivity (State Office of Mining, Energy and Geology, "Landesamt für Bergbau, Energie und Geologie", LBEG)		------	------
	Water and groundwater quality	potential heavy metals and other toxic compounds leaching	water and ground-water sensitivity to potential heavy metals and other toxic compounds leaching on water protected areas (Landscape structure plan, LRP)		------	------
	Visual landscape	mechanisation of the visual landscape	human sensitivity (visual perception) to wind turbines on recreation areas according to the regional planning programme (RROP)		------	------
Biomass	Soil	biomass (maize) harvesting and intensive crop production	soil erosion sensitivity (State Office of Mining, Energy and Geology, "Landesamt für Bergbau, Energie und Geologie", LBEG)			
	Flora and biotopes		ground vegetation sensitivity and values (Landscape structure plan, LRP)		values geographic distribution according to the Shannon Index	Geographic distribution of crop production (2012)
	Fauna		faunistic habitat's sensitivity and values (Landscape structure plan, LRP)			
	Water and groundwater quality	potential nitrate-nitrogen leaching	water and ground-water sensitivity to potential nitrate-nitrogen on water protected areas (Landscape structure plan, LRP)			pollution levels of groundwater and drinking on water protected areas
	Visual landscape	monotonisation of the visual landscape	human sensitivity (visual perception) to maize intensive cultivated areas (proportion of land-use areas designated for maize cultivation)			

Table 5: Definition of environmental indicators on RE-development [21], [42] - [55]

As an example, as indicator for human health sensitivity is defined the sound pressure level at different distances from the wind turbine which is measured in [dB (A)[68]] and compared with the specific hearing threshold levels of the current regulations [56]. The linkage rule, which is used

[68] A-weighted sound pressure level.

here in order to estimate sensitivities and values, is conducted by a Boolean linkage rule, which defines how different indicators are connected to form a new combined indicator, ranging from high via medium to low [41], [57] and is presented in Figure 4.

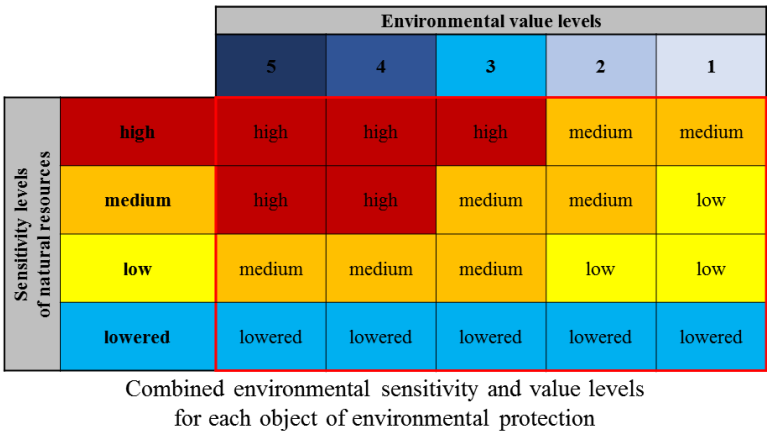

Figure 4: Linkage rule for the combination of sensitivities and values on an ordinal scale

The result of this procedure is a spatially explicit assessment of sensitivity and value levels, which are: high, medium, low and lowered (previous impacts). For the following integration as scenario-inputs, the single sensitivity categories are aggregated and displayed in one map. Additionally, in our analysis we include lowered sensitivities for wind power development.

7 Energy Scenarios Design and Modelling

According to spatial technical potentials and environmental trade-offs, we developed one reference scenario and two RE-development scenarios. They are defined in Figure 5.

Energy scenarios design		
Reference scenario 1	**Scenario "Maximum"**	maximum, technically possible, exploitable RE-production
RE-development scenario 2	**Scenario "Plan"**	Exploitable RE-production, taking into account hard and soft restriction areas
RE-development scenario 3	**Scenario "Environment"**	Exploitable RE-production, in accordance with the environmental sensitivities and values

Figure 5: Defining energy scenarios for identifying suitable and conflict areas for RE-development

Figure 6 illustrates the developed GIS-based scenario modelling. After defining energy scenarios, all polygon feature maps are converted in raster's and overlaid in order to calculate different possible RE energy yields per year [GWh/a] and the installable power [GW], which are then compared with the actual decision-space for RE-development and the political RE energy targets.

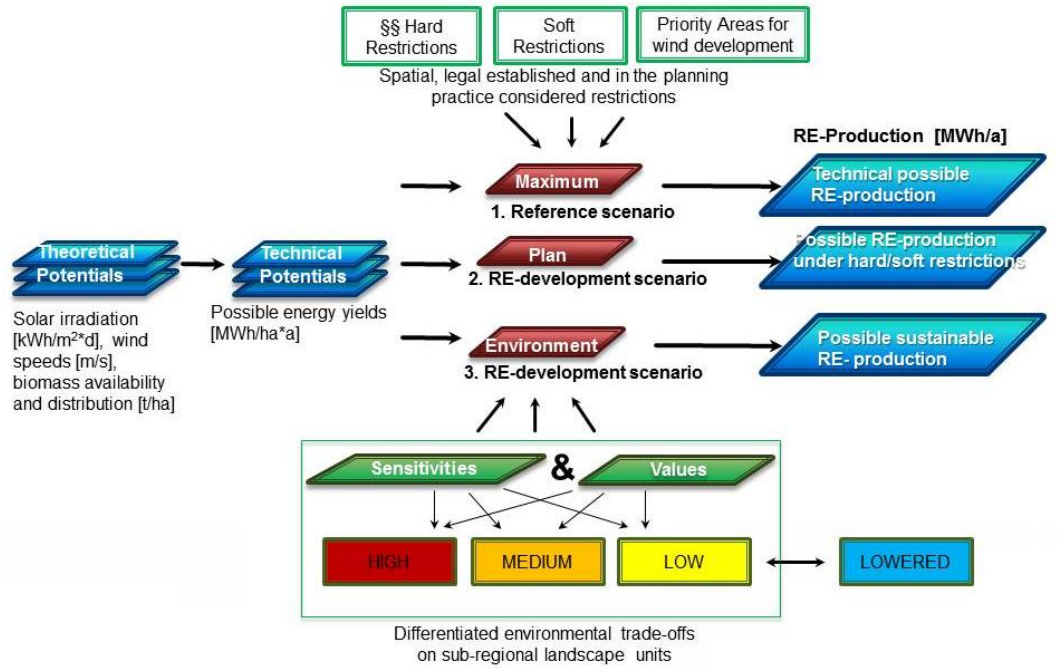

Figure 6: General scenarios modelling methodology

8 Results

After GIS-based modelling according to the geophysical properties of the landscape, the geographical distribution of theoretical RE potentials in the Hanover region was determined. The results are presented in Figure 7: solar irradiation [kWh/m^2*d], wind speeds [m/s], biomass availability and distribution [t/ha].

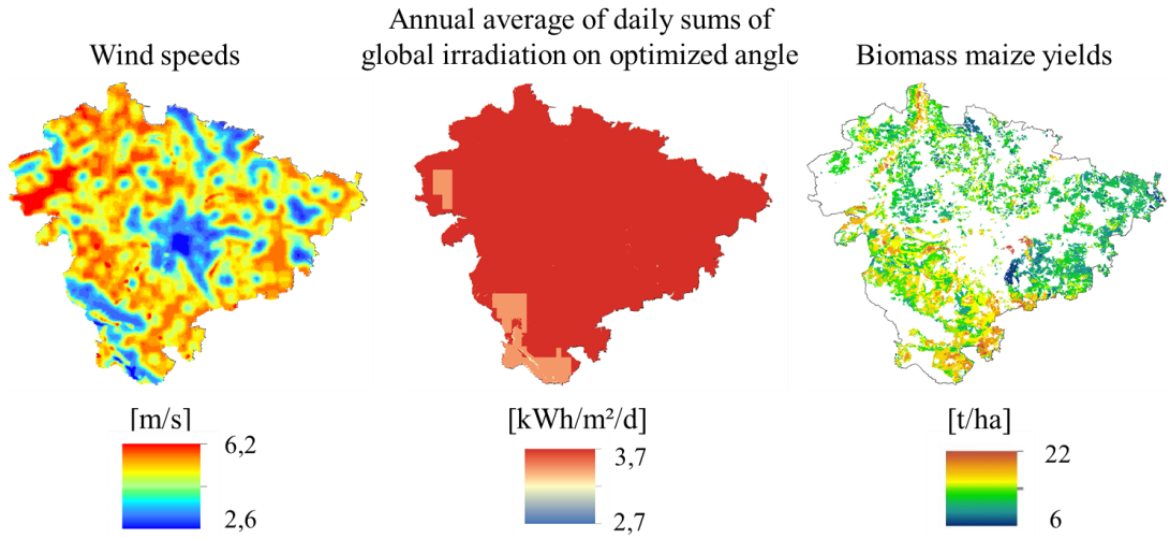

Figure 7: RE-theoretical potentials in the Hanover region

According to the specific power plant technical requirements, the maps quantify the different energy yields expressed per unit area of the Hanover region and calculated for a year [MWh/ha*a]. RE technical potentials are shown in Figure 8. It has to be noted that wind potential is the highest one compared to solar power and biomass (maize) cultivation options. Furthermore, depending on the wind speeds variability, wind electricity yields have a relevant variability all over the region.

However, the average solar electricity yields 420 MWh/ha*a on agricultural areas are similar to the wind ones 441 MWh/ha*a.

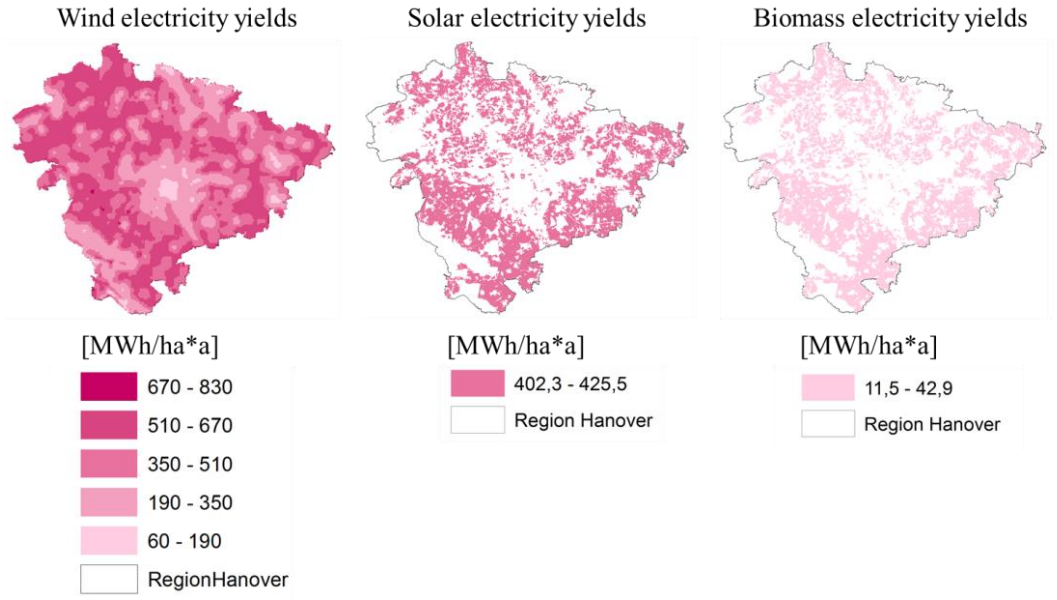

Figure 8: RE technical potentials in the Hanover region

The average biomass electricity production is 27 MWh/ha*a. Furthermore, as heat production as an important by-product of power production from biogas is a relevant component, we estimate the heat yields for biomass (maize) cultivation, which vary from 20.7 to 77.3 MWh/ha*a with an average heat production of 48 MWh/ha*a. As limitation for RE exploitation, we take into account current restrictions for RE development which are either legally binding regulations such as laws, defined as hard restriction areas, or from different recommendations by official planning institutions, mentioned as soft restriction areas. The possible suitable areas are shown in Figure 9, where the percentages displayed are referred to the whole regional area.

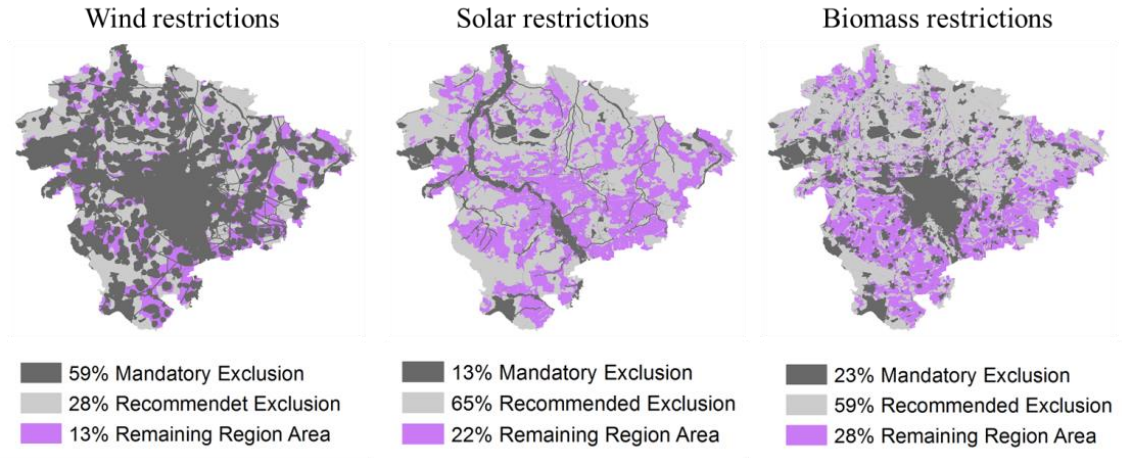

Figure 9: Hard and soft restriction areas, and suitable areas for each RE development, calculated as a percentage of the whole regional area.

In the Hanover region, hard restriction areas differ largely among the assessed possible exploitation of wind power (59 %) on the one hand versus PV power plants (13 %) and energy maize cultivation (23 %) on the other hand. The mapping of soft restriction areas for both, PV power plants and maize cultivation, reveal more than the 50 % of the regions' total area are considered sensitive to development according to planning recommendations; while for wind only 28 % of the total area are classified as sensitive areas. Regarding the remaining areas after subtraction of both hard and soft restricted areas, wind energy exploitation is more limited with 14 %, followed by maize cultivation with 27 % and PV power plants with 37 % share of the regions' total area.

In order to take into account the sensitivity and values of relevant objects of environmental protection, we produce separately sensitivity and values maps, which are then aggregated to complete the spatial environmental analysis. As an example, we show here the aggregated and the single environmental sensitivity and values maps for wind development. Taking into account as relevant environmental objects flora, avifauna and human health, we estimated 56 % of the regions area as highly sensitive and 37 % as medium sensitive, while 7 % were estimated to exhibit a low sensitivity (Figure 10).

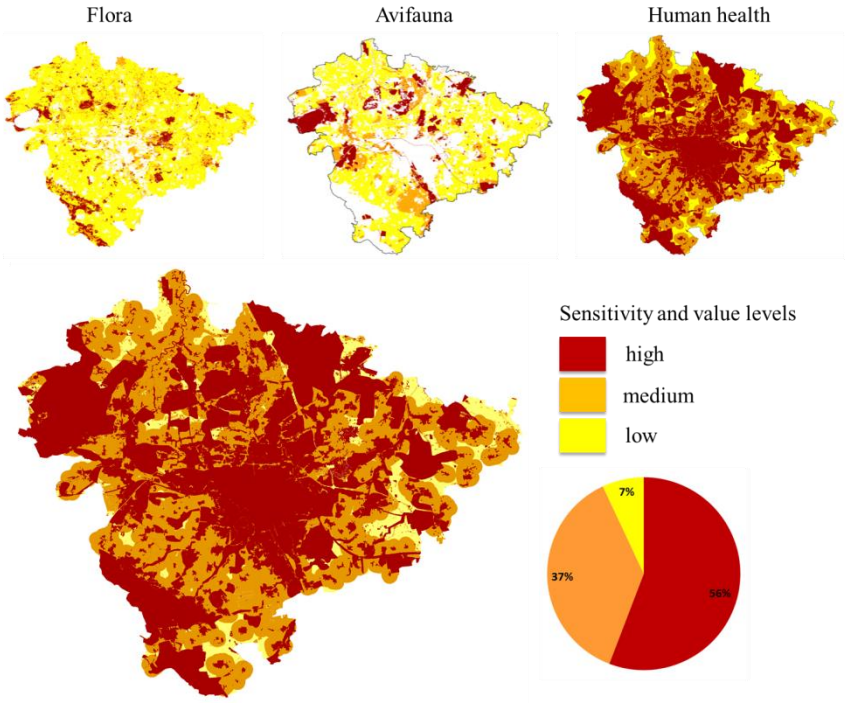

Figure 10: Wind power - map of sensitivity and value levels
of relevant objects of environmental protection

When additionally including areas with previous environmental impacts into the sensitivity analyses (i.e. due to noise emissions from existing main roads), suitable areas for wind development increase, as shown in Figure 11.

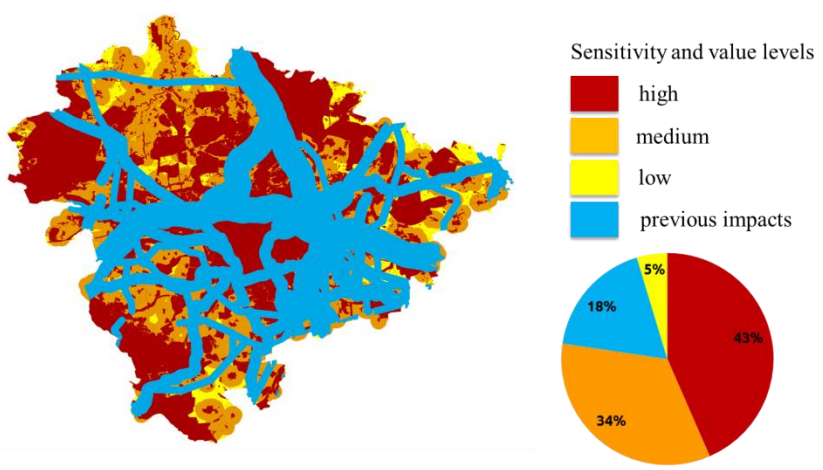

Figure 11: Wind power - map of lowered sensitivities due to previous environmental impacts.

Finally, energy scenarios are modelled taking into account the technical energy potentials and the integration of spatial restrictions and environmental sensitivities and values. Figure 12 and Table 4 show the energy scenarios for wind-development and the combination of wind and solar power. By developing energy scenarios, we estimate potentially producible energy yields under the different RE-development scenarios conditions.

As final results of the Smart Nord sub-project six, Table 7 and Figure 12 illustrate the suitable areas [ha] and possible electricity yields [GWh/a] for wind development according to the reference, named as scenario "Maximum" and the two different RE-development scenarios, named as "Plan" and as "Enviroment". The model allows also calculating the predicted number of wind power plants and, therefore, the installable power [GW].

	Scenario "Maximum"	**Scenario "Plan"**		**Scenario "Environment"**		
	areas and potentials for wind electricity production					
	technical requirements	hard restrictions	soft restrictions	low sensitivities	medium sensitivities	lowered sensitivities (previous impacts)
Area [ha]	229,304	86,978	25,586	7,593	14,225	27,579
Proportion of Area [%]	100	38	11	3	6	12
Wind Power Stations [n]	25,992	10,905	3,520	1,110	2,085	3,774
Energy Yield [GWh/a]	11,473	4,959	1,850	552	1,077	1,780
Installable Power [GW]	79	33	11	3	6	12

Table 7: Wind power - total exploitable electricity yields and suitable areas according to different scenarios

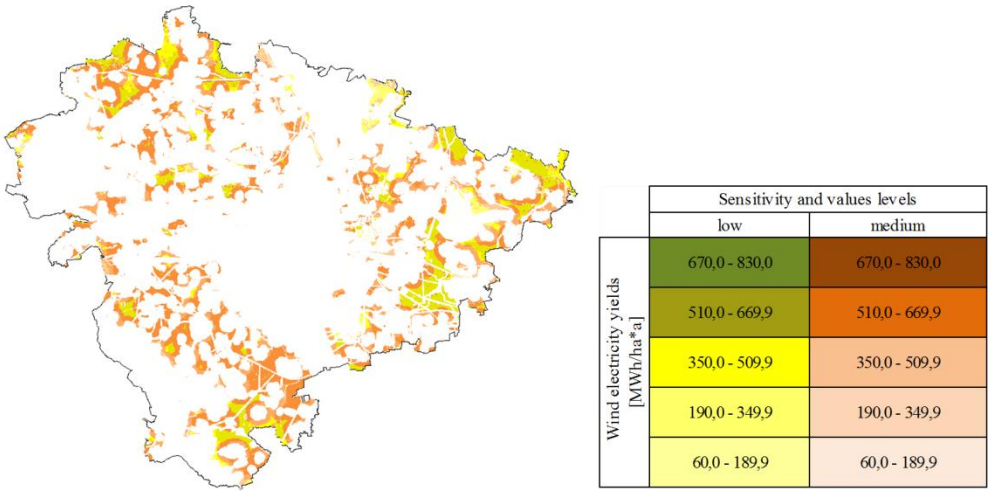

Figure 12: Possible sites for wind development by combining energy potentials and environmental sensitivities and values

The possible wind energy yield according to the technical potential (scenario "Maximum") is estimated around 11,473 GWh/a on the regions total area. According to the scenario "Plan", when hard restriction areas are excluded, the potential is reduced to 4,959 GWh/a on 38 % of that area. If all (hard and soft) restricted areas are excluded from the possible production area, 1,850 GWh/a remain to be exploited on 11 % of the regions area. By contrast, the differentiated environmental analysis assessed in the scenario "Environment" suggests that the low sensitivity areas amount to 853 GWh/a on 5 % of the technically exploitable area.

When considering lowered sensitivities due to previous environmental impacts, we estimated wind energy yields of to 1,780 GWh/a on 12 % of the technically exploitable area.

Table 8 and Figure 13 finally show the combination of wind and biomass (maize) energy on agricultural areas according to combined potentials and environmental analyses, with a total share of 8 % of the total area. Taking into account that we assume a maize cultivation covers approximately 20 % of the agricultural areas, the possible energy yields according to the technical potentials and environmental sensitivity and values (scenario "Environment") is estimated at 99 GWh/a on low sensitivity areas and at 1,139 GWh/a on medium sensitivity areas.

	Scenario "Environment"			
	Areas and potentials for electricity production		Areas and potentials for heat production	
	areas of low sensitivities	areas of intermediate sensitivities	areas of low sensitivities	areas of intermediate sensitivities
Area [ha]	1,455	15,849	1,455	15,849
Proportion of area [%]	1	7	1	7
Wind energy yields [GWh/a]	83	912	-	-
Biomass energy yields [GWh/a]	6	81	10	146

Table 8: Wind and solar power - total exploitable electricity yields and suitable areas according to different scenarios

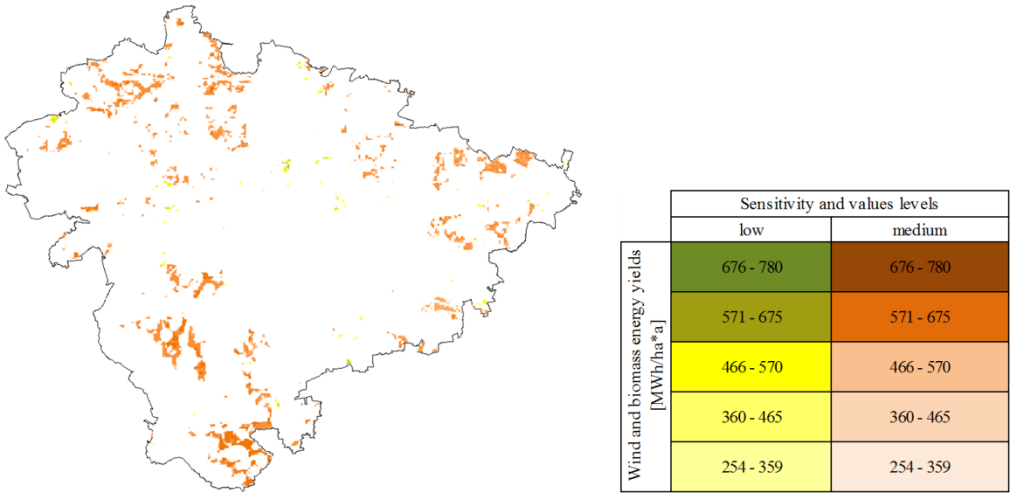

Figure 13: Possible sites for wind and solar development by combining energy potentials and environmental sensitivities and values

9 Discussion

After developing different scenarios for identifying suitable and conflict areas for RE-development, we compare these outcomes with the actual decision-space for RE-development and the political RE energy targets. The priority areas designated for wind development are partially in accordance with our spatial environmental analysis, i.e. by considering bird habitats. Accordingly, we suggest considering sensitivities and values of relevant environmental objects by identifying suitable areas for energy production.

By comparing the soft and hard restrictions with the environmental analysis, it should be mentioned that they might be over or under regulated for the different RE sources [17]. Both these types of restriction areas might differ among the single federal states; also, the restrictions in protected areas may differ as they are defined by individual ordinances of the particular conservation area. Moreover, hard restriction areas as well as associated buffer zones definitions have been subject to continuous change due to increasing land-use pressures [17]. As an example, the case of wind power development, hard restriction areas and estimated sensitivities, respectively 14 % and 7 % of the regions total area exhibit a light under-regulation, supported by the presented analyses, which lead to a stepwise reduction of designated restriction areas, referring to the latest draft of the Wind Energy Decree, produced by the federal state of Lower Saxony ("Windenergieerlass") [27].

Regional energy targets by 2050 according to the trend scenario ("Trend") and to the goal path scenario ("Zielpfad") is to produce electricity yields respectively of 1,372 and 3,244 GWh/a by wind energy [58]. By contrast, we estimate possible electricity yields of 2,332 GWh/a with low environmental sensitivity, which increases up to 3,409 GWh/a, if including medium sensitivity (Figure 14). However, areas with previous impacts are basically based on noise emissions of major roads, without considering obstacles fulfilling sound absorbing functions. At the same time, sensitive areas, designates as medium should be surveyed on the local scale, and possibly many areas might prove unsuitable for sustainable wind power development. Therefore, we suggest for those areas more investigations, because they may vary from case to case, depending on such technical and environmental factors as geographical location, technological power plant features or special ecological sensitivities, e.g. related to protected bird species.

As regional targets for solar electricity do include solar panel installations on roofs and building facades, respectively 1,090 GWh/a ("Trend") and 3,143 GWh/a ("Ziel Pfad"), we calculated

additional possible electricity yields of 1,232 GWh/a on low sensitivity agricultural areas and of 13,931 GWh/a with the addition of the medium sensitivity areas produced by open-space solar panels. However, the construction of open-solar panel on the surveyed agricultural land is currently not politically promoted and, therefore, not supported by the incentive-based Renewable Energy Act [59], [60], [61]. Finally, regional targets for biogas energy production do take into account also wood and sewer gas for the heat component, while we consider maize only. Nevertheless, one arable land will only be used for either maize production or for the production of other energetically usable biomass. But, by the use of different bioenergy crops, negative impacts on the environment can be reduced and more acreage could be used for energy production [62]. However, by comparing the results and selecting the low sensitivity areas, we estimate for electricity production around 232 GWh/a, which is near to 196 GWh/a ("Trend"), but far away to 323 GWh/a ("Ziel Pfad"). On the other hand, heat production of biogas plants on low sensitivity areas accounts 417 GWh/a and 739 GWh/a compared to 462 ("Trend") and 921 GWh/a ("Ziel Pfad").

RE-production	Trend 2050	Ziel Pfad 2050	Lowered and low sensitivities	Lowered, low and medium sensitivities
Wind electricity yields [GWh/a]	1.372	3.244	2.332	3.409
Solar electricity yields [GWh/a]	1.090	3.143	1.232	13.931
Biomass electricity yields [GWh/a]	196	323	232	411
Biomass heat yields [GWh/a]	462	921	417	739

Figure 14: Comparison of regional energy targets by 2050 with environment-oriented scenarios

If the required spatial efficiency and the objectives of climate and environmental protection are to be reached, it is necessary to combine spatial information on both, sectorial and combined RE potentials as well as possible environmental impacts. This way, potential (co-)allocation options for RE development can be analysed in order to maximize energy generation and at the same time minimize environmental trade-offs [17], [20].

As showed for the here presented case study, the developed methodology is an important first step in supporting regional decisions for the development and allocation of RE systems. Based on data that are available for all German and most European regions, SmartSpatial can calculate the trade-offs but also opportunities of regional RE-development at the beginning of the planning decision process in a given region. The regional case study in the Hanover region with its high amount of potentially conflicting land-use demands reveals that both, yields and environmental sensitivities and values can vary widely with RE siting decisions. The differentiated environmental analysis in combination with the spatially differentiated RE potential offers the best opportunities to find optimized solutions which may also integrate political preferences or citizen opinions. If low sensitive areas are not sufficient, medium sensitivity areas can be considered – given adequate compensation of impaired ecosystem functions. This strategy offers the maximal energy yield with a low consumption of land. Furthermore, areas that are already environmentally impacted, e.g. by previously existing infrastructure projects are suitable, as long as they offer satisfactory energy yields. In order to find these areas, the interplay between high potential energy yields and environmental sensitivities should be analysed for each region individually. Of course, input data are decisive for the results. On the one hand, technical wind energy potentials can be more precisely estimated, if wind frequency distributions are available as well as the average wind speeds at 100 m above the ground level. On the other hand, the evaluation of the visual landscape is

strong affected by the values of the Regional planning programme (RROP), in particular on recreational areas. This evaluation had an almost prohibitive effect on the possibility to develop additional RE in the region.

If other options have to be taken into account in order to reach RE production targets, which might be less favourable regarding nature, we recommend considering possible mitigation measures in order to use synergies (e.g. inclusion of previous environmental impacts into development strategies) and therefore prevent invasive impacts. In fact, this general approach has already found its way into planning, with the siting of wind power plants along infrastructure [43], as well as the incentive-based steering by the EEG, with the siting of open-space solar panels exclusively up to 110 m along road infrastructure, on conversion areas from commercial or military utilization, or in commercial and industrial areas[69] [61]. One way to increase the decision space would be to use more differentiated spatial analysis in order to achieve a high spatial efficiency. In this context, spatial efficiency can be defined as appropriate site selection. To avoid possible land-use conflicts and trade-offs between renewable energy production and nature conservation, regional land-use planners need spatially explicit information in order to find the best development alternative. Rather than undifferentiated restriction areas, RE development planning needs to be specific as to which area specific pressures, sensitivities and values are of concern for the particular RE source and their efficient combinations.

10 Conclusions and Recommendations

In SP 6 we develop the SmartSpatial model, which is based on a spatial multi-criteria methodological framework for RE siting, following the objectives of sustainability by simultaneously maximizing the spatial efficiency and minimizing the environmental impacts of RE production. Thus, the model offers a great potential for the improvement of RE planning decisions. Methodologically, the model combines RE-potential analysis with an ecological impact analysis, which is specified for different RE pressure factors. The results obtained offer advanced insights on regional RE development problems and chances. Furthermore, supporting a decentralised energy production, spatial RE potentials can be used as an input to further develop electrical grid infrastructures, in particular micro-grids (SP 1-5).

The spatially explicit approach and the opportunity to calculate RE production possibilities in relation to environmental sensitivities and values, needs to integrate further considerations by minimizing costs (SP 2). Further research development can include economic market constraints, availability of transmission infrastructure, and current and future electricity loads (SP 1-4). The interface between engineering and environmental planning, being currently underdeveloped, can make a major contribution to transdisciplinary research on the one hand, and finding solutions for major social problems on the other hand. Furthermore, the implementation of SmartSpatial at local scale can be suggested for further research improvement. Accordingly, during Smart Nord, we assess energy potentials from solar and geothermal sources for the municipality of Ganderkesee in Lower Saxony, which will be compared in a next step to those estimated in the associated project "EnerGeoPlan". Also the regional energy potentials will be compared with the results at European scale reached in SP 4.

Moreover, the biogas power plant allocation can be optimized by finding optimal site network according to biomass potentials and environmental sensitivities and values and by minimizing maize transportation and extraction costs (SP 5). This can have positive effects on the successful achievement of regional RE production targets including optimized relations between spatial

[69] cfr. §32 EEG.

energy yields and environmental impacts, reducing planning uncertainties and the pitfalls of nature conservation law as well as enhanced acceptance of future RE and electricity grid development. These achievements are supported primarily by spatially explicit visualizations and calculations of diverse RE development scenarios. In future research, economic and social considerations can be integrated and optimized, for representation of a real level of renewable generation that may be then deployed for allocating efficient energy combinations. Having provided basically preparatory work for further optimization processes, we recommend further developing the presented spatial multi-criteria model, which is an effective tool for RE-development, supporting regional and local planning authorities to track changes and identify the best solutions.

References

[1] Bundesministerium für Umwelt, Naturschutz, Bau und Reaktorsischerheit (BMUB), "Erneuerbare Energien. Innovationen für eine nachhaltige Energiezukunft," October 2011.

[2] W. Brücher, "Energiegeographie," in Energiegeographie-Wechselwirkungen zwischen Ressourcen, Raum und Politik, Berlin, Stuttgart, Germany, Gebrüder Bornträger, 2009, ch. 1, pp. 1-280.

[3] J. Nitsch, W. Krewitt, M. Nast, P. Viebahn, S. Gärtner, M. Pehnt, et al., "Ökologisch optimierter Ausbau der Nutzung erneuerbarer Energien in Deutschland," March 2004.

[4] G. Reinhardt, K. Scheurlen, "Naturschutzaspekte bei der Nutzung erneuerbarer Energien," June 2004.

[5] Bosch, Partner, "Vorbereitung und Begleitung der Erstellung des Erfahrungsberichtes 2007 gemäß §20 EEG," November 2007.

[6] Bosch, Partner, "Planerische Steuerung der Naturschutz Erneuerbarer Energien-Möglichkeiten und Grenzen," December 2010.

[7] M. Rodrigues, C. Montañés, N. Fueyo, "A method for the assessment of the visual impact caused by the large-scale deployment of renewable-energy facilities," in Environmental Impact Assessment Review (Ed.) 30, 2010, 240-246.

[8] S. Bosch, G. Peyke, "Raum und Erneuerbare Energien. Anforderungen eines erneuerbaren Energiesystems an die Standortplanung," in Standort, vol.34, Springer-Verlag, Germany, 2010, pp. 11-19.

[9] T. Chang, E. Nielsen, W. Auberle, F. I. Solop, "A quantitative method to analyze the quality of EIA information in wind energy development and avian/bat assessments," in Environmental Impact Assessment Review, 382013, 2013, pp. 142-150.

[10] C. V. Haaren, C. Palmas, T. Boll, M. Rode, M. Reich, F. Niederstadt, et al., "Erneuerbare Energien — Zielkonflikte zwischen Natur- und Umweltschutz," in BBN (Ed.), Neue Energien — Neue Herausforderungen: Naturschutz in Zeiten der Energiewende, Jahrbuch Naturschutz und Landschaftspflege, 59, 2013, pp. 18–33.

[11] M. Althaus, "Schnelle Energiewende — bedroht durch Wutbürger und Umweltverbände? Protest, Beteiligung und politisches Risikopotenzial für Großprojekte im Kraftwerk- und Netzausbau," in Wissenschaftliche Beiträge, 15TH Wildau, 2012, pp. 103–113.

[12] S. Becker, L. Gailing, N. Naumann, "Neue Akteurslandschaften der Energiewende. Aktuelle Entwicklungen in Brandenburg," in Raumplanung162/3, 2012, pp. 42–46.

[13] P. Buschmann, "The German energy (half) turnaround, an analysis of soft-power mechanisms that shape the German energy transformation," Master Thesis, Series in environmental studies and sustainable science, No. 2013 Lund University, 2013, p. 021.

[14] C. Kemfert, J. Horne, "Good governance of the Energiewende in Germany: wishful thinking or manageable? Hertie school experts on the federal elections 2013," July 2013.

[15] K. Calvert, J. M. Pearce, W. E. Mabee, "Toward renewable energy geo-information infrastructures: applications of GIScience and remote sensing that build institutional capacity," in Renewable and sustainable energy reviews, vol. 18, 2013, pp. 416–429.

[16] W. Peters, "Erneuerbare Energien – Strategien für eine naturverträgliche Nutzung," 2013.

[17] C. Palmas, A. Siewert, C. V. Haaren, "Exploring the decision-space for renewable energy generation to enhance spatial efficiency," in Environmental Impact Assessment Review (Ed.), 52, 2014, pp. 9–17.

[18] C. Palmas, E. Abis, C. V. Haaren, A. Lovett, “Renewables in residential development: an integrated GIS-based multicriteria approach for decentralized micro-renewable energy production in new settlement development: a case study of the eastern metropolitan area of Cagliari, Sardinia, Italy,” in Energy, Sustainability and Society 2012, 2, 2012, p. 10.

[19] H. Diefenbacher, “Zum Konfliktpotenzial Erneuerbarer Energien,” in soFid Sozialwissenschaftlicher Fachinformationsdienst. International Beziehungen/Friedens- und Konflitkforschung, vol. 2009/2, 2009, pp. 9–18.

[20] C. V. Haaren, C. Palmas, A. Siewert, T. Boll, “Landschaft: Gesellschaftliche und wissenschaftliche Herausforderungen der Energiewende,” in Eidg. Forschungsanstalt für Wald, Schnee und Landschaft WSL (Hrsg.): Landschaft und Energiewende. Der Einfluss erneuerbarer Energien auf die Landschaft, WSL Berichte 21 – Forum für Wissen, 2014, pp. 25-28.

[21] Region Hannover, “Landschaftsrahmenplan der Region Hannover,” 2013.

[22] Bundesamt für Naturschutz (BfN), May 2014.

[23] Landesamt für Statistik Niedersachsen (LSN), “Statistisches Taschenbuch 2014,” 2014.

[24] Region Hannover, “Regionalplanung in der Region Hannover,” 2014.

[25] J. X. Domínguez Bravo, I. García Casals, I. Pinedo Pascua, “J. X. Domínguez Bravo, I. García Casals, I. Pinedo Pascua” in: Energy Policy, 35, 2007, pp. 4879–4892.

[26] LGLN Niedersachsen, “Auszug aus den Geobasisdaten der Niedersächsischen Vermessungs- und Katasterverwaltung,” ATKIS Basis-DLM (2012) [ESRI ArcMap Digital Edition], 2012.

[27] Ministerium für Umwelt, Energie und Klimaschutz (MU), “Planung und Genehmigung von Windenergieanlagen an Land in Niedersachsen und Hinweise für die Zielsetzung und Anwendung (Windernergieerlass),” July 2012

[28] Niedersächsischen Landkreistag (NLT), “Naturschutz und Windenergie. Hinweise zur Berücksichtigung des Naturschutzes und der Landschaftspflege bei Standortplanung und Zulassung von Windenergieanlagen,” October 2014.

[29] Niedersächsischen Landkreistag (NLT), “Regionalplanung und Windenergie. Empfehlungen des NLT zu den weichen Tabuzonen zur Steuerung der Windenergienutzung mit Ausschlusswirkung in Regionalen Raumordnungsprogrammen,” February 2014.

[30] Ministerium für Umwelt, Energie und Klimaschutz (MU), “Verordnung über Schutzbestimmungen in Wasserschutzgebieten” SchuVO, November 2009.

[31] J. Counihan, “Adiabatic atmospheric boundary layers: a review and analysis of data from the period 1880–1972,” in Atmos Environ, 79, 1975, pp. 871–905.

[32] J. S. Touma, “Dependence of the wind profile power law on stability for various locations,” in Air Pollution Control Association, 27, 1977, pp. 863–866.

[33] EU Joint Research Centre (JRC), “model r.sun,” 2010.

[34] EU Joint Research Centre (JRC), “Clear sky indexes,” May 20014.

[35] S. Azam-Ali, N. M. J. Crout, R. G Bradley, “Perspectives in modelling resource capture by crops,” Nottingham University Press, UK, 1994.

[36] R. Bauböck, “Optimizing Land use and the Yields of Bio-Energy Crops by using site specific Biomass Calculations: Introduction of the Crop Modelling Software BioSTAR,” in R. Seppelt, A.A. Voinov, S. Lange, D. Bankamp (Eds.), Managing Resources of a Limited Planet: Pathways and Visions under Uncertainty, Sixth Biennial Meeting, Bankamp (Hrsg.), Leipzig, 2012, pp. 412–419.

[37] Bayerische Landesanstalt für Landwirtschaft (LfL), “Faustzahlen für die Biogaserzeugung,” 2008.

[38] J. Wiehe, M. Rode, H. Kanning, “Raumanalyse I – Auswirkungen auf Natur und Landschaft,” in M. RODE AND H. KANNING (Eds) Natur- und raumverträglicher Ausbau energetischer Biomassepfade, Stuttgart, ibidem-Verlag, 2010, pp. 21–90.

[39] W. Saathoff, C. Albert, C. V. Haaren, J. Hermes, M. Rode, F. Neuendorf, S. Hermann, “Optimierung des Energiepflanzenbaus im Hinblick auf Natur und Landschaft,” in Abschlussbericht zum Projekt Biomasse im Spannungsfeld. Unpublished.

[40] E. Smeets, R. Weterings, “Environmental Indicators: Typology and Overview,” Technical Report no. 5, EEA, Copenhagen, 1999, pp. 1-35.

[41] R. Bachfischer, “Die ökologische Risikoanalyse: eine Methode zur Integration natürlicher Umweltfaktoren in die Raumplanung,” Ph.D. dissertation, Technische Universität München, München, 1978, pp. 1-298.

[42] Region Hannover, “Regionales Raumordnungsprogramm 2005 für die Region Hannover,” 2005.

[43] Bosch, Partner, "Abschätzung der Ausbaupotenziale der Windenergie an Infrastrukturachsen und Entwicklung von Kriterien der Zulässigkeit," in Final Report, Berlin, client: BMU, Forschungszentrum Jülich PTJ, 2009, pp. 1-199.

[44] A. Garniel, U. Mierwald, "Vögel und Straßenverkehr," Guideline, Michael-Otto-Institut, NABU, Bonn, client: BMV, FE 02.286/2007/LRB, Bonn, 2010, pp. 1-133.

[45] H. Hötker, "Auswirkungen des Repowering von Windkraftanlagen auf Vögel und Fledermäuse," Final Report, Bergenhusen, client: Landesamt für Natur und Umwelt Schleswig Holstein, 2006, pp. 1-40.

[46] Länderarbeitsgemeinschaft der Vogelschutzwarten (LAG-VSW), "Abstandsempfehlungen für Windenergieanlagen zu avifaunistische bedeutenden Vogellebensräumen sowie Brutplätzen besonders störungsempfindlicher oder durch Windenergieanlagen besonders gefährdeter Vogelarten," May 2008.

[47] T. Dürr, "Vogelverluste an Windenergieanlagen in Deutschland, Daten aus der zentralen Fundkartei der Staatlichen Vogelschutzwarte im Landesamt für Umwelt," Gesundheit und Verbraucherschutz Brandenburg, October 2013.

[48] R. Brinkmann, "Möglichkeiten und Grenzen der Integration tierökologischer Daten in die Landschaftsplanung - dargestellt am Beispiel des Landschaftsplans Nenndorf," in Inform. d. Naturschutz Nieders., vol. 19, no. 2, 1999, pp. 90-104.

[49] Blasy, Overland, "Teilfortschreibung Konzentrationsflächen Windenergie. Ermittlung und Bewertung der Konzentrationszonen," August 2012.

[50] K. Runge, "Ökologische Auswirkungen von Freileitungen und Erdkabeln (380 kV)," April 2013.

[51] W. Nohl, "Landschaftsästhetische Auswirkungen von Windenergieanlagen," September 2009.

[52] J. Peters et al., "Studie zur Bewertung der Wirkung von 380-kV-Freileitungen auf das Landschaftsbild," October 2008.

[53] Schallschutz im Städtebau, DIN 18005-1, 2002, July.

[54] Sechzehnte Verordnung zur Durchführung des Bundes-Immissionsschutzgesetzes (Sechzehnte Verkehrslärmschutzverordnung – 16. BImSchV), 1990, June.

[55] Sechste Allgemeine Verwaltungsvorschrift zum Bundes-Immissionsschutzgesetz (Technisce Anleitung zum Schutz gegen Lärm – TA Lärm), 1998, August.

[56] Niedersächsisches Gesetz über Verordnungen der Gemeinden zum Schutz vor Lärm (Niedersächsisches Lärmschutzgesetz - NLärmSchG), 2012, December.

[57] F. Scholles, "Die ökologische Risikoanalyse und ihre Weiterentwicklung," in D. Fürst and F. Scholles, "Handbuch Theorien und Methoden der Raum- und Umweltplanung", Rohn, Dortmund, 2008, ch. 7.6, pp. 458-479.

[58] Region Hannover, "Masterplan Stadt und Region Hannover. 100% für den Klimaschutz. Auf dem Weg zu einer klimaneutralen Region bis 2050," 2012.

[59] Gesetz für den Ausbau erneuerbarer Energien, Erneuerbare-Energien-Gesetz - EEG, 2014, July.

[60] S. Enkhardt, "Bundesregierung schränkt Flächen für Solarparks mit Ausschreibungen doch ein," February 2015.

[61] F. Staiß et al., "Nutzung der solaren Strahlungsenergie nach §11 EEG," in Vorbereitung und Begleitung der Erstellung des Erfahrungsberichtes 2007 gemäß §20 EEG, Report, ZSW, Stuttgart, 2007, ch. 8.9, pp. 68-77.

[62] M. Rode, H. Kanning, "Natur- und raumverträglicher Ausbau energetischer Biomassepfade," Ibidem, Stuttgart, 2010, pp. 1-156.

Annex

List of Publications Written in Smart Nord

- M. Blank, S. Lehnhoff, "A Concept for Reliability Assessment for the Provision of Ancillary Services," in proc. of 2nd International Conference on Smart Grids and Green IT Systems (Smart-Greens), May 9-10, 2013, Aachen, Germany.
- C. Hinrichs, S. Lehnhoff, M. Sonnenschein, "A Decentralized Heuristic for Multiple-Choice Combinatorial Optimization Problems," in Operations Research Proceedings 2012 - Selected Papers of the International Annual Conference of the German Operations Research Society (GOR), Springer, pp. 297-302, 2014.
- J. Bremer, M. Sonnenschein, "A Distributed Greedy Algorithm for Constraint-based Scheduling of Energy Resources," in 1st International Workshop on Smart Energy Networks & Multi-Agent Systems, FedCSIS Proceeding, pp. 1285-1292, 2012.
- S. Beer, "A Formal Model for Agent-based Coalition Formation in Electricity Markets," in 4th IEEE/PES Innovative Smart Grid Technologies Europe (ISGT EUROPE), Kopenhagen, pp. 1-5, 2013.
- M. Blank et al., "Agentenbasierte Vorhaltung und Erbringung von Primärregelleistung," in at – Automatisierungstechnik, Band 62, Heft 5, pp. 347-363, April 2014.
- F. Fuchs, D. V. Pham, A. Mertens, "Analysis of grid current control in consideration of voltage feedforward and cable capacitance demonstrated on a fully sized wind turbine installed in a wind park," Energy Conversion Congress and Exposition (ECCE), 2013 IEEE, pp.3325,3332, 15-19 Sept. 2013.
- M. Blank, S. Lehnhoff, "Assessing Reliability of Distributed Units with Respect to the Provision of Ancillary Services," in proc. of 11th IEEE Conference on Industrial Informatics (INDIN), Special Session on Industrial Informatics in Smart Grids, Bochum, Juli 2013.
- J. Bremer, M. Sonnenschein, "Automatic Reconstruction of Performance Indicators from Support Vector based Search Space Models in Distributed Real Power Planning Scenarios," in Proceedings of the Informatik 2013 - Informatik angepasst an Mensch, Organisation und Umwelt, Koblenz, Germany. LNI 220, pp. 1441-1454, 2013.
- R. Bleiker, S. Lehnhoff, C. Mayer, K. Piech, "Automatisierung heterogener, verteilter Energieanlagen mittels OPC UA," in Zukünftige Stromnetze für Erneuerbare Energien, Berlin, Germany, 2014.
- F. Fuchs, R. Dietz, S. Garske, T. Breithaupt, A. Mertens, L. Hofmann, "Challenges of Grid Integration of Distributed Generation in the Interdisciplinary Research Project Smart Nord," IEEE 5th International Symposium on Power Electronics for Distributed Generation Systems (PEDG), Galway, Ireland, 24.-27. June 2014.
- J. Psola et al., "Characteristics of Energy Storage in Smart Grids," EVER2014, Monaco, Monaco, 2014.
- C. Hinrichs, S. Lehnhoff, M. Sonnenschein, "COHDA: A Combinatorial Optimization Heuristic for Distributed Agents," in Agents and Artificial Intelligence, Communications in Computer and Information Science, Vol. 449, Springer, pp. 23-29, 2014.
- A. Nieße, S. Beer, J. Bremer, C. Hinrichs, O. Lünsdorf, M. Sonnenschein, "Conjoint Dynamic Aggregation and Scheduling Methods for Dynamic Virtual Power Plants," in Proceedings of

the 2014 Federated Conference on Computer Science and Information Systems, pp. 1505-1514, 2014.

- M. Blank, S. Lehnhoff, "Considering Correlations for Reliable Distributed Ancillary Service Provision," in proc. of 5th IEEE PES Innovative Smart Grid Technologies (ISGT) Europe, October 12-14, 2014, Istanbul, Turkey.
- J. Bremer, M. Sonnenschein, "Constraint-Handling for Optimization with Support Vector Surrogate Models: A Novel Decoder Approach," in Proceedings of the 5th International Conference on Agents and Artificial Intelligence, Volume 2, Barcelona, Spain, 15-18 February. SciTePress, pp. 91-105, 2013.
- J. Bremer, M. Sonnenschein, "Constraint-Handling with Support Vector Decoders," in Agents and Artificial Intelligence, Communications in Computer and Information Science, Vol. 449, Springer, pp. 228-244, 2014.
- M. Blank, S. Lehnhoff, "Correlations in Reliability Assessment of Agent-based Ancillary-Service Coalitions," in proc. of 18th Power Systems Computation Conference (PSCC), August 18-22, 2014, Wroclaw, Poland.
- M. Sonnenschein, O. Lünsdorf, J. Bremer, M. Tröschel, "Decentralized control of units in smart grids for the support of renewable energy supply", Environmental Impact Assessment Review (in press).
- C. Köpp, H.-J. von Mettenheim, M. H. Breitner, "Decision Analytics mit Heatmap-Visualisierung von mehrschrittigen Ensembledaten," Wirtschaftsinformatik: 147. doi:10.1007/s11576-014-0417-3.
- A. Nieße, M. Tröschel, M. Sonnenschein, "Designing Dependable and Sustainable Smart Grids - How to Apply Algorithm Engineering to Distributed Control in Power Systems," Environmental Modelling and Software, Vol. 56, pp. 37-51, 2014.
- M. Sonnenschein, H.-J. Appelrath, L. Hofmann, M. Kurrat, S. Lehnhoff, C. Mayer, A. Mertens, M. Uslar, A. Nieße, M. Tröschel, "Dezentrale und selbstorganisierte Koordination in Smart Grids," VDE-Kongress 2012 - Intelligente Energieversorgung der Zukunft, Stuttgart, 2012.
- S. Lehnhoff et al., "Distributed Coalitions for Reliable and Stable Provision of Frequency Response Reserve – An Agent-based Approach for Smart Distribution Grids," in proc. of IEEE International Workshop on Intelligent Energy Systems (IWIES), IEEE Press, 2013.
- C. Hinrichs, J. Bremer, M. Sonnenschein, "Distributed Hybrid Constraint Handling in Large Scale Virtual Power Plants," in IEEE PES Conference on Innovative Smart Grid Technologies Europe (ISGT Europe 2013), Kopenhagen, IEEE Power & Energy Society, 2013.
- F. Fuchs, A. Mertens, "Dynamic modelling of a 2 MW DFIG wind turbine for converter issues: Part 1," Power Electronics and Motion Control Conference (EPE/PEMC), 2012 15th International, pp.DS2d.5-1,DS2d.5-7, 4-6 Sept. 2012.
- A. Nieße, S. Lehnhoff, M. Sonnenschein, M. Tröschel, "Dynamic Virtual Power Plants in Future Energy Grids: Defining the Gap to the Field," in VDE Kongress 2014, VDE Verlag, 2014.
- F. Muuß, N. G. A. Hemdan, M. Kurrat, D. Unger, B. Engel, "Dynamic Virtual Reactive Power Plant in Active Distribution Networks" – Powertec, Eindhoven 2015.

- A. Ohsenbrügge et al., “Efficient Provision of Ancillary Services by Decentralized, Volatile Generating Units,” to appear in proc. of VDE/ETG Fachtagung Von Smart Grids zu Smart Markets, 25.-26. March 2015, Kassel, Germany.
- F. Fuchs, D. V. Pham, A. Mertens, “Einfluss der Netzimpedanz auf die Dynamik der netzseitigen Stromregelung am Beispiel einer Windenergieanlage,” ETG Kongress, Berlin, 2013.
- S. C. Meyer, M. H. Breitner, “Electricity Associations as Marked - Based Steering Mechanism and Alternative to Fixed Feed - in Tariffs,” Proceedings of the 28th EnviroInfo 2014 Conference: 729–734.
- J. Bremer, M. Sonnenschein, “Estimating Shapley Values for Fair Profit Distribution in Power Planning Smart Grid Coalitions,” in Multiagent System Technologies - Proceedings of the MATES 2013, Koblenz, Germany. Springer, LNCS 8076, 2013.
- C. Hinrichs, M. Sonnenschein, “Evaluation Guidelines for Asynchronous Distributed Heuristics in Smart Grid Applications,” in Proceedings of the 28th Conference on Environmental Informatics - EnviroInfo 2014 - ICT for Energy Efficiency, BIS-Verlag, pp. 365 – 372, 2014.
- C. Hinrichs, M. Sonnenschein, S. Lehnhoff, “Evaluation of a Self-Organizing Heuristic for Interdependent Distributed Search Spaces,” in ICAART 2013 - Proceedings of the 5th International Conference on Agents and Artificial Intelligence, Volume 1 - Agents, Barcelona, Spain, 15-18 February. SciTePress, pp. 25-34, 2013
- G. Lohmann, M. R. R. Tabar, P. Milan, M. Anvari, M. Wächter, E. Lorenz, D. Heinemann, J. Peinke, “Flickering Events in Wind and Solar Power,” in Proceedings of the 28th International Conference on Informatics for Environmental Protection, Oldenburg, 2014, S. 723–728.
- G Lohmann, J. Kühnert, E. Lorenz, A. Hammer, D. Heinemann, “Fluctuations in Large-Scale Photovoltaic and Wind Power Feed-In,” in Proceedings of the 4th International Workshop on Integration of Solar Power into Power Systems, Berlin, Germany, 2014.
- S. Lehnhoff, M. Sonnenschein, M. Tröschel, “Forschungsverbund Smart Nord - Dezentrale und selbstorganisierte Koordinationsverfahren für einen sicheren und zuverlässigen Netzbetrieb,” in Konferenz für Nachhaltige Energieversorgung und Integration von Speichern - NEIS 2013 – Tagungsband, S. 7-12, 2013.
- C. Norrenbrock, O. Melchert, A. K. Hartmann, “Fragmentation properties of two-dimensional Proximity Graphs considering random failures and targeted attacks,” (in Vorbereitung).
- H.-J. Appelrath, G. Brunekreeft, A. Weidlich, C. Wissing, C. Mayer, A. Ohsenbrügge, S.-C. Schnabel, M. Tröschel, “Future Energy Markets - Mehr Markt für eine effiziente Energiewende,” acatech Materialien, 2014.
- C. Rosinger, S. Beer, “Glaubwürdigkeit in dynamischen Wirkleistungsverbünden,” DACH-Energieinformatik 2014, Zürich, 2014.
- C. Rosinger, S. Beer, “Glaubwürdigkeit in dynamischen Wirkleistungsverbünden,” in Informatik-Spektrum, pp. 1–8, Dezember 2014.
- M. Calabria, W. Schumacher, “Impact of inverter clustering on the small-signal stability of a grid,” in EnviroInfo, 2013.

- T. Breithaupt, T. Rendel, L. Hofmann, “INES - Integrierte Netz- und Energiemarktsimulation,” 15. Dresdener Kreis 2014, Fachtagung der TU-Dresden, der Universität Hannover, der Universität Magdeburg und der Gesamthochschule Duisburg: Elektroenergieversorgung, Leipzig, Deutschland, 19.-20. März 2014.
- C. Rosinger, M. Uslar, J. Sauer, “Informationssicherheit als Vertrauenswürdigkeitsfacette für selbstorganisierende Energieagenten,” in VDE-Kongress 2014, VDE Verlag, 2014.
- Y. Chen, R. Hesse, D. Turschner, H. P. Beck, “Investigation of the Virtual Synchronous Machine in the Island Mode,” 3rd IEEE PES Innovative Smart Grid Tech-nologies Europe (ISGT Europe), Berlin, 2012.
- M. R. R. Tabar, M. Anvari, G. Lohmann, D. Heinemann, M. Wächter, P. Milan, E. Lorenz, J. Peinke, “Kolmogorov spectrum of renewable wind and solar power fluctuations,” European Physical Journal Special Topics, Bd. 223, Nr. 9, S. 1–8, Juli 2014.
- J. Bremer, M. Sonnenschein, “Kommunikation von Umweltkennzahlen im Smart Grid und deren Integration in die verteilte Wirkleistungsplanung,” in IT-gestütztes Ressourcen- und Energiemanagement, Konferenzband zu den 5. BUIS-Tagen, Oldenburg, Springer, S. 35-47, 2013.
- T. Dewenter, A. K. Hartmann, “Large-deviation properties of power grids,” Münster, 6. März 2014, "Complexity Meets Energy" workshop.
- T. Dewenter, A. K. Hartmann, “Large-deviation properties of power grids,” Dresden, 4. April 2014, DPG Frühjahrstagung.
- T. Dewenter, A. K. Hartmann, “Large-deviation properties of resilience of power grids,” New J. Phys. 17, 015005 (2015).
- T. Dewenter, A. K. Hartmann, “Large-deviation properties of resilience of power grids,” Bad Honnef, 6.-9. Dezember 2014, “HEEECC - Health, Energy & Extreme Events in a Changing Climate”, 577. WE-Heraeus-Seminar.
- A. K. Hartmann, “Large-deviation properties of resilience of transportation networks,” Eur. Phys. J B 87, 114 (2014).
- A. K. Hartmann, “Large-deviation properties of simple energy-grid models,” Regensburg, 12. März 2013, DPG Frühjahrstagung.
- A. K. Hartmann, T. Dewenter, W. Heins, B. Werther, “Large-deviation study of the maximum-disturbance stability of power grids,” 19. März 2014, DPG Frühjahrstagung, Berlin.
- C. Köpp, H. J. von Mettenheim, M. H. Breitner, “Lastmanagement in Stromnetzen - Beiträge für ein Entscheidungsunterstützungssytem für Portfoliobetreiber,” Wirtschaftsinformatik: 1–11. doi:10.1007/s11576-012-0348-9.
- C. Wissing, A. Nieße, M. Tröschel, “Market-Based redispatch in distribution Grids,” IRES, 2013.
- S. Lehnhoff, M. Tröschel, M. Uslar, C. Wissing, H.-J. Appelrath, M. Sonnenschein, “Market-based self-organized provision of active power and ancillary services: An agent-based approach for Smart Distribution Grids,” in Complexity in Engineering (COMPENG), pp. 1-5, 2012.

- T. Breithaupt, S. Garske, T. Rendel, L. Hofmann, “Methodological Approach for Integrated Grid and Market Simulation of Coherent Distribution and Transmission Systems,” EnviroInfo 2013, Hamburg, Germany, 02.-04. September 2013.
- J. Bremer, M. Sonnenschein, “Model-based Integration of Constrained Search Spaces into Distributed Planning of Active Power Provision,” in Computer Science and Information Systems, Vol. 10, No. 4, 1823-1854, 2013.
- J. Psola, et al., “Modeling of a Redox Flow Battery Storage for Grid Applications,” in PCIMasia 2013, Shanghai, China, 2013.
- M. Calabria, W. Schumacher, “Modeling power inverter interactions in a low voltage grid,” in s Control and Modeling for Power Electronics (COMPEL), 2014 IEEE 15th Workshop on, 2014.
- T. Breithaupt, T. Rendel, C. Rathke, L. Hofmann, “Modeling the Reliability of Large Thermal Power Plants in an Integrated Grid and Market Model,” 2012 IEEE International Conference on Power System Technology (Powercon), Auckland, New Zealand, 30. October–2. November 2012.
- Y. Chen, B. Werther, B. Schwake, H.-P. Beck, “Netzstabilisierung durch die "Virtuelle Synchronmaschine" (VISMA) mit überlagerter Frequenz- und Spannungsregelung,” Internationaler ETG-Kongress 2013, Berlin (05.-06. November 2013).
- G. Anders, C. Hinrichs, F. Siefert, P. Behrmann, W. Reif, M. Sonnenschein, “On the Influence of Inter-Agent Variation on Multi-Agent Algorithms Solving a Dynamic Task Allocation Problem under Uncertainty,” in 2012 IEEE Sixth International Conference on Self-Adaptive and Self-Organizing Systems (SASO 2012), Lyon, France, 2012.
- T. Dewenter, B. Werther, A. K Hartmann, H.-P. Beck, “Optimierung des dynamischen Verhaltens netzstützender Anlagen am Beispiel der Virtuellen Synchronmaschine,” 13. Symposium Energieinnovation, Graz/Austria, (12.-14. Februar 2014).
- J. Psola et al., “Optimization of energy output by combining energy storages with renewable energies,” in PCIMasia 2014, Shanghai, China, 2014.
- J. Bremer, M. Sonnenschein, “Parallel tempering for constrained many criteria optimization in dynamic virtual power plants,” in 2014 IEEE Symposium on Computational Intelligence Applications in Smart Grids (CIASG), IEEE, 2014.
- C. Norrenbrock, “Percolation threshold on planar Euclidean Gabriel graphs,” arXiv:1406.0663.
- F. Fuchs, M. Mertens, “Prediction and avoidance of grid-connected converter's instability caused by wind park typical, load-varying grid resonance,” Energy Conversion Congress and Exposition (ECCE), 2014 IEEE, pp.2633,2640, 14-18 Sept. 2014.
- Y. Chen, R. Hesse, D. Turschner, H.-P. Beck, “Propiedades dinamicas da maquina sincrona virtual,” EM Janeiro 2014, S. 58 - 65, (2014).
- N. G. A. Hemdan, F. Muuß, D. Unger, M. Kurrat, “Reactive Power as an Ancillary Service Provision into Transmission Networks through Decentralized Generation” in Cigre Belgium 2014.
- M. Gandor et al., “Reconfiguration Strategies for Electrical Devices for Operation within Feasibility Margins,” in proc. of VDE Kongress 2012 – Smart Grid Applications / Services, 2012, Stuttgart, Germany.

- C. Wissing, H.-J. Appelrath, “ReFlex: Market-Based Redispatch in Distribution Grids - Incentivizing Flexible Behavior of Distributed Energy Resources,” EnviroInfo. Hamburg, September 2013.
- M. R. R. Tabar, M. Anvari, M. Wächter, P. Milan, G. Lohmann, E. Lorenz, D. Heinemann, J. Peinke, “Renewable Power from Wind and Solar: Suppressing The Short-Term Intermittency and Their Resilience,” (submitted).
- C. Rosinger, M. Uslar, F. Hockmann, “Reputationssysteme für selbstorganisierte Multi-Agenten-Systeme in Energiemanagementsystemen,” *VDE-Kongress 2012*, 2012.
- M. R. R. Tabar, M. Anvari, M. Waechter, P. Milan, G. Lohmann, E. Lorenz, D. Heinemann, J. Peinke, “Resilience of Renewable Power from Wind and Solar and Suppressing Their Short-Term Intermittency,” (Submitted).
- J. Bremer, M. Sonnenschein, “Sampling the Search Space of Energy Resources for Self-organized, Agent-based Planning of Active Power Provision,” in Environmental Informatics and Renewable Energies - 27th International Conference on Informatics for Environmental Protection. Shaker Verlag, pp. 214-222, 2013.
- M. Sonnenschein, “Smart Grids - auf dem Weg zu intelligenten Stromnetzen,” in Zukunftswerkstatt Deutschland: Die Energiewende. Vol. 8 Hanse Studien, S. 93-104, 2013.
- M. Sonnenschein, M. Tröschel, O. Lünsdorf, “Smart Grids for Optimised Utilisation of Renewable Energy Supply,” in Environmental Informatics and Renewable Energies - 27th International Conference on Informatics for Environmental Protection. Shaker Verlag, pp. 178-187, 2013.
- M. Calabria, W. Schumacher, “Stability optimization for distributed generation of load-following energy,” in Energy Conference (ENERGYCON), 2014 IEEE International, 2014.
- M. Sonnenschein, C. Hinrichs, A. Nieße, U. Vogel, “Supporting Renewable Power Supply through Distributed Coordination of Energy Resources,” in ICT Innovations for Sustainability, Advances in Intelligent Systems and Computing. Springer, pp. 387-404, 2015.
- M. Kurrat, N. G. A. Hemdan, B. Engel, R. Canders, M. Henke, “Technical challenges for ancillary services provided by decentralized power generation in active distribution systems,” in ETG Kongress Berlin 2013.
- J. Psola, et al., “Technologies and Operational Concepts for Energy Storages,” in Enviroinfo, Hamburg, Germany, 2013.
- C. Hinrichs, M. Sonnenschein, “The Effects of Variation on Solving a Combinatorial Optimization Problem in Collaborative Multi-Agent Systems,” in Multiagent System Technologies. Lecture Notes in Computer Science Volume 8732, pp. 170-187, 2014.
- C. Rosinger, M. Uslar, J. Sauer, “Threat Scenarios to evaluate Trustworthiness of Multi-agents in the Energy Data Management,” in Environmental Informatics and Renewable Energies - 27th International Conference on Informatics for Environmental Protection. Shaker Verlag, 2013.
- B. Küster, A. Koukal, M. H. Breitner, “Towards an Allocation of Revenues in Virtual Clusters within Smart Grids,” IWI Diskussionbeiträge 60 (September), 2013.

- S. Beer, M. Sonnenschein, H.-J. Appelrath, “Towards a Self-Organization Mechanism for Agent Associations in Electricity Spot Markets,” in INFORMATIK 2011 – Informatik schafft Communities., Berlin, 2011.
- S. Lehnhoff, K. Piech, S. Rohjans, “UML-based Modeling of OPC UA Address Spaces for Power Systems,” in IEEE International Workshop on Intelligent Energy Systems (IWIES 2013), Vienna, Austria, 2013.
- C. Wissing, H.-J. Appelrath, “Using automated market analysis for optimized economic operation of DER in Virtual Power Plants,” EEM, 2012.
- A. Nieße, M. Sonnenschein, “Using Grid Related Cluster Schedule Resemblance for Energy Rescheduling,” in SmartGreens 2013 - 2nd Int. Conf. on Smart Grids and Green IT Systems, Aachen, Germany, pp. 22-31, 2013.
- C. Rosinger, M. Uslar, J. Sauer, “Using Information Security as a Facet of Trustworthiness for Self-Organizing Agents in Energy Coalition Formation Processes,” in Proceedings of the 28th Conference on Environmental Informatics - EnviroInfo 2014 - ICT for Energy Efficiency, BIS-Verlag, 2014.

List of Doctoral Theses

- Almut Siewert, “Kumulative Wirkung von EE-Anlagen,” Leibniz Universität Hannover, Institute of Environmental Planning, planned to be submitted 2016.
- Anja Ohsenbrügge, “Entwicklung eines flexiblen Prognosemodells zur dynamischen Regelleistungsbemessung,” University of Oldenburg, Department of Computing Science, planned to be submitted 2015.
- Astrid Nieße, “Verteilte kontinuierliche Einsatzplanung in Dynamischen Virtuellen Kraftwerken,” University of Oldenburg, Department of Computing Science, 2015.
- Carsten Wissing, “ReFlex: Marktbasiertes Redispatch mit Flexibilitäten von Netznutzern für das Verteilnetz,” University of Oldenburg, Department of Computing Science, 2015.
- Christian Hinrichs, “Selbstorganisierte Einsatzplanung dezentraler Akteure in Smart Grids,” University of Oldenburg, Department of Computing Science, 2014.
- Christine Rosinger, “Ein Vertrauensmodell für die Verbundbildung von Multi-Agenten-Systemen im Energiedatenmanagement,” University of Oldenburg, Department of Computing Science, planned to be submitted 2016.
- Felix Fuchs, “Einfluss von Resonanzen der Netzimpedanz auf die Stromregelung von Windenergieanlagen,” Leibniz Universität Hannover, Institut für Antriebssysteme und Leistungselektronik, planned to be submitted 2015.
- Fridolin Muuß, “Blindleistungsregelstrategien - intelligentes Blindleistungsmanagement durch dezentrale Energieanlagen im aktiven Verteilnetz,” Technische Universität Braunschweig, elenia, planned to be submitted 2017.
- Gerald Lohmann, “Kleinskalige stochastische Simulation von Fluktuationen in der Leistungsabgabe dezentraler Photovoltaikanlagen auf Verteilnetzebene,” University of Oldenburg, Institute of Physics and ForWind, 2016.
- Jan-Hendrik Psola, “Betriebs- und Einsatzmöglichkeiten von Energiepseichern,” Technische Universität Braunschweig, Institute for Electrical Machines, Traction and Drives, planned to be submitted 2015.
- Jörg Bremer, “Constraint-Handling mit Supportvektor-Dekodern in der verteilten Optimierung,” University of Oldenburg, Department of Computing Science, 2015.
- Marita Blank, “Reliability Assessment of Coalitions for the Provision of Ancillary Services,” University of Oldenburg, Department of Computing Science, planned to be submitted 2015.
- Phillip Gronstedt, “Systembasierte Integration erneuerbarer Energieumwandlung über die Mehrwegevermarktung virtueller Pools,” Technische Universität Braunschweig, 2013.
- René Dietz, “Wechselwirkungen dezentraler Energieerzeuger kleiner Leistung im Niederspannungsnetz,” Leibniz Universität Hannover, Institut für Antriebssysteme und Leistungselektronik, planned to be submitted 2016.
- Sebastian Beer, “Dynamic Coalition Formation in Electricity Markets,” University of Oldenburg, Department of Computing Science, planned to be submitted 2015.

Closing Remarks

Looking back on the past three years, it can be claimed that the planned aims of Smart Nord were achieved. It should especially be mentioned that due to the large number of participants numerous collaborations between the young scientists resulted at the different research institutes which will hopefully be continued after the end of Smart Nord.

The grant ended with the end of February 2015 where results of Smart Nord were presented to a broad audience of interested visitors at the Smart Nord final conference. At this point, we would like to thank again the organization committee and all speakers and supporters of the conference as well as the contributors of this final report. In addition Dr. Martin Troeschel and Torsten Rendel had to be thanked for their coordination of the project and support of the project management.

Smart Nord's results are currently worked on in the transfer project "iQ –Intelligent Reactive Power Control for Distribution Grids" which is funded by the Lower Saxony Ministry of Science. Also the EXIST transfer project "Dynamic VPP" which revisits topics of Smart Nord must be mentioned here. In addition to these projects directly linked to Smart Nord, two project funded by the federal ministries of BMU and BMWI, one funded by the EU and five federal funded projects are applied for. At last it must be mentioned that one partner is aiming to implement a DFG-Forschergruppe.

A list of publications and adjacent doctoral theses can be found in the annex. For further information do not hesitate to contact the authors of this final report.

We would like to express our gratitude to the Lower Saxony Ministry of Science for supporting Smart Nord through the "Niedersächsisches Vorab" grant programme.

Prof. Dr.-Ing. habil. Lutz Hofmann

Institute of Electric Power Systems
Leibniz Universität Hannover

hofmann@iee.uni-hannover.de

Prof. Dr. rer. nat. habil. Michael Sonnenschein

Department of Computing Science
Carl von Ossietzky Universität Oldenburg

sonnenschein@informatik.uni-oldenburg.de

ISBN: 978-3-00-048757-6